Barts Cancer Institute
Queen Mary, University of London

Barts and The London
School of Medicine and Dentistry

THE ROLE OF EPITHELIAL CELL-DERIVED TUMOUR NECROSIS FACTOR ALPHA IN PANCREATIC CARCINOGENESIS

by Maud Bossard

Thesis submitted to Queen Mary, University of London for the degree of Doctor of Philosophy

March 2012

Centre for Cancer and Inflammation

Barts Cancer Institute - a CR-UK Centre of Excellence

Queen Mary, University of London

3rd floor, John Vane Science Centre

Charterhouse Square

London - EC1M 6BQ

STATEMENT

I hereby certify that, except where acknowledgment is made, the work contained in this thesis was performed by me in the Barts Cancer Institute at Queen Mary, University of London.

Dr Eleni Maniati developed the *kras*^{G12D}/*tnfa*$^{\Delta Pdx}$ mice, Juliana Candido performed the Masson's trichrome staining and Dr Thorsten Hagemann helped with the generation of chimeras here at Barts Cancer Institute, Queen Mary, University of London, London, UK. Histological tissue processing and haematoxylin and eosin staining were carried out by the Barts Cancer Institute pathology department, Queen Mary, University of London, London, UK. FACS analyses were performed by Dr Guglielmo Rosignoli, Barts Cancer Institute, Queen Mary, University of London, London, UK.

Histological analyses were completed with support from Anne Schultheis (University Medical Center Hamburg-Eppendorf, Pathology department, Hamburg, Germany). The kinase assays were performed by Dr Toby Lawrence and his group (Inflammation Biology Group, Centre d'Immunologie Marseille - Luminy, Marseille, France) and the mass spectrometry analyses by Dr Benjamin Thomas and Dr Fernando Martinez-Estrada (Central Proteomics Facility, Oxford University, Oxford, UK).

I also declare that the work described in this thesis is original and has not been previously published by others or submitted for any other degree in this or any other university. Part of the work presented in this thesis has been published in the Journal of Clinical Investigation, December 2011 and a copy is enclosed.

ABSTRACT

Activating mutations of the *kras* proto-oncogene are found in more than 90 % of human pancreatic ductal adenocarcinoma (PDAC) and can result in increased activity of the NF-κB pathway, leading to constitutive production of pro-inflammatory cytokines such as TNF-α. Pancreatic cancer progression occurs through a series of pre-invasive lesions, pancreatic intraepithelial neoplasias (PanIN lesions), which progress into invasive carcinoma.

The aim of this thesis is to understand the autocrine role of TNF-α produced by pre-malignant epithelial cells in pancreatic tumour progression. This cytokine has already been shown to be involved in the progression of cancer. The major hypothesis therefore tested was that TNF-α secreted by pre-malignant epithelial cells promotes the early stages of pancreatic carcinogenesis by sustaining an inflamed microenvironment.

In the spontaneous *kras*$^{+/LSL\text{-}G12D}$; *pdx1*-cre mouse model of pancreatic cancer, concomitant genetic deletion of the TNF-α/IKK2 pathway substantially delayed pancreatic cancer progression and resulted in downregulation of the classical Notch target genes *hes1* and *hey1*. Cell lines from the different PanIN bearing mice were established and used to dissect the cooperation between TNF-α/IKK2 and Notch signalling during PanIN progression. Optimal expression of Notch target genes was induced upon TNF-α stimulation of the canonical NF-κB signalling pathway, in cooperation with basal Notch signals. Mechanistically, TNF-α stimulation resulted in phosphorylation of histone H3 at the *hes1* promoter and this signal was lost upon *ikk2* genetic deletion. HES1 suppressed the expression of *pparg*, which encodes for the anti-inflammatory nuclear receptor PPAR-γ. Thus, crosstalk between TNF-α/IKK2

and Notch sustained an intrinsic inflammatory profile of the transformed cells. The treatment of PanIN bearing mice with rosiglitazone, a PPAR-γ agonist, also delayed PanIN progression.

A malignant cell-autonomous, low-grade inflammatory process was shown to operate from the very early stages of *kras*-driven pancreatic carcinogenesis, which may cooperate with the Notch signalling pathway to promote pancreatic cancer progression.

ACKNOWLEDGMENTS

Special thanks must firstly go to my supervisor, Dr Thorsten Hagemann. He has provided me with an excellent project and continual encouragement, ideas and inspiration throughout my research. I am also thankful to my second supervisor, Professor Frances Balkwill, for her scientific guidance and help. I am grateful to the Medical Research Council for funding my PhD.

I would like to thank the current and previous members of the Centre for Cancer and Inflammation for all their encouragement, advice and help. A special thank you to Richard Thompson for his help, his patience and his expertise with animals.

I am especially indebted to Dr Eleni Maniati for her kindness and availability, our close partnership during this thesis and her expertise. I also would really like to thank Nia Emami-Shahri, for brightening up my days in the lab, for our chitchats and for his friendship.

I wish also to thank all past and present co-workers within Thorsten's group: Bernardo Alvares, Juliana Candido, Jenny Cook, Dr Mónica Escórcio-Correia, Dr Cristina Ghirelli, Dr Simon Hallam, Lily Keane, Dr Eleni Maniati, Dr Fiona McCarthy, Rozita Roshani, Dr Robin Soper and Dr Raphaël Zollinger. Thank you to all of you for giving a helping hand in the lab and especially with any *in vivo* experiments.

Thank you also to the Barts Cancer Institute Biological Services Unit staff, in particular to Alex, for her help with mice husbandry and close monitoring of their

health statuses. I am also thankful to all the people who proofread the chapters of this thesis.

I would like to thank Paul, Gilbert and all the others who encouraged and convinced me to do a PhD. It was a difficult decision which I do not regret, even if there were quite a few challenging moments. I have learnt so much about work and about myself. It has been quite a long journey but a very interesting and rewarding experience.

Special thanks go to all of my friends, who stood by me even through the toughest times: Isabelle, Kristin, Kyra, Sally, Salma, Samia and Samira here in UK, and Emilie, Hugues, Jonathan and Laure in France. I owe a huge personal thank to my friend Anne-Sophie; thank you for who you are, for your help and support throughout my PhD and life in general.

Last but certainly not least, my love and gratitude to my entire extended family; to my brothers Mickaël, Pierre, Romain and Romain, to my sister Agathe, to Brigitte, to my father, to Jean and especially to my mother, for her love, for standing by me and for being an amazing woman; thank you to all of you for your understanding, constant support and encouragement over the phone and/or Skype.

Dans les sciences, le chemin est plus important que le but.

Les sciences n'ont pas de fin.

Erwin Chargaff - Biochemist (1905 - 2002)

Il n'est de médecine qui ne guérisse ce que ne guérit pas le bonheur.

Gabriel García Márquez - Novelist (1927)

TABLE OF CONTENTS

STATEMENT II

ABSTRACT III

ACKNOWLEDGMENTS V

TABLE OF CONTENTS VIII

LIST OF FIGURES XIV

LIST OF TABLES XVII

ABBREVIATIONS XVIII

CHAPTER ONE: INTRODUCTION 26

1.1 CANCER AND INFLAMMATION 27

1.1.1 CANCER 27

1.1.2 INFLAMMATION 30

1.1.3 LINKS BETWEEN INFLAMMATION AND CANCER 30

1.1.4 TUMOUR MICROENVIRONMENT 34

1.2 PANCREATIC CANCER 44

1.2.1 ANATOMY AND DEVELOPMENT OF THE PANCREAS 44

1.2.2 INCIDENCE, MORTALITY AND SURVIVAL OF PANCREATIC CANCER 46

1.2.3 RISK FACTORS FOR PANCREATIC CANCER 47

1.2.4 SYMPTOMS AND DIAGNOSIS OF PANCREATIC CANCER 48

1.2.5 TREATMENTS FOR PANCREATIC CANCER 49

1.2.6 INITIATION, PROGRESSION AND CLASSIFICATION OF PANCREATIC CANCER 52

1.2.7 THE STROMA IN PANCREATIC CANCER 57

1.2.8 *IN VIVO* MODELS 60

1.3 THE TNF-α/NF-κB SIGNALLING PATHWAY 70

1.3.1 THE NF-κB SIGNALLING PATHWAY 70

1.3.2 NF-κB: BETWEEN INFLAMMATION AND CANCER 73

1.4 THE NOTCH SIGNALLING PATHWAY 84

1.4.1 COMPONENTS OF THE PATHWAY 84

1.4.2 THE CANONICAL AND NON-CANONICAL NOTCH SIGNALLING PATHWAYS 84

1.4.3 NOTCH FUNCTIONS - LINKS BETWEEN DEVELOPMENT AND CANCER 86

1.4.4 IMPLICATIONS OF THE NOTCH PATHWAY IN PANCREATIC DEVELOPMENT, PANCREATITIS AND PANCREATIC CANCER 90

1.5 FOCUS OF THESIS 94

CHAPTER TWO: MATERIALS AND METHODS 95

2.1 TRANSGENIC ANIMALS 96

2.1.1 MOUSE MODELS AND BREEDING 96

2.1.2 CHIMERAS 97

2.1.3 *IN VIVO* CELL PROLIFERATION 98

2.1.4 *IN VIVO* EXPERIMENTS WITH SMALL INHIBITORS 98

2.2 TISSUE CULTURE 99

2.2.1 PANIN AND PDAC CELL LINES 99

2.2.2 OP9-DL1 CELLS 101

2.2.3 IMMUNE CELLS 101

2.2.4 CELL CULTURE TREATMENT 102

2.3 CLONING AND TRANSFECTION OF CELLS 104

2.3.1 PLASMID CONSTRUCTS 104

2.3.2 TRANSFORMATION OF BACTERIA 104

2.3.3 RECOVERY OF BACTERIA FROM FROZEN GLYCEROL STOCKS 105

2.3.4 PLASMID DNA EXTRACTION 105

2.3.5 INTEGRITY OF THE PLASMID CONSTRUCTS 107

2.3.6 TRANSCIENT TRANSFECTION OF TARGET CELLS WITH FUGENE®HD 108

2.3.7 SILENCING GENES *IN VITRO* - SMALL INTERFERENCE RNA (SIRNA) 108

2.3.8 LUCIFERASE REPORTER ASSAY 109

2.4 NUCLEIC ACIDS 112

2.4.1 NUCLEIC ACID QUANTIFICATION 112

2.4.2 AGAROSE GEL ELECTROPHORESIS 112

2.4.3 TOTAL RNA ISOLATION - TRIZOL 113

2.4.4 DNASE TREATMENT OF RNA 113

2.4.5 TOTAL RNA ISOLATION - RNEASY TECHNOLOGY 114

2.4.6 CDNA SYNTHESIS 116

2.4.7 QUANTITATIVE REAL-TIME PCR (QRT-PCR) 116

2.5 PROTEIN ANALYSIS 119

2.5.1 PROTEIN EXTRACTION 119

2.5.2 PROTEIN QUANTIFICATION 119

2.5.3 WESTERN BLOT 120

2.5.4 ENZYME-LINKED IMMUNOSORBENT ASSAY (ELISA) 124

2.5.5 KINASE ASSAY 126

2.5.6 CYTOKINE AND CHEMOKINE ARRAYS 126

2.6 PROTEIN-DNA INTERACTIONS 128

2.7 PROTEIN-PROTEIN INTERACTIONS 130

2.7.1 IMMUNOPRECIPITATION 130

2.7.2 COOMASSIE BRILLIANT BLUE STAIN 131

2.7.3 MASS SPECTROMETRY 131

2.8 HISTOLOGY, STAINING AND IMMUNOHISTOCHEMISTRY 134

2.8.1 HISTOLOGY 134

2.8.2 HAEMATOXYLIN AND EOSIN STAINING 134

2.8.3 MASSON'S TRICHROME 135

2.8.4 IMMUNOHISTOCHEMISTRY 136

2.9 CONFOCAL MICROSCOPY - IMMUNOFLUORESCENCE 139

2.10 FLOW CYTOMETRY 141

2.10.1 ANALYSIS OF IMMUNE POPULATIONS FROM THE PANCREAS 141

2.10.2 FLUORESCENCE-ACTIVATED CELL SORTING (FACS) 143

2.11 STATISTICAL ANALYSIS 144

CHAPTER THREE: CHARACTERISATION OF PANCREATIC MURINE MODELS 145

3.1 INTRODUCTION 146

3.2 GENERATION OF *KRAS*^{G12D} MOUSE MODELS WITH CONDITIONAL DELETION OF *IKK2* OR *TNFA* IN THE PANCREAS 148

3.3 ASSESSMENT OF *TNFA* AND *IKK2* GENETIC DELETION IN PANCREATIC EPITHELIAL CELLS *IN VITRO* 150

3.3.1 PANIN AND PDAC CELL LINES SECRETE TNF-α 150

3.3.2 GENETIC DELETION OF *TNFA* 152

3.3.3 GENETIC DELETION OF *IKK2* 152

3.4 EFFECTS ON PANIN FORMATION AND PROGRESSION 154

3.4.1 INCIDENCE OF PANCREATIC TUMOURS 154

3.4.2 GENERAL HISTOPATHOLOGY 156

3.4.3 HISTOLOGICAL QUANTIFICATION 159

3.4.4 ANALYSIS OF PANCREATIC TISSUE SECTIONS 160

3.4.5 INFLAMMATORY INFILTRATE IN THE PANCREAS 167

3.5 DISCUSSION AND CONCLUSION 173

CHAPTER FOUR: THE NF-κB AND THE NOTCH SIGNALLING PATHWAYS 181

4.1 INTRODUCTION 182

4.2 ACTIVATION OF THE NOTCH PATHWAY IN PANCREATIC CANCER 184

4.3 COOPERATION BETWEEN THE TNF-α/IKK2 AND THE NOTCH SIGNALLING PATHWAYS 188

4.3.1 THE EXPRESSION OF NOTCH TARGET GENES OVER TIME 188

4.3.2 NOTCH TARGET GENES ARE EXPRESSED UPON STIMULATION WITH RTNF-α 189

4.3.3 RTNF-α STIMULATION ENHANCES THE PROMOTER ACTIVITY OF THE *HES1* GENE 192

4.3.4 RTNF-α STIMULATION DOES NOT INCREASE THE EXPRESSION OF NOTCH RECEPTORS AND LIGANDS 193

4.3.5 CANONICAL NOTCH SIGNALLING IS REQUIRED 195

4.3.6 ACTIVATION OF THE NOTCH PATHWAY IS IKK2-DEPENDENT 201

4.4 ANALYSIS OF THE CROSSTALK BETWEEN NF-κB AND NOTCH 205

4.4.1 RTNF-α STIMULATION INDUCES NICD CLEAVAGE 205

4.4.2 INTERACTION BETWEEN NICD AND IKK2 *IN VITRO* 207

4.4.3 PHOSPHORYLATION OF HISTONE H3 UPON RTNF-α STIMULATION 211

4.5 DISCUSSION AND CONCLUSION 216

CHAPTER FIVE: HES1 AND INFLAMMATION 223

5.1 INTRODUCTION 224

5.2 LINK BETWEEN HES1 AND PPAR-γ IN PANCREATIC CANCER 227

5.2.1 GENE EXPRESSION LEVELS OF *PPARG* 227

5.2.2 EXPRESSION OF *PPARG* IS INHIBITED BY HES1 229

5.2.3 HES1 IS PRESENT AT THE *PPARG* PROMOTER 232

5.3 DISCUSSION AND CONCLUSION 233

CHAPTER SIX: INFLAMMATION AND TUMOUR PROGRESSION IN PANCREATIC CANCER 235

6.1 INTRODUCTION 236

6.2 INHIBITION OF THE NOTCH AND THE NF-κB SIGNALLING PATHWAYS 239

6.3 INFLAMMATORY STATUS OF THE PANCREAS AFTER DAPT TREATMENT 243

6.4 EFFECTS OF ROSAGLITAZONE TREATMENT ON THE PROGRESSION OF PANCREATIC CANCER 246

6.5 DISCUSSION AND CONCLUSION 252

CHAPTER SEVEN: CONCLUSIONS AND FUTURE PLANS 255

REFERENCES 266

APPENDICES 315

PUBLICATION 325

LIST OF FIGURES

Figure 1.1: Hallmarks of cancer _____29

Figure 1.2: Extrinsic and intrinsic pathways linking inflammation and cancer _____33

Figure 1.3: The tumour microenvironment_____35

Figure 1.4: Anatomy and histology of the pancreas _____44

Figure 1.5: Chronology of pancreatic cancer development _____53

Figure 1.6: *Cre-lox* system _____62

Figure 1.7: Conditional expression of *kras*$^{LSL-G12D}$ allele_____63

Figure 1.8: Schematic representation of cell differentiation during the development of the pancreas _____67

Figure 1.9: Cell types in the adult pancreas and their contribution to PanIN/PDAC formation _____67

Figure 1.10: The TNF-α/IKK2/NF-κB signalling pathway _____70

Figure 1.11: The canonical Notch signalling pathway_____85

Figure 3.1: Generation of *kras*^{G12D} mice with targeted deletion of *ikk2* _____149

Figure 3.2: Morphological characteristics of the cell lines generated _____150

Figure 3.3: TNF-α secretion from PanIN and PDAC cell lines _____151

Figure 3.4: Genetic deletion of *ikk2* and *tnfa* in pancreatic cell lines _____153

Figure 3.5: Tumour incidence and histology grade _____154

Figure 3.6: Liver metastasis_____155

Figure 3.7: Body weight monitoring of the main mouse strains used _____156

Figure 3.8: Haematoxylin and eosin staining of pancreas sections from intermediate strains _____157

Figure 3.9: Haematoxylin and eosin staining of pancreas sections from mouse models ___158

Figure 3.10: Proportion of the pancreas occupied by PanIN lesions _____159

Figure 3.11: Immunohistochemistry staining for SOX9 in tissue sections _____161

Figure 3.12: Masson's Trichrome staining for collagen in tissue sections_____162

Figure 3.13: Immunohistochemistry staining of BrdU in tissue sections _____164

Figure 3.14: Immunohistochemistry staining for PCNA in tissue sections 165

Figure 3.15: Immunohistochemistry staining for cleaved caspase-3 in tissue sections 167

Figure 3.16: Profile of the infiltrated inflammatory cells 169

Figure 3.17: *Ex vivo* TNF-α secretion from immune cells 171

Figure 3.18: Proportion of pancreas occupied by PanIN lesions in chimeras 172

Figure 4.1: Notch target genes mRNA levels in pancreases 185

Figure 4.2: Immunofluorescent staining for HES1 in tissue sections 186

Figure 4.3: Time course of *hes1* and *hey1* expression upon rTNF-α stimulation 188

Figure 4.4: mRNA levels of Notch target genes in cell lines 190

Figure 4.5: Immunofluorescent staining for HES1 and HEY1 in PanIN derived cell lines 191

Figure 4.6: Transcriptional activity of the *hes1* promoter 192

Figure 4.7: Effect of cycloheximide treatment on the expression of Notch target genes 194

Figure 4.8: Effect of pharmacological inhibition of Notch signalling on the expression of TNF-α-induced Notch and NF-κB target genes 196

Figure 4.9: Expression of Notch target genes when maximally engaging Notch receptors 197

Figure 4.10: siRNA knockdown of *rbpj* in cell lines derived from PanIN bearing *kras*^{G12D}/*tnfa*$^{\Delta Pdx}$ mice 199

Figure 4.11: siRNA knockdown of *ikk2* in cell lines derived from PanIN bearing *kras*^{G12D}/*tnfa*$^{\Delta Pdx}$ mice 202

Figure 4.12: siRNA knockdown of *ikk1* in cell lines derived from PanIN bearing *kras*^{G12D}/*tnfa*$^{\Delta Pdx}$ mice 203

Figure 4.13: siRNA knockdown of *nemo* in cell lines derived from PanIN bearing *kras*^{G12D}/*tnfa*$^{\Delta Pdx}$ mice 204

Figure 4.14: NICD and HES1 protein levels by Western blot in PanIN derived cells 206

Figure 4.15: Protein levels by Western blot after co-immunoprecipitations in transfected cells 208

Figure 4.16: Coomassie brilliant blue staining of purified immunocomplexes 210

Figure 4.17: Chromatin immunoprecipitation of histone H3 to the *hes1* promoter 213

Figure 4.18: Chromatin immunoprecipitation of phospho-histone H3 (Ser10) to the *hes1* promoter 214

Figure 4.19: The link between the IKK2 and the Notch signalling pathways 219

Figure 5.1: Nuclear receptor *pparg* gene expression *in vivo* 227

Figure 5.2: Nuclear receptor *pparg* gene expression upon rTNF-α stimulation *in vitro* 228

Figure 5.3: siRNA knockdown of *hes1* in cell lines derived from PanIN bearing $kras^{G12D}$ mice 229

Figure 5.4: Gene expression levels for *pparg* following *hes1* knockdown 230

Figure 5.5: Gene expression levels for *cebpa* following *hes1* knockdown 230

Figure 5.6: Effects of HES1 on the activity of the *pparg* promoter 231

Figure 5.7: Chromatin immunoprecipitation of HES1 to the *pparg* promoter 232

Figure 6.1: Changes in *hes1* expression levels upon inhibition of the Notch or the NF-κB signalling pathways *in vitro* 239

Figure 6.2: Changes in *hes1* expression levels upon inhibition of the Notch or the NF-κB signalling pathways *in vivo* 240

Figure 6.3: TNF-α cytokine levels 241

Figure 6.4: Cytokines and chemokines array data 243

Figure 6.5: Cytokine gene expression levels upon DAPT treatment in $kras^{G12D}$ mice 245

Figure 6.6: Body weight monitoring upon rosiglitazone treatment 247

Figure 6.7: Proportion of the pancreas occupied by PanIN lesions 248

Figure 6.8: Tumour incidence and histology grade 249

Figure 6.9: Liver metastasis 250

Figure 6.10: Macrophage infiltrate 250

Figure 7.1: TNF-α/IKK2 is suggested to cooperate with Notch to sustain an inflammatory environment favouring pancreatic carcinogenesis 265

LIST OF TABLES

Table 1.1: The relationship between chronic inflammation and cancer _____32

Table 1.2: Fibroblast markers _____36

Table 1.3: Transcription factors and genes expressed during pancreatic organogenesis ____46

Table 1.4: Mutations during PDAC progression _____55

Table 2.1: Plasmid constructs used and their characteristics_____104

Table 2.2: Formulation of resolving gels_____121

Table 2.3: Formulation of stacking gels _____121

Table 2.4: Primary antibodies used for Western blot_____123

Table 2.5: Secondary antibodies used for Western blot_____124

Table 2.6: Antibodies used for chromatin immunoprecipitation _____129

Table 2.7: Primary antibodies used for immunohistochemistry_____136

Table 2.8: Secondary antibodies used for immunohistochemistry_____136

Table 2.9: Primary antibodies used for immunofluorescence _____140

Table 2.10: Secondary antibodies used for immunofluorescence _____140

Table 2.11: Antibodies used for flow cytometry analysis_____142

Table 2.12: Flow cytometry spectrum guide_____142

Table 3.1: Characteristics of the mouse strains used _____149

Table 3.2: Surface markers used for the identification of immune cells _____168

ABBREVIATIONS

5-FU/FA	5-fluorouracil and folinic acid
ABC	Avidin biotinylated enzyme complex
AP	Activator protein
APS	Ammonium persulfate
ANOVA	Analysis of variance
ATP	Adenosine-5'-triphosphate
BATF	Basic leucine zipper transcription factor
BCA	Bicinchoninic acid
bHLH	Basic helix-loop-helix
B	B cells
BO	Biliary obstruction
bp	Base pair
BRCA	Breast cancer susceptibility protein
BrdU	5-bromo-2'-deoxyuridine
BSA	Bovine serum albumin
CA 19-9	Carbohydrate antigen 19-9
CAFs	Cancer associated fibroblasts
CCL2	CC chemokine ligand 2
CD	Cluster of differentiation
CDKN2	Cyclin dependent kinase inhibitor 2
cDNA	Complementary deoxyribonucleic acid
CEBPA	CCAAT/enhancer-binding protein alpha
ChIP	Chromatin immunoprecipitation
COX2	Cycloxygenase-2
Cre	Causes recombination

CSF1	Colony stimulating factor 1
Ct	Threshold cycle
CTL	Cytotoxic T lymphocytes
CTLA4	Cytotoxic T lymphocyte antigen
CXCR	CXC chemokine receptor
Da	Daltons
DAB	3,3'-diaminobenzidine
DAPI	4',6-diamidino-2-phenylindole
DAPT	N-[(3,5-Difluorophenyl)acetyl]-L-alanyl-2-phenyl]glycine-1,1-dimethylethyl ester
DC	Dendritic cells
Dlk	Delta like homologue
Dll	Delta like
DMBA	7,12-dimethylbenz[a]-anthracene
DMEM	Dulbecco's modified eagle medium
DMSO	Dimethyl sulfoxide
DNA	Deoxyribonucleic acid
dNTP	Deoxyribonucleotide triphosphate
DPC	Deleted in pancreatic cancer
dsRNA	Double-stranded ribonucleic acid
DTT	Dithiothreitol
EBV	Epstein-Barr virus
ECL	Enhanced chemiluminescence reaction
ECM	Extracellular matrix
EDTA	Ethylenediaminetetraacetic acid
EGF	Epidermal growth factor

EGFR	Epidermal growth factor receptor
EGTA	Ethylene glycol tetraacetic acid
ELISA	Enzyme-linked immunosorbent assay
ER	Oestrogen Receptor
ERCP	Endoscopic retrograde cholangio-pancreatography
ERK	Extracellular signal-regulated kinase
EudraCT	European union drug regulating authorities clinical trials
EYFP	Enhanced yellow fluorescent protein
FACS	Fluorescence-activated cell sorting
FAM	6-carboxyfluorescein
FAP	Fibroblast activation protein
FCS	Fœtal calf serum
FRET	Fluorescence resonance energy transfer
FSP1	Fibroblast specific protein 1
GFP	Green fluorescent protein
GSI	Gamma secretase inhibitor
GTP	Guanosine-5'-triphosphate
Gy	Gray
H3	Histone 3
HBSS	Hank's buffered salt solution
HBV	Hepatitis B virus
H&E	Hematoxylin and eosin
HER	Human epidermal receptor
HES1	Hairy enhancer of split 1
HGF	Hepatocyte growth factor
HIF1α	Hypoxia inducible factor 1 alpha

HPLC	High-performance liquid chromatography
HPV	Human papilloma virus
HRE	Hormone response elements
HRP	Horserardish peroxydase
Hsp90	Heat shock protein 90
IAP	Inhibitor of apoptosis protein
ID	Identification
IFN	Interferon
IGF	Insulin-like growth factor
IGFBP	Insulin-like growth factor-binding protein
IgG	Immunoglobulin G
IκB	Inhibitor of kappa B
IKK	Inhibitor of kappa B kinase
IL	Interleukin
IL-1R	Interleukin 1 receptor
IPI	International protein index
IPMN	Intraductal papillary mucinous neoplasm
JNK	c-Jun N-terminal kinase
kDa	Kilo daltons
KM	Lysine mutant
LC-MS/MS	Liquid chromatography - Mass spectrometry/Mass spectrometry
LDS	Lithium dodecyl sulfate
LN	Lymph node
LoxP	Locus of crossing-over P1
LPS	Lipopolysaccharide
LSL	*loxP* - STOP - *loxP*

MAPK	Mitogen-activated protein kinase
MCN	Mucinous cystic neoplasm
Mf	Macrophages
MHC	Mouse histocompatibility antigene
MMLV-RT	Moloney murine leukaemia virus reverse transcriptase
MMP	Matrix metalloproteinase
MOI	Multiplicity of infection
MOPS	3-(N-morpholino)propanesulfonic acid
MRCP	Magnetic resonant cholangio-pancreatography
MRI	Magnetic resonance imaging
mRNA	Messenger ribonucleic acid
MSCT	Multi-slice computed tomography
MSK	Mitogen- and stress-activated protein kinase
MV	Megavolts
NEB	New England BioLabs
NEMO	NF-κB essential modulator
Nf	Neutrophils
NF-κB	Nuclear factor kappa-light-chain-enhancer of activated B cells
NICD	Notch intracellular domain
NK	Natural killers
NLK	NEMO-like kinase
OD	Optical density
PAMP	Pathogen-associated molecule patterns
PanIN	Pancreatic intraepithelial neoplasia lesions
PBL	Peripheral blood leukocytes
PBS	Phosphate buffered saline

PBS/T	Phosphate buffered saline with Tween
PCNA	Proliferating cell nuclear antigen
PD	Peritoneal disease
PDAC	Pancreatic ductal adenocarcinoma
Pdx1	Pancreatic and duodenal homeobox 1
PE	Phycoerythrin
PE-Cy5	Phycoerythrin-cyanine dye 5
PG	Prostaglandin
PGJ2	Prostaglandin J2
PI3K	Phosphatidylinositol 3-kinase
Poly(I:C)	Polyinosinic:polycytidylic acid
PP	Pancreatic polypeptide
PPAR-γ	Peroxisome proliferator-activated receptor gamma
ppm	Parts per million
PVDF	Polyvinylidene fluoride
qRT-PCR	Quantitative real-time polymerase chain reaction
RANK	Receptor activator of NF-κB
RAS	Rat sarcoma
RBPjκ	Recombining binding protein suppressor of hairless
RIP	Rat insulin promoter
RNA	Ribonucleic acid
RNAi	Ribonucleic acid interference
rpm	Revolutions per minute
rTNF-α	Recombinant tumour necrosis factor alpha
SAv-HRP	Streptavin-horseradish peroxidase
SD	Standard deviation

SDS	Sodium dodecyl sulfate
SDS-PAGE	Sodium dodecyl sulfate polyacrylamide gel electrophoresis
shRNA	Short hairpin ribonucleic acid
siRNA	Short interference ribonucleic acid
α-SMA	Alpha smooth muscle actin
SOX	Sry-related HMG box
STAT3	Signal transducer and activator of transcription 3
T	T cells
TACE	Tumour necrosis factor alpha converting enzyme
TAE	Tris base, acetic acid and EDTA buffer
TAMs	Tumour associated macrophages
TAMRA	Tetramethylrhodamine
TBS	Tris buffered saline
TBS/T	Tris buffered saline with Tween
TEMED	Tetramethylethylenediamine
TGF-β	Transforming growth factor beta
TIMP	Tissue inhibitor of metalloproteinases
TLR	Toll-like receptors
TMB	3,3',5,5'- tetramethylbenzidine
TP53	Tumour protein 53
TPA	12-0-tetradecanoyl-phorbol-13-acetate
TRAF	TNF receptor associated factor
TZD	Thiazolidinedione
TNF-α	Tumour necrosis factor alpha
UK	United Kingdom
USA	United States of America

V	Volts
VEGF	Vascular endothelial growth factor

CHAPTER ONE: INTRODUCTION

1.1 Cancer and inflammation

1.1.1 Cancer

The latest statistical figures show a decrease in cancer incidence and death rates in the United States in 2008. This has been achieved after many years of research, improved diagnostic and treatment options, further understanding of the mechanisms and better prevention and screening throughout the populations. In this same year, cancer accounted for 14 % of all deaths worldwide. Lung, breast and colorectal cancers are the most commonly diagnosed whereas lung, stomach, liver and pancreatic cancers remain the most lethal (Ferlay *et al.,* 2010).

Cancer is a multifactorial disease characterised by an uncontrolled division of cells and the ability of these to spread, either by direct growth into adjacent tissues through invasion, or by migration into distant sites, also called metastasis. Cancer initiation is due to genetic alterations that can be induced by external factors, such as chemicals, or internal factors, such as spontaneous mutations or recombination events, leading to the deregulation of critical pathways such as cell proliferation and cell death.

The most common genetic alterations found in cancers are activating mutations within proto-oncogenes or loss of function mutations within genes encoding for tumour suppressor proteins (Mathers 2007). Conversion of proto-oncogenes into oncogenes can be due to point mutations, which lead to a constitutively active protein (such as KRAS versus $KRAS^{G12D}$) (O'Hagan and Heyer 2011) or it can result from chromosomal translocations, which usually modify the regulation of the gene expression or create new fusion proteins. The chromosomal translocation between

chromosomes 22 and 9 in humans is commonly found in patients with chronic myelogenous leukaemia and results in the production of the BCR-ABL fusion protein (Druker 2008).

Most tumour suppressor genes encode proteins involved in the regulation of cell proliferation, inhibiting directly or not the progression of the cell cycle following DNA damage and/or stress signals (Sherr 2004). For example, loss of function of CDKN2, a cyclin-kinase inhibitor that regulates cell cycle progression, is found in various cancers (Kamb *et al.,* 1994). The tumour suppressor protein p53 is also frequently mutated in cancer, preventing its main functions of activating DNA repair and inducing growth arrest or apoptosis from occurring (Soussi and Lozano 2005).

In 2000, Hanahan and Weinberg proposed that most cancers exhibit six hallmarks, corresponding to the deregulation of six biological processes: evasion of apoptosis, sustained angiogenesis, limitless replicative potential, tissue invasion and metastasis, insensitivity to anti-growth signals and self-sufficiency in growth signals (Hanahan and Weinberg 2000) (Figure 1.1 A). However, genetic alterations alone are not sufficient to fully account for these characteristics. The role of an inflammatory microenvironment, including the role of the tumour microenvironment and its components, has been suggested as the 7th hallmark of cancer (Mantovani 2009). In 2011, Hanahan and Weinberg proposed a revised version of the hallmarks of cancer, including two new emerging hallmarks: deregulation of cellular metabolism and avoidance of immune destruction (Hanahan and Weinberg 2011) (Figure 1.1 B). Two enabling characteristics have also been added as they facilitate the emergence of the hallmarks of cancer mentioned above: genome instability and tumour-promoting inflammation (Hanahan and Weinberg 2011) (Figure 1.1 B).

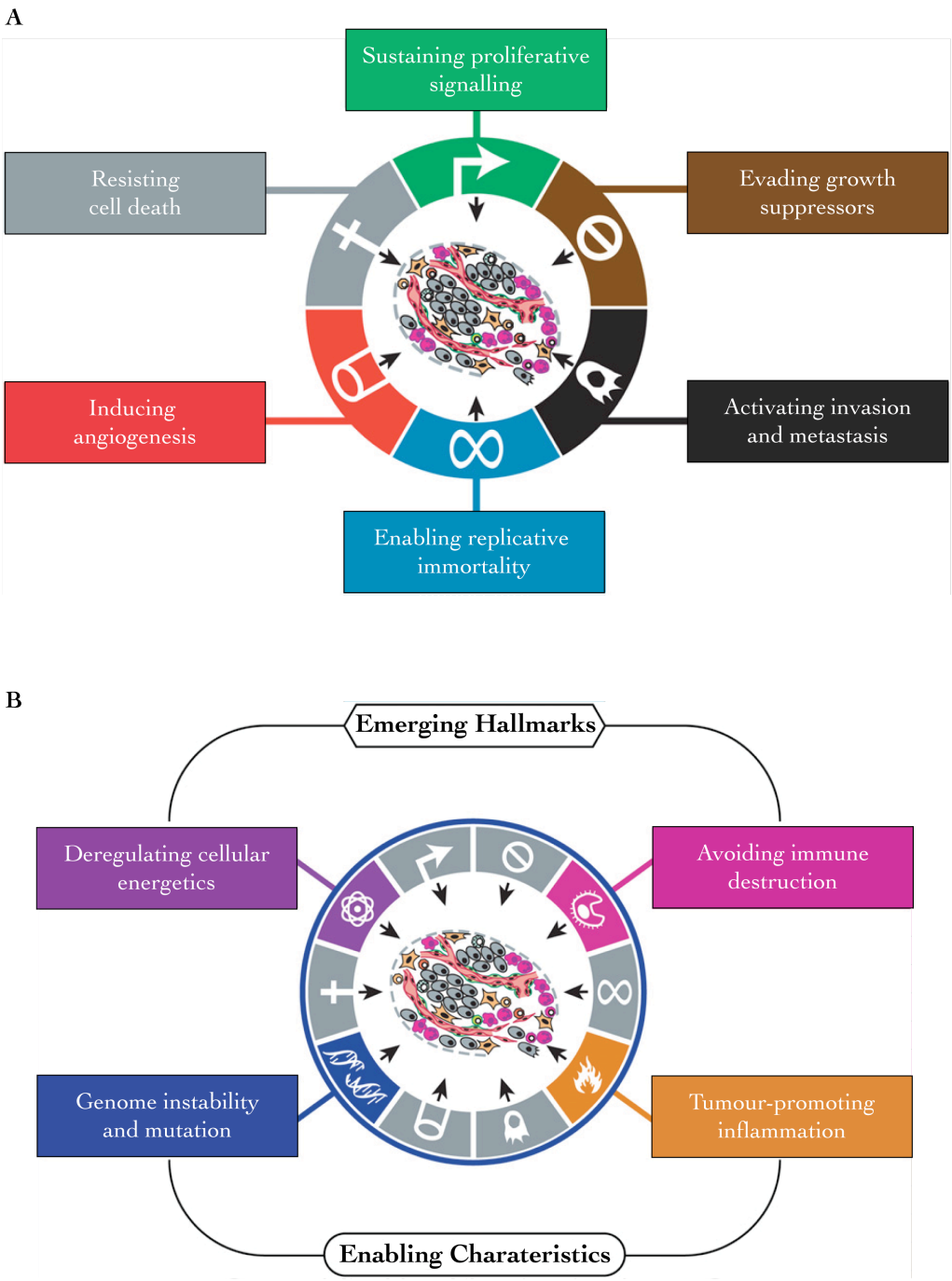

Figure 1.1: Hallmarks of cancer

The diagrams represent the hallmarks of cancer described by Hanahan and Weinberg. (A) The six original hallmarks of cancer were evasion of apoptosis, tissue invasion and metastasis, insensitivity to growth inhibitors, self-sufficiency in growth signals, limitless replicative potential and sustained angiogenesis. (B) The revised version of these hallmarks includes two new emerging hallmarks: deregulation of cellular metabolism and avoidance of immune destruction and two enabling characteristics: genome instability and tumour-promoting inflammation (Hanahan and Weinberg 2011). Adapted from (Hanahan and Weinberg 2011).

1.1.2 Inflammation

Following tissue injury (physical, chemical or microbiological), inflammation is the first response mediated by many molecules and the influx of innate immune cells. This non-specific response is usually temporary, and lasts until its resolution: the repair of the damaged tissue. Macrophages and neutrophils are the main players involved during the acute phase. Tissue-resident innate immune cells are activated and secrete a cascade of signalling molecules (mainly cytokines and chemokines) to recruit more innate immune cells, such as monocytes and neutrophils, until resolution. If the inflammation process occurs in a tissue capable of regeneration, tissue damage will be negligible. However, if the tissue is unable to regenerate, the resolution of inflammation will be associated with scarring and fibrosis (Stramer *et al.,* 2007). If the injury is persistent, or if the acute phase is dysregulated, this short-term response can lead to chronic inflammation (Philip *et al.,* 2004).

This failure of resolution of inflammation has been associated with cancer and tumours were once described as wounds that do not heal (Dvorak 1986). It is now well established and accepted that inflammation can be a promoter of malignancy (Balkwill and Mantovani 2001; Hanahan and Weinberg 2011).

1.1.3 Links between inflammation and cancer

Cancer-related inflammation was first observed and implied by Rudolph Virchow in 1864 (Virchow 1864). Since then, it has been suggested that chronic inflammation can promote cancer initiation and that inflammatory cells are recruited by the cancer cells to support tumour growth and progression (Aggarwal *et al.,* 2006; Balkwill and Mantovani 2001; Balkwill *et al.,* 2005; Coussens and Werb 2002; Kuper *et al.,* 2000; Mantovani *et al.,* 2008; Rakoff-Nahoum 2006). Inflammation is now considered as an

enabling characteristic facilitating malignant growth (Figure 1.1 B) (Hanahan and Weinberg 2011).

This link is also supported by epidemiological data, where 20 % of all cancers are due to infectious agents (Hausen 2006). For example, chronic inflammation induced by *Helicobacter pylori* infection increases the risk of gastric cancer (Zabaleta 2012). Other infectious agents such as viruses also play a role in carcinogenesis. For example, persistent infection with human papilloma virus (HPV) induces the expression of the E6 and E7 viral proteins, which can inactivate tumour suppressor proteins such as p53 and therefore support constant cell proliferation. 95 % of cervix cancers are due to HPV infection (Saha *et al.,* 2010). Epstein-Barr virus (EBV) and hepatitis B virus (HBV) infections are often associated with lymphoma and hepatocellular carcinoma respectively. Integration of the HBV DNA into the host DNA can induce transformation of the cells via genetic alterations such as amplification, deletion, translocation or duplication, further affecting different signalling pathways (Saha *et al.,* 2010).

The table below summarises and illustrates the cause-effect relationship between chronic inflammation and cancer in different clinical situations (Table 1.1).

Inflammatory agent	Inflammatory stimulus	Associated malignancy
Pathogen	Human papilloma virus	Cervix cancer
Pathogen	Hepatitis B and C viruses	Liver cancer
Pathogen	*Helicobacter pylori*	Gastric cancer
Chemicals	Abestos, silica, cigarette smoke, talc	Bronchial cancer, mesothelioma, ovarian cancer, pancreatic cancer
Autoimmune disease	Inflammatory bowel disease	Colorectal cancer
Inflammatory conditions	Pancreatitis, type II diabetes mellitus	Pancreatic cancer
Inflammatory conditions	Prostatitis	Prostate cancer
Inflammatory conditions	Thyroiditis	Thyroid cancer

Table 1.1: The relationship between chronic inflammation and cancer

Table describes some examples of inflammatory agents and stimuli associated with malignant diseases. Adapted from (Balkwill and Mantovani 2001; Porta *et al.,* 2011).

Two pathways have been described to explain the link between inflammation and cancer: the intrinsic and the extrinsic pathways (Mantovani *et al.,* 2008) (Figure 1.2). The intrinsic pathway occurs downstream of genetic events such as oncogene activation or loss of tumour suppressors, whereas the extrinsic pathway is activated in the context of infections or inflammatory conditions. In both cases, a variety of inflammatory mediators are produced and the inflammatory response is activated and regulated through transcription factors such as nuclear factor κB (NF-κB), hypoxia inducible factor 1 alpha (HIF1α) and signal transducer and activator of transcription 3 (STAT3). Activation of the pathways associated with these transcription factors in tumour cells leads to increased secretion of cytokines and chemokines, allowing the recruitment of immune cells such as macrophages and neutrophils. This cytokine rich milieu activates inflammatory pathways in these cells as well as in the stroma, therefore generating a positive feedback loop, "fuelling" the inflammation process and response.

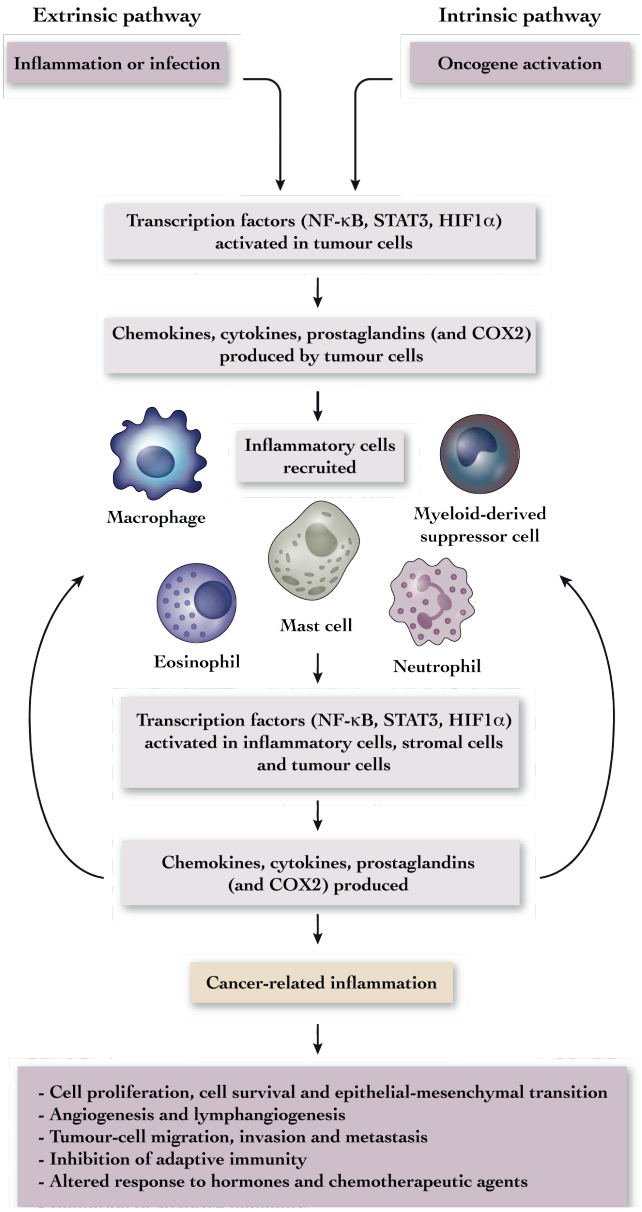

Figure 1.2: Extrinsic and intrinsic pathways linking inflammation and cancer

Two pathways are involved in the connection between inflammation and cancer: the extrinsic pathway, with an inflammatory origin such as infections; and the intrinsic pathway, usually triggered by oncogene activations. In both cases, inflammatory pathways are activated (NF-κB, HIF1α and STAT3) and inflammatory mediators are released to recruit and activate immune cells. The positive feedback loop generated creates a cancer-related inflammatory microenvironment. Adapted from (Mantovani *et al.*, 2008).

Triggers involved in these inflammatory signalling pathways are pattern recognition receptors [mainly Toll-like receptors (TLR) recognising pathogen-associated molecular patterns (PAMP)], cytokines, cycloxygenase-2 (COX2) (involved in the synthesis of lipid inflammatory mediators such as prostaglandin), the transcription

factor NF-κB (discussed in more details in section 1.3), oxidative stress (leading to the production of reactive oxygen species and inducing DNA damage) and finally hypoxia inducible factors (HIF) that regulate pathways according to the oxygen levels (Balkwill and Mantovani 2001; Porta *et al.,* 2011). The combination of these factors contributes to the creation of a cancer-related inflammatory microenvironment.

Overall, any type of inflammation appears to predispose to cancer development as for pancreatitis and pancreatic cancer (Greer and Whitcomb 2009). It has been demonstrated that both intrinsic (*kras* mutation) and extrinsic (pancreatitis) inflammation could accelerate the initiation and progression of pancreatic ductal adenocarcinoma (Morris *et al.,* 2010b).

1.1.4 Tumour microenvironment

The important role of the tumour microenvironment for tumour progression and metastasis was first proposed by Dr Stephen Paget (Paget 1989). He hypothesised that cancer cells could be assimilated as "seeds" that required the appropriate environment ("soil") to proliferate. This "seed and soil" hypothesis is still topical and the microenvironment is now considered as a therapeutic target (Albini and Sporn 2007). The tumour microenvironment, also called the stroma, is composed of an extracellular matrix and a non-malignant cell compartment of fibroblasts, immune cells and blood vessels surrounding the tumour. Its role in tumour progression and angiogenesis involves crosstalk with the tumour cells (Figure 1.3).

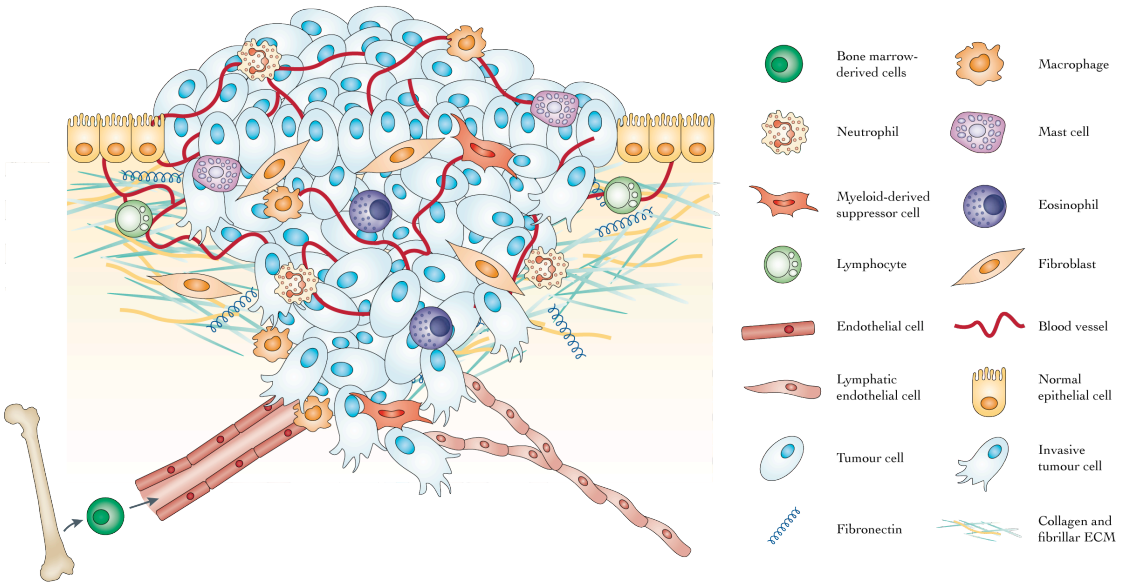

Figure 1.3: The tumour microenvironment

Tumour cells are surrounded by a rich and dense stroma composed of an extracellular matrix (ECM), fibroblasts, immune cells, blood and lymphatic vessels. Bone marrow-derived cells are the precursors for the circulating immune cells, which can be recruited by the tumour cells to support tumour growth. Adapted from (Joyce and Pollard 2009; Kalluri and Zeisberg 2006).

The tumour microenvironment evolves and is shaped by the cancer cells in a process that mimics wound healing in normal homeostasis. Such remodelling involves the secretion of mediators such as cytokines, chemokines and growth factors by the cancer cells to activate other signalling pathways in an autocrine and/or paracrine manner. These signals lead to constant stimulation of cell proliferation, mobility or invasion, which contribute to the generation of a supporting environment for tumour growth, progression and metastasis (Pietras and Ostman 2010). The main growth factors which control the composition of the stroma are hepatocyte growth factor (HGF), insulin-like growth factor (IGF), epidermal growth factor (EGF) and transforming growth factor beta (TGF-β). This dynamic process is constantly amplified over time. Moreover, hypoxic conditions develop in the core of the tumour, contributing to the activation of additional signalling pathways (Ide *et al.*, 2006; Mahadevan and Von Hoff 2007).

1.1.4.1 Extracellular matrix

The extracellular matrix (ECM) provides structural support for the different cells within the tumour microenvironment. The main components of the ECM are proteoglycans, hyaluronan and fibrous proteins such as collagen, fibronectin and fibrin (Dvorak *et al.,* 2011).

1.1.4.2 Cancer-associated fibroblasts

Fibroblasts are widely distributed in tissues and play a role in maintaining their homeostasis. Fibroblasts are highly heterogeneous and no specific markers have been described to characterise them *in vivo*, although fibroblast specific protein 1 (FSP1) is believed to be an accurate marker (Kalluri and Zeisberg 2006) (Table 1.2).

Marker	Function	Located on fibroblast type	Located on other cell types
Vimentin	Intermediate filament associated protein	Miscellaneous	Endothelial cells, myoepithelial cells and neurons
α-smooth muscle actin	Intermediate filament associated protein	Myofibroblasts	Vascular smooth muscle and myoepithelial cells
Desmin	Intermediate filament associated protein	Skin fibroblasts	Muscle and vascular smooth muscle cells
FSP1	Intermediate filament associated protein	Miscellaneous	Invasive carcinoma cells
FAP	Serine protease	Activated fibroblasts	Activated melanocytes
α1β1 integrin	Collagen receptor	Miscellaneous	Monocytes and endothelial cells
ProcollagenI α2	Collagen biosynthesis	Miscellaneous	Osteoblasts and chondroblasts

Table 1.2: Fibroblast markers

Table describes various fibroblast markers, detailing their function as well as expression on different fibroblast types and also on other cells (Kalluri and Zeisberg 2006).

When tissues are injured, residential fibroblasts differentiate into myofibroblasts in response to paracrine signals. These cells, considered to be an intermediate between fibroblasts and smooth muscle cells, contribute to wound healing and undergo apoptosis once the tissue is repaired (Li and Wang 2009). The induction of myofibroblasts can also cause organ fibrosis, which enhances the risk of cancer development (Desmouliere *et al.,* 2004; Radisky *et al.,* 2007). Myofibroblasts are found in the reactive tumour stroma and are also called cancer-associated fibroblasts (CAFs).

CAFs represent a very heterogeneous population in the tumour microenvironment and there is no consensus in the markers used to characterise them (Sugimoto *et al.,* 2006). Furthermore, their origin still remains elusive. CAFs may derive from multiple resident precursors such as endothelial cells, smooth muscle cells and myoepithelial cells (Tomasek *et al.,* 2002; Willis *et al.,* 2006). According to other studies, they may originate from bone marrow-derived stem cells (Brittan *et al.,* 2002; Direkze *et al.,* 2004). In this context, the circulating precursors migrate into the wound and contribute to the wound healing process.

The role of CAFs in the stroma of many different cancers is more and more topical, in particular their contribution to tumour growth and progression (Mueller and Fusenig 2004). Several studies have shown they can promote tumour neoangiogenesis (Dong *et al.,* 2004; Orimo and Weinberg 2006) or that they contribute to the provision of a suitable microenvironment for cancer cells (Koukourakis *et al.,* 2006). However, their exact role is not clearly defined and appears to be context- and tissue-dependant.

Although CAFs were originally considered as quiescent cells, they are now regarded as key players for tumour growth, angiogenesis and metastasis as they represent an important source of pro-tumorigenic signals (Kalluri and Zeisberg 2006; Ostman and Augsten 2009). They can secrete growth factors such as vascular endothelial growth factor (VEGF) and stromal cell-derived factor 1 (SDF-1/CXCL12). CXCL12 allows the recruitment of endothelial progenitor cells, thus promoting tumour neoangiogenesis (Dong *et al.,* 2004; Orimo and Weinberg 2006). In addition, it has been shown in colorectal cancer that CAFs and cancer cells have different metabolic pathways and that CAFs were able to use the toxic products generated by the cancer cells to provide and generate a suitable microenvironment for cancer cell growth and survival (Koukourakis *et al.,* 2006).

A study performed by Spaeth *et al.* demonstrated that mesenchymal stem cells present in the tumour microenvironment can differentiate into CAF-like cells (Spaeth *et al.,* 2009). This was observed in a murine xenograft model with human ovarian cancer cells combined with human mesenchymal stem cells. In the arising tumours, cells expressing CAF markers, such as fibroblast activation protein (FAP) and FSP1 (see Table 1.2), were identified and tumour growth was enhanced (Spaeth *et al.,* 2009).

In mouse models of skin, breast and pancreatic tumours, CAFs express a pro-inflammatory gene signature, which contributes to the support of tumour growth by enhancing neovascularisation and the recruitment of immune cells. These tumour-promoting effects are abolished upon inhibition of the transcription factor NF-κB, suggesting an important role in tumour progression for this inflammatory signalling pathway in stromal cells (Erez *et al.,* 2010).

As described in Table 1.2, FAP is one of the fibroblast markers and FAP^+ stromal cells have been characterised and identified in different tumour models, including Lewis lung carcinoma. FAP^+ cell population is heterogeneous, sharing mesenchymal and/or immunological markers, and represents 2 % of the tumour cells in Lewis lung carcinoma model (Kraman *et al.,* 2010). The depletion of FAP^+ cells in mice with established Lewis lung carcinoma induces necrosis and this biological process is mediated by IFN-γ and TNF-α. Cell lines derived from PDAC bearing $kras^{G12D}trp53^{R172H}$ mice (see section 1.2.8.2) have been used in a subcutaneous model and the depletion of FAP^+ cells after establishement of the tumours has also been associated with tumour regression. In these two models, FAP^+ stromal cells have been described as important mediators for immune suppression, therefore supporting tumour growth (Kraman *et al.,* 2010).

1.1.4.3 Immune cells

1.1.4.3.1 Tumour immune surveillance and immunoediting

The inflammation process triggered in response to tissue injury allows the recruitement of leukocytes attracted by the chemokines, cytokines and growth factors released by the injured cells (see section 1.1.2). The immune system can also efficiently identify and eliminate damaged or transformed cells by a process called tumour immune surveillance. The discovery of this immune reaction originates from the observation that immunodeficient mice develop more spontaneous tumours than immunocompetent animals, but also that they are more susceptible to carcinogen-induced tumour formation. A role for IFN-γ was initially identified in the tumour immune surveillance process as mice lacking IFN proteins are more susceptible to chemically-induced carcinogenesis (Dighe *et al.,* 1994; Kaplan *et al.,* 1998). In addition, mice deficient in adaptive immune cells (B cells and T cells) are also more susceptible to tumour formation (Shankaran *et al.,* 2001). A large number of studies

have been performed and have revealed that all components of the immune system are required for tumour immune surveillance and tumour suppression [reviewed in (Vesely *et al.,* 2011)].

This anti-tumour response requires tumour-specific antigens, which are recognised by tumour-specific T cell precursors. Naïve T lymphocytes present in the lymph nodes and spleen can be activated by direct presentation of these antigens by the transformed cells in the case of haematopoietic malignancies or following metastasis of solid tumours. In most cases however, presentation of tumour specific antigen to naïve T cells requires intermediate antigen presenting cells, such as dendritic cells. Once activated in the lymphoid organs, tumour specific lymphocytes migrate to the site of the transformed cells (Schreiber *et al.,* 2011). Despite this, tumours do develop, introducing the concept of immunoediting, during which the anti-tumour response fails to eliminate all the premalignant cells and under selective pressure new resistant tumour cell variants emerge, allowing tumour development (Ostrand-Rosenberg 2008; Schreiber *et al.,* 2011).

1.1.4.3.2 Tumour infiltrating immune cells

Tumour infiltrating immune cells include myeloid cells (macrophages, neutrophils, and dendritic cells) as well as lymphocytes. It is still not fully understood whether they constitute an immune response against tumour cells or whether they contribute to tumour progression. Cytotoxic T cells, T helper cells (Th1) and M1 macrophages are usually associated with anti-tumour effects, while M2 macrophages, T helper cells (Th2 and Th17) and regulatory T cells are characterised by pro-tumour activities (Fridman *et al.,* 2011). Dendritic cells are often considered as anti-cancer cell types as they are the main players for antigen presentation and T cell activation. Dendritic cell activation is the main strategy for immunotherapies. However, it has recently been

shown that upon tyrosine kinase inhibitors (known to improve the treatment of some leukaemia), dendritic cells can upregulate immune inhibitory receptors, therefore preventing T cell activation (Schwarzbich *et al.,* 2012). As illustrated with dendritic cells, these pro- and anti-tumour characteristics seem to be context-dependent due to the plasticity of immune cells and therefore vary between different tumour types.

The infiltrated cytotoxic T cells express activation markers, which are induced by tumour antigens, suggesting the effective induction of an immune response. In addition, a correlation between patient survival and infiltrated cytotoxic T cells has been shown in various different cancers, such as colorectal cancer (Dunn *et al.,* 2004).

Among T helper cells, Th17 cells can infiltrate different tumour types such as ovarian and prostate tumours and have been associated with poor prognosis in patients with hepatocellular carcinoma (Maniati *et al.,* 2010; Miyahara *et al.,* 2008; Sfanos *et al.,* 2008; Zhang *et al.,* 2009). Th2 cells are characterised by an IL-4 secretion, which despite the leukocyte recruitment this cytokine generates, it also polarises macrophages towards an M2 phenotype, known to have a tumour-promoting role (Ruffell *et al.,* 2010). However, Th1 cells are polarised by and secrete IFN, which corroborates the predominant anti-tumour role of this immune population (Johansson *et al.,* 2008).

Regulatory T cells have also been observed in various different tumours, including hepatocellular carcinoma and pancreatic adenocarcinoma. In these cancers, their presence is associated with poor prognosis (Gao *et al.,* 2007a; Hiraoka *et al.,* 2006). These cells can inhibit anti-tumour immune responses usually induced by T cells and natural killer cells (Ghiringhelli *et al.,* 2005; Shevach *et al.,* 2001).

The leukocyte infiltrate is also composed of tumour associated macrophages (TAMs), which can contribute to tumour progression (Sica 2010). Clinical studies in many different malignancies have shown that high levels of TAMs within the tumour microenvironment correlates with poor prognosis and reduced survival (Lewis and Pollard 2006). TAMs are plastic cells and are usually polarised to a tumour-promoting phenotype when recruited into the tumours, therefore facilitating tumour progression and metastasis (Hallam *et al.,* 2009; Qian and Pollard 2010). It has also been shown that the macrophage phenotype in tumours is plastic and that tissue-specific inhibition of the NF-κB signalling pathway in macrophages can restore their anti-tumour activity (Hagemann *et al.,* 2008).

Tumour cells secrete a variety of growth factors such as colony stimulating factor 1 (CSF1), and chemokines, such as CCL2, to recruit TAMs (Qian and Pollard 2010). Macrophages can have different phenotypes in response to the variety of signals present in the environment: the "classical activated " phenotype, also called M1, mainly induced in response to microbial infection and IFN-γ, and the "alternatively activated" or M2 phenotype, generated by cytokines such as IL-4 and IL-10 (Qian and Pollard 2010). This distinction between M1 and M2 phenotypes is a simplified view of the variety of phenotypes these cells can have. TAMs are often associated with an M2-like phenotype and pro-tumoural properties (Biswas and Mantovani 2010; Mantovani *et al.,* 2011).

Considering the context-specific role of each immune cell population, a balance between pro- and anti-tumour immunity is required within the tumour microenvironment. Immunotherapy is a strategy that has been used to stimulate and reactivate the host immune system to effectively fight cancer cells (Couzin-Frankel

2010; Sharma *et al.,* 2011b). As described in section 1.1.4.3.1, an anti-tumour response requires T cell activation and proliferation, which are induced after the presentation of tumour specific antigens by antigen presenting cells and the activation of costimulatory signals between the CD80 and CD86 receptors on the antigen presenting cells and the CD28 or CTLA4 ligands on the T cells (Foell *et al.,* 2007). Signalling through CTLA4 generates signals which are inhibitory to the T cells as opposed to CD28 (Krummel and Allison 1995). Ipilumimab is an anti-CTLA4 antibody which has recently shown promising anti-tumour activity and activation of T cells in patients with advanced melanoma (Fong and Small 2008; Weber *et al.,* 2011). In the context of pancreatic cancer, combination of a chemotherapeutic agent with an agonist antibody for CD40 induces tumour regression in human patients. This involves the activation of macrophages into an anti-tumour phenotype (see also section 1.2.7) (Beatty *et al.,* 2011).

1.2 Pancreatic cancer

1.2.1 Anatomy and development of the pancreas

The pancreas is an organ of the digestive system and is a mixed gland with exocrine and endocrine functions. Figure 1.4 represents its anatomy and histological characteristics.

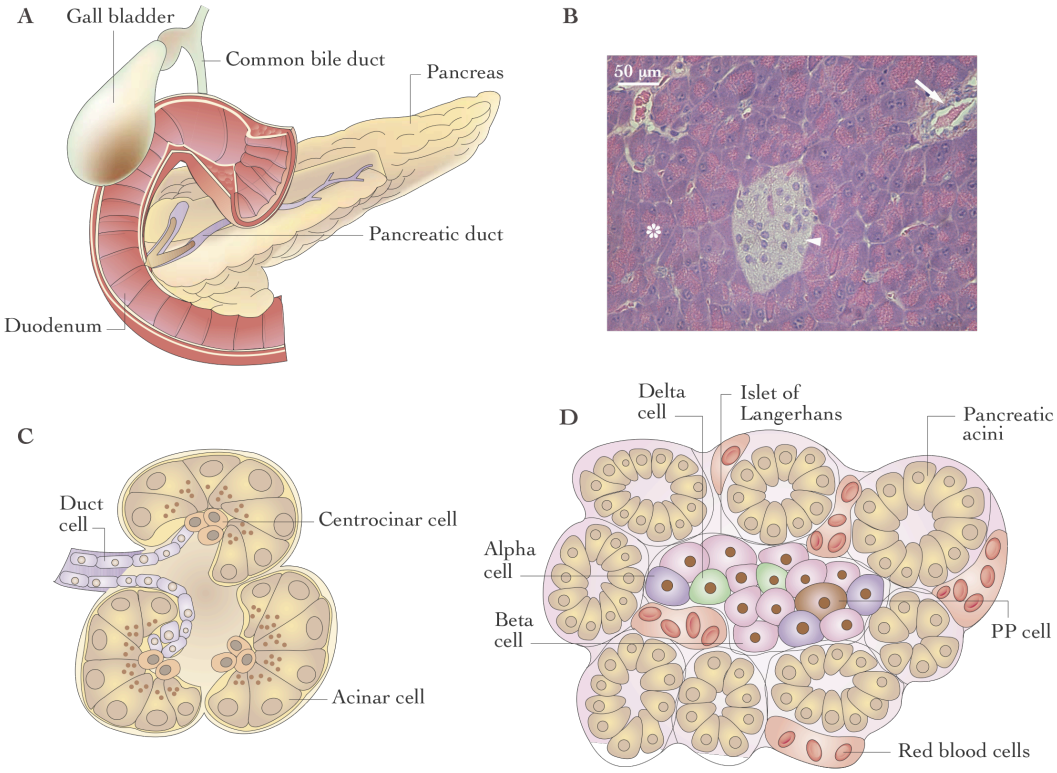

Figure 1.4: Anatomy and histology of the pancreas

(A) Gross anatomy of the pancreas. (B) Histological aspect of the pancreas with an islet of Langerhans (arrowhead), ducts (solid arrow) and acinar cells within the exocrine pancreas (asterisk). (C) Schematic representation of an acinus. (D) Schematic representation of an islet of Langerhans surrounded by exocrine pancreas. Adapted from (Bardeesy and DePinho 2002).

The exocrine pancreas, representing 80 % of the organ, is composed of acinar and duct cells that secrete a pancreatic juice containing enzymes into the small intestine for food digestion. Centroacinar cells are also present between the acinar and the duct cells. The endocrine pancreas secretes hormones into the bloodstream to regulate metabolism and glucose homeostasis (Hezel *et al.,* 2006). Clusters of

endocrine cells, also called islets of Langerhans, are composed of five different cell types, individually characterised by their specific hormone secretion (Assmann *et al.,* 2009; Herrera 2002):

- α-cells secrete glucagon to increase blood glucose levels
- β-cells produce insulin to reduce blood glucose levels
- δ-cells release somatostatin to regulate α- and β-cells
- PP cells secrete pancreatic polypeptide
- ε-cells produce ghrelin

A tight regulation of insulin and glucagon secretion is required to regulate glycaemia, as well as the uptake and release of the glucose stored into the different tissues (Quesada *et al.,* 2008).

The pancreas is endodermal in origin and its development, as well as the differentiation of cell lineages, involve various signalling pathways and transcription factors. The main one required in these processes is the Notch signalling pathway (Apelqvist *et al.,* 1999; Fujikura *et al.,* 2006; Jensen *et al.,* 2000; Lammert *et al.,* 2000; Murtaugh *et al.,* 2003).

The earliest and most important transcription factor involved at different stages of the development of this organ is the pancreatic and duodenal homeobox 1 (*Pdx1*), which can give rise to the three different cell lineages within the pancreas (duct, acinar and islet cells) (Cano *et al.,* 2007). It has been demonstrated that the expression of *Pdx1* is required at the early stages of pancreatic development, as animals lacking this transcription factor are born without a pancreas and are not viable (Jonsson *et al.,* 1994; Offield *et al.,* 1996). Inactivation of *Pdx1* at a specific time

during pancreatic development can block and prevent islet and acinar cell differentiation (Hale *et al.,* 2005). Finally, animals heterozygote for this gene have an impaired regulation of insulin secretion, showing that it also plays a role in β-cell function in the adult mouse (Brissova *et al.,* 2002). *Pdx1* is expressed in pancreatic progenitor cells, whereas in the adult tissue it is mainly found in β- and PP-cells within the endocrine compartment (Cano *et al.,* 2007). Another transcription factor, *P48*, has been described to be involved in pancreatic organogenesis (Kawaguchi *et al.,* 2002; Krapp *et al.,* 1998). The transcription factor neurogenin 3 (*Ngn3*) has also been shown to be important for endocrine development (Cano *et al.,* 2007). The development of the exocrine compartment of the pancreas depends on the expression of specific transcription factors such as *Mist1* (Johnson *et al.,* 2004; Pin *et al.,* 2000) but also on the expression of genes such as *Elastase* (Hammer *et al.,* 1987) and *Nestin* (Delacour *et al.,* 2004; Esni *et al.,* 2004).

The table below summarises the main transcription factors and genes involved in the development of the pancreas (Table 1.3).

Transcription factors or genes	Expression in the pancreas from	Cell lineages
Pdx1	E8.5	Pancreatic progenitors
P48	E9.5	Pancreatic progenitors
Ngn3	E9.5	Endocrine progenitors
Nestin	E10.5	Exocrine progenitors
Elastase	E14	Acinar cells
Mist1	E14.5	Acinar cells

Table 1.3: Transcription factors and genes expressed during pancreatic organogenesis

Table describes the transcription factors and genes expressed during the embryonic development of the pancreas, the embryonic day (E) from which they are expressed and their cell lineage specificity.

1.2.2 Incidence, mortality and survival of pancreatic cancer

Pancreatic cancer is the tenth most common cancer and the fifth leading cause of cancer-related death in the UK; it has a five-year survival rate of approximately 3 %,

the lowest among the most common cancers (Rachet *et al.,* 2009). This low survival rate is mainly due to the fact that symptoms and therefore diagnosis, occurs at a late and advanced stage, meaning that surgery is not feasible for a large majority of patients.

1.2.3 Risk factors for pancreatic cancer

The main risk factor involved in the development of pancreatic cancer is smoking, which is linked with up to 20 % of pancreatic cancers in the UK. Regular smokers have a 50 % increased risk to develop this cancer as opposed to non-smokers (Iodice *et al.,* 2008). "Passive" smoking also enhances the possibility of developing pancreatic cancer by approximately 50 % (Vrieling *et al.,* 2010).

A patient's medical history can impact upon pancreatic cancer risk. For example, patients presenting chronic pancreatitis, mainly caused by alcohol consumption (Tapia *et al.,* 2010), are more susceptible to pancreatic cancer (Malka *et al.,* 2002). However, the role of chronic pancreatitis in increasing the risk of developing pancreatic cancer is controversial and this inflammatory condition might instead be a consequence of early and non-detected pancreatic cancer (Sharma *et al.,* 2011a). A true positive association between these two conditions has been demonstrated in patients with hereditary pancreatitis (Lowenfels *et al.,* 1997; Whitcomb *et al.,* 1999). Two studies have shown that patients with type II diabetes mellitus have an increased risk of developing pancreatic cancer (Huxley *et al.,* 2005; Stolzenberg-Solomon *et al.,* 2005). This is also the case for people with type I diabetes mellitus (Stevens *et al.,* 2007). Other diseases such as gastric ulcers, ulcerative colitis, Crohn's disease, respiratory and skin allergies or other cancers were also linked to pancreatic cancer development (Bao *et al.,* 2010; Gandini *et al.,* 2005; Hemminki *et al.,* 2008, 2009; Shen *et al.,* 2006).

Other risk factors include an advanced age (8 out of 10 pancreatic cancers are diagnosed after 60 years of age), gender (men have a higher incidence rate than women) and family history when a first-degree relative is affected by pancreatic or prostate cancer (correlated with a 50 and 45 % increased risk, respectively) (Jacobs *et al.,* 2010; Permuth-Wey and Egan 2009).

A synergy between these risk factors has been demonstrated in women, in particular an interaction between cigarette smoking and family history (approximately 13 % versus 3 % when considering the risk factors individually) and between cigarette smoking and diabetes mellitus (approximately 9 % versus 3.8 % when considering the risk factors individually) (Hassan *et al.,* 2007).

1.2.4 Symptoms and diagnosis of pancreatic cancer

The symptoms for pancreatic cancer are not unique and usually appear at a late stage of the disease. The medical risk factors (acute pancreatitis or diabetes) described earlier could be considered symptoms if present at advanced stages. However, the most common symptoms are obstructive jaundice, weight loss and abdominal and/or back pain (Kalser *et al.,* 1985; Okusaka *et al.,* 2001).

Early diagnosis remains a critical challenge. Trans-abdominal ultrasound is used to detect tumours larger than 2 cm (Minniti *et al.,* 2003). Other imaging techniques can be used, such as multi-slice computed tomography (MSCT) or magnetic resonance imaging (MRI) to effectively identify pancreatic tumours (Catalano *et al.,* 2003; Lopez Hanninen *et al.,* 2002). Endoscopic retrograde cholangio-pancreatography (ERCP) is typically favoured over magnetic resonant cholangio-pancreatography (MRCP) as it offers the advantage of gaining tissue samples for diagnosis but also because inserting a biliary stent relieves obstructive jaundice (Adamek *et al.,* 2000).

Levels of carbohydrate antigen 19-9 (CA 19-9) in the blood are increased in patients with pancreatic cancer as opposed to healthy individuals and thus its measurement is also assessed (Kim *et al.,* 2004; Steinberg 1990). However, this marker is not specific for pancreatic cancer and some humans do not synthesise this protein at all (Cascinu *et al.,* 2010). Despite the lack of specificity, its measurement influences treatment decisions and patient follow-up care (Cascinu *et al.,* 2010). The identification of new potential markers in other physiological fluids such as urine or serum, which would allow earlier detection, prediction of recurrence and measurement of efficacy of treatments, is still under investigation (Brand *et al.,* 2011; Weeks *et al.,* 2008). A variety of potential serum biomarkers have been identified in patients with pancreatic cancer. Examples of these are invasion and adhesion mediators (matrix metalloproteinases MMP and tissue inhibitor of metalloproteinases TIMP), cytokines, chemokines and receptors, such as TNFRI and TNFRII, or apolipoproteins (Brand *et al.,* 2011). However, their validation as useful "true" markers needs to be awaited.

1.2.5 Treatments for pancreatic cancer

1.2.5.1 Resectable tumours

The only curative treatment for pancreatic cancer is surgical resection. If the cancer is already at an advanced stage with metastases to the peripheral organs (liver and peritoneal cavity) and/or to distant lymph nodes, the patient will not be eligible for surgical removal. Recurrence after surgery is high (90 %) and usually appears within 1 or 2 years (Kayahara *et al.,* 1993). Pancreatectomy, which could be considered as an alternative to partial surgical resection, is not recommended as unseen metastases at the time of surgery are sufficient to induce recurrence (Amikura et al., 1995; Karpoff et al., 2001).

1.2.5.2 Non resectable tumours

Patients with advanced pancreatic cancer are usually not operable and are treated with chemotherapy. Therapies for these patients are aimed at increasing survival, improving quality of life and reducing the pain associated with the different symptoms.

The nucleoside analogue gemcitabine is so far widely used for the treatment of pancreatic cancer, although with limited success. Once incorporated into the cells and phosphorylated, gemcitabine can have two different modes of action: inhibition of the synthesis of new deoxynucleosides and competition with existing deoxynucleosides for their incorporation into the newly synthesised DNA (Plunkett *et al.,* 1995). Once incorporated into the DNA strand, the repair machinery of the cell is unable to remove this analogue, leading to cell death. Patients treated with gemcitabine achieved a clinical benefit over that of 5-FU/FA (Burris *et al.,* 1997). Since then, gemcitabine is considered the "standard of care" for pancreatic cancer, even though the benefits remain minimal.

Irinotecan, a cytotoxic agent, or specific inhibitors such as marimastat (an MMP inhibitor) or tipifarnib (which inhibits farnesyltransferase, an enzyme involved in post-translational modification of RAS) did not show a clinical advantage when used alone or in combination with gemcitabine (Berlin *et al.,* 2002; Bramhall *et al.,* 2002; Rocha Lima *et al.,* 2004; Van Cutsem *et al.,* 2004). Recently, the combination of gemcitabine with erlotinib, targeting the HER1/EGFR receptor often overexpressed in pancreatic cancers (Fjallskog *et al.,* 2003; Tobita *et al.,* 2003), has shown some modest effect in improving patient survival (Moore *et al.,* 2007). The results of a phase III clinical trial showed that the overall survival of patients with pancreatic

cancer can be slightly improved (approximately 1 month) by treating them with the combination of gemcitabine and capecitabine (Xeloda® - Roche) as compared with gemcitabine alone (Cunningham *et al.,* 2009). Combination of oxaliplatin, irinotecan, fluorouracil and leucovorin (FOLFIRINOX) was used in phase II expansion trial as a first-line therapy in metastatic pancreatic cancer and compared with single agent gemcitabine. The toxicity associated with FOLFIRINOX was significantly increased, but the FOLFIRINOX combination led to significant increase in tumour response and provided a survival advantage (Conroy *et al.,* 2011).

Using a genetically engineered mouse model of pancreatic cancer, Olive *et al.* have demonstrated that phosphorylated gemcitabine (active form) is not detectable in the core of pancreatic tumours, possibly explaining the chemoresistance observed in patients. However, they have shown an improvement in gemcitabine delivery by combining it with an inhibitor of the Hedgehog signalling pathway, which is known to be activated in pancreatic cancer and to contribute to desmoplasia (Bailey *et al.,* 2008). This was demonstrated by revascularisation of the pancreatic tumours and a better response to the chemotherapeutic agent (Olive *et al.,* 2009). This inhibitor has been used in a phase I clinical trial and has proven to be safe and to provide some promising effects on patients with basal cell carcinoma or medulloblastoma (LoRusso *et al.,* 2011). However, clinical trials in pancreatic cancer using the combination of gemcitabine with this Hedgehog inhibitor have shown to be unsatisfying thus far (Olson and Hanahan 2009). This suggests that, in human patients, drug resistance might not only be due to ineffective drug delivery, as illustrated above with the efficacy of FOLFIRINOX.

Other potential mechanisms of gemcitabine resistance have been described to try to identify combination therapies. Resistance to gemcitabine in pancreatic cancer cell lines but also in lymphoma cell lines has been associated with a deficiency in the deoxycytidine kinase, or a deficiency in some nucleoside transporters on tumour cells or an increased activity of the ERK kinase (Fryer *et al.,* 2011; Galmarini *et al.,* 2004).

These pre-clinical data are encouraging for the potential development of new combinational therapies which would be able to increase the survival of pancreatic cancer patients.

1.2.6 Initiation, progression and classification of pancreatic cancer

The development of pancreatic cancer is a multifactorial and multistep process. The early stages of the disease are characterised by pancreatic intraepithelial neoplasia lesions (PanIN), which represent the main precursors of the invasive form. Morphological and genetic changes contribute to the progression from PanIN to pancreatic ductal adenocarcinoma (PDAC) (Feldmann *et al.,* 2007). A detailed chronology is shown in Figure 1.5.

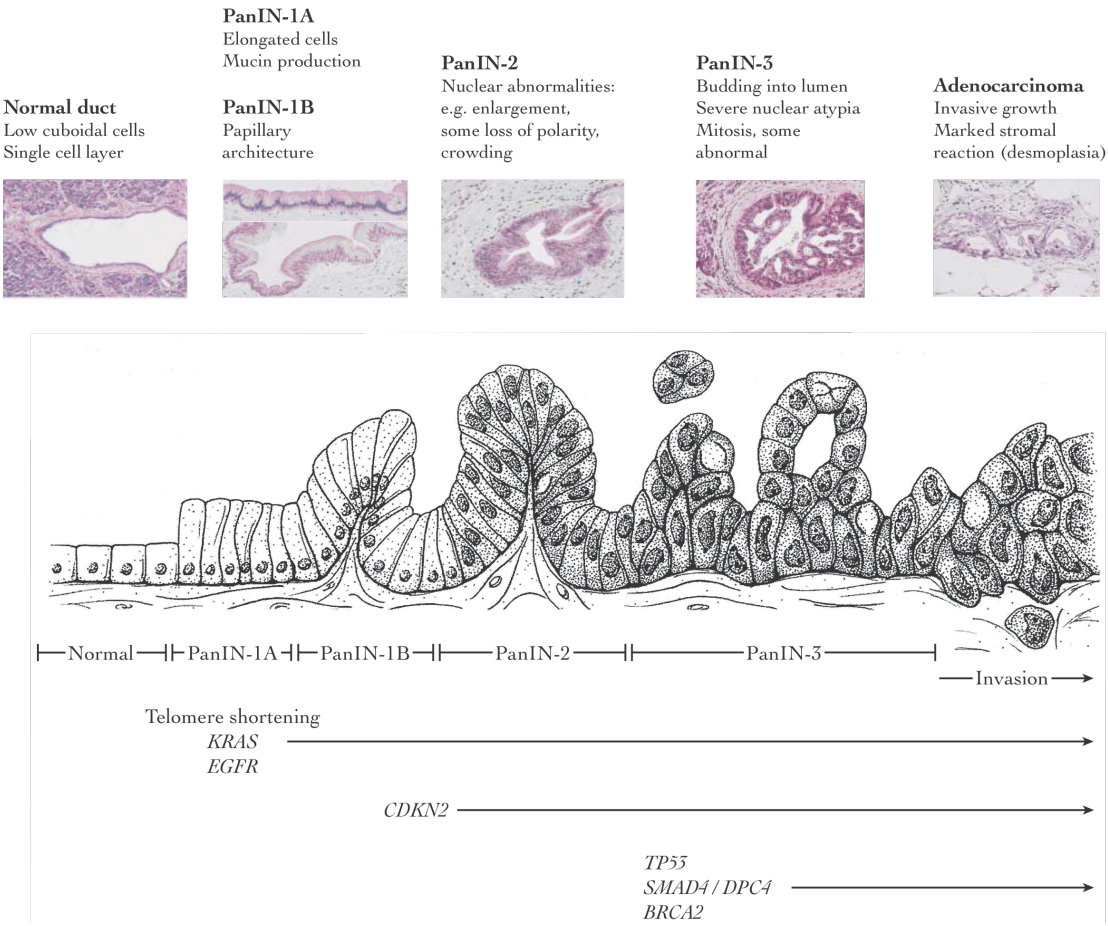

Figure 1.5: Chronology of pancreatic cancer development

It is well accepted that pancreatic cancer follows a linear development, evolving from normal cells to PanIN lesions (PanIN-1A, PanIN-1B, PanIN-2 and PanIN-3) and invasive PDAC. Each stage is characterised by morphological and genetic changes within proto-oncogenes or tumour suppressor genes. Adapted from (Bardeesy and DePinho 2002; Maitra *et al.,* 2003).

The origin of PanIN lesions has not been identified and remains under investigation (Ijichi 2011; Morris *et al.,* 2010b). Considering the characteristics of this organ, such lesions can arise from the duct cells, the acinar cells, the centroacinar cells or the endocrine cells. Using genetically engineered mouse models of pancreatic cancers, the involvement of each cell type has been tested, without providing a clear answer so far (see section 1.2.8.3).

1.2.6.1 Classification of duct lesions - morphological characteristics

PDAC can arise from three different lesions: mucinous cystic neoplasm (MCN), intraductal papillary mucinous neoplasm (IPMN) and pancreatic intraepithelial

neoplasia (PanIN) (Hezel *et al.,* 2006). Only the progression from PanIN to PDAC, which is the most common, will be presented and discussed in this section. The nomenclature used to classify the pancreatic duct lesions is now well established and each stage is well characterised (Hruban *et al.,* 2001). PanIN lesions are separated into four different stages: PanIN-1A, PanIN-1B, PanIN-2 and PanIN-3 and their morphological characteristics are summarised in Figure 1.5.

PanIN-1A lesions are characterised by elongated cells that secrete mucin. The epithelium of these lesions remains flat whereas it becomes papillary in the PanIN-1B lesions. At these stages, nuclear atypia is minimal. Low-grade dysplasia is more characteristic of the PanIN-2 stage lesions, presenting more frequent nuclear abnormalities (enlarged nuclei, hyperchromatism - excess of chromatin - and degeneration of the nuclei, increasing its staining capacity) and loss of polarity with cells no longer correctly ordered within the basement membrane. PanIN-3 lesions have high-grade dysplasia, with emphasised nuclear atypia and they also present some "budding" into the lumen. Although these lesions resemble carcinoma, they remain within the basement membrane and are not invasive. PDAC is characterised by an invasive growth beyond the basement membrane and by an important desmoplastic reaction. The stroma, mainly composed of fibroblasts and immune cells, is very dense and plays an important role in cancer progression. PDAC presents a glandular structure and different levels of cellular atypia and/or differentiation (Hezel *et al.,* 2006; Hruban *et al.,* 2001; Ottenhof *et al.,* 2009). PDAC is characterised and graded depending on the differentiation status of these glandular structures. Undifferentiated structures are more malignant and indicate a poor prognosis (Pan and Wang 2007).

1.2.6.2 Pancreatic cancer and genetics

Pancreatic tumorigenesis requires several gene mutations (gain or loss of function), usually occurring within proto-oncogenes or tumour suppressor genes affecting different pathways. Genetic analyses of different PanIN lesions from human patients have been performed. Although the genetic changes identified did not seem to appear in a specific and repetitive order in all cases, a tendency regarding some mutations occurring at earlier stages than others was identified (Hruban *et al.,* 2008). This simplified vision of a sequential order for genetic mutations is represented in Figure 1.5 and is now well accepted as the standard progression model for pancreatic cancer development. The table below summarises the genes most commonly mutated in PDAC and the frequency of these mutations (Table 1.4).

Gene	Mutation frequency (%)
KRAS	75 - 100
EGFR	70
CDKN2	80 - 95
TP53	50 - 75
SMAD4 / DPC4	55
BRCA2	7 - 10

Table 1.4: Mutations during PDAC progression

Table describes the most common genes mutated in PDAC and the frequency of mutation. Data adapted from (Yonezawa *et al.,* 2008).

According to this progression model, the main genetic changes observed in each PanIN grade lesions will be described and discussed.

The first main genetic changes occurring at the PanIN-1 stage include telomere shortening (Hong *et al.,* 2011; van Heek *et al.,* 2002) and an activating mutation in the *KRAS* proto-oncogene (DiGiuseppe *et al.,* 1994; Moskaluk *et al.,* 1997). KRAS is a GTP-binding protein and its activation and deactivation regulates many cellular

processes, such as cell growth and survival via the RAS/RAF/MAPK and PI3K/AKT effector pathways (Castellano and Downward 2011). The most frequent point mutation in *KRAS* replaces a glycine with an aspartate at the twelfth codon ($KRAS^{G12D}$) which generates a constitutively active protein leading to constant cell proliferation. Expression of the $KRAS^{G12D}$ mutant protein is associated with an upregulation of epidermal growth factor (EGF) (Watanabe *et al.,* 1996) and overexpression of EGF receptor (EGFR) has been detected in early PanIN-1 pancreatic lesions (Day *et al.,* 1996). Activating mutations in this tyrosine kinase receptor have also been described and its expression is associated with enhanced tumour aggressiveness and poor survival (Friess *et al.,* 1999; Kwak *et al.,* 2006). Activation of this growth factor receptor controls, via various downstream signalling pathways, many cellular processes such as cell migration, adhesion and proliferation (Oliveira-Cunha *et al.,* 2011).

Inactivating mutations of the tumour suppressor *CDKN2* (coding for the p16 protein) are detected in PanIN lesions in PanIN-2 stage disease (Moskaluk *et al.,* 1997). This protein negatively regulates cell cycle and alteration of the gene encoding this protein leads to uncontrolled cell proliferation (Romagosa *et al.,* 2011).

In PanIN-3 lesions, two other tumour suppressor genes are inactivated: *SMAD4*/*DCP4* and *TP53* (Luttges *et al.,* 2001; Wilentz *et al.,* 2000). Inactivation or loss of expression of these proteins contributes further to PanIN progression. The main roles of the p53 transcription factor are to block cell cycle progression or to induce apoptosis in response to stress signals (Suzuki and Matsubara 2011). SMAD4 is also a transcription factor and is activated by the transforming growth factor beta (TGF-β) signalling pathway (Massague *et al.,* 2005). Inactivation of the wild type

BRCA2 allele is also a late event in pancreatic cancer progression (Goggins *et al.,* 2000). *BRCA2* is a tumour suppressor gene encoding for a protein mainly involved in the repair of DNA double strand breaks. Mutations in this gene were first associated with an increased risk of developing breast cancer but are now related to many different cancers (Yoshida and Miki 2004).

1.2.7 The stroma in pancreatic cancer

One of the characteristics of pancreatic adenocarcinoma is the presence of a rich and dense desmoplasia (stroma with fibrous and connective tissue), which can account for up to 90 % of the tumour mass (Neesse *et al.,* 2010). As described in section 1.1.4, the tumour microenvironment contributes to cancer development and invasion in different types of cancer, and this also applies to pancreatic adenocarcinoma.

In pancreatic adenocarcinoma, the stroma is mainly composed of fibroblasts, pancreatic stellate cells, endothelial cells and macrophages (Farrow *et al.,* 2008). Pancreatic stellate cells are similar to myofibroblasts in that they express smooth muscle actin (α-SMA) when activated, but they also express additional specific markers such as desmin. Once activated by the pancreatic cancer cells, these cells secrete high levels of ECM components such as collagen, therefore playing a critical role in the development of the pancreatic tumour stroma (Apte *et al.,* 2004; Farrow *et al.,* 2008; Hwang *et al.,* 2008). Pancreatic stellate cells can promote pancreatic cancer progression; their co-injection with pancreatic cancer cells in an orthotopic mouse model is associated with an increased tumour growth and metastasis, as well as a reduction in the efficacy of the chemotherapy treatment (Hwang *et al.,* 2008).

Gene expression profiling has been used to identify potential genes involved in tumour-stroma interactions by co-culturing pancreatic cancer cells with stromal

fibroblasts. Interestingly, the *Cox-2* gene was overexpressed in both cell types and the pancreatic cancer cells had an increased invasive potential, which could be suppressed using a COX-2 inhibitor (Sato *et al.,* 2004). As mentioned in section 1.1.3, this enzyme contributes to the generation of a more inflamed microenvironment.

Clark *et al.* studied the immune response in the spontaneous *kras*^{G12D} mouse model of pancreatic cancer (see section 1.2.8.2 for a detailed description of this mouse model) and showed that leukocyte infiltration in the stroma increased during pancreatic cancer progression from PanIN to PDAC stage. They further analysed the leukocyte populations and found that T cells did not have an activated phenotype, excluding the presence of an immune T cell response during pancreatic cancer progression in this model. Furthermore, macrophages were able to infiltrate the surrounding stroma from the early stages of the disease and were still present at the PDAC stage. These data indicate that the anti-tumour immune response, usually initiated by T cells, may not exist in this context. In addition, tumour-promoting and immunosuppressive cells, such as macrophages, were recruited from the early events of pancreatic carcinogenesis, demonstrating their important role in the stroma during cancer progression (Clark *et al.,* 2007). Another study revealed that macrophages in the pancreatic stroma express angiogenic factors and can therefore contribute to tumour development-supporting angiogenesis (Esposito *et al.,* 2004).

More recently, in a spontaneous mouse model of pancreatic cancer (see section 1.2.8 for a detailed description of *in vivo* models), Ijichi *et al.* showed that pancreatic cancer epithelial cells secrete high levels of CXC chemokines. These chemokines induce the secretion of connective tissue growth factor by the surrounding fibroblasts and accelerate tumour progression. They identified the CXCR2 receptor as being

important in this tumour-stroma interaction and its inhibition *in vivo* reduces tumour progression and angiogenesis (Ijichi *et al.,* 2011).

The density of the surrounding stroma has proven to be an obstacle for the efficient delivery of chemotherapeutic drugs, in particular due to the absence of an effective blood vessel network (Olive *et al.,* 2009). Therefore, targeting the tumour microenvironment, at least in the context of pancreatic cancer, seems to be a novel approach to assist the current treatments.

Paracrine Hedgehog signalling from neoplastic cells to stromal cells has been shown to promote desmoplasia in pancreatic carcinogenesis (Bailey *et al.,* 2008). Olive *et al.* have demonstrated that treating pancreatic cancer bearing $kras^{G12D}trp53^{R172H}$ mice with an inhibitor of the Hedgehog signalling pathway can deplete the desmoplastic stroma, and that this process was associated with revascularisation of the core of the tumour and thus improvement of drug delivery (Olive *et al.,* 2009).

The activation of the CD40 receptor has been shown to be critical for T cell-dependent anti-tumour immune response (Vonderheide 2007). Moreover, it was suggested that such an anti-tumour immune response might be absent in the context of pancreatic cancer (Clark *et al.,* 2007). Recently, a study combining gemcitabine and an agonist antibody for CD40 led to pancreatic tumour regression, both in mice and humans (Beatty *et al.,* 2011). Surprisingly, when deciphering the mechanisms involved, they showed that macrophages, and not T cells, responded to CD40 activation and that once activated, these macrophages had an anti-tumour phenotype and could not only infiltrate the tumour, but could also participate in a stromal depletion reaction (Beatty *et al.,* 2011).

Several clinical trials for stromal depletion compounds (alone or in combination with chemotherapeutic agents) have been launched, especially with the Hedgehog inhibitor described earlier in section 1.2.5.2 (Garber 2010; LoRusso *et al.,* 2011; Neesse *et al.,* 2010). Combining existing treatments with molecules targeting the tumour microenvironment is a promising strategy for the treatment of pancreatic cancer. The current treatments available for patients with pancreatic cancer are discussed in section 1.2.5.

1.2.8 *In vivo* models

1.2.8.1 Cre-lox system

The *Cre-lox* system is derived from the P1 bacteriophage and was rapidly identified as a very powerful tool to excise specific portions of DNA flanked by two *loxP* sites in both prokaryotic cells (Sauer 1987) and eukaryotic cells (Sauer and Henderson 1988). This system has also been applied *in vivo* to specifically delete DNA sequences in selected cell types of transgenic animals (Gu *et al.,* 1994; Orban *et al.,* 1992). This technology is widely used throughout the world to help understand the function of genes in specific cell types and conditions, without facing the main problem encountered with loss-of-function animal models: lethal phenotypes. Once the experimental difficulties of inserting the *loxP* sites into the genome by homologous recombination and maintaining a functional gene have been overcome, conditional gene knockout animals are relatively straightforward to generate. However, in these models, due to the variability of the expression of CRE recombinase, genetic deletion is often incomplete and tissues contain cells expressing the wild type allele and cells deleted for the gene of interest (Schulz *et al.,* 2007). This can be disadvantageous when gene and protein function analyses are performed. However, the mosaic therefore created in the tissue represents a positive aspect to study cancer development in mice as cancers arise from spontaneous and/or random genetic

alterations (see section 1.1.1). Another limitation with the C*re-lox* system is the impossibility to control temporal gene expression as opposed to spatial expression. Genes can have multiple known and/or unknown functions in different tissues but also at different stages of the development process. The use of inducible systems has been presented as one possible tool to be able to control when and where recombination events will occur. The tamoxifen inducible system is one of them. In this model, a mutant of the ligand-binding domain of the human oestrogen receptor (ER) is fused with CRE recombinase (Danielian *et al.,* 1993; Metzger *et al.,* 1995). This protein fusion retains the recombinase in the cytosol complexed with Hsp90 until tamoxifen administration (an antagonist of the ER) releases this inhibition, allowing its translocation to the nucleus, thus permitting inducible recombination of *loxP* sites (Mattioni *et al.,* 1994). However, the main disadvantage observed with inducible promoters is the detection of CRE recombinase activity in absence of tamoxifen (leakage), which in mouse models of cancer for example allows disease initiation and slower progression (Strachan and Read 1999).

The *Cre-lox* system is not only used to knockout gene expression but also to turn on the expression of a foreign or mutant gene, by removing an upstream STOP cassette (Figure 1.6).

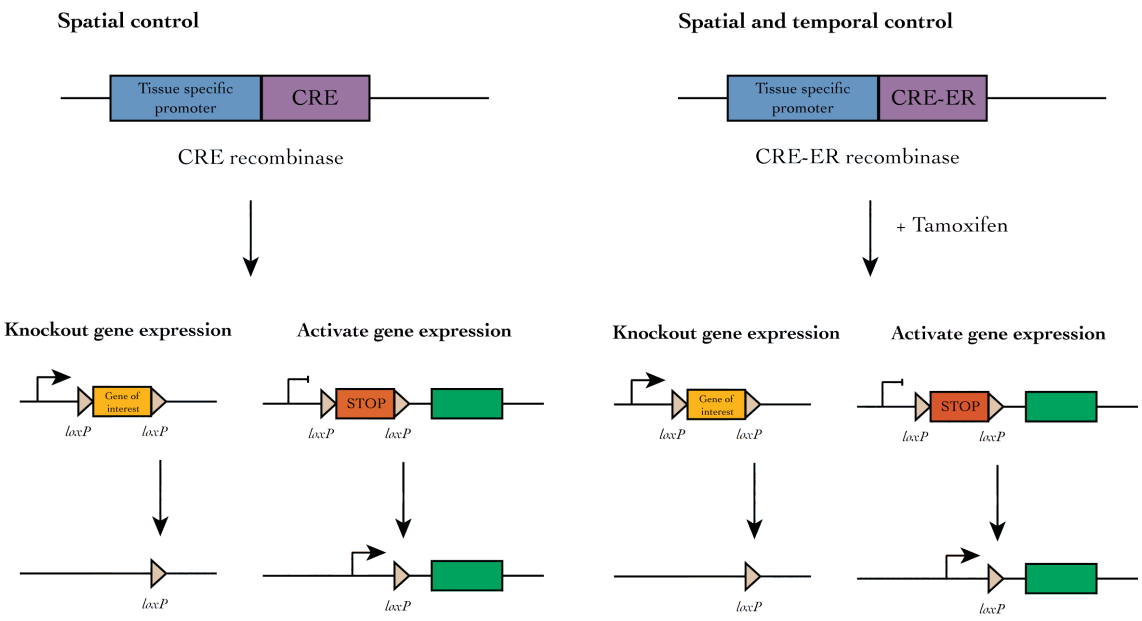

Figure 1.6: *Cre-lox* system

The *Cre-lox* technology allows the knockout of gene expression in a specific tissue when the recombinase CRE is expressed under the control of a tissue specific promoter. This constitutive model can become inducible following the expression of the CRE-ER protein fusion and its translocation to the nucleus upon tamoxifen administration.

1.2.8.2 Modelling pancreatic cancer - kras^{G12D} mouse model

Considering the genetic changes involved and required during pancreatic cancer progression but also the morphological and histological characteristics of the different PanIN lesions (see section 1.2.6), a progression model for human pancreatic cancer has been suggested (Figure 1.5). To better understand the molecular processes operating during pancreatic cancer development and to overcome the limitations encountered with orthotopic mouse studies, genetic mouse models were developed.

A wide range of genetically engineered mouse models modelling human pancreatic cancer have been generated. The first genetic mouse model that fully recapitulated human pancreatic cancer progression, from PanIN lesions to invasive carcinoma, was the *kras*^{G12D} mouse model, created by Dr David Tuveson (Cancer Research UK

Cambridge Research Institute, Cambridge, UK) (Hingorani *et al.,* 2003). This model harbours a *kraʃ* mutation, which is the most frequent genetic alteration in this disease and is considered an early event in pancreatic carcinogenesis (as described in section 1.2.6.2). This model, described below in Figure 1.7, has kindly been provided by Dr David Tuveson and used in the research detailed in this thesis. In this mouse model, two genetic modifications have been introduced (Hingorani *et al.,* 2003):

- expression of the mutated *kraʃ*$^{LSL\text{-}G12D}$ gene, controlled by a STOP cassette flanked by two *loxP* sites (l*oxP*-STOP-*loxP* cassette - LSL).
- *Cre* expression, allowing recombination between the *loxP* sites and removal of the STOP cassette, under the control of the pancreas specific promoter: *Pðx1*.

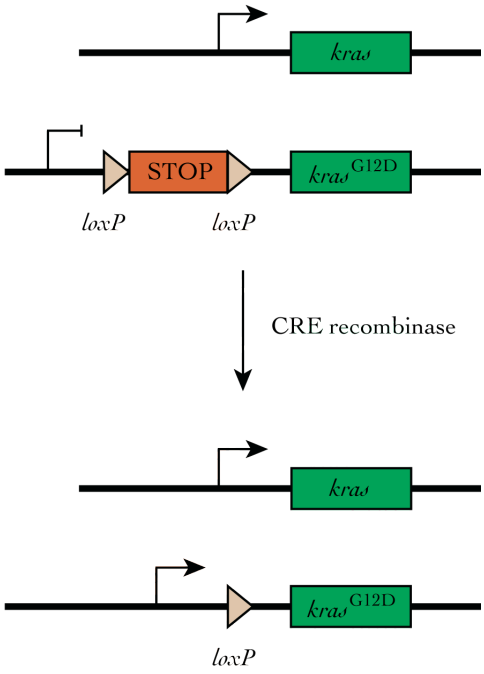

Figure 1.7: Conditional expression of *kraʃ*$^{LSL\text{-}G12D}$ allele

A l*oxP*-STOP-*loxP* cassette upstream of the *kraʃ*$^{LSL\text{-}G12D}$ allele allows its expression upon CRE-recombination only.

As explained in section 1.2.1, *Pðx1* is initially expressed in pancreatic progenitors and later in the adult pancreas. KRAS^{G12D} production therefore followed the same temporal pattern and can be modulated to induce duct-lesion formation in the murine pancreas. In these genetically engineered mice, PanIN development occurs in all

animals from 2 months of age onwards while progression towards the invasive carcinoma is observed in only 10 % of the mice and from 12 months of age onwards (Hingorani *et al.,* 2003). Mutant *kras* has been shown to be sufficient to induce cell transformation, but additional genetic mutations are usually required to allow complete cancer progression (Grippo *et al.,* 2003; Hingorani *et al.,* 2005; Tuveson *et al.,* 2004). This mouse model clearly confirms that mutated *kras* is sufficient to initiate PanIN development and is therefore a very useful tool to study pancreatic cancer initiation and progression in a molecular context similar to the human disease.

Previous mouse models resulted in acinar cell carcinoma and did not recapitulate the stepwise progression observed in humans. This was mainly due to the fact that the oncogene was expressed consitutively and at higher levels in transgenic models (Brembeck *et al.,* 2003; Grippo *et al.,* 2003; Ornitz *et al.,* 1987; Quaife *et al.,* 1987). However, in the $kras^{G12D}$ model, mutated *kras* is expressed at endogenous levels using the native *Pdx1* promoter, mimicking the spontaneous activation of this oncogene in humans. However, low penetrance was observed following the reduced frequency in the expression of the *kras* mutated gene (O'Hagan and Heyer 2011).

To study and/or test inhibitors or new therapeutic strategies, mouse models harbouring additional mutations were introduced as PDAC development occurs faster and more frequently (Hingorani *et al.,* 2005).

1.2.8.3 Other mouse models of pancreatic cancer

Since the creation of the mosaic $kras^{G12D}$ mouse model in 2003, similar genetic approaches have led to the development and creation of additional models. The variety of these existing models was recently reviewed and some are described below (Ijichi 2011; O'Hagan and Heyer 2011).

1.2.8.3.1 Modelling human PDAC

Other models of PDAC, which are more invasive, have been developed by combining the expression of mutated oncogenic *kras* with another genetic alteration, such as the knockout of a tumour suppressor gene. In these mice, the expression of mutant *kras* and the knockout of a tumour suppressor gene were mediated by *Cre* expression, which was in turn controlled by the *Pdx* or *P48* promoters.

C*dkn2* knockout along with mutant *kras* expression in the mouse pancreas, leads to an accelerated development of PanIN and PDAC compared with the *kras*^{G12D} mouse model (Aguirre *et al.,* 2003). All animals develop invasive carcinoma and 100 % mortality occurs at 11 weeks. Concomitant expression of oncogene *kras* and mutant *trp53* (*trp53*^{R172H}) also generates metastatic PDAC, further imitating human disease development (Hingorani *et al.,* 2005). In this model, 100 % mortality occurs by 12 months.

Mice harbouring expression of mutant *kras* and *smad4* knockout have been simultaneously generated by different research groups (Bardeesy *et al.,* 2006; Izeradjene *et al.,* 2007; Kojima *et al.,* 2007). These groups have shown that in this model, PanIN development is accelerated (100 % mortality at 24 weeks), but MCN and IPMN are also generated as additional precursors of PDAC.

The effects of knocking out non-tumour suppressor genes on PanIN and PDAC development have also been investigated. Many other proteins are mutated or overexpressed in pancreatic cancer (see Table 1.4) and signalling pathways involving growth factors are involved in PDAC progression. *Tgfbr2* knockout in cooperation with mutant *kras* expression promotes and accelerates PDAC progression,

recapitulating the human progression of the disease. All animals are moribund within six months (Ijichi *et al.,* 2006). This observation has reinforced the role of the TGF-β signalling in pancreatic cancer. In this same model, inhibition of the CXCL-CXCR2 axis inhibits tumour growth and angiogenesis *in vivo*, showing the importance of the tumour-stromal interactions (see section 1.2.7) (Ijichi *et al.,* 2011).

All the mouse models described in this section harbour an endogenous expression of the mutated oncogene *kras*, combined with a null allele within the pancreatic progenitor cells, as the recombinase CRE was under the control of *Pdx* or *P48* promoters only.

1.2.8.3.2 Understanding the origin of PanIN lesions

The exact origin of PanIN lesions is still a topic of extensive investigation, as the *Pdx* and *P48* promoters used to model pancreatic carcinogenesis are expressed before the differentiation step between the three pancreatic cell lineages (Figure 1.8) (Ijichi 2011; Morris *et al.,* 2010b). To investigate the potential role of the different cell types of the adult pancreas in PanIN formation, cell lineage specific promoters have been used to control *Cre* expression and consequently $KRAS^{G12D}$ production (Figure 1.8 and Figure 1.9).

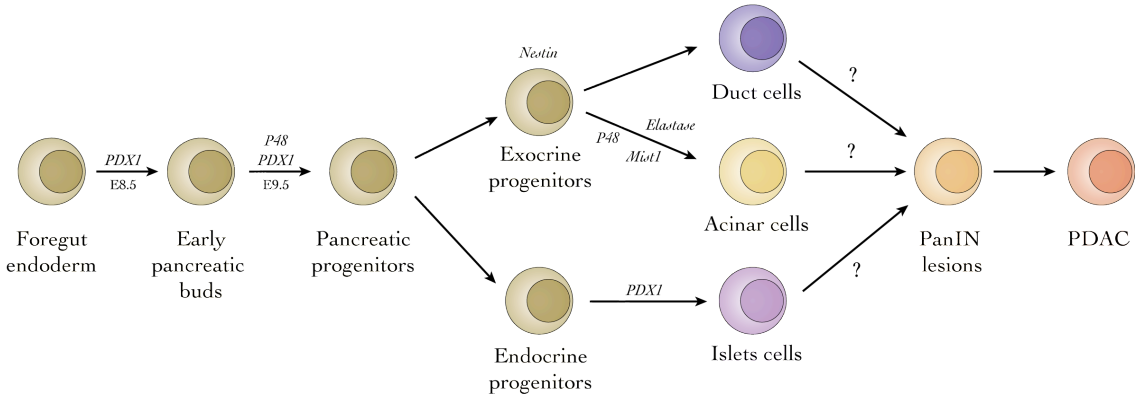

Figure 1.8: Schematic representation of cell differentiation during the development of the pancreas

Pancreatic development is a well-orchestrated process, which involves the expression of different transcription factors and genes that regulate cell differentiation. The origin of PanIN lesions is still not understood. E: Embryonic day - Adapted from (Carriere *et al.,* 2007; Ijichi 2011).

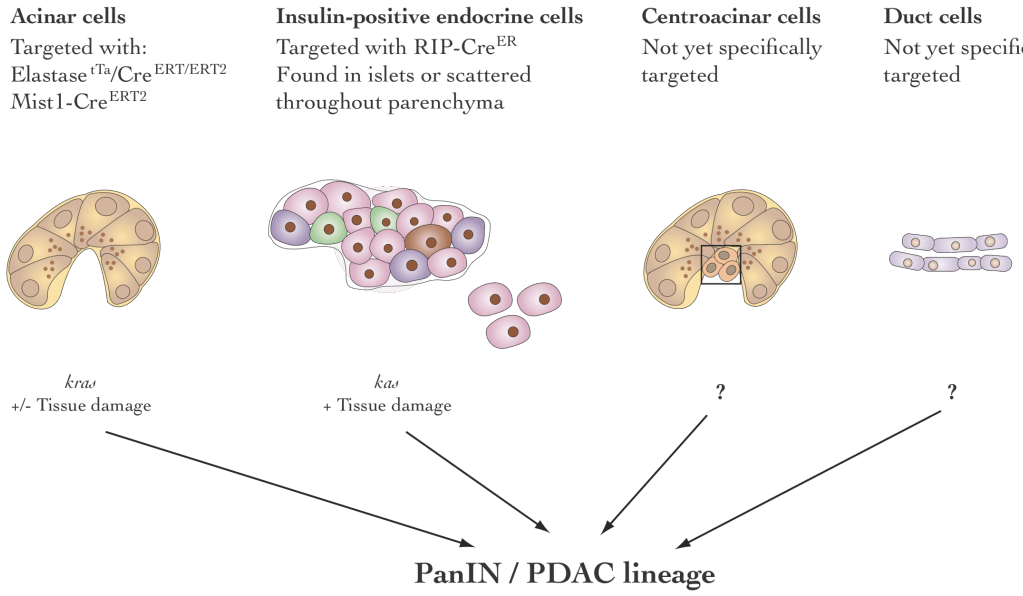

Figure 1.9: Cell types in the adult pancreas and their contribution to PanIN/PDAC formation

The exocrine pancreas is composed of acinar cells, duct cells and centroacinar cells, while the endocrine compartment is composed of islet cells, mainly β-cells producing insulin (pink). Acinar cells and insulin-positive cells have been targeted to express mutant *kras* and to evaluate their implication in PanIN and PDAC formation and progression in the presence or absence of a formely inflamed pancreas. RIP: rat insulin promoter. Adapted from (Bardeesy and DePinho 2002; Morris and Hebrok 2009).

The main hypothesis regarding the origin of PanIN lesions is that they arise from normal duct cells. However, this has yet to be proved, as mouse models with specific endogenous expression of mutant *kras* in these cells have not been generated (Ijichi 2011).

Several research groups have reported that using a specific acinar cell marker to target *kras* expression under the promoter of genes such as *Elastase* or *Mist1*, thus allowing endogenous expression of mutated *kras* in acinar cells during development, could lead to PanIN formation (Grippo *et al.,* 2003; Shi *et al.,* 2009; Tuveson *et al.,* 2006). Targeting endogenous expression of mutated *kras* in adult and mature acinar cells has also been effective in inducing PanIN formation (De La *et al.,* 2008; Habbe *et al.,* 2008; Shi *et al.,* 2009). As opposed to the mouse models described so far, these animals are inducible models allowing the control of the expression of the transgene in the adult animals only. Not only is the expression of the mutated *kras* allele under the control of the CRE recombinase, whose expression is regulated by an acinar cell specific promoter (*Elastase* or *Mist1*), but the CRE recombinase is retained in an inactive state and its activity is induced upon tamoxifen administration (CRE-ER protein fusion described in section 1.2.8.1). The endogenous expression of mutated *kras* in P48 positive cells is not cell lineage specific, because this transcription factor is ubiquitous and is expressed in all pancreatic progenitor cells. However, one scientific group analysed early PanIN-1 lesions from these mice and suggested that they may arise from acinar cells (Zhu *et al.,* 2007).

Another scientific research group has tested the effects of endogenous expression of mutated *kras* in Nestin positive cells. Nestin is a specific marker for progenitors of the exocrine pancreas and the mutant mice develop PanIN lesions in a similar pattern to

the *kras*^{G12D} model used (Carriere *et al.,* 2007). Interestingly, Nestin is a neuronal progenitor cell marker and an increased expression has been identified in various cancer cells as well as a correlation with enhanced aggressiveness and metastasis in some tumours (Ishiwata *et al.,* 2011).

Although pancreatic carcinoma mostly arise from exocrine tumours, endocrine tumours are also detected in human patients, though at a lower incidence (Halfdanarson *et al.,* 2008). Gidekel Friedlander *et al.* considered the insulin-producing cells as a possible origin for PanIN formation, with *Cre* expression being controlled by the rat insulin promoter (RIP) (Gidekel Friedlander *et al.,* 2009). They have shown that when mutant *kras* is expressed in endocrine cells, PanIN formation is induced if mice are previously treated with caerulein to induce chronic pancreatitis. The requirement of a formely injured or inflamed pancreas for PanIN formation has already been suggested (Guerra *et al.,* 2007).

Pancreatic cancer is linked to inflammation and two major signalling pathways are found to be "switched on" in this pathology: the NF-κB signalling pathway, which is a key regulator of inflammation and the Notch signalling pathway, which is associated with cell fate decisions and organ development. These two important signalling mechanisms will be described in the following two sections.

1.3 The TNF-α/NF-κB signalling pathway

1.3.1 The NF-κB signalling pathway

The NF-κB family of transcription factors is important and can be activated by many different stimuli. It can regulate the transcription of many different genes encoding for proteins, such as cytokines and chemokines (TNF-α and IL-6), immunoreceptors (TNFR and mouse histocompatibility antigene MHC), cell adhesion molecules (Tenascin-c), regulators of apoptosis (inhibitor of apoptosis protein IAP and Fas-ligand), growth factors or other transcription factors (Pahl 1999). Originally described as a "central mediator of the human immune response", it regulates many different cellular processes such as cell survival, cell proliferation, cell adhesion, migration and stress response (Oeckinghaus *et al.,* 2011).

This signalling pathway is represented in the figure below (Figure 1.10).

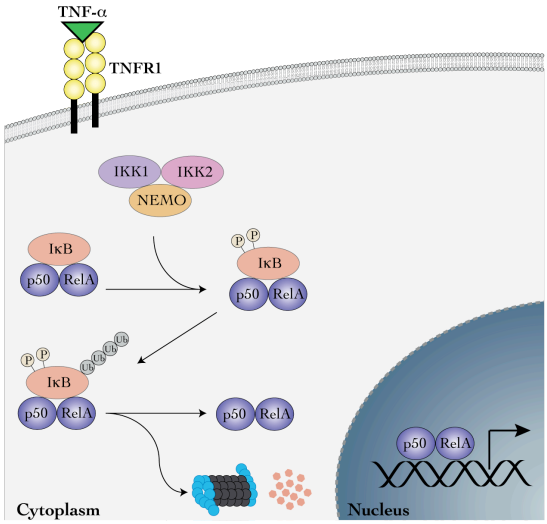

Figure 1.10: The TNF-α/IKK2/NF-κB signalling pathway

NF-κB dimers (p50/Rel A) are sequestred into the cytoplasm by binding to IκB proteins. Activation of the signalling pathway via TNF-α for example, activates the IKK complex which targets IκB to proteosomal degradation, releasing NF-κB for nuclear translocation and regulation of gene transcription.

1.3.1.1 Components of the pathway

In vertebrates, the NF-κB transcription factor family is comprised of 5 different members: Rel A (also called p65), Rel B, c-Rel, p50 and p52 respectively processed from the precursors NF-κB1 (also called p105) and NF-κB2 (also called p100) (Hayden and Ghosh 2004). These proteins usually exist as homodimers or heterodimers and they are maintained in an inactive status by binding to an inhibitor of κB (IκB) in the cytosol. The presence of a Rel homology domain within their N-terminus allows their dimerisation, but also their binding to the IκB proteins and DNA to regulate gene transcription (Hayden and Ghosh 2004). The dimers most frequently found in physiological conditions are the following: p50/Rel A (classically called NF-κB), p52/Rel B and p50/c-Rel (Shih *et al.,* 2011). The presence of a transactivation domain is essential for the heterodimers to be able to promote transcription. This domain is only found in the Rel A, Rel B and c-Rel proteins (Gerondakis *et al.,* 1999).

The phosphorylation of the IκB proteins allows for ubiquitination and protosomal degradation, therefore releasing the NF-κB complexes and allowing their translocation to the nucleus for specific gene activation (Oeckinghaus *et al.,* 2011). IκB phosphorylation is mediated by the inhibitor of κB kinase (IKK) complex, which consists of two catalytic subunits, IKK1 and IKK2 and the regulatory protein IKK3 (or NEMO) (Hagemann *et al.,* 2009) (Figure 1.10).

1.3.1.2 Classical and alternative pathways

There are two NF-κB activation pathways in cells: the classical (canonical) pathway and the alternative (non-canonical) pathway (Bonizzi and Karin 2004). The stimuli and the cell-receptors involved are different, but in both cases activation of the pathway will lead to NF-κB nuclear translocation and subsequent gene transcription.

The canonical pathway is dependent on IKK2, NEMO and Rel A. Their respective knockout has proved to be lethal and animals show similar phenotypes, with severe liver degeneration due to apoptosis (Beg *et al.,* 1995; Li *et al.,* 1999; Rudolph *et al.,* 2000). The canonical NF-κB activation pathway is mostly involved in the regulation of innate immunity (Alcamo *et al.,* 2001; Senftleben *et al.,* 2001). Following infections, its activation leads to the transcription of genes coding for cytokines and chemokines which are required for the inflammatory process.

During canonical NF-κB signalling, signals mostly arise from cytokine receptors, such as TNF receptor or interleukin 1 receptor (IL-1R), but also from Toll-like receptors, which recognise pathogen-associated molecule patterns (PAMP). Pro-inflammatory stimuli, including cytokines such as TNF-α or IL-1, will signal via these receptors leading to IKK2 activation by phophorylation on two serine residues (177 and 181) (Delhase *et al.,* 1999). Once activated, IKK2 can phosphorylate IκB-α, allowing the recruitment of ubiquitin ligase, which will mark this protein for proteosomal degradation (Chen *et al.,* 1996). NF-κB heterodimers (mostly containing p65) are then released and translocate to the nucleus to regulate the transcription of an important variety of genes involved in various cellular processes, such as inflammation and immune responses (Shih *et al.,* 2011).

The non-canonical pathway depends on the activation of the IKK1 subunit of the IKK complex. Once activated, IKK1 can process the p100 precursor into its active form (p52), allowing the formation of the p52/Rel B heterodimers. This pathway is induced by different ligands, including lymphotoxin-β, B cell activating factor BAFF and CD40 ligand and is implicated in lymphoid organ development and adaptive immunity (Bonizzi and Karin 2004).

Interestingly, the NF-κB signalling pathway is involved in the control of some of the hallmarks of cancer cells described in section 1.1.1 (Figure 1.1), such as cell proliferation, evasion of apoptosis, angiogenesis, invasion and metastasis. Links between this pathway and oncogenesis have also been shown, such as the ability of oncoproteins to activate the NF-κB signalling pathway (Basseres and Baldwin 2006) (further discussed in section 1.3.2.2).

1.3.2 NF-κB: between inflammation and cancer

As described in the previous section, the canonical NF-κB pathway is involved in inflammation. Upon its activation, a wide variety of genes are activated, mainly encoding for cytokines and chemokines such as TNF-α and IL-6 (Pahl 1999). TNF-α is also an effector of this pathway and the resulting positive feedback loop can rapidly induce a constitutive activation of the pathway.

The role of canonical NF-κB signalling as a link between inflammation and cancer has been shown in a number of models. Constitutive activation of this pathway can act as a tumour promoter in different types of cancer (see section 1.3.2.2) (Ben-Neriah and Karin 2011).

Activation of NF-κB signalling has been associated with abnormal growth of cells in a variety of organisms, from *Drosphila melanogaster* to mammals (Ben-Neriah and Karin 2011). In the context of Scribble deficiency, a gene involved in cell polarity, and the expression of the oncoprotein RAS, hemocyte-derived TNF-α enhances tumour growth and migration in *Drosphila melanogaster* (immune responses in invertebrates are mediated by hemocytes) (Cordero *et al.,* 2010). In human lung cancer, inhibition of the NF-κB axis enhances cell death, associating this signalling with tumour growth (Bivona *et al.,* 2011).

IKK2 has been shown to be essential for tumour growth in a model of inflammation-induced carcinogenesis (colitis-associated cancer). The deletion of this kinase in either intestinal epithelial cells or myeloid cells leads to a reduction in tumour incidence and tumour growth. This is due to an increase in apoptosis when the deletion occurs in the enterocytes. However, deletion in the myeloid cells leads to a reduction in the production of inflammatory mediators which usually contribute to tumour growth (Greten *et al.,* 2004).

Inactivation of the NF-κB signalling pathway does not always inhibit tumorigenesis; its role in tumour initiation has been shown in skin and hepatic mouse models (Dajee *et al.,* 2003; Sakurai *et al.,* 2006). Inhibition of the NF-κB signalling pathway concomitant with activation of the RAS signalling pathway (*hras* mutant) has been observed in patients with squamous cell carcinoma. Although RAS induces cell cycle arrest, this is counterbalanced by the inhibition of the NF-κB signalling pathway, which restores cell proliferation (Dajee *et al.,* 2003). The second study involved genetic deletion of the IKK2 kinase in the liver, after which mice are more susceptible to chemically-induced hepatocarcinogenesis (Maeda *et al.,* 2005; Sakurai *et al.,* 2006). It has been shown that this enhanced formation of hepatocellular carcinoma is due to the absence of JNK inhibition, usually induced by TNF-α, therefore leading to an increase in hepatocyte proliferation (Deng *et al.,* 2003; Kamata *et al.,* 2005; Maeda *et al.,* 2005; Sakurai *et al.,* 2006)

This project focuses on the autocrine role of TNF-α in pancreatic cancer and therefore the function of this cytokine in the context of the NF-κB signalling pathway will be the main topic of discussion.

1.3.2.1 TNF-α, IL-1β and IL-6: the main cytokines involved

TNF-α is a major inflammatory cytokine and a classical stimulus of the canonical NF-κB signalling pathway. It recognises two different receptors, TNFRI and TNFRII, expressed in most cell types or on haemopoietic cells, respectively (Balkwill 2006). Its activation via TNFRI leads to NF-κB activation as described in the previous section.

Originally described as a tumour necrosis factor, when TNF-α is administrated locally and at high doses in tumours, it induces necrosis (Balkwill *et al.,* 1986; Talmadge *et al.,* 1988). However, the tumour-promoting action of this cytokine came to light when mice deficient for *tnfa* were found to be protected from developing skin tumours following experimental induction of skin carcinogenesis with the classical DMBA/TPA protocol (Moore *et al.,* 1999).

TNF-α is expressed by many different tumours and a real balance between a tumour-promoting or a tumour-necrotic role exists (Balkwill 2002). The reasons for such contrary effects still remain a major point of interest and investigation. The cell types involved in the secretion of this cytokine and its concentration in the milieu seem to be critical for this balance as high local doses of TNF-α are associated with tumour necrosis (Balkwill *et al.,* 1986; Talmadge *et al.,* 1988). This cytokine is involved in tumour progression and in some models, this is dependent on the NF-κB pathway (Balkwill 2006). TNF-α produced by tumour cells or by cells in the tumour microenvironment such as immune cells, contributes to oncogene activation, to DNA damage and consequently to tumour development. TNF-α can therefore be considered as a therapeutic target for cancer treatment (Balkwill 2009).

Immune and endothelial cell-derived TNF-α in the liver tumour microenvironement leads to the activation of the NF-κB signalling pathway and anti-TNF-α treatment can decrease tumour incidence (Pikarsky *et al.,* 2004). Similar to the fact that *tnfa* deficient mice are resistant to chemically-induced skin carcinogenesis (Moore *et al.,* 1999), *tnfr1* knockout mice are resistant to chemically-induced hepatocellular carcinoma (Knight *et al.,* 2000). TNF-α-treatment of pancreatic cancer cell lines *in vitro* or of mice bearing orthotopic pancreatic tumours induces and enhances tumour growth and invasiveness. The use of anti-TNF-α antibodies *in vivo*, such as infliximab or etanercept, reduces tumour growth and metastasis, therefore suggesting this cytokine as a therapeutic target for pancreatic cancer (Egberts *et al.,* 2008).

Constitutive expression of TNF-α by epithelial ovarian cancer cells contributes to the maintenance of the production of other cytokines and chemokines within the tumour microenvironment, providing a network of inflammatory molecules and contributing to tumour development (Kulbe *et al.,* 2007; Kulbe *et al.,* 2011).

IL-1β is another pro-inflammatory cytokine, which, as opposed to TNF-α, can activate the NF-κB pathway in an IKK2-independent manner (Solt *et al.,* 2007). An enhanced production of this cytokine has been associated with an increased risk of gastric cancer (El-Omar *et al.,* 2000). IL-1β is known to be upregulated in different types of cancer and to have a tumour-promoting role, favouring angiogenesis and increasing metastasis (Lewis *et al.,* 2006). Tumours secreting high amounts of IL-1β are often associated with poor prognosis (Apte *et al.,* 2006; Elaraj *et al.,* 2006). This cytokine has also been shown to be responsible for the increased activity of the NF-κB signalling pathway observed in pancreatic adenocarcinoma cell lines, also contributing to explain their chemoresistance (Arlt *et al.,* 2002). This IL-1β secretion

by the pancreatic epithelial cells is induced by the production of nitric oxide by the fibroblasts surrounding the tumour cells (Muerkoster *et al.,* 2004).

IL-6 induction during inflammation is one of the consequences of the activation of the NF-κB signalling pathway by TNF-α and/or IL-1β. IL-6 activates another inflammatory signalling pathway, STAT3, which is also activated in cancer and which has been shown to cooperate with the NF-κB signalling pathway to promote tumorigenesis (Grivennikov and Karin 2010). IL-6 is upregulated in human ovarian cancer cells (Chou *et al.,* 2005), in human lung adenocarcinoma (Gao *et al.,* 2007b) and in human breast cancer (Sansone *et al.,* 2007). IL-6 contributes to inflammation-associated carcinogenesis and this has been demonstrated in a mouse model of colitis-associated cancer and hepatocellular carcinoma (mostly induced by inflammatory conditions) (Naugler and Karin 2008). A research group has recently demonstrated that the activation of STAT3 signalling in pancreatic cancer cells is induced by paracrine IL-6 from myeloid cells in the *kras*^{G12D} genetic mouse model of pancreatic cancer. Genetic inactivation of IL-6 trans-signalling or of the STAT3 signalling pathway in this model inhibits PanIN progression (Lesina *et al.,* 2011).

1.3.2.2 Constitutive activation of NF-κB in cancer

The constitutive activation of the NF-κB signalling pathway observed in many different cancers has been shown to have several origins: genetic mutations or alterations in the different components of the pathway and exposure to inflammatory mediators or genetic mutations in other pathways (mainly affecting oncogenes and tumour suppressor genes) leading to an activation of the NF-κB signalling pathway (Ben-Neriah and Karin 2011).

1.3.2.2.1 Mutations in the components of the NF-κB pathway and exposure to inflammatory mediators

A chromosomal translocation leading to a constitutive activation of a Rel transcription factor has been identified in B cell lymphoma (Neri *et al.,* 1991). The constitutive activation of NF-κB signalling observed in diffuse large B cell lymphoma has recently been attributed to oncogenic mutations affecting MYD88, a protein required for TLR activation (Ngo *et al.,* 2011). Overexpression of cytokines, chemokines and growth factors by the cancer cells themselves also leads to activation of this pathway (Lu and Stark 2004; Lu *et al.,* 2004).

In human PDAC, a constitutive activation of the transcription factor Rel A was shown (Wang *et al.,* 1999). Blocking NF-κB activation in pancreatic cancer cell lines and tumours with a proteasome inhibitor leads to a reduction in cell proliferation and to induction of apoptosis (Shah *et al.,* 2001). Pancreatic cancer cell lines expressing a mutant form of the IκB-α protein that blocks the activity of NF-κB cannot induce tumour formation *in vivo* (Fujioka *et al.,* 2003b).

Constitutive secretion of different cytokines, such as IL-1α and IL-8, in human pancreatic cancer cells have been identified as activators of the NF-κB pathway, contributing to increased growth and tumorigenesis (Le *et al.,* 2000; Melisi *et al.,* 2009; Niu *et al.,* 2004). Many of these studies indicate that autocrine secretion of proinflammatory cytokines is one of the routes which leads to the activation of the NF-κB signalling pathway and contributes to tumour progression. Constitutive NF-κB signalling in epithelial lung cells increases the risk of lung carcinogenesis (Zaynagetdinov *et al.,* 2011). Persistent activated NF-κB signalling in human breast cancer cells contributes to maintain abnormal cell proliferation (Biswas *et al.,* 2004).

As described in section 1.1.4, a variety of cell types are present in the tumour microenvironment. The previous examples illustrated the role of autocrine signalling of epithelial cell-derived inflammatory mediators. However, the effects of paracrine signalling of these molecules on tumour cells is also very important and can originate from the stromal cells (Mantovani *et al.,* 2008).

In a genetic mouse model of prostate cancer, it has been demonstrated that immune infiltrating cells expressing the ligand for the receptor activator of NF-κB (RANK) could activate the respective receptor on prostate cancer cells, leading to IKK1 activation and subsequently to an enhanced metastatic phenotype (Luo *et al.,* 2007). *In vitro* studies have shown that the co-culture of macrophages with ovarian tumour cells can increase the invasive capacity of the tumour cells in a TNF-α and NF-κB-dependent manner (Hagemann *et al.,* 2005; Hagemann *et al.,* 2006).

Fibroblasts are also a main component of the tumour microenvironment. Activation of NF-κB signalling by IL-1α in this cell type in breast cancer stroma induces the secretion of IL-6 and promotes angiogenesis and metastasis (Bhat-Nakshatri *et al.,* 1998).

The NF-κB pathway has also been shown to regulate apoptosis by controlling the expression of antiapoptotic proteins, such as IAP1, IAP2, TRAF1 (TNF receptor associated factor) and Bcl-2, therefore providing an additional route to enhance tumour cell growth. This has been shown in the context of pancreatic tumour progression (Holcomb *et al.,* 2008).

Furthermore, NF-κB controls the production of angiogenic factors such as IL-8 and VEGF in human pancreatic cancer cells (Holcomb *et al.,* 2008). Several studies have shown that inhibiting the NF-κB pathway in pancreatic cancer cells reduces and prevents tumour angiogenesis (Holcomb *et al.,* 2008; Xiong *et al.,* 2004). However, reducing angiogenesis in an originally poorly vascularised tumour might prevent efficient delivery of therapeutic drugs (Olive *et al.,* 2009). Inhibition of NF-κB also significantly prevents pancreatic tumour metastasis into the liver and the peritoneal cavity (Fujioka *et al.,* 2003a; Xiong *et al.,* 2004).

Finally, NF-κB activity is associated with chemoresistance in pancreatic cancer and the combination of a chemotherapeutic agent with a specific inhibitor of the pathway has been shown to improve the responsiveness of the cancer cells and reduce tumour growth (Arlt *et al.,* 2001; Arlt *et al.,* 2003; Muerkoster *et al.,* 2003).

1.3.2.2.2 Oncogenes and NF-κB in cancer: kras, myc and tp53

Oncogenes can drive the activation of inflammatory signalling pathways such as the NF-κB axis. The main oncogenes involved in human cancers belong to the *RAS* family and 25 % of human tumours have a mutated form of these small GTPases (Castellano and Downward 2011). More than 90 % of human pancreatic cancers are associated with a *KRAS* mutation (see section 1.2.6.2) (Yonezawa *et al.,* 2008). Constitutive activation of the main downstream pathway (RAF/MEK/ERK) results in the production of inflammatory cytokines and chemokines controlling cell proliferation and survival (Montagut and Settleman 2009). Mutant RAS proteins are known to be able to activate the canonical pathway of NF-κB signalling. This has been shown in lung epithelial cells and in prostate epithelial cells following *kras* overexpression (Basseres *et al.,* 2010; Kim *et al.,* 2002), but also in fibroblasts with

overexpression of mutant *hras* (Finco *et al.,* 1997). Overexpression of oncogenic *kras* can induce lung adenocarcinoma and is associated with activation of the NF-κB signalling pathway (Basseres *et al.,* 2010; Meylan *et al.,* 2009). Overexpression of mutant *hras* in melanocytes deficient for a specific tumour suppressor gene (*cdkn2*) can induce melanoma. In this spontaneous model, additional genetic deletion of *ikk2* in melanocytes impairs the development of melanoma, confirming the importance of the NF-κB signalling pathway in cancer initiation (Yang *et al.,* 2010). In all these models, activation of the NF-κB signalling pathway was due to overexpression of oncogenic *kras* rather than endogenous expression, allowing physiological levels like in the $kras^{G12D}$ mouse model used.

The cooperation between oncogene activation and inflammatory conditions for tumour development is well described and in the context of pancreatic carcinogenesis is associated with pancreatitis and *kras* activation (see section 1.2). This has been shown in a mouse model of pancreatic cancer associated with caerulein-induced pancreatitis (Guerra *et al.,* 2007).

The RAS signalling pathway can activate inflammatory cytokines such as IL-8, therefore increasing tumour growth and angiogenesis in mouse xenograft models (Sparmann and Bar-Sagi 2004). It has also been demonstrated that in melanoma, RAF mutations contribute to the maintenance of a constitutively active ERK and STAT3 signalling, enhancing the secretion of inflammatory mediators such as VEGF and IL-6 (Sumimoto *et al.,* 2006).

The *MYC* transcription factor controls various cellular processes such as cell proliferation and apoptosis. Mutations in this oncogene contribute to tumour

development and its overexpression has been shown to control and modulate the tumour microenvironment, favouring tumour angiogenesis and stimulating inflammation (Whitfield and Soucek 2011). In a mouse model of B cell lymphoma (driven by *myc*), constitutive activation of two main inflammatory signalling pathways was observed: NF-κB and STAT3 (Han *et al.,* 2010). In addition, the transcription factor NF-κB controls the expression of *myc*, demonstrating a bidirectional cooperation in tumour development (Kanda *et al.,* 2000).

Inactivating mutations in the tumour suppressor gene *tp53*, which codes for p53, are also frequently found in human cancers (at least 50 % of the tumours) (Soussi and Wiman 2007). This protein is a transcription factor, which plays a critical role in the control of the cell cycle by activating the expression of genes involved in cell cycle arrest or apoptotic signals in response to DNA damage. Crosstalk between the p53 and the NF-κB signalling pathways has been demonstrated in lung and pancreatic cancer cells, showing that p53 mutants can activate the NF-κB promoter and enhance some tumour-promoting responses such as anti-apoptotic signals (Schneider *et al.,* 2010; Scian *et al.,* 2005). In mouse embryonic fibroblasts, *kras* activation associated with loss of *trp53* (mouse gene homologue for *tp53*) activates the NF-κB signalling pathway (Meylan *et al.,* 2009). Lung tumour cell lines derived from animals with mutant *kras* and *trp53* loss also present with enhanced NF-κB activity, suggesting the cooperation between the two oncogenes and the activation of an inflammatory signalling pathway (Meylan *et al.,* 2009). Interestingly, mycoplasma infection has been shown to be associated with an activated NF-κB signalling and a reduced p53 signalling, increasing the sensibility of mouse embryonic fibroblasts to *kras*-induced transformation (Logunov *et al.,* 2008).

Along with NF-κB, a number of other signalling pathways are deregulated in pancreatic cancer such as Notch, Wnt and Hedgehog (De La *et al.,* 2008; Pasca di Magliano *et al.,* 2006; Pasca di Magliano *et al.,* 2007; Thayer *et al.,* 2003). The present work focuses on the interplay between the NF-κB and the Notch pathways. The Notch signalling cascade and the evidence of its implication in pancreatic cancer are described in the following section.

1.4 The Notch signalling pathway

1.4.1 Components of the pathway

Notch receptors and ligands are transmembrane proteins, allowing communication between a signal-sending cell and a signal-receiving cell (Figure 1.11). In mammals, four different Notch receptors have been identified (Notch1 to Notch4) and five different ligands belonging to two distinct families: the Jagged family (Jagged1 and Jagged2) and the delta-like family (Dll1, Dll3 and Dll4) (Lobry *et al.,* 2011).

Following Notch ligand-receptor interaction, the Notch protein is cleaved by a metalloprotease TACE (TNF-α converting enzyme), releasing the extracellular part of the Notch receptor, which is endocytosed by the signal-sending cell (Kopan and Ilagan 2009). The mechanisms triggered after this endocytosis are still unclear and under investigation. In the signal-receiving cell, proteolytic cleavage of the Notch receptor results in the release of the Notch intracellular domain (NICD), which can translocate to the nucleus and regulate the transcription of different genes via the canonical or the non-canonical Notch signalling mechanisms (Lobry *et al.,* 2011).

1.4.2 The canonical and non-canonical Notch signalling pathways

When NICD translocates to the nucleus, it cannot directly bind to the DNA. In the context of the canonical signalling pathway, it associates and forms a complex with RBPjκ, which is already present at the promoter of the Notch target genes. In the absence of NICD, RBPjκ forms a complex with corepressor proteins, to repress the transcription of Notch target genes. NICD binding with RBPjκ switches this repressed state to an activated state, associated with the recruitment of coactivator proteins to allow gene transcription (Borggrefe and Oswald 2009; Kopan and Ilagan 2009) (Figure 1.11).

The main Notch target genes regulated by the canonical pathway are proteins belonging to bHLH families (basic helix-loop-helix) such as HES and HEY (Fischer and Gessler 2007; Iso *et al.,* 2003). HES and HEY proteins are transcriptional repressors, mainly thought to bind to the promoter region of their target genes on N-box and/or E-box sequences (Fischer and Gessler 2007).

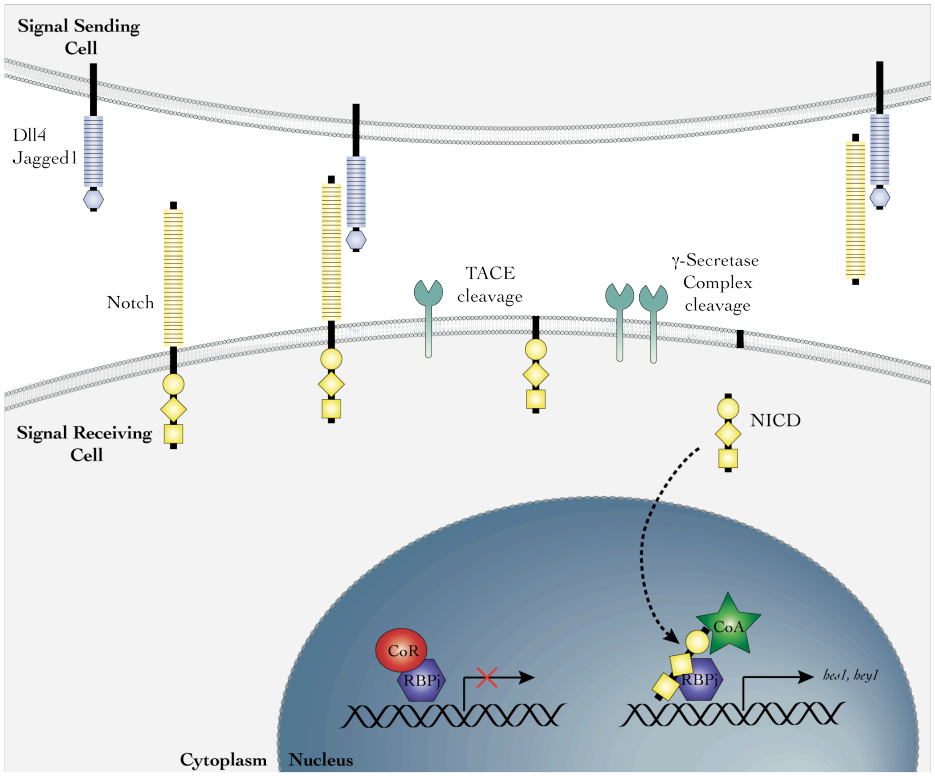

Figure 1.11: The canonical Notch signalling pathway

A signal-sending cell expressing a Notch ligand (Jagged1, Jagged2, Dll1, Dll3 or Dll4) interacts with a signal-receiving cell expressing a Notch receptor (Notch1 to Notch4). Upon receptor-ligand recognition, two successive proteolytic cleavages occur in the signal receiving cells and are mediated by TACE and γ-secretase complex cleavage. The intracellular domain of Notch (NICD) is therefore released and translocates to the nucleus to regulate gene transcription. In the context of canonical Notch signalling, NICD binds to RBPjκ, releasing the corepressor proteins (CoR) and recruiting coactivator proteins (CoA) to allow the transcription of Notch target genes, such as *hes1* and *hey1*.

The non-canonical Notch signalling pathway is RBPjκ independent and still not well described and understood (Martinez Arias *et al.,* 2002). NICD can bind to other signalling molecules including the transcription factor Deltex (Matsuno *et al.,* 1995; Ordentlich *et al.,* 1998; Ramain *et al.,* 2001; Yamamoto *et al.,* 2001). Binding of NICD to IKK complex contributes to the maintenance of the NF-κB signalling pathway in an active state (Vacca *et al.,* 2006; Vilimas *et al.,* 2007) and NICD has also been shown to interact with SMAD proteins (Blokzijl *et al.,* 2003; Dahlqvist *et al.,* 2003; Itoh *et al.,* 2004). These interactions highlight that the Notch signalling pathway can cooperate and interact with many other signalling pathways such as NF-κB, TGF-β and bone morphogenic protein signalling (via SMAD).

Notch ligands can activate or inhibit the Notch signalling pathway. The activity of these ligands can be regulated by post-translational modifications, such as glycosylation or ubiquitination, but also via cellular mechanisms such as endocytosis or proteolysis. All these regulation processes add to the complexity and diversity of this pathway as they also involve cross-signalling with other signalling pathways (D'Souza *et al.,* 2008).

1.4.3 Notch functions - links between development and cancer

1.4.3.1 Context- and tissue-dependent

The Notch signalling pathway is involved in the embryonic development of many organs and tissues in all multicellular organisms, showing high genetic conservation (Artavanis-Tsakonas *et al.,* 1999; Gridley 1997). Notch not only regulates tissue homeostasis but also cell fate, and was originally identified as involved in neurogenesis in flies and vertebrates. It is now established that the Notch pathway is implicated in the development of a variety of organs, such as the organs of the central nervous system or of the cardiovascular system, but also the pancreas, the gut and

bones (Bolos *et al.,* 2007). Controlling various cellular processes, deregulation of this pathway has been identified in a number of pathological conditions, including cancer.

The Notch signalling pathway has been shown to be involved in the regulation of lymphocyte development and in particular of B and T cell lineages (Tanigaki and Honjo 2007). Chromosomal translocations or genetic mutations in components of the Notch signalling pathway leading to its constitutive activation have been associated with the development of chronic lymphocytic leukaemia and T lymphoblastic neoplasms (Allenspach *et al.,* 2002; Ellisen *et al.,* 1991; Puente *et al.,* 2011).

Appropriate kidney development requires Notch signalling and its reactivation in the adult organ contributes to the development of inflamed renal pathologies (Bielesz *et al.,* 2010; Cheng and Kopan 2005). Notch is involved in the regulation of differentiation of the human epidermis and a downregulation has been observed and associated with basal cell carcinoma (Thelu *et al.,* 2002). Cervix development is also regulated by Notch signalling and both an upregulation or a downregulation of the pathway have been associated with cervical cancer, the latest occurring when carcinogenesis is induced by human papillomavirus infection (Maliekal *et al.,* 2008; Talora *et al.,* 2002; Zagouras *et al.,* 1995).

For the purpose of this thesis, the effects of the Notch signalling pathway on pancreas development and the status of this pathway in the context of pancreatitis and pancreatic cancer are described in more detail in section 1.4.4.

Notch signalling has also been implicated in the induction of the epithelial-mesenchymal transition process, which is usually associated with solid tumour

development and aggressiveness. Activation of this pathway in epithelial cells leads to the expression of specific mesenchymal markers such as α-SMA. This contribution is in agreement with the reactivation of the Notch signalling pathway observed in many epithelial cancers and inhibiting this pathway may represent a therapeutic strategy to prevent this mesenchymal transformation (Wang *et al.,* 2010).

Targeting the Notch signalling pathway is now considered as a new strategy for cancer treatment, as its inappropriate reactivation has been observed in various cancers and it is also associated with cancer progression (Sethi and Kang 2011). Several inhibitors, such as γ-secretase inhibitors or antibodies against Notch ligands, are being investigated (Garber 2007). A Cancer Research UK sponsored phase I/II clinical trial is currently evaluating the efficacy of a γ-secretase inhibitor in combination with gemcitabine in patients with metastatic pancreatic carcinoma (EudraCT number 2008-004829-42).

1.4.3.2 Notch: oncogene or tumour suppressor gene?

Due to its tissue- and context-dependent implications, it is difficult to classify the Notch protein as an oncogene or a tumour suppressor (Lobry *et al.,* 2011; Ranganathan *et al.,* 2011). Notch was for a long time considered an oncogene in different cancers and was first identified in T cell acute lymphoblastic leukaemia (Ellisen *et al.,* 1991). Activating mutations in the Notch1 receptor have been identified in human cases of chronic lymphocytic leukaemia (Fabbri *et al.,* 2011; Puente *et al.,* 2011). Increased expression of Notch or Jagged1 have also been shown to correlate with poor prognosis in human breast cancer (Reedijk *et al.,* 2005).

A tumour suppressor role has been shown in the skin where loss of Notch function can lead to spontaneous skin carcinoma (Nicolas *et al.,* 2003). In a genetic mouse

model of hepatocellular carcinoma, cancer development is associated with an upregulation of the genes coding for the components of the Notch pathway, therefore suggesting an oncogenic role. However, inhibition of the Notch pathway with a γ-secretase inhibitor accelerates the development of hepatocellular carcinoma in this mouse model, therefore suggesting a tumour suppressor role. This observation has been corroborated by the detection of an increased expression of *HES1* in patients with hepatocellular carcinoma and presenting a better survival (Viatour *et al.,* 2011). Finally, constitutive activation of Notch in fibroblasts in the microenvironment of melanoma can reduce tumour growth and angiogenesis (Shao *et al.,* 2011).

1.4.3.3 Notch and oncogenes in cancer

In section 1.3.2.2, the ability of oncogenes such as *kras*, *myc* or *tp53* to activate inflammatory signalling pathways was discussed. However, the same oncogenes do not appear to be able to activate Notch signalling directly, but a cooperation between these different signalling pathways is suggested, especially in pancreatic cancer and in leukaemia.

Expression of oncogenic *kras* cooperates with the activation of Notch signalling to promote tumour progression (De La and Murtaugh 2009). This cooperation has only been shown in the context of pancreatic carcinogenesis (see also section 1.4.4.3) and the exact mechanisms involved are still unknown.

The *MYC* oncogene is activated in acute lymphoblastic T cell leukaemia and its expression, associated with Notch signalling, induces tumour progression. A recent study qualified Notch as a dominant oncogene in acute lymphoblastic T cell leukaemia (Demarest *et al.,* 2011). Notch activation has also been shown to be

upstream of *MYC* and that Notch directly regulates *MYC* expression, contributing to the growth of leukemic cells (Palomero *et al.,* 2006).

The *TP53* oncogene is often mutated or lost in the setting of chronic lymphocytic leukaemia (Zenz *et al.,* 2008). In these cells, a cooperation between p53 and Notch pathways has been demonstrated: leukemic cell lines expressing the wild type *TP53* gene have an upregulated expression of Notch, which is absent upon loss of functional *TP53* (Secchiero *et al.,* 2009). Notch therefore appears to be an antiapoptotic target of p53 and inhibiting the induction of Notch in chronic lymphocytic leukaemia can represent a new treatment approach (Wickremasinghe *et al.,* 2011).

1.4.4 Implications of the Notch pathway in pancreatic development, pancreatitis and pancreatic cancer

1.4.4.1 The Notch pathway in the developing and adult pancreas

The components of the Notch pathway (receptors, ligands and target genes) are expressed during pancreatic organogenesis which reveals that this pathway is activated in this process (Apelqvist *et al.,* 1999; Jensen *et al.,* 2000; Lammert *et al.,* 2000). Notch signalling is important for the development of the endocrine cells of the pancreas as inactivation of some components of the pathway leads to an accelerated differentiation of the endocrine compartment (Apelqvist *et al.,* 1999; Jensen *et al.,* 2000). However, inappropriate and constitutive activation of the Notch signalling pathway in pancreatic precursor cells prevents the development of both exocrine and endocrine lineages (Hald *et al.,* 2003; Murtaugh *et al.,* 2003). The Notch signalling pathway has also been shown to be active in adult mouse pancreatic islets and its inhibition can induce apoptosis in the endocrine β-cells (Dror *et al.,* 2007).

1.4.4.2 Notch in acute pancreatitis

Following experimentally induced pancreatic injury, pancreatic regeneration involves acinar cell dedifferentiation, with the re-expression of the components of the Notch pathway, normally expressed in undifferentiated pancreatic progenitor cells during the development stage (Jensen *et al.,* 2005; Rooman *et al.,* 2006). Simultaneous inhibition of the Notch signalling pathway and induction of acute pancreatitis in a mouse model impairs the regeneration of the exocrine compartment of the pancreas (Siveke *et al.,* 2008). Genes coding for different components of the Notch signalling pathway are rapidly expressed after experimental induction of acute pancreatitis (Gomez *et al.,* 2004).

1.4.4.3 Notch in pancreatic cancer

The Notch pathway, normally quiescent in the adult pancreas, is reactivated in pancreatic cancer from PanIN to PDAC progression (Mazur *et al.,* 2010a; Miyamoto *et al.,* 2003; Plentz *et al.,* 2009). An active Notch signalling pathway is identified by the expression of classic target genes such as *hes1* and *hey1*. These genes are also found to be upregulated in early PanIN lesions and throughout PDAC, but not in normal pancreatic epithelium (Hingorani *et al.,* 2003; Miyamoto *et al.,* 2003). However, Notch-independent HES1 production has been shown in other cell types, such as endothelial cells or neuroblastoma cells, involving the RAS/RAF/MAPK and/or the JNK signalling pathways (Curry *et al.,* 2006; Katoh 2007; Stockhausen *et al.,* 2005).

Transgenic overexpression of TGF-α in the acinar cells of the pancreas is accompanied by activation of the Notch signalling pathway in PanIN lesions (Miyamoto *et al.,* 2003). The presence of TGF-α is therefore shown to be an initiating event in neoplasia and an increase of acetylated-histone H3 at the *hes1* promoter is

associated with this process (Miyamoto *et al.,* 2003). However, adenovirus-mediated overexpression of Notch target gene *hes1* in normal pancreatic epithelial cells does not induce metaplasia, as opposed to NICD overexpression (Miyamoto *et al.,* 2003). Moreover, in response to TGF-α, the matrix metalloproteinase MMP7 is expressed and contributes to Notch activation during pancreas metaplasia (Sawey *et al.,* 2007).

Experiments inhibiting or downregulating Notch signalling in pancreatic cancer cell lines have shown that this pathway is required to maintain the transformed status of these cells, rather than to initiate transformation. This has been observed using either a γ-secretase inhibitor leading to a reduction in tumour growth and PDAC progression (Plentz *et al.,* 2009) or siRNAs against Notch, leading to increased apoptotic events and a reduction in cell proliferation in human pancreatic cell lines (Wang *et al.,* 2006).

In pancreatic cancer, the Notch pathway has been shown to cooperate with other signalling pathways, in particular with oncogenic KRAS. PanIN lesions induced by the expression of mutated *kras* express Notch target genes, suggesting the presence of an activated Notch pathway in this context (Guerra *et al.,* 2007). In the context of mutant *kras*, the Notch pathway activation has been shown to have a tumour-promoting role and was implicated in mediating metaplasia of acinar to ductal epithelium, a critical process in pancreatic carcinogenesis (De La *et al.,* 2008; Mazur *et al.,* 2010a; Morris *et al.,* 2010a).

A clinical trial is currently evaluating the efficacy of a γ-secretase inhibitor in combination with gemcitabine on patients with metastatic pancreatic cancer (see section 1.4.3.1). Even though currently used γ-secretase inhibitors present some side

effects, such as diarrhoea, they can be safely tolerated (Mysliwiec and Boucher 2009). Moreover, an additional study has shown that Notch activation is mostly due to an overexpression of Notch ligand in pancreatic cancer cells, reinforcing the idea of inhibiting this pathway with small molecule inhibitors (Mullendore *et al.,* 2009).

1.5 Focus of thesis

Most pancreatic tumours express an activating mutation in the *KRAS* proto-oncogene (Yonezawa *et al.,* 2008) and activation of NF-κB signalling upon expression of this oncogene has been established in other cancers (Basseres et al., 2010; Meylan et al., 2009).

The aim of this thesis is to study the role of TNF-α produced by pre-malignant epithelial cells in the early stages of pancreatic tumour progression, hypothesising that autocrine effects of this cytokine can promote pancreatic carcinogenesis.

The *kras*^{G12D} genetic mouse model of pancreatic carcinogenesis was used as this model recapitulates PanIN progression with a low penetrance of the invasive form. To study the role of the TNF-α/IKK2 signalling pathway on pancreatic carcinogenesis, new genetic mouse models were generated combining mutant *kras* expression with *ikk2* or *tnfa* genetic deletion in pancreatic epithelial cells. *In vitro* studies using cell lines generated from PanIN bearing animals were performed to investigate the molecular mechanisms downstream of the TNF-α/IKK2 pathway that may contribute to the carcinogenic process. This work focused on the cooperation between the TNF-α/IKK2 and the Notch signalling pathways, which suppresses the expression of anti-inflammatory proteins and promotes pancreatic carcinogenesis in mice.

CHAPTER TWO: MATERIALS AND METHODS

Buffer recipes can be found in Appendix A: Solutions.

2.1 Transgenic animals

Mice were maintained in the Biological Services Unit of Barts Cancer Institute, Queen Mary, University of London, in a specific pathogen-free environment and used according to established institutional welfare guidelines under the authority of a UK Home Office project licence (PL 70/6578) (Guidance on Operation of Animals Scientific Procedures - Act 1986). Experimental protocols and procedures were also approved by the UK Home Office and performed under the following personal licence number: PIL 70/21874.

2.1.1 Mouse models and breeding

kras$^{+/LSL\text{-}G12D}$, *pdx1-cre*, *tnfa*$^{flox/flox}$ and *ikk2*$^{flox/flox}$ strains were interbred to obtain *kras*^{G12D}, *kras*^{G12D}/*tnfa*$^{\Delta Pdx}$ and *kras*^{G12D}/*ikk2*$^{\Delta Pdx}$ triple mutant mice on a mixed C57BL/6/129/SvJae background (See Figure 3.1 for breeding plan). Dr Eleni Maniati developed the *kras*^{G12D}/*tnfa*$^{\Delta Pdx}$ mice (Barts Cancer Institute, Queen Mary, University of London, London, UK). The *ikk2*$^{flox/flox}$ mice were kindly provided by Dr Toby Lawrence (Inflammation Biology Group, Centre d'Immunologie Marseille - Luminy, Parc Scientifique de Luminy Case 906, 13288 Marseille, France) (Fong *et al.,* 2008). The *tnfa*$^{flox/flox}$ mice were a kind gift from Dr Sergei Nedospasov (Laboratory of Molecular Immunology, Engelhardt Institute of Molecular Biology, 119991, Moscow, Russia) (Grivennikov *et al.,* 2005). The *kras*$^{+/LSL\text{-}G12D}$ and *pdx1-cre* strains were generated and provided by Dr David Tuveson (Cancer Research UK Cambridge Research Institute, Robinson Way, Cambridge CB2 0RE, UK) (Hingorani *et al.,* 2003; Johnson *et al.,* 2001). The *Mx-cre* mice (The Jackson Laboratory - stock number 005673 - BALB/cJ background) were interbred with the *tnfa*$^{f/f}$ (Grivennikov *et al.,* 2005) to generate *tnfa*$^{f/f}$/*Mx-cre* mice on a mixed

C57BL/6/BALB/cJ background. The *ROSA26-LSL-EYFP* mice (The Jackson Laboratory - stock number 006148 - C57BL/6 background) were crossed with the *kras*^{G12D} mice to obtain the composant mutant strain on a mixed C57BL/6/129/SvJae background. All mice were genotyped at weaning by a commercial vendor (Transnetyx, Tennessee, USA).

2.1.2 Chimeras

To delete *tnfa* expression in the bone marrow-derived cells, *tnfa*$^{f/f}$*/Mx-cre* mice were injected intravenously once a day, for 3 days with poly(I:C) at 5 µg/g body weight (Invivogen - tlrl-picw). *tnfa*$^{f/f}$*/Mx-cre* mice treated with poly(I:C) are abbreviated as *tnfa*$^{\Delta Mx}$ mice. Bone marrow-derived cells were isolated from the bones of *tnfa*$^{f/f}$ and *tnfa*$^{\Delta Mx}$ mice (described in section 2.2.3.1). Six weeks old *kras*^{G12D} and *kras*^{G12D}*/tnfa*$^{\Delta Pdx}$ female mice (n=10 per strain) were irradiated with a single dose of 10 Gy using a linear accelerator with 15 MV nominal photon energy and set to deliver a dose rate of 3.6 Gy/min. The irradiated mice were left to rest for 6 hours and were then reconstituted with 5x10^6 bone marrow-derived cells from *tnfa*$^{f/f}$ or *tnfa*$^{\Delta Mx}$ mice injected intravenously. To reduce the risk of infection following irradiation, mice were treated with a fluoroquinolone antibiotic (enrofloxacin - Baytril) for 4 weeks (0.56 mg/ml in drinking water). To allow complete reconstitution of the immune system and repopulation of the organs with immune cells, mice were maintained for 8 weeks in individually ventilated microisolator cages and were given sterilised food and acidified sterile water. Peripheral leukocytes from transplanted mice were collected and cultured *in vitro* to measure TNF-α secretion upon LPS stimulation by ELISA (see sections 2.2.3.2 and 2.5.4). Chimera mice were generated with the help of Dr Thorsten Hagemann, Barts Cancer Institute, Queen Mary, University of London, London, UK.

2.1.3 *In vivo* cell proliferation

To detect proliferating cells in the pancreas, *kras*, *kras*^{G12D} and *kras*^{G12D}/*ikk2*$^{\Delta Pdx}$ mice were injected intraperitoneally with 250 µl of 5-bromo-2'-deoxyuridine (BrdU - Sigma-Aldrich - B9285) at 50 µg/g of total body weight. 90 minutes after BrdU injection, mice were sacrificed and each pancreas was processed and stained as described in sections 2.8.1 and 2.8.4.2. BrdU is a synthetic nucleoside which is an analogue of thymidine and which can therefore be incorporated into the newly synthesised DNA of live replicating cells.

2.1.4 *In vivo* experiments with small inhibitors

In the *in vivo* experiments described, mice were treated with the following compounds:

- Rosiglitazone (Cayman Chemical - 71740) was incorporated into standard rodent chow at 3 mg/kg/day.
- Notch antagonist N-[N-(3,5-difluorophenacetyl)-L-alanyl]-S-phenylglycine t-butyl ester (DAPT/γ secretase inhibitor IX) (Cayman Chemical - 13197) was injected intraperitoneally at 100 mg/kg/day.
- Bay11-7082 (Alexis Biochemicals Corporation) was injected intraperitoneally at 10 mg/kg/day.
- Anti-murine-TNF-α (R&D Systems - AB-410-NA) was injected intraperitoneally at 10 mg/kg/day.
- IgG control antibody (R&D Systems - AB-105-C) was injected intraperitoneally at 10 mg/kg/day.

The age of the mice and the duration of treatment varied and are specified in the figure legend of each individual experiment.

2.2 Tissue culture

2.2.1 PanIN and PDAC cell lines

2.2.1.1 Collection and generation

PanIN and PDAC cell lines derived from the different mouse strains were generated by Dr David Tuveson's laboratory as previously described (Schreiber *et al.,* 2004). PanIN cell lines were derived from PanIN lesions with no invasive cancer present within the pancreas of the mouse.

Pancreases from the required mice genotype and age were harvested, minced and digested by incubation in Hank's buffered salt solution (HBSS) with glucose (1 g/l), calcium chloride (0.185 g/l) (Sigma Aldrich - H8264) and complemented with 2 mg/ml of collagenase V (Sigma Aldrich - C9263) for 30 minutes at 37°C. The cell suspension obtained (mainly containing immune cells) was filtered through a 100 µm cell strainer and tissue fragments left in the cell strainer were further digested in 0.05 % w/v Trypsin-EDTA for 2 minutes at 37°C to obtain epithelial cells. Trypsin was inhibited by adding fresh complete Dulbecco's modified Eagle medium (DMEM) supplemented with 10 % v/v foetal calf serum (FCS). The tissue was washed three times with HBSS buffer and the fragments were plated in plastic dishes, previously precoated with rat tail collagen type I at 2.3 mg/ml (BD Biosciences - 354236) in fresh complete medium (DMEM supplemented with 10 % v/v FCS). Monolayers of cells were rapidly obtained and cells were expanded and frozen as described in the next section.

2.2.1.2 Culture conditions

PDAC and PanIN cell lines were maintained in culture with DMEM (PAA - E15-810), 10 % v/v FCS (PAA - A15-102), 1 % v/v penicillin/streptomycin (PAA - P11-010) under sterile conditions at 37°C and in a 5 % v/v CO_2 atmosphere. The cells were passaged and divided twice weekly or when 80 % confluency was reached. All cell-lines were adherent and were detached from the culture flask using Trypsin-EDTA (0.1 % w/v and 0.05 % w/v in PBS respectively) (PAA - L11-003). The cells were washed with phosphate buffered saline (PBS) (PAA - H15-002) to remove any excess FCS. Trypsin-EDTA was added and cells were incubated at 37°C until they were completely detached. The action of Trypsin was stopped by adding fresh complete medium. Cells were centrifuged at 450 x *g* for 5 minutes. Following centrifugation, the supernatant was removed and cells were resuspended in the appropriate culture medium.

To freeze the cells down, cell numbers and viability were determined by counting live cells using a Vi-CELL™ image analyzer (Beckman Coulter). Cells were stained with trypan blue to distinguish the live population from the non-viable cells. Cells were resuspended in fresh complete medium at $4x10^6$ cells/ml. In parallel, a solution of 10 % v/v DMSO (Sigma Aldrich - D2650) in FCS was prepared. This freezing medium was added to the cells (1:1 v/v) and 1 ml of solution was aliquoted into cryovials. Cells were slowly frozen down by incubating them in a freezing container (Mr Frosty - Nalgene®) containing isopropanol, overnight at -80°C. Isopropanol allows an optimal cooling rate of -1°C per minute. Vials can be stored in liquid nitrogen (-196°C), thus retarding the growth of ice crystals. When thawing, the cells should be warmed very quickly in a 37°C water bath to maximize the recovery rate. Once completely melted, cells were diluted into prewarmed to 37°C fresh complete

medium and pelleted by centrifugation at 450 x *g* for 5 minutes in order to remove DMSO, which is toxic to cells. The cells were resuspended in the appropriate culture medium and placed in culture under sterile conditions at 37°C and in a 5 % v/v CO_2 atmosphere.

2.2.2 OP9-DL1 cells

OP9 cells stably transfected with the Notch ligand Delta-like 1 (OP9-DL1) were obtained from Dr Juan-Carlos Zuniga-Pflucker (Schmitt and Zuniga-Pflucker 2002). This mouse bone marrow-derived stromal cell line was co-cultured with cells derived from PanIN bearing *kras*^{G12D}/*tnfa*$^{\Delta Pdx}$ mice. OP9-DL1 stromal cells were cultured in Minimum Essential Medium Alpha (Invitrogen - 12561056), supplemented with 20 % v/v FCS and 1 % v/v penicillin/streptomycin.

2.2.3 Immune cells

2.2.3.1 Collection of bone marrow-derived cells

Donor mice (*tnfa*$^{f/f}$ or *tnfa*$^{\Delta Mx}$) were sacrificed by cervical dislocation and their femurs and tibias were collected in ice-cold PBS. Bones were scraped clean with a scalpel under sterile conditions and the ends of the bones were removed at the epiphyses, also with a scalpel. Holding the shaft of the bone with forceps, PBS was used to flush the bone marrow with a 27G needle. The suspension obtained was washed with PBS and after centrifugation at 450 x *g* for 5 minutes, the cells were resuspended in 5 ml of 1X red blood cell lysis buffer (BD Biosciences - 555899). The action of the lysis buffer was stopped by adding 30 ml of PBS and cells were pelleted by centrifugation at 450 x *g* for 5 minutes. Cells were resuspended in 1 ml of PBS, passed through a 70 µm cell strainer, centrifuged at 450 x *g* for 5 minutes and resuspended at 25x10^6 cells/ml, to be injected into irradiated mice for adoptive transfer (see section 2.1.2).

2.2.3.2 Collection of peripheral blood leukocytes

Mice were anaesthetised with isoflurane (Baxter Healthcare - FDG9623) delivered at 3 % v/v for induction and 1.5 % v/v for maintenance in oxygen. Blood was collected by cardiac puncture using a 27G needle in heparin-loaded syringes (5,000 units/ml) and collection tubes (a drop of this anti-coagulant was sufficient). Mice were sacrificed by cervical dislocation. Under sterile conditions, red blood cells were lysed as described above and peripheral blood leukocytes (PBL) and other immune cells were placed in culture in Petri dishes in complete DMEM. Immune cells were simultaneously treated with LPS (Sigma Aldrich - L2630) at 10 ng/ml for 16 hours to activate them and to induce TNF-α secretion. Supernatants were collected and cell debris, membranes and dead cells were removed by centrifugation at 450 x *g* for 15 minutes at 4°C. Supernatants were stored at - 80°C until TNF-α measurement by ELISA.

2.2.4 Cell culture treatment

Cells derived from PanIN bearing *kras*^{G12D}, *kras*^{G12D}/*ikk2*$^{\Delta Pdx}$ or *kras*^{G12D}/*tnfa*$^{\Delta Pdx}$ mice were plated in complete medium in 6-well plates and left to adhere overnight at 37°C in a 5 % v/v CO_2 atmosphere ($0.3x10^6$ cells per well). The following day, cells were treated with the following compounds:

- Recombinant mouse TNF-α (Peprotech - AF-300-01A) at a final concentration of 1 ng/ml.
- Cycloheximide (Sigma Aldrich - C7698) at a final concentration of 15 µM.
- Recombinant Jagged 2 (R&D Systems - 4748-JG-050) at a final concentration of 20 µg/ml.
- L685458 (γ-secretase inhibitor) (5S)-(tert-Butoxycarbonylamino)-6-phenyl-(4R)-hydroxy-(2R)-benzylhexanoyl)-L-leucy-L-phenylalaninamide (Shearman *et al.,* 2000) (Sigma Aldrich - L1790) at a final concentration of 5 µM.

- Bay11-7082 (NF-κB inhibitor) ((E)-3-[4-methylphenylsulfonyl]-2-propenenitrile) (Pierce *et al.,* 1997) (Sigma Aldrich - B5556) at a final concentration of 1 μM.

The origin of the cells used and the duration of treatment varied and are specified in the figure legend of each individual experiment.

2.3 Cloning and transfection of cells

2.3.1 Plasmid constructs

The plasmids used are described in Table 2.1 below and their map can be found in Appendix B: Plasmid Maps.

pCR-FLAG-IKK2 (Addgene plasmid 15465) and pCR-FLAG-IKK2-KM (Addgene plasmid 15466) were received as a stab culture from Addgene (Nakano *et al.,* 1998). pDEST40-NICD-V5 plasmid was kindly provided by Dr Michael Potente, Goethe University, Frankfurt, Germany.

Plasmid	Insert	Fusion Protein	*E. coli* resistance	Transfection reagent
pCR-FLAG-IKK2	IKK2	FLAG	Ampicillin	FuGENE® HD
pCR-FLAG-IKK2-KM	IKK2-KM	FLAG	Ampicillin	FuGENE® HD
pDEST40-NICD-V5	NICD	V5	Ampicillin	FuGENE® HD

Table 2.1: Plasmid constructs used and their characteristics

Table describes the plasmids used, the insert, the protein fusion, the gene of selection and the transfection reagent used.

2.3.2 Transformation of bacteria

JM109 competent *E. coli* cells (Promega - L2001) were transformed by a standard heat shock protocol. 100 µl of competent cells were used per transformation reaction. pDEST40-NICD-V5 plasmid was received on Whatman paper and was reconstituted by incubation in 50 µl of 10 mM Tris, pH 7.6 for 15 minutes at room temperature. 10 µl of this supernatant was added to the competent bacteria (or 10 µl of water as negative control) and incubated on ice for 30 minutes. A brief heat shock at 42°C was performed for 45 seconds and samples were incubated on ice for 5 minutes. 400 µl of lysogeny broth (L. broth) was added and samples were incubated for 1 hour at 37°C with shaking (225 rpm). Samples were spread on L. agar plates

containing ampicillin at a final concentration of 60 µg/ml. Plates were incubated overnight at 37°C to allow individual clones to develop. The following day, colonies were picked with sterile pipette tips and grown in 5 ml of L. broth, containing ampicillin at a final concentration of 60 µg/ml for 16 hours at 37°C with shaking at 225 rpm. 750 µl of bacterial culture was added to 150 µl of autoclaved 70 % v/v glycerol for long-term storage at -80°C (glycerol stock). The remaining bacterial culture was pelleted by centrifugation for 10 minutes at 4,500 x *g* and plasmid DNA was isolated using a mini-prep kit as described in section 2.3.4.

The plasmids pCR-FLAG-IKK2 and pCR-FLAG-IKK2-KM were received as a stab culture. Samples were streaked on L. agar plates containing ampicillin at a final concentration of 60 µg/ml, allowing isolation of a single colony, and the same steps as above were followed.

2.3.3 Recovery of bacteria from frozen glycerol stocks

Using a sterile pipette tip, a small amount of frozen stock was added to 5 ml of L. broth medium with ampicillin (60 µg/ml) and cultured for 16 hours at 37°C with shaking at 225 rpm. Plasmid DNA was extracted with a miniprep kit (Qiagen - 27106) (see section 2.3.4.1) or further expanded into 150 ml of L. broth with ampicillin (60 µg/ml). In the latter case, bacteria were cultured for a further 16 hours at 37°C with shaking at 225 rpm and plasmid DNA was extracted with a maxiprep kit (Qiagen - 12262) (see section 2.3.4.2).

2.3.4 Plasmid DNA extraction

2.3.4.1 Miniprep

Plasmid DNA from *E. coli* bacteria was extracted using the QIAprep® Spin Miniprep Kit (Qiagen - 27106). Bacterial cultures were pelleted by centrifugation for

10 minutes at 4,500 x *g* and after removing the L. broth supernatant, the bacteria pellet was resuspended in 250 µl buffer P1. Bacteria were lysed in alkaline solution with 250 µl buffer P2. Buffer N3 was added to neutralise the samples and therefore stop the lysis process but also allow plasmid DNA renaturation. Tubes were thoroughly mixed by inversion until a white precipitate containing bacteria and genomic DNA formed. This precipitate was removed by centrifugation for 10 minutes at 16,100 x *g* and the supernatant, containing the plasmid DNA, was applied to a column containing a DNA binding matrix. Columns were then washed with two different buffers: PB (500 µl, isopropanol solution) and PE (750 µl, ethanol based solution). Each buffer was applied to the column and eliminated via a centrifugation step (1 minute at 16,100 x *g*). Plasmid DNA was finally eluted by adding 50 µl of deionised water to the spin column and centrifuging for 1 minute at 16,100 x *g* into a clean 1.5 ml centrifuge tube. Plasmid DNA concentration was determined using the ND-100 spectrophotometer (Nanodrop Technologies).

2.3.4.2 Maxiprep

The QIAfilter™ Plasmid Maxi Kit (Qiagen - 12262) was used to prepare high amounts of plasmid DNA (up to 500 µg for high-copy plasmids). Bacterial cultures were pelleted by centrifugation for 15 minutes at 6,000 x *g*. The bacterial pellet was resuspended in 10 ml of buffer P1. Once fully resuspended, bacteria were lysed with 10 ml of buffer P2 for no more than 5 minutes at room temperature. To neutralise the cells, 10 ml of pre-chilled buffer P3 was added. Tubes were thoroughly mixed by inversion until a white material had formed and the lysate was no longer viscous. To prevent later disruption of the precipitate layer, lysates were immediately transferred into a closed QIAfilter cartridge and incubated for up to 10 minutes at room temperature, allowing the precipitate to form a layer on top of the solution. The cap from the QIAfilter cartridge was removed and with a plunger, the cell lysate was

filtered into a QIAGEN-tip, which was previously equilibrated with 10 ml of buffer QBT. Once the lysate entered the resin by gravity flow, the QIAGEN-tip was washed twice with 30 ml of buffer QC. Plasmid DNA was eluted from the resin with 15 ml of buffer QF and precipitated with 0.7 volumes (10.5 ml) of isopropanol. DNA was pelleted by centrifugation at ≥ 15,000 x *g* for 30 minutes at 4°C. After carefully decanting the supernatant, DNA pellets were washed with 70 % v/v ethanol, air-dried and redissolved in a suitable volume of slightly alkaline TE buffer. Plasmid DNA concentration was determined using the ND-100 spectrophotometer (Nanodrop Technologies).

2.3.5 Integrity of the plasmid constructs

The integrity of the plasmid constructs pCR-FLAG-IKK2 and pCR-FLAG-IKK2-KM was assessed by digesting the DNA with the appropriate restriction enzymes and buffers (New England BioLabs - NEB) to cut out bands which depending in the size would indicate the presence of the insert. The following were incubated for 2 hours at 37°C and 15 minutes at 65°C (for heat inactivation) and for 5 minutes on ice.

200 ng plasmid DNA

2 µl NEBuffer 4 (NEB - B7004)

1 µl EcoR1 (NEB - R0101)

1 µl Xho1 (NEB - R0146)

0.5 µl BSA (100X) (NEB - B9001)

deionised water up to 20 µl final volume

Plasmid DNA fragments were separated on an agarose gel as described in section 2.4.2.

2.3.6 Transcient transfection of target cells with FuGENE®HD

The pCR-FLAG-IKK2 and pCR-FLAG-IKK2-KM vectors were transfected into target cells derived from PDAC bearing *kras*^{G12D} mice using the transfection reagent FuGENE® HD (Promega - E2311).

Cells were plated in penicillin/streptomycin-free medium in 6-well plates and left to adhere overnight at 37°C in a 5 % v/v CO_2 atmosphere ($0.5x10^6$ cells per well). When cells reached 80 % confluency, transfection complexes were prepared by diluting 5 µg of DNA into 135 µl of OptiMEM® reduced serum medium (Invitrogen - 31985.047) and 15 µl of FuGENE® HD (3:1 ratio µl FuGENE® HD:µg DNA) and incubated for 20 minutes at room temperature. Complexes were added drop-wise onto the cells and the preparations were gently mixed by rocking the plates. Cells were incubated for 24 to 36 hours at 37°C in a 5 % v/v CO_2 atmosphere. Proteins were extracted as described in section 2.5.1.

2.3.7 Silencing genes *in vitro* - small interference RNA (siRNA)

RNA interference (RNAi) is a gene-silencing pathway active in most eukaryotes cells (Fire *et al.,* 1998), which uses short interference RNA (siRNA) to target specific mRNA degradation.

Commercially validated *rbpj-*, *ikk1-*, *ikk2-*, *nemo-* and *hes1*-specific individual siRNAs and non-targeting control individual siRNAs were purchased from Dharmacon (3 individual siGENOME siRNAs per target gene). These were resuspended in sterile, nuclease-free water at a final concentration of 20 µM.

The siRNAs were transfected into target cells derived from PDAC bearing *kras*^{G12D} mice using the transfection reagent Lipofectamine™ RNAiMAX (Invitrogen - 13778-

075), according to the manufacturer's instructions. Cells ($0.1x10^6$ cells in 5 ml) were plated in penicillin/streptomycin-free medium in small Petri dishes (60 mm ∅) and left to adhere overnight. When the cells had reached 50-70 % confluency, transfection complexes were prepared by adding 150 pmol of siRNA to 500 µl of OptiMEM® reduced serum medium (Invitrogen - 31985-047) and incubating this solution for 5 minutes at room temperature. In parallel, 10 µl of Lipofectamine™ RNAiMAX were also diluted in 500 µl of OptiMEM® reduced serum medium and incubated for 5 minutes at room temperature. The siRNA/OptiMEM® mix was slowly added to the centre of the diluted Lipofectamine™ RNAiMAX and incubated for 20 minutes at room temperature. Complexes were added drop-wise onto the cells and the preparations were gently mixed by rocking the plates. This gave a final volume of 6 ml and a final siRNA concentration of 25 nM. Cells were incubated for 24 to 36 hours at 37°C in a 5 % v/v CO_2 atmosphere. RNA extraction was performed as described in section 2.4.3.

2.3.8 Luciferase reporter assay

For *hes1* reporter gene assays, primary *kras*^{G12D}/*tnfa*$^{\Delta Pdx}$ and *kras*^{G12D}/*ikk2*$^{\Delta Pdx}$ cells were transfected in duplicate in 24-well plates. A *hes1* luciferase reporter construct containing the -194 to +160 promoter fragment of the *hes1* gene inserted upstream of the luciferase gene in pGL2 (gift from Prof Sangram Sisodia, Department of Neurobiology, The University of Chicago, Chicago, USA) (Berechid *et al.,* 1999; Jarriault *et al.,* 1995) and an internal control plasmid encoding renilla luciferase pRL-CMV (Promega - E2261) were used. These reporters were transfected using Lipofectamine™ LTX (Invitrogen - 15338-100). On the next day, cells were stimulated with rTNF-α for 6 h, and cell lysates were prepared and analysed for firefly and renilla luciferase activity with the Dual-Luciferase Reporter Assay System (Promega - E1910).

The reporter construct allows the expression of the firefly luciferase from the firefly *Photinus pyralis* while the internal control allows the expression of the renilla luciferase from the anthozoan coelenterate *Renilla reniformis*. These enzymes do not catalyse the same substrate: with the firefly luciferase, the light is produced by oxidation of luciferine and this reaction involves ATP and Mg^{2+}. The renilla luciferase produces light after oxydising coelenterazine, in an ATP and Mg^{2+} independent manner (Nieuwenhuijsen *et al.,* 2003). As these enzymes catalyse two different substrates, their activity can be measured in a single reaction. The activity of the reporter is correlated with the effect associated with the experimental conditions while the activity associated with the control provides a baseline response. Results are shown as firefly luciferase activity normalised to renilla luciferase activity, to minimise experimental variability due to cell viability and/or transfection efficiency.

For cell lysate preparation from adherent cells, the medium was aspirated and the cells washed twice with ice-cold PBS. Cells were treated with lysis buffer for 15 minutes at room temperature on a rocking platform. Cells were harvested using a cell scraper and membranes, debris and DNA were eliminated by centrifugation at 16,100 x *g* for 15 minutes at 4°C. Cleared lysates (20 µl) were transferred into tubes containing 100 µl of Luciferase Assay Substrate and firefly luciferase activity was measured using a luminometer (Tecan - Infinite® F200). The reaction was then quenched and the renilla luciferase activity was simultaneously initiated by adding 100 µl Stop & Glo® reagent. Renilla luciferase activity was measured using the same luminometer.

The *pparg* luciferase reporter gene and *hes1* plasmid (gifted by Prof Marc Montminy Salk Institute for Biological Studies, La Jolla, USA) were previously described

(Herzig *et al.,* 2003). Cells were transfected with the *pparg* luciferase reporter plasmid and an expression plasmid encoding *hes1* or a control vector (as described for *hes1* reporter gene assays). Luciferase activity was measured in presence of luciferin at 150 µg/ml final concentration (Caliper Life Science - 122796) using a luminometer (Tecan - Infinite® F200) and was proportional to the activity of the promoter.

2.4 Nucleic acids

2.4.1 Nucleic acid quantification

DNA and RNA concentrations were determined using the ND-100 spectrophotometer (Nanodrop Technologies). To assess the purity of DNA and RNA, two ratios of absorbance were considered:

- A ratio of sample absorbance at 260 and 280 nm (260/280). A value of ~ 1.8 for DNA or ~ 2.0 for RNA are generally accepted as "pure". A lower value may indicate the presence of protein, phenol or other contaminants absorbing close to the 280 nm region.
- A ratio of sample absorbance at 260 and 230 nm (260/230). The 260/230 values for "pure" nucleic acid are often higher than the respective 260/280 values. They are usually between 1.8 and 2.2. A lower ratio may indicate the presence of co-purified contaminants.

2.4.2 Agarose gel electrophoresis

In order to visualise DNA fragments, agarose gel electrophoresis was used. Typically, 1.2 % w/v agarose gels were prepared by melting the agarose (Invitrogen - 16500-500) in 1X TAE buffer, adding GelRed™ Nucleic Acid Gel Stain (Cambridge Bioscience - BT41003) at a final concentration of 4 % v/v and cooling the mix to 55°C in a water bath. The gel was allowed to solidify in a tray with combs inserted for sample loading and equilibrated in 1X TAE buffer. 6X loading buffer was added to the samples to a final concentration of 1X and the samples were loaded into the gel and allowed to run at 90 V for 30 minutes (6 V/cm). DNA samples and a DNA ladder (Invitrogen - 15615-016) were visualised using a UV lamp and photographed (Alpha Innotech - Red™ Imaging System).

2.4.3 Total RNA isolation - Trizol

For RNA isolation from adherent cells, medium was first removed and cells were washed once with PBS. Cells were detached with Trypsin-EDTA (PAA - L1-003) for 3 minutes at 37°C and the action of Trypsin was stopped by adding fresh complete medium. Cells were then centrifuged at 300 x *g* for 5 minutes. Following centrifugation, the supernatant was removed leaving only approximately 100 µl (by eye) of medium, in the tube, to which 900 µl of Trizol (Sigma Aldrich - T9424) was added. Once in Trizol, cell suspensions were mixed well and incubated at 4°C for 10 minutes or stored at - 80°C for long term storage. After this incubation, 200 µl of chloroform ($CHCl_3$) was added. The sample was mixed well and incubated at 4°C for another 10 minutes and centrifuged at 16,100 x *g* for 15 minutes at 4°C to separate the RNA, in the aqueous phase, from the chloroform, which remained in the bottom organic phase. The supernatant (~ 500 µl) was transferred to a fresh tube containing 1.2 µl of RNAse-free glycogen at 5 mg/ml (Ambion - AM9510) to facilitate its pelleting and mixed well. An equal volume (500 µl) of isopropanol was added to precipitate the RNA and incubated at 4°C for 5 minutes, centrifuged at 16,100 x *g* for 15 minutes at 4°C. The RNA pellet was washed with 70 % v/v ethanol and either stored at - 80°C as a pellet or resuspended in 40 µl RNAse-free water.

2.4.4 DNase treatment of RNA

In order to remove contaminating DNA, all RNA samples used for cDNA preparation were treated with RQ1 DNAse (Promega - M6101), according to the manufacturer's instructions. DNAse was added to the RNA preparation (at least one unit of enzyme/µg of RNA) and incubated in a total volume of at least 50 µl for 30 minutes at 37°C, in the presence of the appropriate enzyme buffer. Following this treatment, the RNA was purified by adding an equal volume of Phenol:Chloroform:Iso-amyl alcohol (pH 5.2, Sigma Aldrich - P1944), mixing well

and centrifuging at 16,100 x *g* for 5 minutes to separate the aqueous and organic phases, respectively containing RNA and proteins. The upper phase was transferred to a fresh microfuge tube. RNA precipitation was performed by adding sodium acetate (3 M, pH 5.2 - 10 % of total volume of sample) and mixing well, followed by the addition of 2x volumes of ice-cold 100 % v/v ethanol. The sample was well mixed and RNA was allowed to precipitate at 4°C for 15 to 30 minutes. The RNA pellet was recovered by centrifugation at 16,100 x *g* for 15 minutes at 4°C and resuspended in 40 µl RNase-free water.

2.4.5 Total RNA isolation - RNeasy technology

2.4.5.1 From adherent mammalian cells

To obtain high-quality RNA, the RNeasy technology was used to purify RNA from adherent mammalian cells, according to the manufacturer's instructions (Qiagen - 74104).

Cells were harvested as described in section 2.4.3 and the pelleted cells were detached thoroughly by flicking the tube and finally disrupted by adding 600 µl of buffer RLT. After mixing well and to ensure a good homogenisation, the lysate was directly pipetted into a QIAshredder spin column (Qiagen - 79654), placed in a 2 ml collection tube and centrifuged at 16,100 x *g* for 2 minutes. To provide appropriate binding conditions, 600 µl of 70 % v/v ethanol was added to the homogenised lysate and mixed well by pipetting. The sample was applied to an RNeasy spin column, where the total RNA binds to the membrane of the column and contaminants are efficiently washed away after centrifugation at 11,200 x *g* for 30 seconds (discarded in the flow-through). Membrane-bound RNA was then washed with 350 µl of buffer RW1 after centrifugation at 11,200 x *g* for 30 seconds (flow-through discarded). To digest contaminating DNA, the RNase-free DNase Set (Qiagen - 79254) was used,

applying 70 µl of buffer RDD and 10 µl of DNase onto the membrane for 15 minutes at room temperature. The spin column membrane was washed a second time with 350 µl of buffer RW1 after centrifugation at 11,200 x *g* for 30 seconds (flow-through discarded). The spin column membrane was again washed twice with 500 µl of buffer RPE after centrifugation at 11,200 x *g* for 30 seconds (flow-through discarded). To eliminate any possible carryover of buffer RPE or any residual flow-through, the RNeasy spin column was placed into a new 2 ml collection tube and centrifuged at 16,100 x *g* for 1 minute. High-quality RNA was eluted in 30 µl of RNase-free water by centrifugation at 11,200 x *g* for 1 minute. RNA was stored at - 80°C.

2.4.5.2 From animal tissues

Pancreases from age-matched mice were harvested in a cryovial and snap frozen by immersion in liquid nitrogen. Fractions of these pancreases were disrupted and homogenised by placing them into gentleMAC™ M tubes (Miltenyi Biotec - 130-093-236) with 1 ml of buffer RLT (Qiagen - *74104*) supplemented with *4* % v/v β-mercaptoethanol. Samples were processed using the gentleMACS dissociator (Miltenyi Biotec) set to the RNA-02 program. The lysate was centrifuged at 1,200 x *g* for 1 minute and 350 µl of the supernatant was directly pipetted into a QIAshredder spin column (Qiagen - *79654*) and placed in a 2 ml collection tube. The rest of the lysate was stored at - 80°C. After one centrifugation at 16,100 x *g* for 2 minutes and another one for 3 minutes to remove tissue debris, the supernatant was transferred into a new 1.5 ml microfuge tube. The same volume of *70* % v/v ethanol was added to the homogenised lysate and mixed well by pipetting. The sample was applied to an RNeasy spin column and the RNA was extracted following the same steps described above in the section 2.4.5.1.

2.4.6 cDNA synthesis

To perform cDNA synthesis, all RNA samples were treated with M-MLV Reverse Transcriptase (Promega - M1705), according to the manufacturer's instructions. 1.2 µg of DNAse treated RNA was added to 1 µg of random primers (Invitrogen - 48190-011) in a final volume of 14 µl. Samples were incubated at 75°C for 5 minutes to allow primer annealing and to remove any secondary structures, and then cooled on ice for 5 minutes to prevent the reformation of these structures. 200 units of M-MLV RT were then added to the RNA along with 5 µl of the appropriate buffer (Promega - M5313), 5 mM dNTPs (Applied Biosystems - N8080007) and 0.6 µl of RNAsin Ribonuclease inhibitor (Promega - N2111). Samples were incubated at room temperature for 10 minutes followed by 50 minutes at 40°C for cDNA synthesis. The final sample volume was adjusted to 100 µl with deionised water and stored at - 80°C.

2.4.7 Quantitative Real-Time PCR (qRT-PCR)

The references of the assays used for each gene of interest are described in Appendix C: Quantitative RT-PCR assays. Each assay contains one gene specific fluorogenic probe, two primers and the AmpliTaq Gold® DNA polymerase and were purchased from Applied Biosystems. The first two letters in the assay ID represent the species (Mm for *Mus musculus*) and the suffix designates the assay placement: "_m" indicates that the probe crosses over an exon junction and will therefore not detect genomic DNA; "_s" indicates that the probe and primers will bind specific sequences within a single exon, allowing genomic DNA detection ; "_g" indicates that the probe and the primers of this assay may bind specific sequences within a single exon.

2.4.7.1 TaqMan® qRT-PCR - Principle of the method

qRT-PCR was developed to allow the quantitation of different mRNA expression levels but also to increase the sensitivity of detection when small amounts of RNA are

used. Various fluorescent chemistries exist to detect PCR products, the most well-known of which are TaqMan® and SYBR®-Green.

TaqMan® chemistry uses a fluorogenic probe coupled to a reporter fluorescent dye on the 5' end (usually FAM or VIC) and a quencher fluorescent dye on the 3' end (usually TAMRA). When the probe is intact, fluorescence resonance energy transfer (FRET) occurs, and the quencher reduces the fluorescence emitted by the reporter. However, when annealed to its target, the probe is cleaved by the 5' nuclease activity of the DNA polymerase, separating the dyes and increasing the reporter dye signal. The fluorescent intensity measured is therefore proportional to the amount of amplicon produced.

2.4.7.2 TaqMan® qRT-PCR - Protocol

qRT-PCR reactions were prepared by adding 500 ng of cDNA (2 µl at 250 ng/µl), 10 µl master mix (Applied Biosystems - 4364340), 1 µl assay for the gene of interest and 1 µl assay for the eukaryote 18S gene (Applied Biosystems - 4310893E) and deionised water to a final volume of 25 µl. The reaction was set up in a MicroAmp optical 96-well reaction plate (Applied Biosystems - 4306737) and amplified in an ABI Prism 7700 sequence detection system (Applied Biosystems). Data were collected and analysed using the SDS software, version 1.9.1, (Applied Biosystems) in order to determine Ct (threshold cycle) values for each sample. Induction values were calculated using the formula $2^{-\Delta\Delta Ct}$. ΔCt represents the difference between the Ct values of the target genes and Ct values of the reference gene 18S. ΔΔCt represents the difference between the ΔCt values of each sample and the ΔCt of the reference sample (i.e. non-stimulated cells). The following thermal cycling conditions were used:

Step 1:	50°C for 2 minutes
Step 2:	95°C for 10 minutes
Step 3:	95°C for 15 seconds
Step 4:	60°C for 1 minute
Step 5:	Repeat steps 3 and 4 for 39 cycles

2.5 Protein analysis

2.5.1 Protein extraction

Procedures were carried out on ice, with ice-cold buffers and materials.

2.5.1.1 From adherent mammalian cells

For total protein extraction from adherent cells, medium was aspirated and cells were washed twice with ice-cold PBS. Cells were treated with 80 µl of complete lysis buffer per well for 30 minutes at 4°C. Cells were harvested using a cell scraper and the membranes, debris and DNA were eliminated by centrifugation at 16,100 x *g* for 15 minutes at 4°C. Supernatants were transferred into new tubes and stored at - 80°C. Protein concentration was measured as described in section 2.5.2.

2.5.1.2 From animal tissues

Pancreases from age-matched mice were harvested in a cryovial and snap frozen by immersion in liquid nitrogen. Fractions of these pancreases were disrupted and homogenised by placing them into gentleMAC™ M tubes (Miltenyi Biotec - 130-093-236) with complete lysis buffer (up to 15 mg of tissue was used per ml of lysis buffer). Samples were processed using the gentleMACS dissociator (Miltenyi Biotec) set to the Protein-01 program. The lysate was centrifuged at 4,000 x *g* for 5 minutes at 4°C. Supernatants were transferred into new tubes and stored at - 80°C. Protein concentration was measured as described in section 2.5.2.

2.5.2 Protein quantification

For each sample, the concentration of protein was determined using the bicinchoninic acid (BCA) protein assay. This method combines the reduction of Cu^{2+} to Cu^{+} by proteins in an alkaline medium (the biuret reaction) with the highly sensitive and selective colorimetric detection of the cuprous cation (Cu^{+}) using bicinchoninic acid.

A purple-coloured reaction product is formed by the chelation of two molecules of BCA with one cuprous cation. This water-soluble complex exhibits a strong absorbance at 562 nm that is nearly linear with increasing protein concentrations. Bovine Serum Albumin (BSA) standard stock solution was diluted in PBS to final concentrations ranging from 0 to 10 mg/ml to create a standard curve. In a 96-well plate, 10 µl of BSA standard, sample or control were pipetted. Working reagent was prepared by combining 50 parts BCA solution (Sigma Aldrich - B9643-L) with one part of Copper (II) sulfate solution (Sigma Aldrich - C2284). This working reagent was dispensed into each well (200 µl) and samples were incubated at 37°C for 30 minutes. The optical density (OD) was read by spectrophotometry at 595 nm and the protein concentration (mg/ml) of each sample was calculated by comparison with the BSA standard curve.

2.5.3 Western blot

To analyse and identify several proteins within a sample, they first need to be denatured chemically and by heating, and then separated according to their molecular weight in a Bis-Tris buffered sodium dodecyl sulfate (SDS) polyacrylamide gel under an electric field. Higher concentrations of acrylamide in these gels will lead to better separation of small proteins. Proteins are then transferred onto a polyvinylidine fluoride (PVDF) membrane to enable detection using antibodies.

Resolving and stacking gels were prepared to the desired specification using 40 % w/v 19:1 acrylamide:bis-acrylamide (Fisher Scientific - ELR/138/010H), Tris HCl and SDS. Gels were polymerised by the addition of ammonium persulphate (APS - Sigma-Aldrich - A3678) and tetramethylethylenediamine (TEMED - Sigma-Aldrich - T8133). Gel formulations are summarised below in Table 2.2 and Table 2.3.

Resolving Gel	8 %	10 %	12 %
H_2O	5.3 ml	4.8 ml	4.3 ml
40 % acrylamide	2 ml	2.5 ml	3 ml
1.6 M Tris HCl pH 8.8	2.5 ml	2.5 ml	2.5 ml
10 % SDS	100 µl	100 µl	100 µl
10 % APS	100 µl	100 µl	100 µl
TEMED	20 µl	20 µl	20 µl

Table 2.2: Formulation of resolving gels

Table describes the formulation for 8 %, 10 % and 12 % w/v acrylamide resolving gels.

Stacking Gel	4 %	6 %
H_2O	2.9 ml	3.1 ml
40 % acrylamide	0.75 ml	0.5 ml
1.6 M Tris HCl pH 8.8	1.25 ml	1.25 ml
10 % SDS	50 µl	50 µl
10 % APS	50 µl	50 µl
TEMED	5 µl	5 µl

Table 2.3: Formulation of stacking gels

Table describes the formulation for 4 % and 6 % w/v acrylamide stacking gels.

Cell lysates were diluted in cell lysis buffer to a final concentration of 1 µg/µl. 4X lithium dodecyl sulfate (LDS) sample buffer was added to the sample to a final concentration of 1X. Samples were then heated to 95°C for 10 minutes followed by brief centrifugation at 12,000 x *g* for 30 seconds. After cooling on ice, denatured samples were loaded into the gel. Prestained molecular weight standards (SeeBlue Plus2 Pre-Stained Standards - Invitrogen - LC5925) were also run on every gel to monitor electrophoresis, and were used to calibrate the mobility and hence apparent mass (kDa) of proteins of interest. Gels were run by electrophoresis in 1X running buffer for 15 minutes at a constant voltage of 90 V, and then for 1 hour and 30 minutes at a constant voltage of 120 V (Mini-PROTEAN Tetra Electrophoresis System - BioRad - 165-8029).

Resolved proteins were transferred to PVDF membranes (PerkinElmer - NEF1002001PK) by tank transfer (Mini Trans-Blot Cell - BioRad - 165-8029). PVDF membranes are hydrophobic and need to be hydrated in methanol for 1 minute followed by a rinse in 1X transfer buffer. The transfer cassette, comprising pre-equilibrated gel and PVDF membrane, was sandwiched between chromatography paper (Grade 3MM Chr - Whatman - 30306189) and Scotch-Brite pads. The cassette was placed in a transfer tank, immersed in transfer buffer, and electrotransfer was performed at a constant voltage of 75 V for 1 hour and 30 minutes.

To prevent non-specific antibody binding, the membranes were blocked with 5 % w/v milk powder in 1X tris buffered saline (TBS) with 0.1 % v/v Tween-20 (TBS/T) for 45 minutes at room temperature on a rocking platform. Primary antibodies were diluted in antibody dilution buffer and applied to the membrane overnight at 4°C or for 1 hour at room temperature. Membranes were washed three times for 5 minutes each wash in TBS/T and then incubated for 45 minutes in horseradish peroxidase (HRP)-conjugated secondary antibodies (Amersham ECL™-HRP Linked Secondary Antibodies - GE Healthcare) in TBS/T (Table 2.5). After again washing the membrane as described earlier, immunodetection was carried out by adding a substrate for the HRP (Amersham ECL™ Western Blotting Detection Reagents - GE Healthcare - RPN2106) followed by an exposure onto Super RX autoradiography films (Fujifilm - P10M000266A) to detect the light emitted. The HRP enzyme catalyses the oxidation of luminol to 3-aminophthalate and this reaction is accompanied by emission of low intensity light. However, in the presence of certain chemicals (p-iodophenol), the light emitted can be enhanced to increase the sensitivity of the reaction. This enhancement of light emission is called enhanced

chemiluminescence (ECL). The intensity of light emitted is a measure of the number of enzyme molecules reacting and thus of the amount of protein.

Once the proteins of interest were revealed, membranes could be stripped to remove previous antibodies and could be re-incubated with a different primary antibody. This was done by briefly washing the membranes in water to eliminate the excess of reagent, and then incubating them in Reblot solution (Millipore - 2504) diluted 1:10 in water for 10 minutes at room temperature, followed by a 5 minutes incubation in TBS/T 5 % w/v milk powder. Membranes were blocked in fresh TBS/T 5 % w/v milk powder for 45 minutes and primary and secondary antibodies were then applied as described earlier and proteins were revealed using ECL™ reagent, again as above.

All primary and secondary antibodies used are listed below in Table 2.4 and Table 2.5 respectively.

Antibody	Supplier	Cat. Ref.	Isotype	Dilution Concentration
β-Actin	Sigma Aldrich	A1978	Mouse IgG1	1:10,000
FLAG	Sigma Aldrich	SAB4200071	Rat IgG1	1 µg/ml
HES1	Santa Cruz	Sc-25392	Rabbit IgG	1:500
IKK2	Cell Signaling	2370	Rabbit IgG	1:1,000
NICD	Cell Signaling	2421	Rabbit IgG	1:500
p-Thr	Cell Signaling	9381	Rabbit IgG	1:1,000
p-Tyr	Millipore	05-321	Mouse IgG2b	1:5,000
RBPjκ	Cell Signaling	5442	Rabbit IgG	1:1,000
V5	Invitrogen	R960-25	Mouse IgG2a	1:5,000

Table 2.4: Primary antibodies used for Western blot

Table describes the primary antibodies used for Western blot listing the supplier, catalogue reference (Cat. Ref.) and antibody isotype. Appropriate dilutions and concentrations are shown for each antibody.

Antibody	Supplier	Cat. Ref.	Dilution
anti-goat IgG HRP	Santa-Cruz	Sc-2056	1:5,000
anti-mouse IgG HRP	GE Healthcare	NXA931	1:5,000
anti-rabbit IgG HRP	GE Healthcare	NA934	1:2,000
anti-rat IgG HRP	GE Healthcare	NA935	1:5,000

Table 2.5: Secondary antibodies used for Western blot

Table describes the secondary antibodies used for Western blot listing the supplier, catalogue reference (Cat. Ref.) and appropriate dilutions.

2.5.4 Enzyme-linked immunosorbent assay (ELISA)

Mouse pancreatic cancer cell lines derived from PanIN or PDAC bearing mice were cultured for 24 hours and their supernatants were collected. Cell debris, membranes and dead cells were removed by centrifugation at 450 x *g* for 15 minutes at 4°C. Supernatants were stored at - 80°C until analysis by ELISA.

ELISA kits from BD Biosciences (catalogue numbers in brackets) were used to measure mouse IL-1β (559603), IL-6 (555240), IL-10 (555252), IL-12p40 (55165), IL-12p70 (555256) and TNF-α (558534) protein levels, according to manufacturer's instructions. Mouse IL-23p19/p40 protein levels were detected with an eBiosience ELISA kit (88-7234). ELISA tests were performed in half area 96-well microplates (Fisher - DPS150030Q).

Plates were coated by overnight incubation at 4°C with a capture antibody (50 µl) diluted 1:250 in PBS. The following day, wells were washed three times with 150 µl PBS with 0.05 % v/v Tween-20 (PBS/T). To prevent non-specific binding, blocking was performed by adding 50 µl per well of PBS with 10 % v/v FCS for 1 hour at room temperature. Meanwhile, standards were diluted in blocking solution according to the manufacturer's instruction (usually to final concentrations ranging from 15.6 to

1,000 pg/ml, 31.3 to 2,000 pg/ml or 62.5 to 4,000 pg/ml, depending on the protein measured) to create a standard curve. If necessary, samples were also diluted 1:2 in blocking solution. Wells were washed three times with 150 µl PBS/T and samples, controls and standards were plated in duplicate (50 µl) and incubated for 2 hours at room temperature. Wells were once again washed three times with 150 µl of PBS/T and diluted detection antibody (1:250, 1:500 or 1:1,000 in blocking solution depending on the kit used) was added and incubated for 1 hour at room temperature. Detection antibodies used were biotinylated. The streptavidin-horseradish peroxidase (SAv-HRP) system was used as the detection method. Streptavidin and biotin have a high affinity, allowing the HRP enzyme to be nearby the detection antibody and therefore nearby the protein of interest. Again, depending on the kit used, the SAv-HRP reagent was incubated pre-mixed with the detection antibody or separately for 30 minutes at room temperature. After washing the wells with 150 µl of PBS/T, 50 µl of the HRP substrate was added (Kirkegaard & Perry Laboratories - 507600). Equal volumes of 3,3',5,5'-tetramethylbenzidine (TMB) at 0.4 g/l in organic base and 0.02 % v/v hydrogen peroxide (H_2O_2) in citric acid buffer were mixed and added to the wells for 30 minutes at room temperature in the dark. In this case, the HRP enzyme will catalyse the oxidation of the chromogenic substrate (TMB) in the presence of hydrogen peroxide as an oxidising agent, converting it into a coloured molecule detectable by spectrophotometry. The developing reaction was stopped by addition of 50 µl of 1 M phosphoric acid (H_3PO_4). Optical densities were measured at 450 nm within 30 minutes on a spectrophotometer. Protein concentrations (pg/ml) in each sample were calculated by comparison with the corresponding standard curve.

2.5.5 Kinase assay

In vitro IKK2 kinase activity assays were performed by Dr Toby Lawrence and his group (Inflammation Biology Group, Centre d'Immunologie Marseille - Luminy, Marseille, France). Pancreatic cell lysates from the different mouse models were obtained as described in sections 2.2.1 and 2.5.1. The IKK complex containing the kinase of interest (IKK2) was immunoprecipitated using 20 µl of Protein A/G PLUS-Agarose (Santa Cruz - Sc-2003) and 2 µg of antibody against NEMO (Cell Signaling - 2685) for 1 hour at 4°C on a rotating device (for a more detailed protocol on immunoprecipitation, see section 2.7.1). The purified protein was incubated with 200 µM ATP (Cell Signaling - 9804) and 1.5 µM of the biotinylated IκB-α peptide (Cell Signaling - 1146) in kinase buffer. The reaction was incubated for 30 minutes at 30°C and stopped with 50 mM EDTA, pH 8.0. The samples were transferred into a 96-well plate precoated with an anti-phospho-IκB-α (Ser32/36) antibody (Cell Signaling - 9246), overnight at 4°C. Samples were incubated for 2 hours at room temperature and direct detection was carried out as described in the previous section 2.5.4 using SAv-HRP. Optical densities were measured by spectrophotometry and IKK2 kinase activity was calculated by setting the expression of the control sample (without substrate) as 100 %.

2.5.6 Cytokine and chemokine arrays

ChemiArray™ Mouse Cytokine Antibody Arrays III (Chemicon International - AA1003M) were used to measure cytokine and chemokine levels (62 proteins) in the pancreases of wild type mice and *kras*^{G12D} mice either untreated or treated with a γ-secretase inhibitor (DAPT).

Mice were sacrificed by cervical dislocation and the pancreases were collected in ice-cold PBS. Protein extraction was performed as described in section 2.5.1.2.

ChemiArrays were used according to the manufacturer's instructions. Membranes were blocked with blocking buffer for 30 minutes at room temperature. Pancreatic protein extracts from untreated or treated mice (n=5) were pooled and diluted 1:10 with blocking buffer and incubated with the membranes for 2 hours at room temperature. Membranes were washed three times with wash buffer I for 5 minutes with gentle shaking. After an additional two washes with wash buffer II in the same conditions, diluted biotin-conjugated anti-cytokines primary antibody was applied for 2 hours at room temperature. The washing step was repeated and membranes were incubated with HRP-conjugated streptavidin for 2 hours at room temperature. After washing the membrane as described before, immunodetection was carried out by adding a substrate for the HRP, followed by an exposure to Super RX autoradiography films to detect the light emitted. Relative levels of cytokine were evaluated by performing image densitometry analysis with the Image J software (public domain) and data were represented graphically as normalised to the signal intensity obtained for the wild type mice.

2.6 Protein-DNA interactions

Chromatin immunoprecipitation assays (EZ-ChIP™ Assay Kit) were performed according to the manufacturer's instruction (Millipore - 17-371). Adherent cells were treated with 1 % v/v formaldehyde for 10 minutes at room temperature. This treatment leads to covalent cross-linking of proteins to DNA. The excess of formaldehyde was quenched by adding glycine at 1.25 M and incubating the cells for 5 minutes on ice. Medium was removed and cells were washed twice with ice-cold PBS. Cells were incubated with ChIP lysis buffer and harvested using a cell scraper. Cells were pelleted by centrifugation at 700 x *g* for 5 minutes at 4°C. Cells were resuspended in 1 ml ChIP SDS lysis buffer containing 1X protease inhibitor cocktail (Millipore - 20-283) to break cell membranes and remove the nuclei. Lysates were sonicated or stored at - 80°C.

Sonication was performed on wet ice, to shear DNA into appropriately sized fragments (around 300 bp). 5 sets of 10 second pulses using a Sanyo - Soniprep 150 sonicator were sufficient to obtain DNA fragments of the required length (verified on a 1.2 % w/v agarose gel - see section 2.4.2). Insoluble material was removed by centrifugation at 10,000 x *g* for 10 minutes at 4°C. Supernatants were transferred into new tubes and stored at - 80°C.

Cross-linked Protein/DNA were immunoprecipitated with protein G agarose. To firstly remove proteins or DNA that would unspecifically bind to the protein G agarose, 100 µl of sheared chromatin was incubated with 900 µl of ChIP dilution buffer containing 1X protease inhibitor cocktail (Millipore - 20-283) and 60 µl of protein G agarose. Samples were incubated for 1 hour at 4°C on a rotating device and the agarose was pelleted by centrifugation at 4,000 x *g* for 1 minute. 10 µl of the

supernatant were saved and stored at 4°C as the input. The remaining supernatant was dispensed into new tubes and 1 µg of the immunoprecipitating antibody or isotype control was added (Table 2.6). Samples were incubated for 10 hours at 4°C on a rotating device. 60 µl of Protein G Agarose was added and samples were once again incubated overnight at 4°C on a rotating device. Immunoprecipitates were collected by centrifugation at 4,000 x *g* for 1 minute at 4°C. Supernatants were carefully aspirated and discarded and the pellets were successively washed once with low salt immune complex wash buffer (Millipore - 20-154), once with high salt immune complex wash buffer (Millipore - 20-155), once with LiCl immune complex wash buffer (Millipore - 20-156) and twice with TE buffer (Millipore - 20-157). Protein/DNA complexes were eluted by incubating the samples and the input for 15 minutes at room temperature with 100 µl of elution buffer (Millipore - 20294).

Cross-link reversal was performed by incubating the samples and the input with 200 mM of NaCl overnight at 65°C. Samples were treated with RNase A (Millipore - 20297) for 30 minutes at 37°C and with Proteinase K in 40 mM EDTA, 40 mM Tris-HCl for 2 hours at 45°C for protein digestion. DNA was purified using the spin columns provided (Millipore - 17-371). qRT-PCR was performed on the samples and the input as described in section 2.4.7.2 with *hes1* or *pparg* promoter-specific primers.

Antibody	Supplier	Cat. Ref.	Isotype	Amount
Histone H3	Cell Signaling	2650	Rabbit IgG	1 µg
Phospho-Histone H3 (Ser10)	Cell Signaling	9701	Rabbit IgG	1 µg
Isotype control	R&D	AB-105-C	Rabbit IgG	1 µg

Table 2.6: Antibodies used for chromatin immunoprecipitation

Table describes the antibodies and the isotype control used for chromatin immunoprecipitation listing the supplier, catalogue reference (Cat. Ref.), isotype and quantity.

2.7 Protein-Protein interactions

2.7.1 Immunoprecipitation

Cells derived from PDAC bearing *kras*^{G12D} mice were transiently transfected with either pCR-FLAG-IKK2, pCR-FLAG-IKK2-KM or pDEST40-NICD-V5 as described in section 2.3.6. Cells were stimulated with recombinant TNF-α for 12 hours before performing protein extraction and quantification as described in sections 2.5.1 and 2.5.2.

500 µg of total cellular protein were diluted in 1 ml PBS and incubated with 2 µg of antibody against the fusion protein (FLAG or V5) for 10 hours at 4°C on a rotating device. 20 µl of Protein A/G PLUS-Agarose (Santa Cruz - Sc-2003) were added. Samples were incubated overnight at 4°C on a rotating device. Immunoprecipitates were collected by centrifugation at 1,000 x *g* for 5 minutes at 4°C. Supernatants were carefully aspirated and discarded and the pellets were washed four times with 1 ml PBS, each time repeating the centrifugation step described. After the final wash, samples were resuspended in a small volume (15 µl) of PBS with LDS sample buffer to a final concentration of 1X. Samples were heated at 95°C for 10 minutes, cooled on ice and centrifuged to pellet the agarose beads before loading them into an SDS-NuPAGE® pre-cast 4-12 % w/v gradient bis tris gel (Invitrogen - NP0336BOX). Prestained molecular weight standards (Precision Plus Protein Dual Color Standards - BioRad - 161-0374) were also run on every gel to monitor electrophoresis, and were used to calibrate the mobility and hence apparent mass (kDa) of proteins of interest. Gels were subjected to electrophoresis in 1X 3-(N-morpholino)propanesulfonic acid (MOPS) SDS running buffer for 15 minutes at a constant voltage of 110 V, and then for 1 hour at a constant voltage of 150 V (NuPAGE® System - Invitrogen).

2.7.2 Coomassie brilliant blue stain

To estimate the complexity of the samples after immunoprecipitation, resolved proteins were stained with EZBlue™ gel staining reagent (Sigma Aldrich - G1041). In a clean container, the gel was rinsed three times for 5 minutes with an excess of deionised water to remove the SDS from the gel, which causes background staining. The proteins were fixed by incubating the gel for 15 minutes in 50 % v/v methanol, 10 % v/v acetic acid and the gel was then rinsed again for 15 minutes with an excess of deionised water. The gel was stained by adding 40 ml of EZBlue™ gel staining reagent and mixing with gentle shaking for 45 minutes to 1 hour. The protein band development was periodically checked and the staining process was usually stopped after approximately 1 hour. Because the pre-cast gels used were quite thick (1.5 mm) and had a high percentage of SDS especially at the bottom, the background was slightly blue. For full background destaining, the gel was washed three times for 15 minutes with deionised water and left overnight in fresh deionised water.

2.7.3 Mass Spectrometry

After performing immunoprecipitation as described in section 2.7.1, immunocomplexes were once again resolved by electrophoresis on an SDS-NuPAGE® pre-cast 4-12 % w/v gradient bis tris gel (Invitrogen - NP0336BOX). Gels were subjected to electrophoresis in 1X MOPS SDS running buffer for 15 minutes at a constant voltage of 110 V (NuPAGE® System - Invitrogen). The electrophoresis was stopped when the leading edge of the electrophoretic front had approximately run 2 cm. Lanes were cut into 1 to 2 mm^3 cubes and sent for analysis to Central Proteomics Facility, Oxford University, Oxford, UK. Gel bands were excised on a clean surface with a clean scalpel blade to avoid any keratin contamination. The use of detergents such as Triton®-X-100 and Tween was avoided during the experiments and when washing the glassware used as they contain

polyoxyethylene which is a source of contaminants and which can bind to the proteins and slow down their migration.

Gel bands were washed twice for 30 minutes with 25 mM ammonium bicarbonate dissolved in v/v ratio of water/acetonitrile, followed by one wash in pure acetonitrile for 10 minutes to completely dehydrate the bands. Once dried, gel bands were incubated with 10 mM DTT for 30 minutes at 37°C and then washed twice with 25 mM ammonium bicarbonate and once in pure acetonitrile. They were then incubated in 55 mM iodoacetamide for 60 minutes in the dark and once again washed twice for 10 minutes with 25 mM ammonium bicarbonate dissolved in v/v ratio of water/acetonitrile, then once in pure acetonitrile and finally dried. Trypsin (Promega - V5111) digestion was performed overnight at 37°C, to hydrolyse the proteins at the lysine and arginine residues and to release them from the gel. The digestion was stopped with formic acid and the supernatants were collected. Complete extraction of the proteins from the gel was performed adding 0.1 % v/v formic acid in water/acetonitrile (1:1 v/v) for 30 minutes. The supernatant obtained was pooled with the previous one. Samples were dried and reconstituted in 0.1 % v/v formic acid in HPLC grade water.

Samples were desalted on a C18 packed pipette tip and injected onto an Ultimate 3000 RSLC nano high-performance liquid chromatography (HPLC - Dionex) system coupled to LTQ XL Orbitrap mass spectrometer (Thermo Electron). They were resolved on a 12 cm by 75 µm inner diameter picotip column (New Objective) which was packed in-house with Reprosil-Pur C18-AQ phase (Dr. Maisch). A 120 minutes gradient was used to separate the peptides and each sample was injected three times and data merged in order to increase sample coverage. In these columns,

the stationary phase is composed of hydrophobic alkyl chains to capture peptides and small molecules. The peptides were eluted with 0.1 % v/v formic acid in HPLC grade acetonitrile. The mass spectrometer was operated in a data dependent acquisition mode. Precursor scans were performed in the Orbitrap instrument at a resolving power of 60,000, from which five precursor ions were selected and fragmented in the linear ion trap. Charge state +1 ions were rejected. Peak lists were generated using DTAsupercharge and searched using Mascot (Matrixscience). Data were searched against international protein index (IPI) database, restricting the taxonomy to mouse. Variable modifications were set as carbamidomethyl cysteine and oxidised methionine and deamidation of asparagine and glutamine. Precursor mass accuracy tolerance was set at 10 ppm and MS/MS at 0.5 Da.

Mass Spectrometry analyses were performed by Dr Benjamin Thomas and Dr Fernando Martinez-Estrada (Central Proteomics Facility, Oxford University, Oxford, UK).

2.8 Histology, staining and immunohistochemistry

All sections were visualised and images were taken using AxioVision 4.8 with an AxioCam HRc camera (Zeiss) coupled to an Axiophot microscope (Zeiss).

2.8.1 Histology

Histological analysis of pancreases was carried out by standard procedures. Specimens were harvested from time-matched animals and fixed in 4 % v/v buffered formalin overnight at 4°C. The following day, the organs were progressively dehydrated in gradient alcohols (30 minutes at room temperature in 30, 50 and 70 % v/v ethanol). Tissues were embedded in paraffin and sections were cut with a microtome (5 µm thickness) and prepared by the Barts Cancer Institute pathology department. Tumour incidence and histology grades of PanIN lesions and PDAC were assessed as previously described (Hruban *et al.,* 2001) and with the help of Anne Schultheis (University Medical Center Hamburg-Eppendorf, Pathology department, Hamburg, Germany).

2.8.2 Haematoxylin and eosin staining

Systematically, one section of each embedded-tissue was stained with haematoxylin and eosin (H&E) by the Barts Cancer Institute pathology department to assess the general histopathology. Sections were deparaffinised in xylene (Fisher Scientific - X020017) for 5 minutes and again in fresh xylene for another 5 minutes. Sections were progressively rehydrated in gradient alcohols (twice for 2 minutes each in 100, 95, 70 and 50 % v/v ethanol and water). Sections were stained with Harris haematoxylin solution for 8 minutes and washed in running deionised water for 5 minutes. Haematin (the oxidation product of haematoxylin) binds to lysine residues of nuclear histones in the presence of aluminium ions. Such a long incubation time allows saturation of all binding sites and overstaining of the tissue. 1 % v/v acid

alcohol was applied onto the sections to differentiate the tissue, followed by addition of alkaline solution (0.2 % v/v ammonia water) to stop the differentiation, turning the haematin into a blue colour for identification of cell nuclei. This process is also known as "blueing". Finally, tissue sections were counterstained with a mix of eosin and phloxine to enhance the colouration. Sections were dehydrated by incubating them twice for 5 minutes each in 95, 100 % v/v ethanol and xylene sequentially. Slides were air-dried and mounted with DPX mounting medium (Fisher Scientific - D/5319/05). This staining resulted in the following colours: pale pink for collagen, red for acidophilic cytoplasm, purple for basophilic cytoplasm, blue for nuclei and cherry red for erythrocytes.

2.8.3 Masson's trichrome

Sections were deparaffinised and rehydrated as described previously in section 2.8.2. To re-fix and intensify the final colouration of the tissues, sections were incubated in Bouin's solution (Sigma Aldrich - HT10132) overnight at room temperature. After several washes with tap water, sections were incubated in Weigert's Iron Haematoxylin solution (Sigma Aldrich - HT1079) for 5 minutes, to allow nuclei to be stained in blue/black. Sections were washed for 5 minutes with tap water and rinsed with deionised water before incubating them in Biebrich Scarlet-Acid Fuchsin (Sigma Aldrich - HT151) for 5 minutes, to stain cytoplasm and muscle in red. Sections were rinsed with deionised water and incubated in phosphotungstic acid solution (Sigma Aldrich - HT152) for 10 minutes to allow the uptake of the aniline blue (Sigma Aldrich - HT154) stain in which the sections were directly incubated for 10 minutes, to stain the collagen in blue. Slides were incubated for 2 minutes in 1 % v/v acetic acid, rinsed with deionised water and finally dehydrated by dipping them in 95 % v/v ethanol for 3 minutes, twice in 100 % v/v ethanol for 3 minutes and three times in xylene for 5 minutes. Slides were then air-dried and mounted with DPX

mounting medium (Fisher Scientific - D/5319/05). Masson's trichrome staining was performed by Juliana Candido, Barts Cancer Institute, Queen Mary, University of London, London, UK.

2.8.4 Immunohistochemistry

All primary and secondary antibodies used for immunohistochemistry are listed below in Table 2.7 and Table 2.8 respectively.

Antibody	Supplier	Cat. Ref.	Isotype	Dilution Concentration
BrdU	Roche	11299964001	Mouse IgG	1:10
Cleaved caspase-3	Cell Signaling	9664	Rabbit IgG	1:200
SOX9	Chemicon	AB5535	Rabbit IgG	10 µg/ml
PCNA	BD Biosciences	610665	Mouse IgG1	1:50
Isotype control	BD Biosciences	550875	Rabbit IgG	1:200 or 10 µg/ml
Isotype control	BD Biosciences	349040	Mouse IgG1	1:10 or 1:50

Table 2.7: Primary antibodies used for immunohistochemistry

Table describes the primary antibodies and isotype controls used for immunohistochemistry listing the supplier, catalogue reference (Cat. Ref.) and antibody isotype. Appropriate dilutions and concentrations are shown for each antibody.

Antibody	Supplier	Cat. Ref.	Dilution
anti-mouse IgG Biotinylated	Vector Labs	BA-9200	1:200
anti-rabbit IgG Biotinylated	Vector Labs	BA-1000	1:200
anti-rat IgG Biotinylated	Vector Labs	BA-4001	1:200

Table 2.8: Secondary antibodies used for immunohistochemistry

Table describes the secondary antibodies used for immunohistochemistry listing the supplier, catalogue reference (Cat. Ref.) and appropriate dilutions.

2.8.4.1 Specific markers

Sections were stained using a standard streptavidin-peroxidase complex technique and the following steps were carried out at room temperature using immunoboxes for washes. Sections were deparaffinised and rehydrated as described previously in section 2.8.2. Following fixation in formalin, methylene bridges are formed, which

cross-link proteins and therefore mask antigenic sites. To improve the exposure of antigen sites on the sections, an antigen retrieval step is usually necessary, which is specific for each primary antibody used. The heat-mediated method was used, which involves immersing the sections in antigen citric acid based unmasking solution (Vector Labs - H-3300) and heating for 9 minutes in a microwave. Sections were allowed to cool down at room temperature for at least 20 minutes and washed three times for 3 minutes each wash in PBS. Sections were circled with ImmEdge™ hydrophobic barrier pen (Vector Labs - H4000) and blocked for non-specific binding with PBS/BSA/Goat serum for 1 hour at room temperature in a humidified chamber. Sections were incubated in primary antibody or isotype control diluted in blocking solution, as described in Table 2.7, overnight at 4°C in a humidified chamber. The following day, the sections were again washed three times for 3 minutes each wash in PBS and subsequently the biotinylated secondary antibody was applied (Table 2.8) and the sections were incubated for 45 minutes at room temperature in a humidified chamber. Sections were again washed three times for 3 minutes each wash in PBS and the endogenous peroxidase activity was quenched by incubating the sections in 0.3 % v/v H_2O_2 diluted in 100 % v/v methanol for 20 minutes at room temperature.

The sections were then washed three times for 3 minutes each wash in PBS and avidin biotinylated peroxidase complex (Vector Labs - Vectastain Elite ABC Kit - PK-6100) was added onto the sections and incubated for 30 minutes at room temperature in a humidified chamber. The sections were once again washed three times for 3 minutes each wash in PBS and the peroxidase activity was visualised by using SIGMA*Fast*™ 3,3'-diaminobenzidine (DAB) at a final concentration of 0.7 mg/ml DAB, 0.67 mg/ml urea hydrogen peroxide and 0.06 M Tris buffer (Sigma-Aldrich - D4418). DAB solution was applied on each section for at least 3 minutes or

until a brown colour developed. Subsequently, sections were briefly washed in water to stop DAB development and counterstained by dipping in haematoxylin solution (Sigma-Aldrich - GSH316) for 30 seconds, washed in water and dipped 10 times in ammonium hydroxide (44.4 mM in water) for acid differentiation. Sections were dehydrated by dipping them 20 times in isobutanol (Fisher Scientific - B/5100/PB17) and incubated again in fresh isobutanol for 4 minutes and then twice in xylene for 5 minutes. Slides were air-dried and mounted with DPX mounting medium (Fisher Scientific - D/5319/05).

2.8.4.2 BrdU staining

To detect proliferating cells in the pancreas, mice were injected intraperitoneally with BrdU (see section 2.1.3). 90 minutes after BrdU injection, mice were sacrificed and each pancreas was processed as described in section 2.8.1. The protocol described in section 2.8.4.1 was followed using the BrdU antibody from the BrdU labelling and detection kit (Roche - 11299964001) and the peroxidase activity was visualised using SIGMA*Fast*™ 3,3'-diaminobenzidine (DAB) with metal enhancer at a final concentration of 0.5 mg/ml DAB, 0.2 mg/ml cobalt chloride, 0.3 mg/ml urea hydrogen peroxide, 0.05 M Tris buffer and 0.15 M sodium chloride (Sigma-Aldrich - D0426).

2.9 Confocal Microscopy - Immunofluorescence

All confocal microscopy images were acquired with a laser scanning-microscope LSM 510 (Zeiss) with a digital signal processor using the LSM software.

The day previous to immunofluorescence imaging, glass cover slips (13 mm Ø VWR - 631-0150) were washed in 70 % v/v ethanol, air-dried and transferred to a 24-well plate. Cell lines derived from PanIN bearing *kras*^{G12D} mice were plated (30,000 cells/well) and grown overnight at 37°C in a 5 % v/v CO_2 atmosphere.

Cells were first rinsed twice with cold PBS and fixed with 4 % v/v paraformaldehyde (Ecolab - 416479) at room temperature for 15 minutes. Cells were rinsed twice with PBS and permeabilised with 0.1 % v/v Triton®-X-100 (Sigma Aldrich - X100) in PBS at room temperature for 5 minutes. Cells were again rinsed twice with PBS and quenched with 50 mM ammonium chloride (NH_4Cl) in PBS at room temperature for 15 minutes. They were then washed once with PBS and blocked with PBS/BSA/Goat serum at room temperature for 45 minutes. Cells were incubated with primary antibody or isotype control diluted in blocking solution or with rhodamine-labelled phalloidin (which binds F-Actin) at room temperature for 1 hour (Table 2.9). Cells were rinsed three times with PBS and incubated with secondary antibody diluted 1:500 in blocking solution at room temperature for 1 hour in the dark (Table 2.10). After this, cells were rinsed three times in PBS and once in water and the cover slips were mounted on clean slides using Prolong Gold antifade reagent with DAPI (Invitrogen - P36931).

Antibody Probe	Supplier	Cat. Ref.	Isotype	Dilution Concentration
E-cadherin	Invitrogen	13-1900	Rat IgG2a	10 µg/ml
F-actin	Invitrogen	R415	n/a	1:200
HES1	Santa Cruz	Sc-25392	Rabbit IgG	1:50
HEY1	Santa Cruz	Sc-28746	Rabbit IgG	1:50
Isotype control	eBioscience	14-4321	Rat IgG2a	10 µg/ml
Isotype control	BD Biosciences	550875	Rabbit IgG	1:50

Table 2.9: Primary antibodies used for immunofluorescence

Table describes the primary antibodies or probe and isotype controls used for immunofluorescence listing the supplier, catalogue reference (Cat. Ref.) and antibody isotype. Appropriate dilutions and concentrations are shown for each antibody. n/a: not applicable.

Antibody	Supplier	Cat. Ref.	Dilution
anti-rabbit Alexa Fluor® 488	Invitrogen	A11008	1:500
anti-rat Alexa Fluor® 568	Invitrogen	A11077	1:500

Table 2.10: Secondary antibodies used for immunofluorescence

Table describes the secondary antibodies used for immunofluorescence listing the supplier, catalogue reference (Cat. Ref.) and appropriate dilutions.

A modified protocol combining immunohistochemistry and immunofluorescence was used to stain pancreatic paraffin sections from *kras*^{G12D}, *kras*^{G12D}/*tnfa*$^{\Delta Pdx}$ and *kras*^{G12D}/*ikk2*$^{\Delta Pdx}$ mice. The protocol described in section 2.8.4.1 was followed but before blocking, cells were permeabilised with 0.1 % v/v Triton®-X-100 and quenched with ammonium chloride as described above. The method described for immunofluorescence was subsequently followed but before mounting the slides, sections were dehydrated by immersion in isobutanol followed by xylene as described in section 2.8.4.1.

2.10 Flow cytometry

2.10.1 Analysis of immune populations from the pancreas

Pancreases were harvested from time-matched PanIN bearing *kras*^{G12D}, *kras*^{G12D}/*ikk2*$^{\Delta Pdx}$ or *kras*^{G12D}/*tnfa*$^{\Delta Pdx}$ mice and minced. Tissue samples were digested by incubation in Hank's buffered salt solution (HBSS) without calcium and without magnesium (Sigma Aldrich - H6648) complemented with 2 mg/ml of collagenase V (Sigma Aldrich - C9263) for 30 minutes at 37°C. The cell suspension obtained (mainly containing immune cells) was filtered through a 100 µm cell strainer and the cells in the flowthrough were washed three times with HBSS buffer. After each wash, the cells were pelleted by centrifugation at 450 x *g* for 5 minutes and the supernatants were discarded. The cells were finally resupsended in HBSS buffer and counted using a Vi-CELL^{TM} image analyzer (Beckman Coulter).

The cells were then plated in a 96-well plate ($5x10^5$ cells/well) and cell surface markers were stained for flow cytometry analysis. To do this, the plates were centrifuged at 515 x *g* for 5 minutes at 4°C and the pelleted cells were washed once in FACS buffer. After another centrifugation at 515 x *g* for 5 minutes at 4°C, cells were resuspended and incubated for 15 minutes at 4°C in 50 µl of anti-mouse CD16/CD32 (eBioscience - 14-0161-81) diluted 1:200 in FACS buffer to block unspecific binding sites (CD16 and CD32 receptors are expressed by most immune cells and recognise the mouse IgG Fc portion). Primary antibodies and isotype controls (Table 2.11) diluted in 50 µl FACS buffer were added to each well and the cells were incubated for 30 minutes at 4°C. The cells were pelleted by centrifugation at 515 x *g* for 5 minutes at 4°C and washed twice with FACS buffer. They were finally resuspended and fixed in 100 µl of 2 % v/v formaldehyde (Ecolab - 3036850) in PBS and the cells

were stored at 4°C in the dark until analysis by flow cytometry (usually within 48 hours).

Antibody	Clone	Supplier	Cat. Ref.	Isotype	Dilution
F4/80 Alexa Fluor® 488	BM8	eBioscience	53-4801	Mouse IgG2a	1:200
CD11b PE	M1/70	eBioscience	12-0112	Rat IgG2b	1:200
Gr1 PE-Cy5	RB6-8C5	eBioscience	15-5931	Rat IgG2b	1:200
Isotype control Alexa Fluor® 488	n/a	eBioscience	53-4724	Mouse IgG2a	1:200
Isotype control PE	n/a	eBioscience	12-4031	Rat IgG2b	1:200
Isotype control PE-Cy5	n/a	eBioscience	15-4031	Rat IgG2b	1:200

Table 2.11: Antibodies used for flow cytometry analysis

Table describes the antibodies used for flow cytometry listing the clone, supplier, catalogue reference (Cat. Ref.) and appropriate dilutions. PE: Phycoerythrin and PE-Cy5: Phycoerythrin-cyanine dye 5. n/a: not applicable.

Individual cells are passed through a beam of light and will scatter the ray. Depending on the fluorophore used to label them, they will be excited and will emit a light at a longer wavelength than the light source (Table 2.12). The light emitted is picked up by detectors, converted into electric signals and each event (each cell being analysed) is shown on a graphical scale.

Three-colour flow cytometry was performed using an LSRFortessa cell analyser (BD Biosciences) and FACSDiva software Version 6.2. The fluorescence of 50,000 events was acquired for each sample. Data were transferred and analysed using the FlowJo software (Tree Star, Oregon, USA).

Dye	Excitation wavelength (nm)	Emission wavelength (nm)
Alexa Fluor® 488	495	519
PE	496	578
PE-Cy5	496	667

Table 2.12: Flow cytometry spectrum guide

Table describes the different dyes used for flow cytometry and their respective excitation and emission wavelengths in nanometers (nm). PE: Phycoerythrin and PE-Cy5: Phycoerythrin-cyanine dye 5.

2.10.2 Fluorescence-activated cell sorting (FACS)

Pancreases from *kras*^{G12D} mice carrying the *ROSA26-LSL-EYFP* allele were first minced and digested with collagenase V as described in section 2.10.1. However, the flowthrough was discarded and the tissue fragments left in the cell strainer were further digested in 0.05 % w/v Trypsin-EDTA for 2 minutes at 37°C to obtain epithelial cells. Trypsin was inhibited by adding fresh complete medium (DMEM supplemented with 10 % v/v FCS). The cell suspension obtained was filtered through a 100 µm cell strainer and cells in the flowthrough were washed three times with HBSS buffer. After each wash, the cells were pelleted by centrifugation at 450 x *g* for 5 minutes and the supernatants were discarded. Once resuspended in HBSS buffer, EYFP positive cells were sorted using the FACSAria™II sorter (BD Biosciences) and FACSDiva software Version 6.2. These cells were used for RNA extraction and qRT-PCR (see sections 2.4.5 and 2.4.7). FACS analyses were performed by Dr Guglielmo Rosignoli, Barts Cancer Institute, Queen Mary, University of London, London, UK.

2.11 Statistical analysis

All data were expressed as the mean of the individual experiments + the standard deviation of the mean (SD), represented as an error bar, unless otherwise stated in the figure legend.

The statistical method used to determine significant differences between two populations was the unpaired Student's t test (Figure 3.4 B, Figure 3.4 C, Figure 6.5 and Figure 6.10). For multiple comparisons, results were tested for statistical significance using one-way or two-way ANOVA and Bonferroni's multiple comparisons tests. Tumour incidence and liver metastasis were analysed by Fisher's exact test. All statistical analyses were performed on the GraphPad Prism software Version 4.0c.

All p values of 0.05 or less were considered statistically significant and the level of statistical significance was indicated by asterisks as follows: * $p<0.05$, ** $p<0.01$ and *** $p<0.001$.

CHAPTER THREE: CHARACTERISATION OF PANCREATIC MURINE MODELS

The work presented in this chapter was performed in collaboration with a postdoc in the research group, Dr Eleni Maniati, Barts Cancer Institute, Queen Mary, University of London, London, UK.

3.1 Introduction

As described in Chapter 1, oncogenic *KRAS* mutations are found in almost all PDAC cases and play an important role in pancreatic tumour induction (see section 1.2.6). It is also known that the expression of mutant *kraʂ* activates NF-κB, a major transcription factor in the inflammatory response (Basseres et al., 2010; Meylan et al., 2009). Various studies indicate that IKK2 and the p65 subunit of NF-κB are required in both murine and human *kraʂ*-induced transformation of lung epithelial cells and in models of inflammation-induced carcinogenesis (Basseres *et al.,* 2010; Greten *et al.,* 2004; Meylan *et al.,* 2009; Yang *et al.,* 2010).

kraʂ$^{+/LSL\text{-}G12D}$; *pđx1-cre* mice (abbreviated as *kraʂ*^{G12D}) express an endogenous oncogenic *kraʂ* allele, initially in pancreatic progenitors and later in the adult pancreas (Hingorani *et al.,* 2003). In this model, PanIN formation usually occurs from 2 months of age and evolves towards a PDAC phenotype from 12 months of age. In order to understand the mechanisms and to decipher the signalling pathways involved in *kraʂ*-induced pancreatic cancer, cell lines derived from PanIN and PDAC bearing *kraʂ*^{G12D} mice were generated (Schreiber *et al.,* 2004).

In these cell lines, constitutive secretion of the TNF-α cytokine was identified by ELISA. This has already been shown in other cell types such as ovarian cancer cells (Kulbe *et al.,* 2007). Further experiments were carried out to determine and understand the role of the TNF-α/IKK2 signalling pathway in the formation and progression of PanIN lesions and also to assess the autocrine role of malignant cell-

derived TNF-α. The starting point was to genetically delete *ikk2* or *tnfa* in *kras*^{G12D} mice in order to generate *kras*^{G12D}/*ikk2*$^{\Delta Pdx}$ and *kras*^{G12D}/*tnfa*$^{\Delta Pdx}$ mice, respectively.

This chapter describes the preliminary data that instigated the study of the role of the TNF-α/IKK2 signalling pathway in pancreatic cancer, how the triple mutant mice were generated and their characterisation. These new mutant mice were used to obtain pancreatic epithelial cell lines from early cancerous lesions and to delineate *in vitro* molecular mechanisms involved in the carcinogenic process.

3.2 Generation of *kraɔ*^{G12D} mouse models with conditional deletion of *ikk2* or *tnfa* in the pancreas

The triple mutant mouse strains were generated by interbreeding C57BL/6 mice carrying "floxed" *ikk2* or *tnfa* alleles with the *kraɔ*$^{+/LSL\text{-}G12D}$ and *pðx1-cre* strains. The intermediate mouse strains were generated and kindly provided by various collaborators (detailed in the Materials and Methods chapter).

The *ikk2*$^{flox/flox}$ mice (Li *et al.,* 2003) were first crossed with *kraɔ*$^{+/LSL\text{-}G12D}$ mice or *pðx1-cre* mice (Hingorani *et al.,* 2003; Johnson *et al.,* 2001) to generate double heterozygote transgenic *kraɔ*$^{+/LSL\text{-}G12D}$/*ikk2*$^{+/flox}$ mice or *ikk2*$^{+/flox}$/*pðx1-cre* mice respectively. These mice were interbred to generate triple mutants on a mixed C57BL/6/129/SvJae background, abbreviated to *kraɔ*^{G12D}/*ikk2*$^{\Delta Pdx}$. The strategy described is illustrated in Figure 3.1 and the different mouse strains used in this thesis are summarised in Table 3.1. *kraɔ*^{G12D}/*tnfa*$^{\Delta Pdx}$ were developed using a similar strategy by Dr Eleni Maniati, Barts Cancer Institute, Queen Mary, University of London, London, UK.

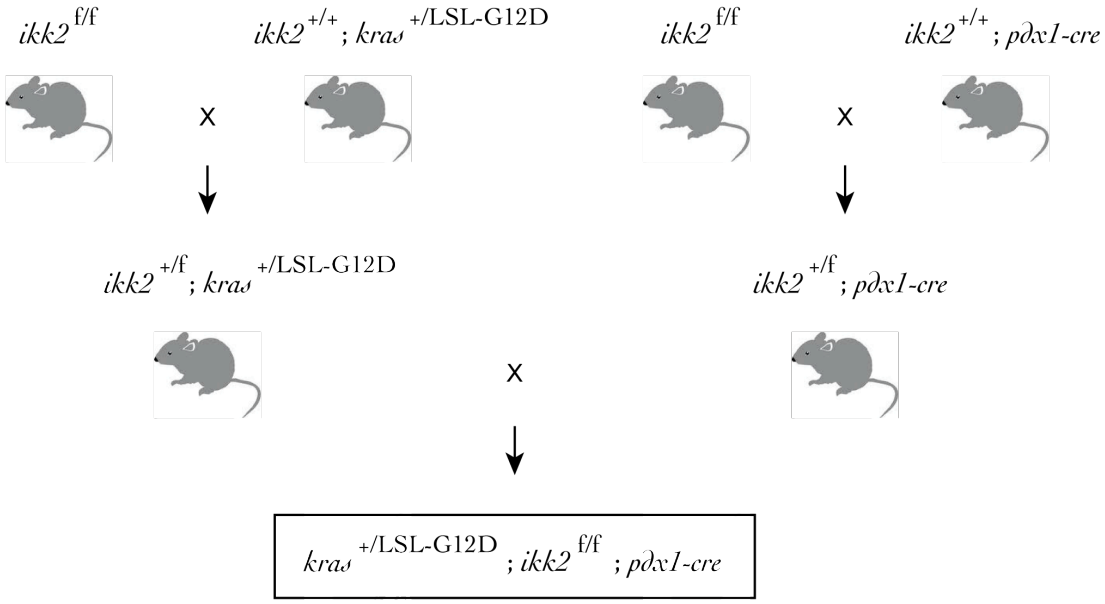

Figure 3.1: Generation of *kras*^{G12D} mice with targeted deletion of *ikk2*

kras$^{+/LSL-G12D}$ and *pdx1-cre* mice were crossed with the *ikk2*$^{flox/flox}$ strain. Progenies were intercrossed to generate *kras*^{G12D}/*ikk2*$^{\Delta Pdx}$ triple mutant mice. A similar strategy was used to develop the *kras*^{G12D}/*tnfa*$^{\Delta Pdx}$ triple mutant mice.

Strain	*Cre*	*kras*	*ikk2*	*tnfa*	Genetic background
ikk2	-	+/+	f/f	+/+	C57BL/6
tnfa	-	+/+	+/+	f/f	C57BL/6
kras	-	+/G12D	+/+	+/+	C57BL/6/129/SvJae
kras/ikk2	-	+/G12D	f/f	+/+	C57BL/6/129/SvJae
kras/tnfa	-	+/G12D	+/+	f/f	C57BL/6/129/SvJae
pdx1-cre	+	+/+	+/+	+/+	C57BL/6
kras^{G12D}	+	+/G12D	+/+	+/+	C57BL/6/129/SvJae
ikk2$^{\Delta Pdx}$	+	+/+	-/-	+/+	C57BL/6
tnfa$^{\Delta Pdx}$	+	+/+	+/+	-/-	C57BL/6
kras^{G12D}/*ikk2*$^{\Delta Pdx}$	+	+/G12D	-/-	+/+	C57BL/6/129/SvJae
kras^{G12D}/*tnfa*$^{\Delta Pdx}$	+	+/G12D	+/+	-/-	C57BL/6/129/SvJae

Table 3.1: Characteristics of the mouse strains used

Table describes the mouse strains used, their genotype for each allele ("+" for wild type; "f" for floxed and "-"for floxed out) and their genetic background.

3.3 Assessment of *tnfa* and *ikk2* genetic deletion in pancreatic epithelial cells *in vitro*

To confirm CRE-mediated recombination and therefore *ikk2* or *tnfa* genetic deletion in the mouse strains, PanIN cell lines were generated by collaborators using pancreases from 3-, 6- and 9-month old *kras*^{G12D}, *kras*^{G12D}/*ikk2*$^{\Delta Pdx}$ and *kras*^{G12D}/*tnfa*$^{\Delta Pdx}$ mice as described in section 2.2.1. Cell lines from age-matched *kras* and *kras/tnfa Cre* negative mice were similarly generated. PDAC cell lines were generated from 1-year old *kras*^{G12D} mice. No significant difference of *in vitro* proliferation was observed between the PanIN cell lines or the PDAC cell lines from the different mouse strains (personal communication Dr Eleni Maniati, Barts Cancer Institute, Queen Mary, University of London, London, UK).

3.3.1 PanIN and PDAC cell lines secrete TNF-α

PanIN and PDAC cell lines grew in clusters and had morphological characteristics typical of epithelial cells (Figure 3.2).

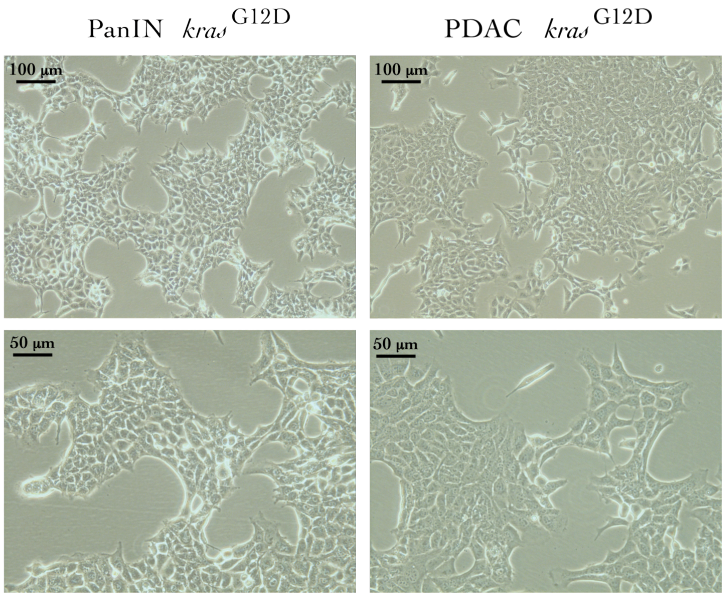

Figure 3.2: Morphological characteristics of the cell lines generated

Cell lines derived from PanIN and PDAC bearing *kras*^{G12D} mice were generated and cultured *in vitro*. Cells grew in clusters, with little or no intercellular space, which is characteristic of epithelial cells.

These cells were positive for intermediate filament proteins from the cytokeratin group, which further confirmed their epithelial nature (personal communication Dr David Tuveson's laboratory, Cancer Research UK Cambridge Research Institute, Cambridge, UK).

The profile of cytokines released after 24 hours in culture was examined, showing that these cells secrete IL-6 and IL-1β but not IL-10, IL-12 and IL-23 (Figure 3.4 and unpublished data from Dr Thorsten Hagemann's group, Barts Cancer Institute, Queen Mary, University of London, London, UK). High levels of TNF-α were also produced (Figure 3.3).

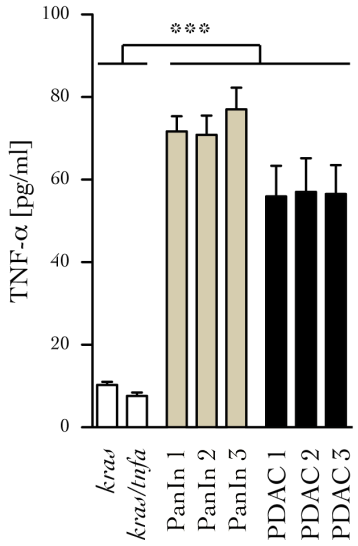

Figure 3.3: TNF-α secretion from PanIN and PDAC cell lines

TNF-α secretion by cell lines derived from PanIN or PDAC bearing *kras*^{G12D} mice measured by ELISA. Control cells were generated from the pancreases of *kras* and *kras/tnfa Cre* negative mice. Data are shown as mean + SD of triplicate experiments and are representative of three independent experiments. ***p<0.001, detection limit 10 pg/ml.

3.3.2 Genetic deletion of *tnfa*

Levels of TNF-α secreted by PanIN and PDAC cell lines derived from *kras*^{G12D}/*tnfa*$^{\Delta Pdx}$ mice *in vitro* after 24 hours in culture were evaluated by ELISA. As shown in Figure 3.4 A, cells secreted minimal levels of TNF-α (around 10 pg/ml, the detection limit of the assay) confirming *tnfa* genetic deletion following CRE recombination.

3.3.3 Genetic deletion of *ikk2*

The absence of IKK2 in the pancreas was verified by performing kinase activity assays on cells derived from *kras*^{G12D} and *kras*^{G12D}/*ikk2*$^{\Delta Pdx}$ mice. IKK complexes were purified and incubated *in vitro* with ATP and the phosphorylation of the IκB-α substrate was measured by colorimetric reaction (see section 2.5.5).

The activity of the IKK complex was abolished in cells derived from PanIN bearing *kras*^{G12D}/*ikk2*$^{\Delta Pdx}$ mice (Figure 3.4 B), therefore confirming excision of the *ikk2* locus. Their capacity to secrete TNF-α and IL-6, whose expression is regulated by NF-κB, was also significantly decreased (Figure 3.4 C), further confirming the genetic inactivation of the *ikk2* gene.

Due to the IKK complex being purified via NEMO to preserve the integrity of the IKK2 kinase, the phosphorylation of the IκB-α substrate could have been due to the IKK1 or the IKK2 kinase. However, IKK2 was identified as the main kinase responsible for the IκB-α phosphorylation, implying that the absence of the kinase activity from the IKK complex was due to the genetic deletion of *ikk2* (Yamamoto *et al.,* 2000). The kinase assays were performed by Dr Toby Lawrence and his group (CIML, Marseille, France).

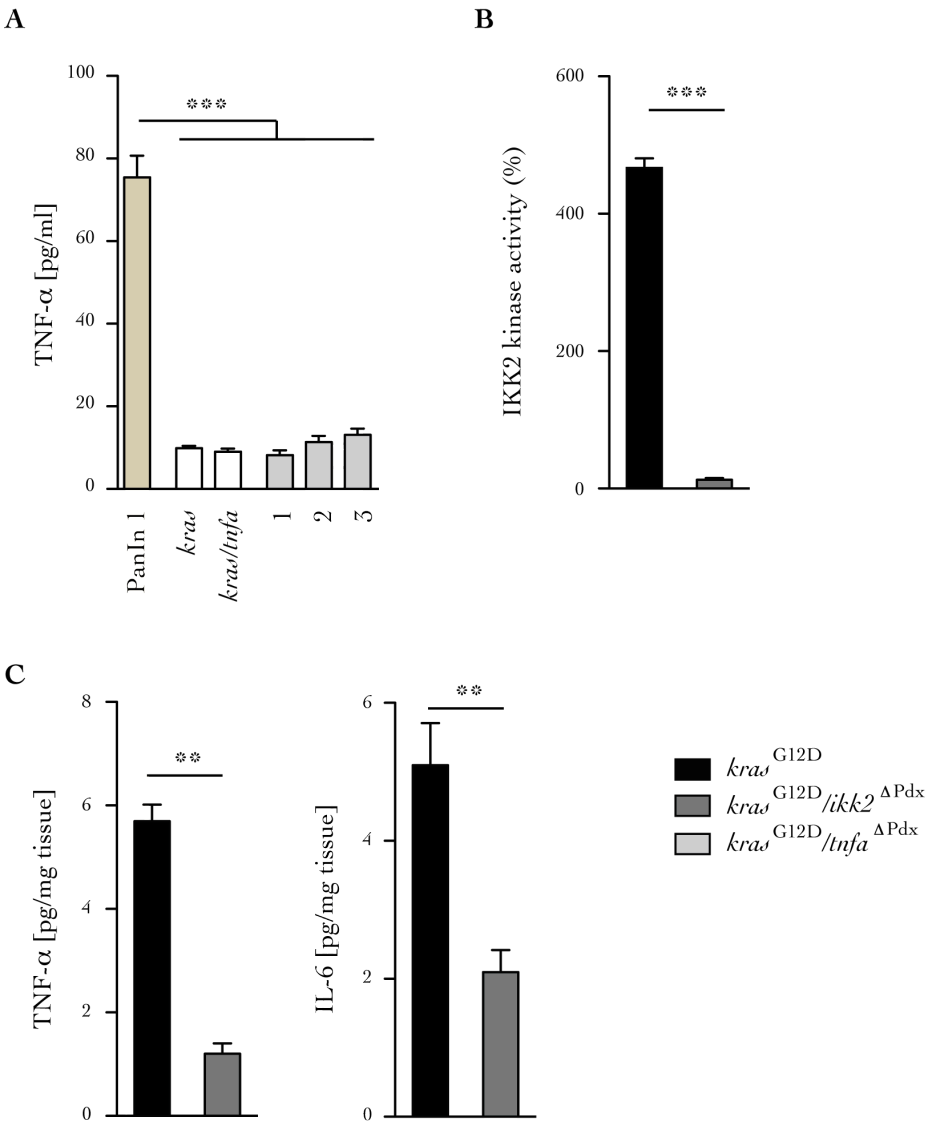

Figure 3.4: Genetic deletion of *ikk2* and *tnfa* in pancreatic cell lines

Cell lines were derived from PanIN bearing *kras*^{G12D}, *kras*^{G12D}/*ikk2*$^{\Delta Pdx}$ or *kras*^{G12D}/*tnfa*$^{\Delta Pdx}$ mice. (A) TNF-α secretion measured by ELISA. Control cells were generated from *kras* and *kras/tnfa Cre* negative pancreases. (B) Cellular IKK2 kinase activity. (C) TNF-α and IL-6 secretion measured by ELISA (n=6). Data are shown as mean + SD of triplicate experiments and are representative of three independent experiments, **p<0.01, ***p<0.001. (A) and (C) detection limit 10 pg/ml.

3.4 Effects on PanIN formation and progression

To establish whether *ikk2* or *tnfa* genetic deletion has an impact on PanIN formation and PDAC progression in the *kras*^{G12D}/*ikk2*$^{\Delta Pdx}$ and *kras*^{G12D}/*tnfa*$^{\Delta Pdx}$ mice compared with the *kras*^{G12D} mice, tumour incidence and histology grade were evaluated. General histopathology analyses were also performed with support from Anne Schultheis (University Medical Center Hamburg-Eppendorf, Pathology department, Hamburg, Germany).

3.4.1 Incidence of pancreatic tumours

To evaluate the long-term impact of *ikk2* genetic deletion, cohorts of 40 *kras*^{G12D} mice and 50 *kras*^{G12D}/*ikk2*$^{\Delta Pdx}$ mice were monitored for nearly two years (Appendices D and E). Mice were sacrificed when they developed any signs of distress or reached the UK Home Office limits. For each mouse, tumour incidence and histology grade were evaluated and the sites of metastasis (liver or lung), the presence of peritoneal disease, ascites, skin lesions (such as papilloma), biliary obstruction and atrophy were also recorded. Significant differences were identified regarding tumour incidence only (Figure 3.5).

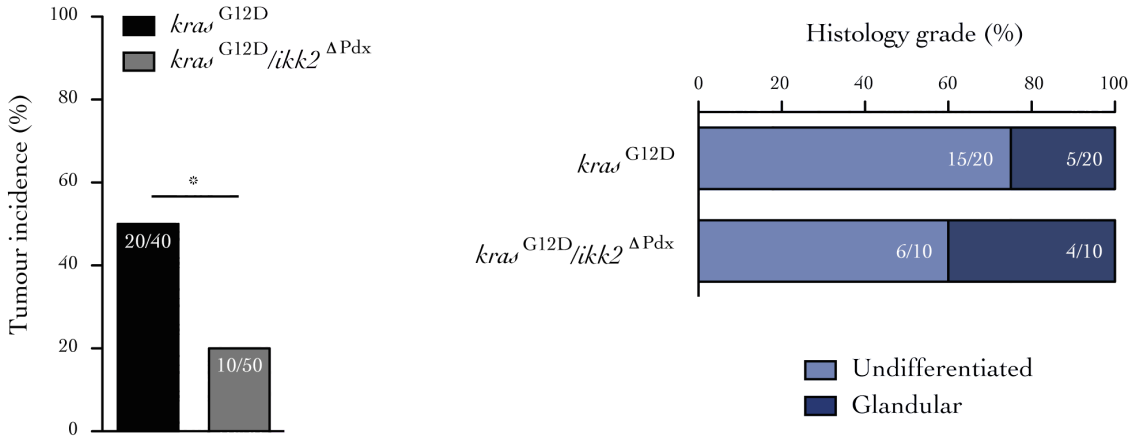

Figure 3.5: Tumour incidence and histology grade

Tumour incidence and histology grade in *kras*^{G12D} (n=40) and *kras*^{G12D}/*ikk2*$^{\Delta Pdx}$ (n=50) mice, *p<0.05. Respectively, 50 % and 20 % of *kras*^{G12D} and of *kras*^{G12D}/*ikk2*$^{\Delta Pdx}$ mice developed PDAC. The number of mice presenting undifferentiated tumours was more important in the *kras*^{G12D} group.

Figure 3.5 shows that only 20 % of *kras*^{G12D}/*ikk2*$^{\Delta Pdx}$ mice succumbed to PDAC, while there was a 50 % tumour incidence in *kras*^{G12D} mice. Tumours, including pancreatic adenocarcinoma, are characterised and graded depending on the differentiation status of their glandular structures. Undifferentiated structures are more malignant and suggest a poorer prognosis (Pan and Wang 2007). Interestingly, three-quarters of the *kras*^{G12D} mice which developed PDAC presented with undifferentiated tumours. However, even though this ratio was reduced by almost half in *kras*^{G12D}/*ikk2*$^{\Delta Pdx}$ mice (Figure 3.5), this difference was not significant. Genetic deletion of *ikk2* appears to be sufficient to induce changes in histopathological features and to delay PDAC development in the genetic *kras*^{G12D} mouse model. Moreover, the frequency of liver metastasis was reduced in *kras*^{G12D}/*ikk2*$^{\Delta Pdx}$ mice (60 % compared with 75 % for the *kras*^{G12D} mice) (Figure 3.6), but this difference was again not significant. This observation confirms that the pancreatic cancer in these mice is at a less advanced stage.

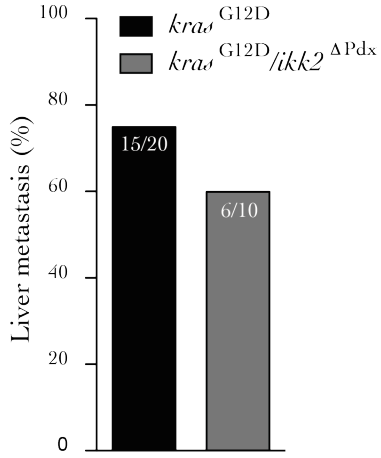

Figure 3.6: Liver metastasis

Liver metastasis was reduced in *kras*^{G12D}/*ikk2*$^{\Delta Pdx}$ (n=50) mice compared with the *kras*^{G12D} (n=40) mice. Respectively, 75 % and 60 % of *kras*^{G12D} and of *kras*^{G12D}/*ikk2*$^{\Delta Pdx}$ mice presented liver metastasis.

In genetically modified mouse models, monitoring the weight of the mice ensures that the genetic modifications introduced do not affect the well-being of the animal. Body

weight also indicates the health status of the animal and cancer development can be accompanied by a significant loss of weight (Tian *et al.,* 2010). Moreover, The Animals (Scientific Procedures) Act 1986 established that if a mouse looses 20 % of its initial body weight, it should be culled using an appropriate and humane method.

The body weight of the main mouse strains used was monitored weekly (Figure 3.7) and no significant loss of weight was observed over a period of 20 weeks. Weight recording was stopped as over this time period *ikk2* genetic deletion did not affect the general health status of the animal. However, as the mice aged, they developed cancer and they had to be culled as mentioned above.

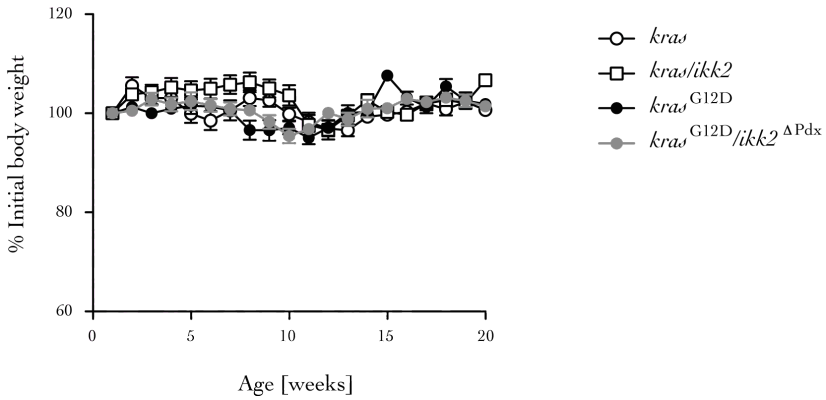

Figure 3.7: Body weight monitoring of the main mouse strains used

The percentage of the initial body weight was assessed weekly for *kraS*, *kraS/ikk2*, *kraS*^{G12D} and *kraS*^{G12D}*/ikk2*$^{\Delta Pdx}$ mice. Data are shown as mean ± SD, n = 10.

3.4.2 General histopathology

The haematoxylin and eosin (H&E) stain is the most widely used staining technique to access the general histopathology of any tissue. This classical method detects any obvious and major abnormality in the tissue structure. Staining was carried out by the Barts Cancer Institute pathology department. A magnification from the pancreases of 5-month old mice is shown in Figure 3.8, indicating no gross pathology in all intermediate strains.

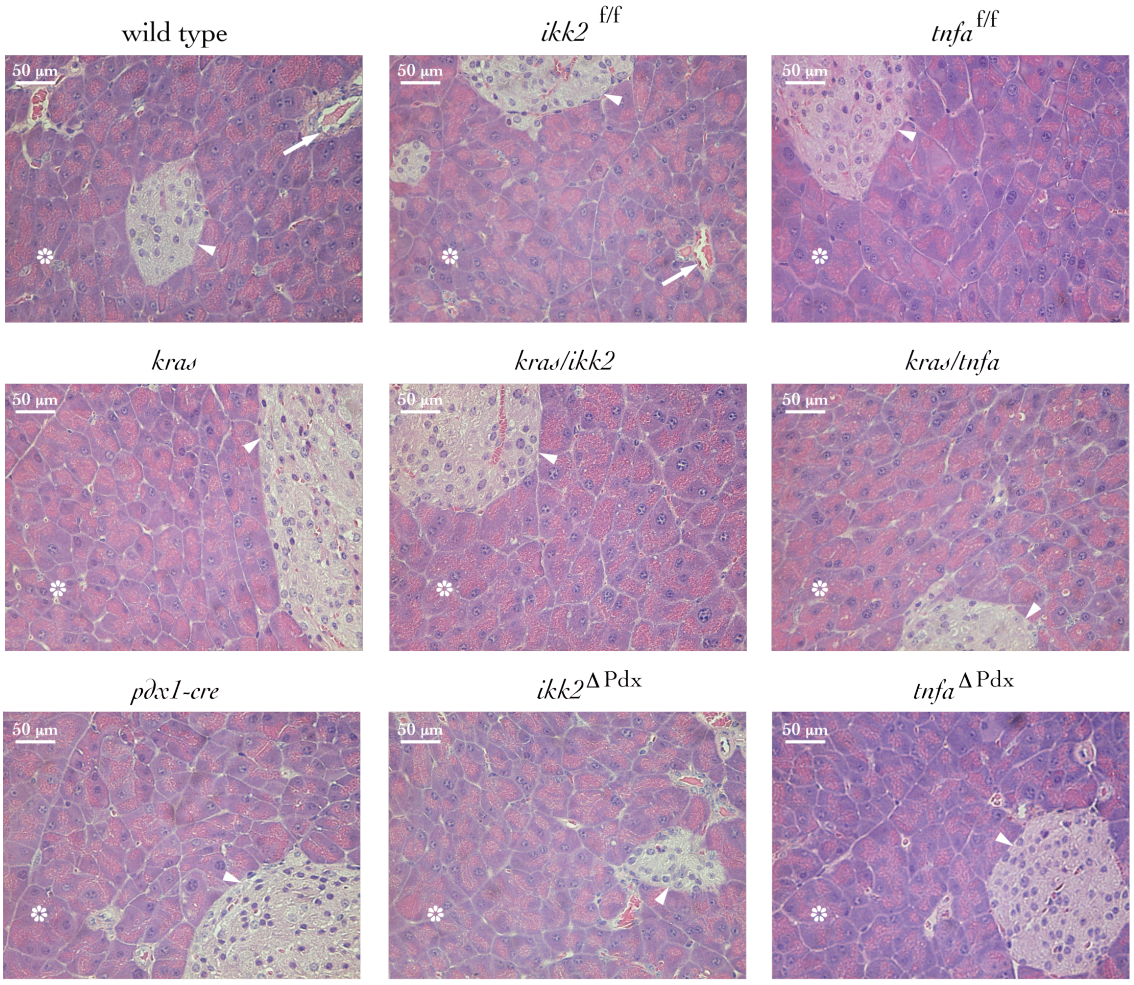

Figure 3.8: Haematoxylin and eosin staining of pancreas sections from intermediate strains

Histological aspect of the pancreas from the indicated strains at 5 months of age. Normal epithelium is shown with islets of Langerhans (arrowhead), ducts (solid arrow) and acinar cells within the exocrine pancreas (asterisk). Each picture is representative of three mice examined for each genotype. blue = nuclei and pink to red = cytoplasm.

In Figure 3.9, the pancreases from the pancreatic cancer mouse models were analysed and compared with the intermediate strains. As shown previously in Figure 3.8, *kras* and *kras/ikk2* strains did not present any PanIN lesions. As expected, the presence of PanIN lesions in the pancreases of 4-month old $kras^{G12D}$ mice was clearly visible (Hingorani *et al.,* 2003). Conversely, those PanIN structures were less frequent in the pancreases of age-matched $kras^{G12D}/ikk2^{\Delta Pdx}$ mice. This was an interesting observation, suggesting that the genetic deletion of *ikk2* can delay PanIN formation and that signalling pathways leading to IKK2 activation seem to be

involved in pancreatic carcinogenesis. The IKK complex can be activated by Toll-like receptors or by the classical receptors involved in NF-κB activation (see section 1.3.1.2). Additional experiments were carried out to further investigate the underlying mechanisms.

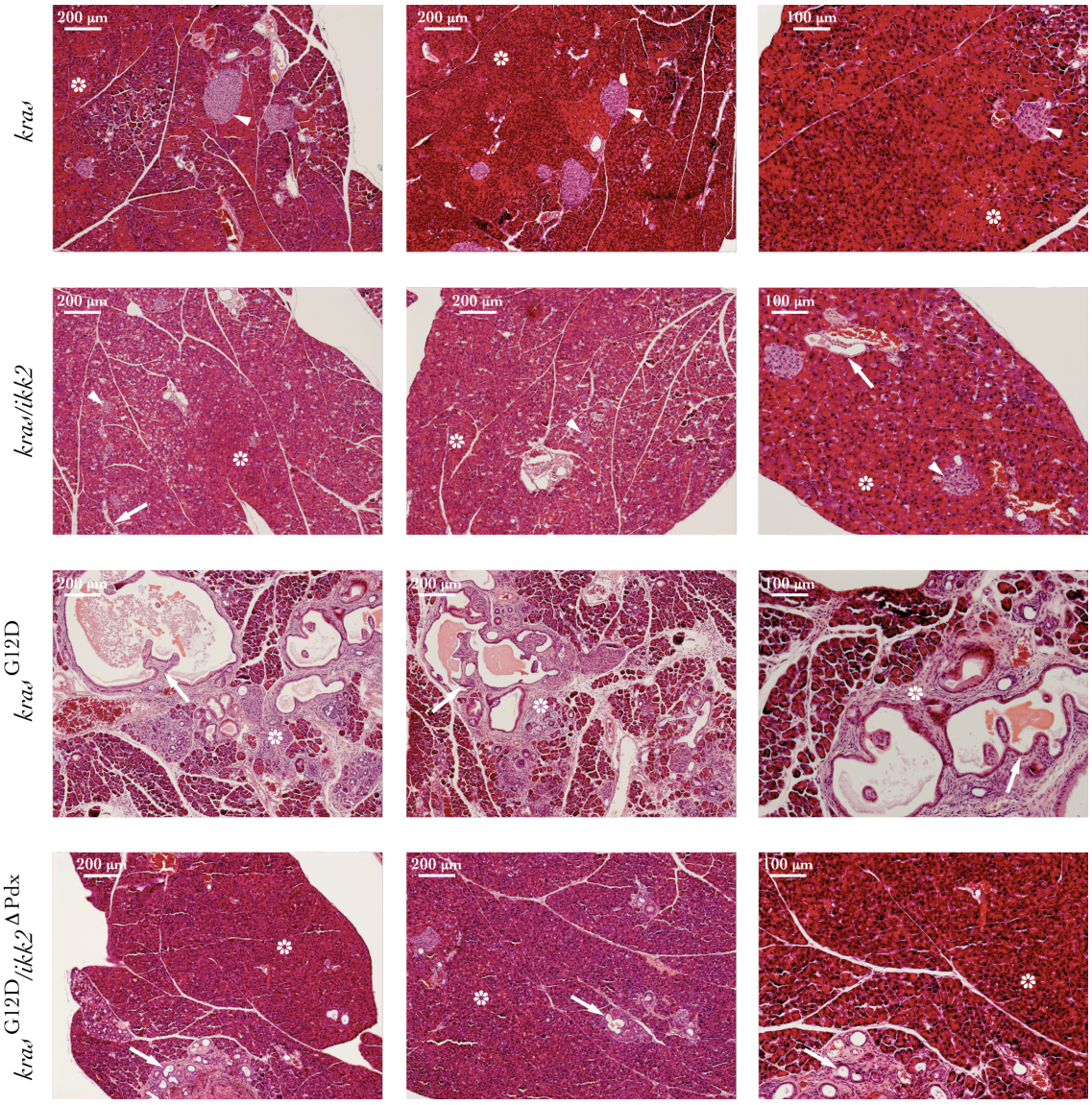

Figure 3.9: Haematoxylin and eosin staining of pancreas sections from mouse models

Histological aspect of the pancreas from the indicated strains at 4 months of age. *kraS*: normal epithelium with an islet of Langerhans (arrowhead) and acinar cells within the exocrine pancreas (asterisk). *kraS/ikk2*: normal epithelium with an islet of Langerhans (arrowhead), ducts (solid arrow) and acinar cells within the exocrine pancreas (asterisk). *kraS*^{G12D}: high-grade PanIN-3 lesions with loss of cell polarity, "budding" into the lumen (solid arrow) and surrounding stroma (asterisk). *kraS*^{G12D}*/ikk2*$^{\Delta Pdx}$: PanIN-1B lesion with papillary epithelium (solid arrow) surrounded by normal exocrine tissue (asterisk). Each picture is representative of three mice examined for each genotype. blue = nuclei and pink to red = cytoplasm.

3.4.3 Histological quantification

To quantify and evaluate the effect of *ikk2* and *tnfa* genetic deletion on PanIN formation, the proportion of the pancreas occupied by PanIN lesions and their stage were histologically assessed in *kras*^{G12D}, *kras*^{G12D}/*ikk2*$^{\Delta Pdx}$ and *kras*^{G12D}/*tnfa*$^{\Delta Pdx}$ mice. This was performed according to the universal classification system for pancreatic duct lesions (Hruban *et al.,* 2001). Cohorts of 12 mice for each strain at 2, 5 or 8 months of age were analysed and the results are presented in Figure 3.10.

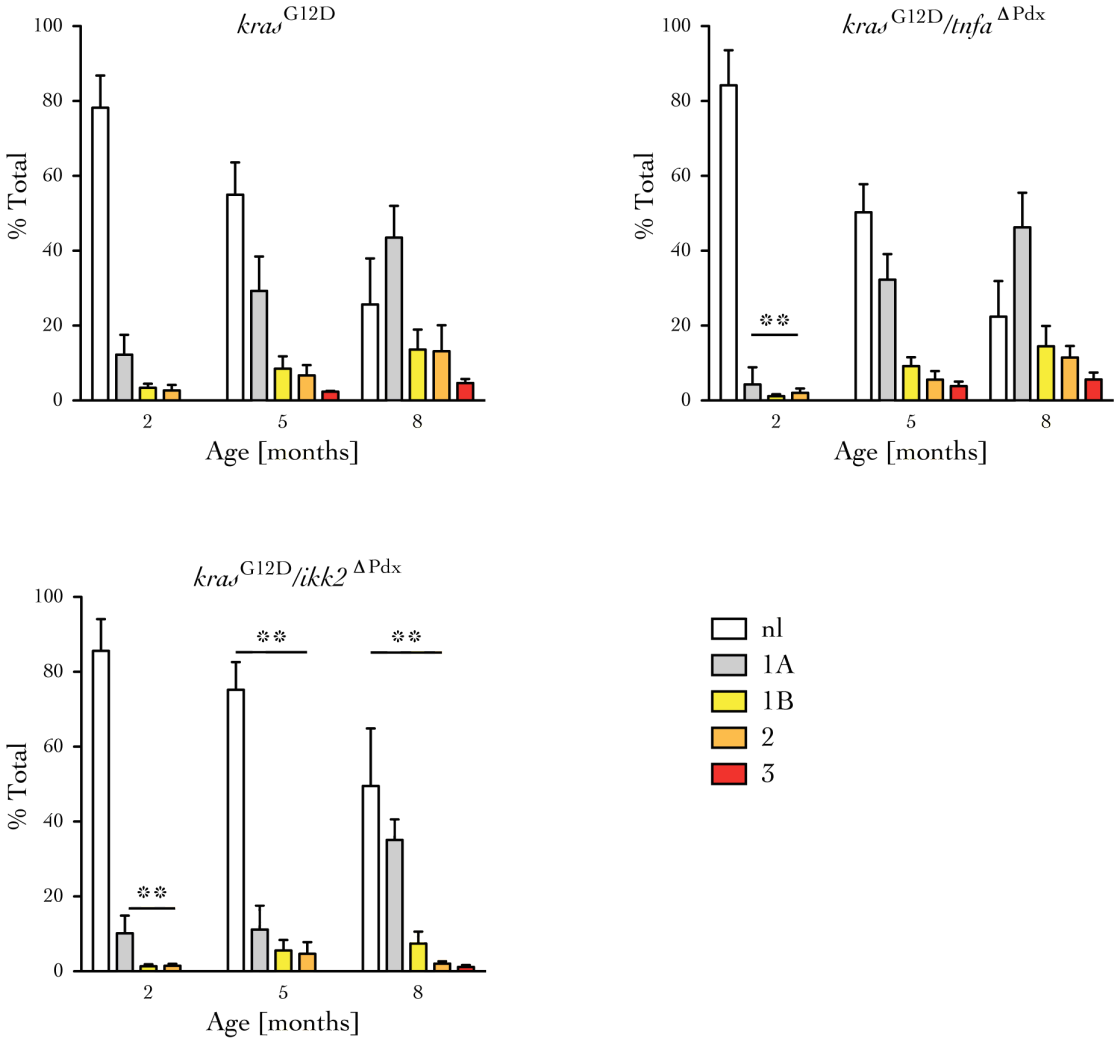

Figure 3.10: Proportion of the pancreas occupied by PanIN lesions

Quantification of the proportion of the pancreas occupied by normal tissue (nl, no lesion) and PanIN lesions. Frequency and grade of the lesions were assessed at 2, 5 and 8 months of age. *Ikk2* deletion reduces the frequency of PanIN lesions while *tnfa* deletion has an impact only on 2-month old mice. Data are shown as mean + SD, **p<0.01, n=12.

Ikk2 deletion in *kras*^{G12D}/*ikk2*$^{\Delta Pdx}$ mice resulted in a profound decrease in the frequency of high-grade PanIN-3 lesions compared with *kras*^{G12D} mice. At 5 and 8 months of age, almost 80 % and 60 %, respectively, of the pancreatic parenchyma retained normal exocrine tissue. Even at 8 months of age, the formation of PanIN-2 and PanIN-3 lesions was minimal and the frequency of PanIN-1 was lower compared with both *kras*^{G12D} and *kras*^{G12D}/*tnfa*$^{\Delta Pdx}$ mice.

However, *tnfa* deletion in *kras*^{G12D}/*tnfa*$^{\Delta Pdx}$ mice had an impact only in young mice. More specifically, 2-month old *kras*^{G12D}/*tnfa*$^{\Delta Pdx}$ mice exhibited a significant reduction in early PanIN lesions, but by 5 months of age, PanIN lesions had formed and progressed in a pattern similar to the one observed in *kras*^{G12D} mice.

In the context of mutant *kras*, these results suggest that IKK2 signalling is important for the development and progression of PanIN lesions. However, deletion of *tnfa* in pancreatic progenitors affects only the early stages of carcinogenesis.

3.4.4 Analysis of pancreatic tissue sections

3.4.4.1 Pancreatic progenitor marker SOX9

As reviewed by Morris *et al., kras* mutations are very common in pancreatic cancer and can be sufficient to drive PanIN and PDAC development (Morris *et al.,* 2010b). In the *kras*^{G12D} model, mutant *KRAS*^{G12D} was produced in *Pdx1* positive cells (making up most cells in the developing pancreas), but it was not clear whether PanIN lesions were arising from the exocrine or the endocrine pancreas (see section 1.2.1 for pancreas biology and section 1.2.8.3 for possible origins of PanIN lesions).

SOX9 is a transcription factor that has been discovered to be involved primarily in many development processes such as chondrogenesis and osteogenesis (skeletogenic processes corresponding to cartilage and bone development respectively) (Akiyama *et al.,* 2005; Lefebvre *et al.,* 1997; Wright *et al.,* 1995) but also gonadogenesis (Kent *et al.,* 1996; Morais da Silva *et al.,* 1996). More recently, SOX9 has been shown to be a critical transcription factor for the development of many tissues and organs, in particular for the pancreas (Lioubinski *et al.,* 2003; Piper *et al.,* 2002). SOX9 is not only a marker of early pancreatic progenitor cells, but it can also drive pancreatic cells to differentiate into endocrine cells (Seymour *et al.,* 2007; Seymour *et al.,* 2008).

Using SOX9 as a marker for islets of Langerhans, immunohistochemistry on pancreas sections was performed on the mouse strains (Figure 3.11) to identify whether the PanIN lesions could arise from the endocrine compartment.

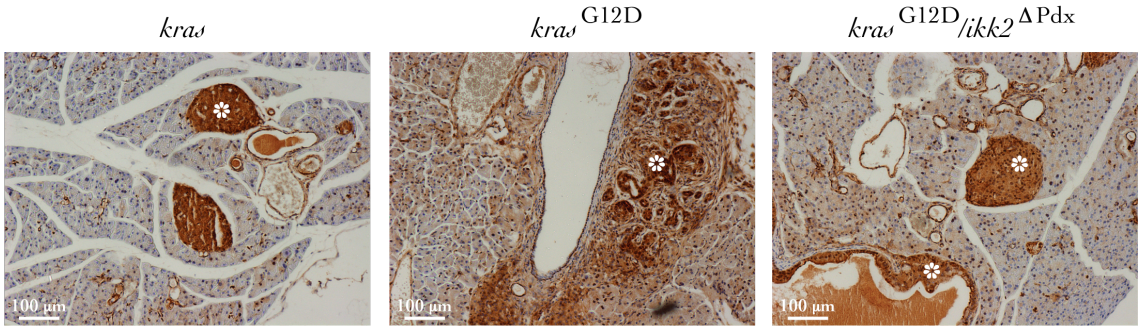

Figure 3.11: Immunohistochemistry staining for SOX9 in tissue sections

Pancreas sections of 4-month old *kras*, *kras*^{G12D} and *kras*^{G12D}/*ikk2*$^{\Delta Pdx}$ mice stained with anti-SOX9. Islets of Langerhans and PanIN lesions are both positive for this transcription factor in each mouse strain (dark brown and asterisk). Each picture is representative of three mice examined for each genotype.

Figure 3.11 confirms that SOX9 is a marker for islets of Langerhans but also demonstrates that PanIN lesions in the pancreases of *kras*^{G12D} and *kras*^{G12D}/*ikk2*$^{\Delta Pdx}$ mice express SOX9. This suggests that PanIN lesions can have an endocrine origin or that this protein is abnormally overexpressed during pancreatic carcinogenesis,

similarly to the Notch signalling pathway. SOX9 staining was weaker in the pancreases of *kras*^{G12D}/*ikk2*$^{\Delta Pdx}$ mice and normal islets structures were still visible.

3.4.4.2 Desmoplasia

One of the features of PDAC is an abundant fibrosis, also called desmoplastic reaction. This dense stroma, absent in normal pancreases, surrounds the malignant cells and is mainly composed of collagen (Hezel *et al.,* 2006; Mahadevan and Von Hoff 2007).

Masson's trichrome staining distinguishes cells from their neighbouring connective tissue (Goldner 1938). This method was used to evaluate the desmoplastic reaction in the pancreases of the different mouse models. To better visualise the more advanced stage of the PanIN lesions in the pancreases of *kras*^{G12D} mice compared with the ones observed in the pancreases of *kras*^{G12D}/*ikk2*$^{\Delta Pdx}$ mice, Masson's trichrome staining was performed (Figure 3.12). Staining was carried out by Juliana Candido, Barts Cancer Institute, Queen Mary, University of London, London, UK.

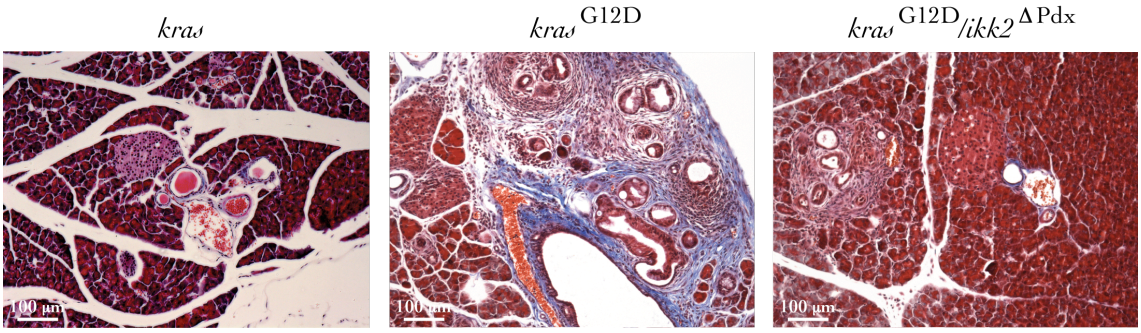

Figure 3.12: Masson's Trichrome staining for collagen in tissue sections

Pancreas sections of 4-month old *kras*, *kras*^{G12D} and *kras*^{G12D}/*ikk2*$^{\Delta Pdx}$ mice stained with Masson's trichrome. Stroma is absent in *kras* and *kras*^{G12D}/*ikk2*$^{\Delta Pdx}$ mice, while *kras*^{G12D} present a dense stromal reaction (blue). Each picture is representative of three mice examined for each genotype. blue = collagen, red = cytoplasm and black = nuclei.

Histological analysis after Masson's trichrome staining showed no desmoplastic reaction in the pancreases of *kras* mice. However, in the pancreases of *kras*^{G12D} mice, a very dense stroma was visible (blue stain) around the PanIN structures characterised earlier. Furthermore, stromal reaction was profoundly delayed in the pancreases of *kras*^{G12D}*/ikk2*$^{\Delta Pdx}$ mice, demonstrating a less advanced stage in PanIN formation.

3.4.4.3 Cell proliferation

In order to detect proliferating cells in tissue sections, two differents strategies were used: the measurement of 5-bromo-2'-deoxyuridine (BrdU) uptake and the detection of PCNA by immunohistochemistry on tissue sections (see the Materials and Methods chapter).

3.4.4.3.1 BrdU uptake

In vivo cell proliferation analyses evolved from the early days of using [^{3}H]thymidine to using BrdU and from high doses and frequent injections to a single BrdU injection (Kempermann *et al.,* 1997b, 1997a; Nowakowski *et al.,* 1989). Sacrificing the animal as soon as 90 minutes after the injection allows sufficient time to visualise BrdU uptake and therefore measurement of cell proliferation. To evaluate cell proliferation in the pancreases of the different mouse models, BrdU was injected intraperitoneally into each mouse and their pancreases were harvested 90 minutes afterwards. BrdU immunohistochemistry staining was performed and data are shown in Figure 3.13.

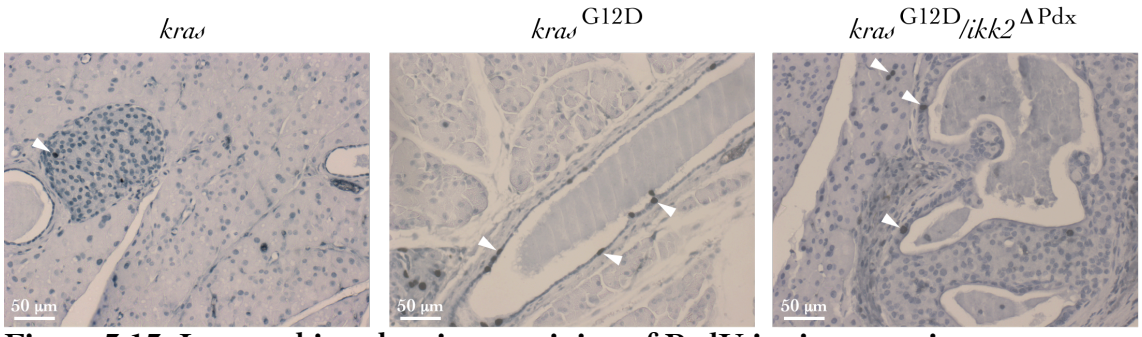

Figure 3.13: Immunohistochemistry staining of BrdU in tissue sections

Pancreas sections of 4-month old *kras*, *kras*^{G12D} and *kras*^{G12D}/*ikk2*$^{\Delta Pdx}$ mice stained with anti-BrdU. Proliferating cells are stained in dark blue (arrowhead) and no significant difference between the mouse strains is observed. Each picture is representative of three mice examined for each genotype.

No major differences were visible between the three mouse strains analysed (Figure 3.13). Only a few number of positive cells were detected in the endocrine part of the pancreases of *kras* mice and in PanIN structures of *kras*^{G12D} and *kras*^{G12D}/*ikk2*$^{\Delta Pdx}$ mice.

Pancreas regeneration after chemically-induced damage is known to be very slow in healthy mice (Fendrich *et al.,* 2008), but recent studies have shown that following tissue damage, pancreatic regeneration can occur, involving the islets of Langerhans (Georgia and Bhushan 2004, 2006; Kushner *et al.,* 2005; Teta *et al.,* 2005) or the acinar cells (Desai *et al.,* 2007; Jensen *et al.,* 2005). Malignant cells and PanIN development are characterised by enhanced proliferation (Klein *et al.,* 2002). However, an increase in the number of BrdU positive cells was not detected in the pancreas of the different mouse strains, suggesting that at that stage either the cells were not hyperproliferating, or that the assay was not sensitive enough to detect the differences from the surrounding normal tissue.

3.4.4.3.2 Proliferating cell nuclear antigen staining

Proliferating cell nuclear antigen (PCNA) is a nuclear protein and acts as a chaperone protein, assisting DNA polymerase δ during DNA replication. PCNA is therefore mainly expressed during the S-phase of the cell cycle and is used as a specific marker for cell proliferation (Kubben *et al.,* 1994; Miyachi *et al.,* 1978; Prives and Gottifredi 2008). Immunohistochemistry staining for PCNA in the pancreases of *kras*, *kras*^{G12D} and *kras*^{G12D}/*ikk2*$^{\Delta Pdx}$ mice was performed and data are shown in Figure 3.14.

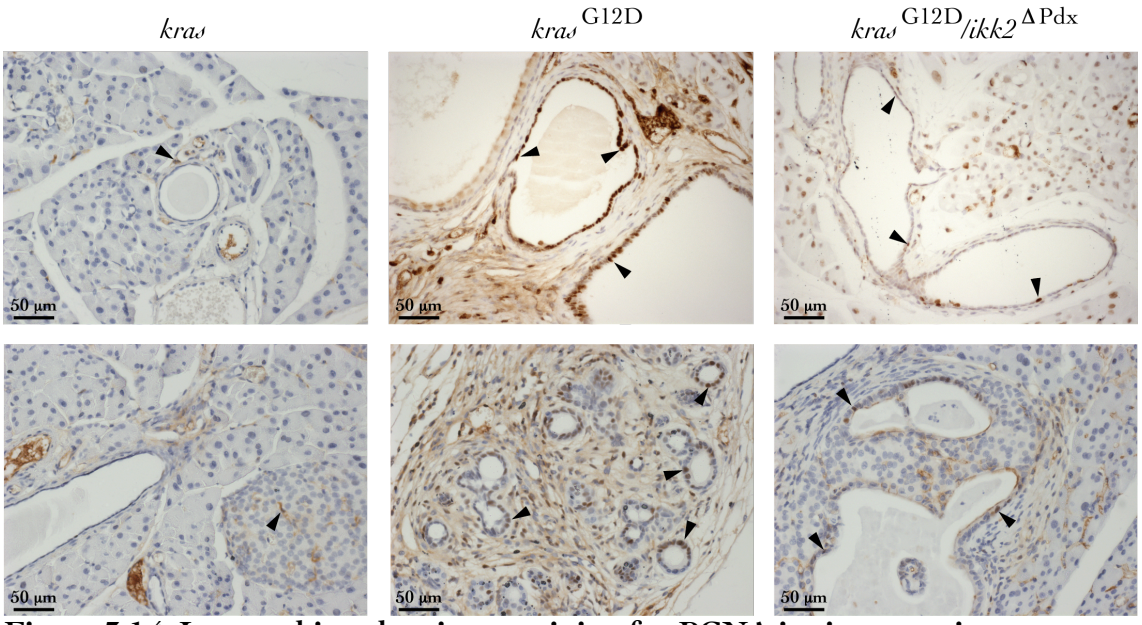

Figure 3.14: Immunohistochemistry staining for PCNA in tissue sections

Pancreas sections of 4-month old *kras*, *kras*^{G12D} and *kras*^{G12D}/*ikk2*$^{\Delta Pdx}$ mice stained with anti-PCNA. PCNA positive cells are stained in dark brown (arrowhead) and an increase in the number of PCNA positive cells is observed in *kras*^{G12D} mice compared with *kras* mice. However, this number is reduced in the pancreases of *kras*^{G12D}/*ikk2*$^{\Delta Pdx}$ mice. Each picture is representative of three mice examined for each genotype.

Very little PCNA protein was observed in the pancreases of *kras* mice. PCNA positive cells were clearly visible and abundant in the pancreases of *kras*^{G12D} mice, especially in PanIN areas (arrowheads). There was, however, a reduction in the number of proliferating cells in the pancreases of *kras*^{G12D}/*ikk2*$^{\Delta Pdx}$ mice compared with *kras*^{G12D} mice. As it was previously shown that *kras*^{G12D}/*ikk2*$^{\Delta Pdx}$ mice presented

less PanIN lesions, a reduction in the number of PCNA positive cells was therefore not surprising. However, it should be noted that PCNA protein has been shown to play a role in DNA repair processes and that its detection may not be totally specific for cell proliferation (Muskhelishvili *et al.,* 2003).

The reduction in the number of PCNA positive cells observed in the pancreases of *kras*^{G12D}*/ikk2*$^{\Delta Pdx}$ mice does not correlate with the results obtained from BrdU staining (Figure 3.13).

Overall and despite the divergence of the results obtained with BrdU and PCNA staining, it seems that on *ikk2* genetic deletion, malignant cell proliferation is reduced *in vivo*, even though no effect was shown in the PanIN cell lines generated from the different mouse models and cultured *in vitro* (see section 3.3).

3.4.4.4 Apoptosis

Caspase activation is a hallmark of apoptosis (Mazumder *et al.,* 2008), and caspase-3 is activated when cleaved by an initiator caspase following an apoptotic signal.

To determine whether *ikk2* genetic deletion results in higher levels of apoptosis as opposed to a reduction in proliferation, pancreas sections from different mouse strains were stained for cleaved caspase-3 by immunohistochemistry (Figure 3.15).

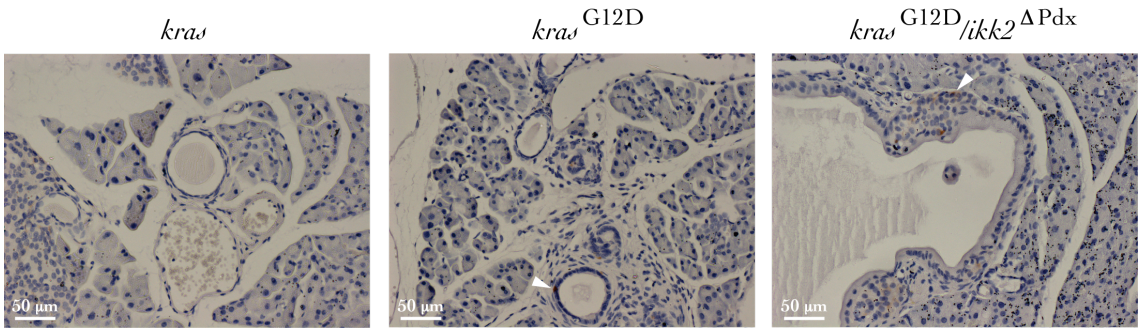

Figure 3.15: Immunohistochemistry staining for cleaved caspase-3 in tissue sections

Pancreas sections of 4-month old *kraS*, *kraS*^{G12D} and *kraS*^{G12D}/*ikk2*$^{\Delta Pdx}$ mice stained with anti-cleaved caspase-3. Apoptotic cells are stained in dark brown (arrowhead) and no significant difference between the mouse strains is observed. Each picture is representative of three mice examined for each genotype.

Low amounts of cleaved caspase-3 protein was identified in the pancreases of *kraS*, *kraS*^{G12D} and *kraS*^{G12D}/*ikk2*$^{\Delta Pdx}$ mice, revealing no differences between the genotypes, but also showing a very low level of apoptosis in general (Figure 3.15). This is in agreement with other published data, showing that apoptotic events are quite rare in any grade of PanIN lesion (Hamacher *et al.,* 2008; Luttges *et al.,* 2003).

3.4.5 Inflammatory infiltrate in the pancreas

As described in section 1.2.7, pancreatic cancer is characterised by a very dense stroma. The dynamics of the infiltration of immune cells in the pancreases of mice spontaneously developing pancreatic cancer (*kraS*^{G12D} mouse model) has been studied by Clark *et al.* and correlates with the progression of the disease (Clark *et al.,* 2007).

The formation of PanIN lesions is affected following *ikk2* genetic deletion in the pancreas, therefore the impact of this genetic modification on the infiltration of the immune cells was evaluated. In addition, many cytokines and chemokines are secreted by immune cells and their potential effect in this context was also explored.

3.4.5.1 Characterisation of the inflammatory infiltrate

A major source of inflammatory cytokines at tumour sites is the infiltrating immune cells. To measure and identify which immune cells infiltrate the pancreases of *kras*^{G12D}, *kras*^{G12D}/*ikk2*$^{\Delta Pdx}$ and *kras*^{G12D}/*tnfa*$^{\Delta Pdx}$ mice, the relative mRNA expression of different markers in whole organs was measured by qRT-PCR and the percentage of CD11b^{+}Gr1^{-}F4/80^{+} and CD11b^{+}Gr1^{+}F4/80^{-} cells was analysed by flow cytometry, both at 2 and 5 months of age (Figure 3.16).

Immune cells can be identified by the expression of specific markers (Joyce and Pollard 2009). Table 3.2 summarises the markers used to identify different immune cell populations.

Cell markers	Immune cells
B220	B cells
CD11b^{+} Gr1^{-} F4/80^{+}	Macrophages
CD11b^{+} Gr1^{+} F4/80^{-}	Neutrophils
CD208	Dendritic Cells
CD2r	T cells
CD8a	Cytotoxic T cell
CXCR1	Neutrophils
NK1.1	NK cells

Table 3.2: Surface markers used for the identification of immune cells

Table describes cell markers and the immune cell types they can be found on. The presence or absence of these markers can be assessed by measuring mRNA levels with qRT-PCR or protein levels by flow cytometry.

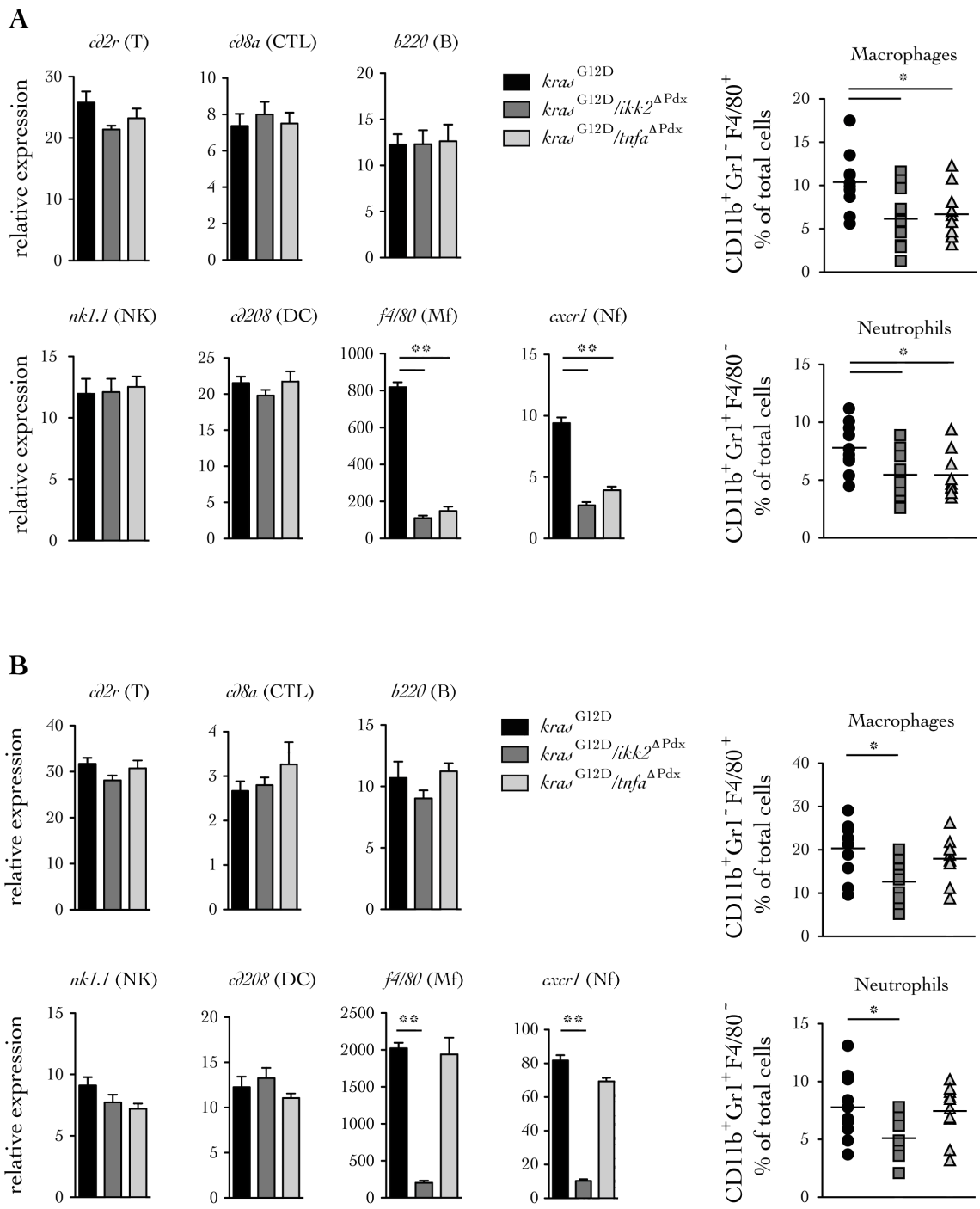

Figure 3.16: Profile of the infiltrated inflammatory cells

Relative mRNA expression of immune cells markers in whole pancreases of (A) 2- and (B) 5-month old mice. *cd2r* for T cells (T), *cd8a* for cytotoxic T cells (CTL), *b220* for B cells (B), *nk1.1* for natural killers (NK), *cd208* for dendritic cells (DC), *f4/80* for macrophages (Mf) and *cxcr1* for neutrophils (Nf). Gene expression was quantified by qRT-PCR and normalised to mRNA levels of 18S. Data are shown as mean + SD. Percentage of $CD11b^{+}Gr1^{-}F4/80^{+}$ and $CD11b^{+}Gr1^{+}F4/80^{-}$ cells in the pancreas was measured by flow cytometry. Each individual data point represents an individual mouse and mean values are depicted by horizontal lines, $^{*}p<0.05$, $^{**}p<0.01$, n=10.

Figure 3.16 A illustrates the immune cell types present in the pancreases of 2-month old mice. For the infiltrated immune cell populations analysed, no difference between the three mouse strains was observed. However, *kras*^{G12D}*/ikk2*$^{\Delta Pdx}$ and *kras*^{G12D}*/tnfa*$^{\Delta Pdx}$ mice had reduced mRNA levels of *f4/80* and *cxcr1*, indicating a lower number of macrophages and neutrophils. This was confirmed by flow cytometry analysis. At 5 months of age, *f4/80* and *cxcr1* expression levels in pancreases from *kras*^{G12D}*/tnfa*$^{\Delta Pdx}$ mice were elevated compared with 2-month old mice (Figure 3.16 B). Flow cytometry analysis also confirmed these results (Figure 3.16 A and B).

3.4.5.2 Adoptive transfer

To investigate the role of TNF-α secreted by the immune cells, *tnfa*$^{f/f}$*/Mx-cre* mice were generated. In these mice, *Cre* expression is under the control of the promoter of the *Mx* gene. This gene is silent in healthy mice but its expression can be induced by IFN-α, IFN-β or synthetic dsRNA such as poly(I:C), mimicking a viral infection (Hug *et al.,* 1988; Kuhn *et al.,* 1995; Staeheli *et al.,* 1986). This model, where *tnfa* deletion was temporally controlled by treating the mice with the immunostimulant poly(I:C), was used to obtain bone marrow cells lacking *tnfa*. *tnfa*$^{f/f}$*/Mx-cre* mice treated with poly(I:C) are abbreviated as *tnfa*$^{\Delta Mx}$ mice.

Bone marrow-derived cells from female *tnfa*$^{f/f}$ or *tnfa*$^{\Delta Mx}$ mice were transplanted into previously lethally irradiated 6-week old *kras*^{G12D} or *kras*^{G12D}*/tnfa*$^{\Delta Pdx}$ female mice, therefore generating two chimera strains. Peripheral leukocytes from these transplanted mice, but also from *kras*, *kras*^{G12D}, *kras/tnfa* and *kras*^{G12D}*/tnfa*$^{\Delta Pdx}$ mice (used as negative controls), were collected and cultured *in vitro*. Chimeras were generated in Barts Cancer Institute Biological Services Unit with the help of Dr Thorsten Hagemann.

The levels of TNF-α released in the culture medium upon *ex vivo* LPS stimulation were measured by ELISA (Figure 3.17). As expected, immune cells from *tnfa*$^{\Delta Mx}$ mice transplanted into *kras*^{G12D} or *kras*^{G12D}/*tnfa*$^{\Delta Pdx}$ mice were not able to secrete TNF-α.

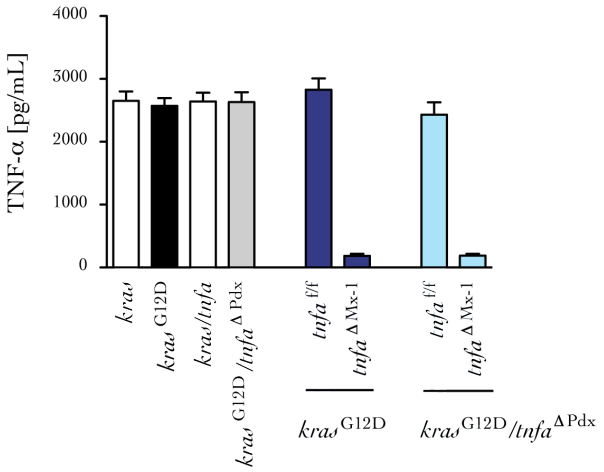

Figure 3.17: *Ex vivo* TNF-α secretion from immune cells

Lethally irradiated *kras*^{G12D} and *kras*^{G12D}/*tnfa*$^{\Delta Pdx}$ mice were transplanted with bone marrow cells from *tnfa*$^{f/f}$ or *tnfa*$^{\Delta Mx}$ mice. Immune cells were collected and the levels of secreted TNF-α were measured by ELISA upon *ex vivo* LPS stimulation (16 hours). Control cells were generated from *kras*, *kras*^{G12D}, *kras*/*tnfa* and *kras*^{G12D}/*tnfa*$^{\Delta Pdx}$ mice. Data are shown as mean + SD of triplicate experiments and are representative of three independent experiments, n=10.

The proportion of the pancreas occupied by PanIN lesions and their histological stage were assessed in the generated chimeras (Figure 3.18). As opposed to *tnfa* deletion in the pancreas only, *tnfa* deletion in the pancreas as well as in the immune cells resulted in a significant decrease in the frequency of PanIN lesions at all time points. PanIN profiles were similar to those observed for *kras*^{G12D}/*ikk2*$^{\Delta Pdx}$ mice in Figure 3.10.

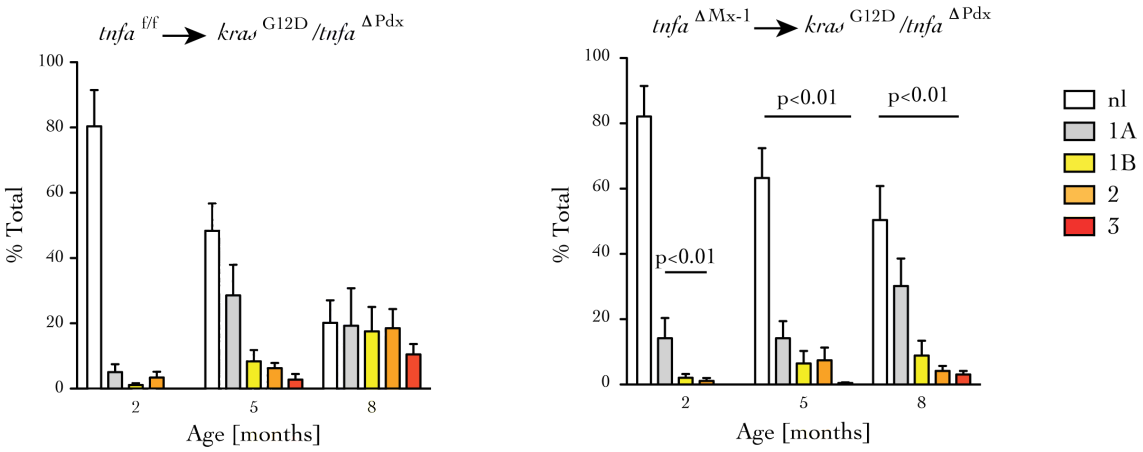

Figure 3.18: Proportion of pancreas occupied by PanIN lesions in chimeras

Quantification of the proportion of pancreas occupied by normal tissue (nl, no lesion) and PanIN lesions. Frequency and grade of the lesions were assessed at 2, 5 and 8 months of age. Data are shown as mean + SD, **p<0.01, n=10.

These results confirm previous observations and conclusions that IKK2 signalling is important for the development and progression of PanIN lesions in the context of mutant *kras*. Moreover, the development of PanIN lesions observed from 5 months of age in *kras*^{G12D}/*tnfa*$^{\Delta Pdx}$ mice is due to the production of TNF-α by the immune cells recruited in the tumour site. Therefore, production of TNF-α by transformed epithelial cells, as opposed to immune cell-derived TNF-α secretion, is a critical step in the initial steps and early stages of pancreatic cancer promotion.

3.5 Discussion and conclusion

This chapter describes how new triple mutant mice were generated and what the phenotypic characteristics of these new mouse models were, in the context of pancreatic cancer.

In the triple mutant mice, *Cre* expression is under the control of the pancreas specific promoter *Pdx*. Its expression is therefore restricted to *Pdx* expressing cells (pancreatic progenitors), allowing recombination events in a specific tissue. *ikk2* or *tnfa* genes were flanked by two *loxP* sites and were subsequently knocked out upon CRE-recombination, while a mutated *kras* allele had an upstream STOP cassette flanked by two *loxP* sites and its expression was activated upon CRE-recombination.

In the endogenous $kras^{G12D}$ model, *Cre* expression, and therefore $KRAS^{G12D}$ production, has previously been shown to create a genetic mosaicism in the organ, inducing PanIN formation in a focal manner (Hingorani *et al.,* 2003). This observation implies that PanIN lesions might have a cell-specific origin. This mosaicism was useful in this model, allowing a better comparison with human disease, where *kras* mutations occur spontaneously and randomly in different cells. It should be noted that although *Pdx* is predominantly expressed in the pancreas, it can also be found in other cell types and organs. A recent publication suggests that *Pdx* is also expressed in the skin (Mazur *et al.,* 2010b) and that recombination events can also occur in leukocytes (personal communication Dr David Tuveson, Cancer Research UK Cambridge Research Institute, Cambridge, UK). This suggests that $KRAS^{G12D}$ production and *ikk2* or *tnfa* genetic deletion can occur in the skin and/or in the leukocyte compartment of the different mouse models. However, in the three mouse models used ($kras^{G12D}$, $kras^{G12D}/ikk2^{\Delta Pdx}$ and $kras^{G12D}/tnfa^{\Delta Pdx}$ mice) no

recombination events were identified in the skin or in the leukocytes (unpublished data from Dr Thorsten Hagemann's group, Barts Cancer Institute, Queen Mary, University of London, London, UK).

NF-κB is a classical target of TNF-α and is activated via IKK2. This signalling pathway is activated during inflammation but several studies have also demonstrated the requirement of IKK2 in tumour formation, such as in a model of colitis-associated cancer (Greten *et al.,* 2004) and more recently in a spontaneous mouse model of melanoma (Yang *et al.,* 2010). The TNF-α/IKK2/NF-κB pathway has been shown to be activated in pancreatic cancer cell lines (Basseres and Baldwin 2006; Lu *et al.,* 2011). However, the role of this pathway in pancreatic cancer progression has so far been unexplored.

Epithelial cell lines derived from the pancreases of the different mouse models were generated to create a simplified and controlled *in vitro* system to initially identify malignant cell autonomous cytokine secretion and also to study the role of TNF-α signalling on pancreatic cancer cells. Constitutive secretion of TNF-α is an interesting finding, as this major inflammatory cytokine can have a tumour-promoting role (Balkwill 2002) and has been shown to be secreted by many different cancer cells (Balkwill 2006; Szlosarek *et al.,* 2006). Moreover, previous work performed in our laboratory describes how ovarian cancer cells also produce TNF-α in a constitutive manner (Kulbe *et al.,* 2007; Kulbe *et al.,* 2011), thus providing and maintaining a tumour-promoting environment. Production of IL-6 and IL-1β by the PanIN and PDAC cell lines tested was not surprising as their expression is known to be induced by NF-κB signalling (Naugler and Karin 2008) and also because

constitutive secretion of IL-1β by pancreatic cancer cells has already been observed (Arlt *et al.,* 2002; Lu and Stark 2004).

The combination of oncogenic mutations and chronic inflammation has already been proven to be necessary for the development of pancreatic cancer (Guerra *et al.,* 2007; Guerra *et al.,* 2011). In order to investigate whether a similar process is operating in the context of *kras*-driven pancreatic cancer in absence of an exogenous inflammatory insult, the hypothesis that autocrine TNF-α secreted by pre-malignant epithelial cells can drive pancreatic cancer progression was tested. Histological analysis of the pancreases of the mutant mice indicated that *tnfa* deletion had a positive effect on young mice only. This suggests that production of TNF-α by transformed epithelial cells facilitates the development and progression of PanIN lesions at the onset of the disease. However, by 5 months of age, $kras^{G12D}/tnfa^{\Delta Pdx}$ mice had already developed PanIN lesions similar to the ones observed in $kras^{G12D}$ mice. Genetic deletion of *ikk2* had a greater effect on the development and progression of PanIN lesions. Indeed, the pancreases of 4-month old $kras^{G12D}$ mice presented high numbers of PanIN lesions at quite advanced stages, whereas the pancreases of age-matched $kras^{G12D}/ikk2^{\Delta Pdx}$ mice presented only a few numbers of low-grade PanIN lesions (Figure 3.9). Genetic deletion of *ikk2* delays pancreatic tumour formation but no significant differences in terms of histological grade and metastatic potential were observed (Figure 3.5 and Figure 3.6).

The tumour microenvironment plays an important role in many cancers (reviewed in section 1.1.4) (Hezel *et al.,* 2006; Mahadevan and Von Hoff 2007). Secretion of cytokines and chemokines such as CSF1 and CCL2 by the small amount of low-grade PanIN lesions present in 2-month old $kras^{G12D}/tnfa^{\Delta Pdx}$ mice was probably

sufficient to trigger immune cell recruitment (primarly macrophages and neutrophils) (Hagemann *et al.,* 2008). Inflammatory cells, especially macrophages, secrete high levels of a range of inflammatory cytokines including IL-6, IL-1β and TNF-α (Qian and Pollard 2010). As the disease progressed, these cytokines probably compensated for the early protective effect of the *tnfa* genetic deletion in the pre-malignant epithelial cells. Analysis of the immune cell infiltrate analysis confirmed this process. Infiltration of macrophages and neutrophils was low in the pancreases of *kras*^{G12D}*/ikk2*$^{\Delta Pdx}$ and *kras*^{G12D}*/tnfa*$^{\Delta Pdx}$ mice at 2 months of age. However, the infiltrate appeared to be increased in 5-month old *kras*^{G12D}*/tnfa*$^{\Delta Pdx}$ mice but not in *kras*^{G12D}*/ikk2*$^{\Delta Pdx}$ mice (Figure 3.16).

The role of infiltrating immune cells, in particular macrophages, in promoting tumour development, progression and metastasis is well documented (Hagemann *et al.,* 2005; Mantovani *et al.,* 2006) and has been described in section 1.1.4.3. The reduced infiltration of macrophages in *kras*^{G12D}*/tnfa*$^{\Delta Pdx}$ mice and more profoundly in *kras*^{G12D}*/ikk2*$^{\Delta Pdx}$ mice may represent an important factor for the delayed disease progression observed. Besides leukocytes, fibroblasts are also a main component of the tumour stroma and are also involved in the generation of a tumour-promoting microenvironment by releasing additional soluble factors that enhance tumour growth. Fibroblasts mostly secrete growth factors and angiogenic factors and nothing is known regarding a potential secretion of TNF-α (Angeli *et al.,* 2009). Nevertheless, fibroblasts within the tumour stroma are likely to be responsive to the presence of cytokines such as TNF-α and further contribute to tumour progression. Investigation of the role of these cells in the context of *tnfa* or *ikk2* genetic deletion is however beyond the scope of the work presented here.

In *kras*^{G12D}*/ikk2*$^{\Delta Pdx}$ mice, not only could pancreatic transformed epithelial cells not secrete TNF-α, but they could not be activated by this cytokine, as the *ikk2* gene coding for the IKK2 kinase from the TNF-α/IKK2/NF-κB signalling pathway is deleted. Genetic deletion of *ikk2* impairs the recruitment of immune cells, contributing to a less inflammatory tumour microenvironment that may explain the absence of PanIN lesions. However, to identify whether the TNF-α/IKK2 signalling pathway is solely implicated in this phenomenon, additional experiments, described in the following chapters, were performed. Inactivation of this pathway has been shown to influence other signalling pathways which have a direct link with cytokine or chemokine production (Oeckinghaus *et al.,* 2011).

The impact of TNF-α derived from immune cells, as opposed to from malignant cells was further addressed with adoptive transfer experiments, where the immune system of *kras*^{G12D}*/tnfa*$^{\Delta Pdx}$ mice was reconstituted with bone marrow cells from *tnfa*$^{\Delta Mx}$ mice. These mice had a significant reduction in the number and grade of PanIN lesions compared with the *kras*^{G12D}*/tnfa*$^{\Delta Pdx}$ mice reconstituted with bone marrow cells with intact *tnfa* expression (Figure 3.18). This result highlights the importance of malignant cell-derived TNF-α during the early process of pancreatic carcinogenesis.

The mouse *Mx* gene, also called influenza virus-resistance gene, is not activated in healthy mice, but can be expressed upon treatment with IFN-α, IFN-β or poly(I:C), an inducer of IFN production (Finkelman *et al.,* 1991), mimicking the cell response when infected by a virus (Hug *et al.,* 1988; Staeheli *et al.,* 1986). Combining the properties of this *Mx* gene with the *Cre-lox* system was the first step in controlling gene inactivation over time, but *Cre* recombination occurs in every cell type in the whole animal. *Mx-cre* mice have been generated, where CRE recombinase is

expressed only when the mice are exposed to viral infections or stimulated with IFN or poly(I:C) (Kuhn *et al.,* 1995). These mice were specifically used to delete *tnfa* in each circulating immune cell, regardless of its specific functions and markers. Although *tnfa* knockout animals do not have a lethal phenotype (Pasparakis *et al.,* 1996), *tnfa* expression may play a role during the development of the mouse immune system. The use of bone marrow-derived cells from $tnfa^{\Delta Mx}$ mice, rather than $tnfa^{f/f}$ mice, was then favoured, to avoid the introduction of more genetic disruption and to remain as close as possible to the wild type phenotype.

Cre activation was induced by three injections of the immunostimulant poly(I:C). However, the impact poly(I:C) could have on PanIN initiation and PDAC progression was not assessed due to time constraints. Its effects were considered as negligible because poly(I:C) was injected at a low dose (5 µg/g body weight) and because the mice were sacrificed quite rapidly afterwards. Moreover, the main scope of the project was to investigate the role of autocrine TNF-α, and not of poly(I:C) on pancreatic cancer initiation and progression.

To further characterise the $kras^{G12D}/ikk2^{\Delta Pdx}$ mutant mice generated, the presence of various markers, to assess cell lineage, cell proliferation and apoptosis, was analysed by immunohistochemistry (Figure 3.11 to Figure 3.15). Immunohistochemistry data for SOX9 suggest an endocrine origin for the PanIN lesions observed in the pancreases of $kras^{G12D}$ mice as they stained positive. However, as explained in section 1.2.8.3, the origin of PanIN lesions is still unknown and may require a combination of genetic and non-genetic events in one or several cell types. In addition, SOX9 expression could reflect the overexpression of the protein in the transformed cells and thereby not be indicative of their origin.

The analysis of two cell proliferation markers (BrdU and PCNA) suggests that malignant cell proliferation was reduced in the pancreas of *kraɹ*^{G12D}*/ikk2*$^{\Delta Pdx}$ mice *in vivo*. To further confirm these results, other methods of measuring cell proliferation can be used, such as immunohistochemistry staining for Ki-67, which is frequently assessed for tumour diagnosis. Ki-67 is a human nuclear protein, so antibodies have been developed to recognise the mouse equivalent. In-situ hybridisation can also be performed to detect histone mRNA on tissue sections. It has been shown that histone protein synthesis occurs only during the S-phase of the cell cycle, therefore providing another specific technique to evaluate cell proliferation (Heintz *et al.,* 1983). A study comparing these four methods, performed by Muskhelishvili *et al.,* identified a suitable technique to substitute immunohistochemistry staining for BrdU in paraffin sections of rat tissues (Muskhelishvili *et al.,* 2003). Immunohistochemistry staining for Ki-67 and in-situ hybridisation for histone mRNA were the two best substitutes. Neither of these techniques were performed due to time and cost constraints but they would have provided additional data to better estimate the effect of *ikk2* genetic deletion on cell proliferation.

Apoptotic events were not frequent in the pancreases of the *kraɹ*^{G12D} mice and genetic deletion of *ikk2* did not appear to affect apoptotic levels. Caspase activation is a characteristic for apoptosis, but cell death could also have been evaluated by other methods, including measurement of DNA fragmentation (identification of a ladder pattern on an agarose gel), staining with Annexin V, which has a high affinity for phosphatidylserine residues normally hidden within the plasma membranes but which are revealed on the cell surface during apoptosis, or to measure the release of cytochrome C from the mitochondria to the cytosol, as mitochondrial physiology and

permeability is also affected during apoptosis (Goldstein *et al.,* 2005; Martin *et al.,* 1995; Oberhammer *et al.,* 1993).

All immunohistochemical analyses were qualitative rather than quantitative. The presence or absence of the protein of interest was more relevant in order to identify the effects of *ikk2* genetic deletion on the different cellular processes analysed. When the protein of interest was detectable, the differences between the phenotypes were not noticeable and thus quantification was not necessary.

Overall, in this chapter, it was demonstrated that genetic inactivation of *ikk2* blocks the progression of PanIN lesions in the context of *kras*-driven pancreatic carcinogenesis, and that the production of TNF-α by transformed pancreatic epithelial cells is a critical step in pancreatic cancer promotion and progression. To unravel the mechanisms causing the delayed PanIN development profile observed in the $kras^{G12D}/ikk2^{\Delta Pdx}$ mice, additional analyses investigating the role of TNF-α/IKK2 signalling in pancreatic carcinogenesis were required. Its cooperation with the Notch signalling pathway, known to be upregulated in pancreatic cancer, is addressed in the next chapter.

CHAPTER FOUR: THE NF-κB AND THE NOTCH SIGNALLING PATHWAYS

4.1 Introduction

A critical role of NF-κB signalling in pancreatic cancer promotion was described in the previous chapter. Even though the NF-κB and the Notch signalling pathways are respectively the archetypical pathways of inflammation and development, they are both implicated in cancer (Bolos *et al.,* 2007; Oeckinghaus *et al.,* 2011; Roy *et al.,* 2007). As described in section 1.4.4, Notch can act as an oncogene, but also as a tumour suppressor in different types of cancer. Normally quiescent in the adult pancreas, the Notch signalling pathway is reactivated in pancreatic carcinogenesis and a specific role in pancreatic cancer tumour promotion and progression in the context of mutated *kras* has been identified (De La *et al.,* 2008; Mazur *et al.,* 2010a; Miyamoto *et al.,* 2003; Plentz *et al.,* 2009). It is thought to be required throughout PanIN and PDAC development, but the exact mechanisms behind the activation of this pathway at the early stages of the disease are not very clear. Activation of the EGF receptor in the exocrine pancreas induces neoplasia and the formation of PanIN lesions, and this is associated with an activation of Notch signalling (Miyamoto *et al.,* 2003). Activation of the Notch pathway is evaluated by measuring the expression levels of *hes1*, a Notch target gene (Hingorani *et al.,* 2003; Miyamoto *et al.,* 2003).

The Notch pathway can also be activated following experimental induction of pancreatitis, in a cancer-independent context (Gomez *et al.,* 2004; Jensen *et al.,* 2005; Siveke *et al.,* 2008). Upon caerulein-induced pancreatitis, the Notch signalling pathway normally expressed during pancreatic organogenesis is reactivated to allow pancreatic regeneration. This has been demonstrated by the measurement of increased levels of different components of the Notch pathway, including ligands (Dll1), receptors (Notch1), transcription factors (RBPjκ) and targets (HES1) (Gomez *et al.,* 2004). Inhibition of the Notch pathway impairs pancreas regeneration

after caerulein-induced pancreatitis and this is associated with a cooperation between Notch and Wnt signalling, characterised by an inhibition of β-catenin-mediated gene activation (Siveke *et al.,* 2008).

The existence of a link between the Notch and the NF-κB signalling pathways is well documented in the scientific literature. For example, Notch1 can activate NF-κB in different cancers such as T cell leukaemia (Vilimas *et al.,* 2007) or cervical cancer (Song *et al.,* 2008). Moreover, Notch can regulate the transcription of different members of the NF-κB signalling pathway (Cheng *et al.,* 2001) and protein-protein interactions between these two partners have been shown in cell specific contexts (Wang *et al.,* 2001). However, the reciprocal crosstalk from NF-κB to Notch is less well described. Expression of the *Jagged1* gene, encoding for one of the Notch receptor ligand, has been shown to be controlled by NF-κB subunits in B cells (Bash *et al.,* 1999). In marginal zone B cells, NF-κB can also cooperate with the Notch signalling pathway, regulating the transcription of some of its target genes (Moran *et al.,* 2007).

Upon consideration of the role of Notch signalling in cancer and especially its activation in pancreatic carcinogenesis, the impact of NF-κB activation in the regulation of downstream Notch targets was investigated in this chapter. The main hypothesis tested in this chapter was whether TNF-α/IKK2 activation can synergise with Notch signalling during pancreatic tumour development and progression. In this chapter, the Notch pathway is shown to be activated in the different mouse models during pancreatic cancer progression and its direct cooperation with the TNF-α/IKK2 signalling pathway in the context of mutant *kras* in pancreatic carcinogenesis is demonstrated.

4.2 Activation of the Notch pathway in pancreatic cancer

In the *kras*^{G12D} mouse model developed by Hingorani *et al.*, activation of the Notch signalling pathway has been shown by immunohistochemistry staining of the transcription factor HES1 (Hingorani *et al.,* 2003). To evaluate the activation of the Notch signalling pathway in the mouse models, the Notch target gene expression levels of *hes1* and *hey1* were measured (Figure 4.1).

Notch can also activate the transcription of other genes, such as *vegf* (Chadwick *et al.,* 2009) *tenascin-c* (Sivasankaran *et al.,* 2009), the transcription factor *c-myc* (Mazur *et al.,* 2010a; Palomero *et al.,* 2006; Sharma *et al.,* 2006; Weng *et al.,* 2006) and the AP-1 family transcription factor *batf* (Johansen *et al.,* 2003; Strobl *et al.,* 2000). To assess the expression of Notch target genes in PanIN bearing *kras*^{G12D}, *kras*^{G12D}*/ikk2*$^{\Delta Pdx}$ and *kras*^{G12D}*/tnfa*$^{\Delta Pdx}$ mice, mRNA levels for *batf*, *c-myc*, *hes1*, *hey1*, *tenascin-c* and *vegf* were measured in whole pancreases by qRT-PCR (Figure 4.1). In agreement with previous studies (Hingorani *et al.,* 2003), *hes1* and *hey1* genes were highly expressed in the pancreases of *kras*^{G12D} PanIN bearing mice. However, their expression was decreased in the pancreases of age-matched PanIN bearing *kras*^{G12D}*/ikk2*$^{\Delta Pdx}$ and *kras*^{G12D}*/tnfa*$^{\Delta Pdx}$ mice, with a more profound reduction for *kras*^{G12D}*/ikk2*$^{\Delta Pdx}$ mice (Figure 4.1). Among other Notch target genes, a significant reduction of *vegf* and *tenascin-c* expression was also observed in the pancreases of *kras*^{G12D}*/ikk2*$^{\Delta Pdx}$ mice only, whereas expression levels for *c-myc* and *batf* were not altered (Figure 4.1).

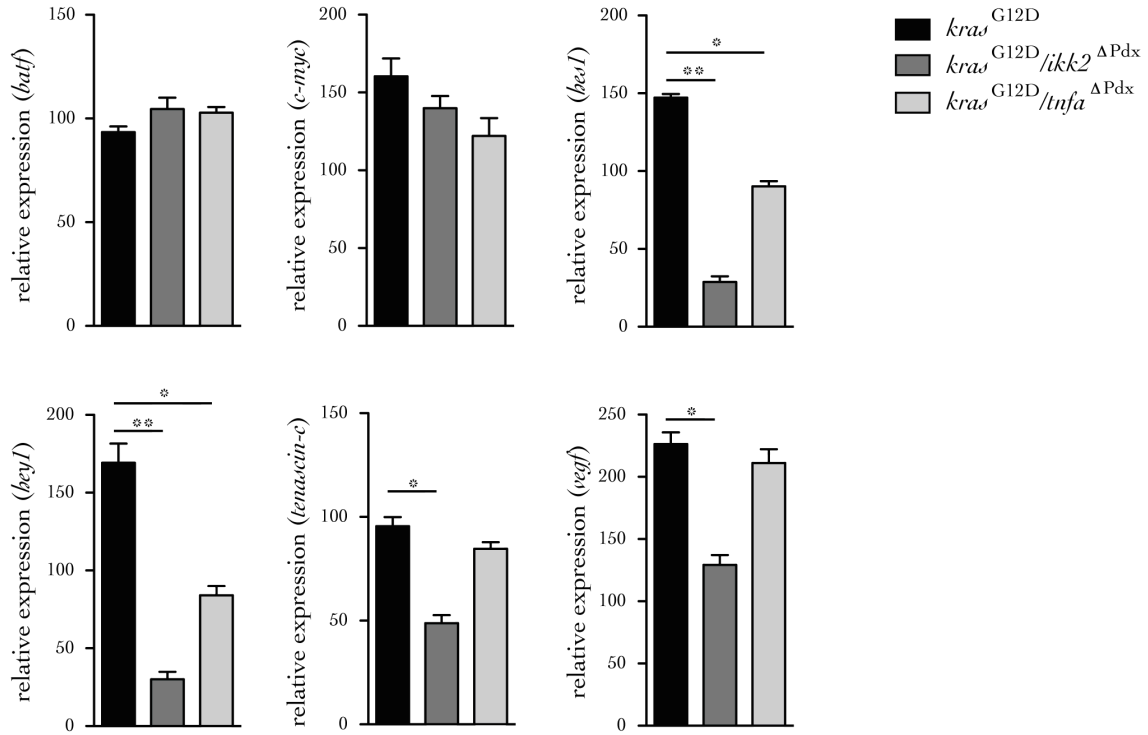

Figure 4.1: Notch target genes mRNA levels in pancreases

Relative mRNA expression of *batf*, *c-myc*, *hes1*, *hey1*, *tenascin-c* and *vegf* in the pancreases of PanIN bearing *kras*^{G12D}, *kras*^{G12D}*/ikk2*$^{\Delta Pdx}$ and *kras*^{G12D}*/tnfa*$^{\Delta Pdx}$ mice at 3 months of age measured by qRT-PCR. Data are shown as mean + SD of duplicate experiments, *p<0.05, **p<0.01, n=6.

Therefore, expression levels of most Notch target genes are affected following *ikk2* inactivation, whereas *tnfa* genetic deletion has a lower impact. These results indicate a concurrent activity between the classical NF-κB and Notch signalling pathways and that activation of the NF-κB signalling pathway can differentially regulate the expression of Notch target genes.

HES1 protein levels were also assessed by immunofluorescent staining on pancreatic tissue sections from PanIN bearing *kras*^{G12D}, *kras*^{G12D}*/ikk2*$^{\Delta Pdx}$ and *kras*^{G12D}*/tnfa*$^{\Delta Pdx}$ mice at 3 months of age (Figure 4.2). To enhance the visualisation of the tissue structure and the cell outline, sections were co-stained with the epithelial cell marker E-cadherin (red) and cell nuclei were counterstained with DAPI (blue).

PanIN lesions from 3-month old *kras*^{G12D} mice were found to be positive for HES1, confirming data obtained by others (Hingorani *et al.,* 2003). Similar levels of HES1 were found in the pancreas sections of *kras*^{G12D}/*tnfa*$^{\Delta Pdx}$ mice but a significant reduction was observed in age-matched *kras*^{G12D}/*ikk2*$^{\Delta Pdx}$ animals (Figure 4.2).

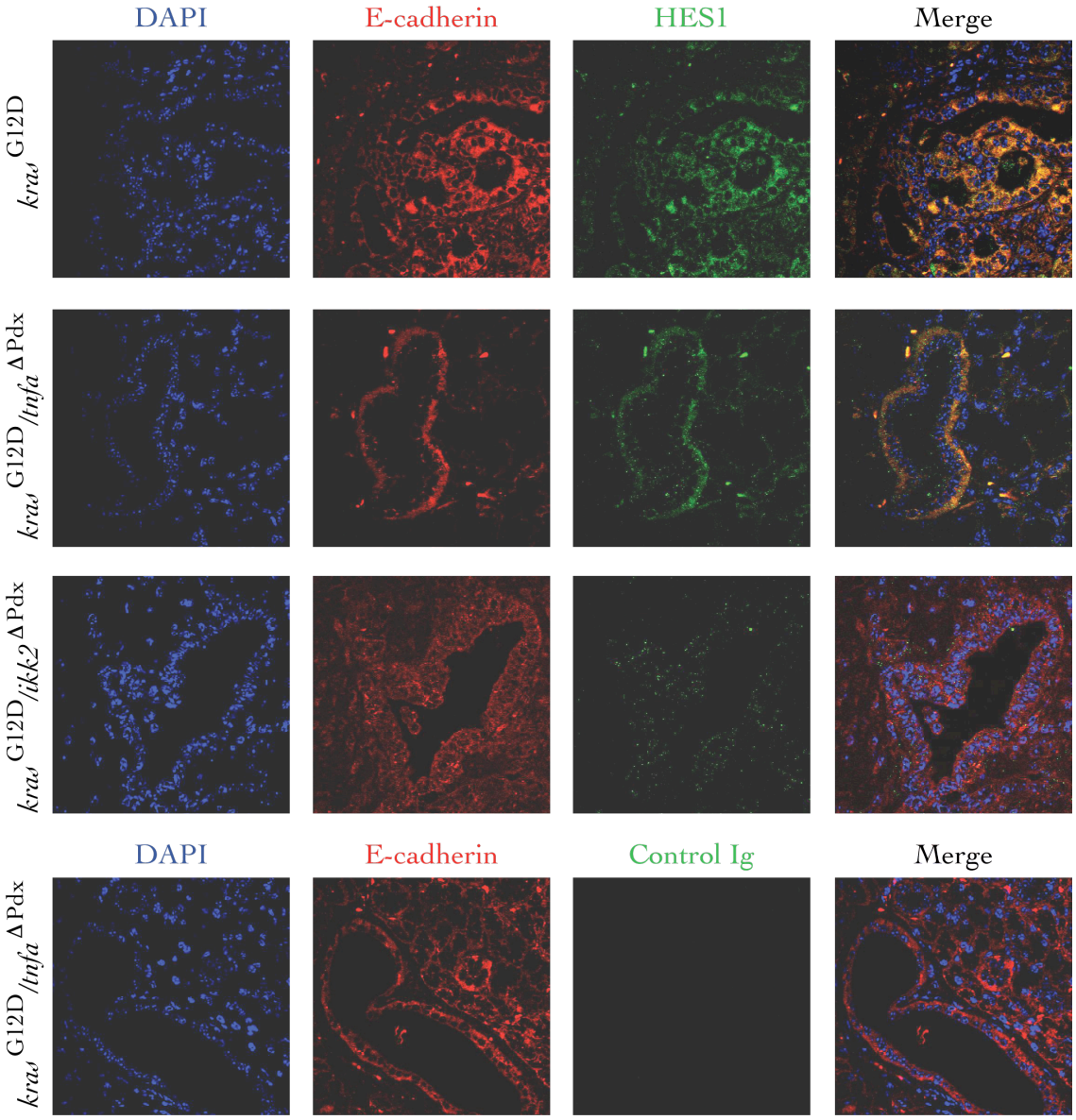

Figure 4.2: Immunofluorescent staining for HES1 in tissue sections

Pancreas sections of 3-month old *kras*^{G12D}, *kras*^{G12D}/*ikk2*$^{\Delta Pdx}$ and *kras*^{G12D}/*tnfa*$^{\Delta Pdx}$ mice stained for HES1, E-cadherin and counterstained with DAPI. Magnification X40. blue = DAPI, red = E-cadherin and green = HES1. HES1 is expressed in *kras*^{G12D} and *kras*^{G12D}/*tnfa*$^{\Delta Pdx}$ mice but absent in *kras*^{G12D}/*ikk2*$^{\Delta Pdx}$ mice. Each picture is representative of three mice examined for each genotype.

Taken together, these data suggest that the Notch signalling pathway is activated in PanIN bearing *kraɔ*^{G12D} and *kraɔ*^{G12D}/*tnfa*$^{\Delta Pdx}$ mice at 3 months of age but not in age-matched *kraɔ*^{G12D}/*ikk2*$^{\Delta Pdx}$ mice. The genetic deletion of *ikk2* is therefore sufficient to block the activation of the Notch pathway in the context of *kraɔ*-driven pancreatic carcinogenesis, suggesting a cooperation between the TNF-α/IKK2 and the Notch signalling pathways. The effects of pharmacological inhibition of NF-κB signalling on the activation of the Notch signalling pathway, rather than those of genetic inactivation, are described in Chapter 6 of this thesis.

4.3 Cooperation between the TNF-α/IKK2 and the Notch signalling pathways

To further dissect and analyse the link between the TNF-α/IKK2 and the Notch signalling pathways, the response of the cell lines derived from PanIN bearing *kras*^{G12D}, *kras*^{G12D}/*tnfa*$^{\Delta Pdx}$ and *kras*^{G12D}/*ikk2*$^{\Delta Pdx}$ mice to recombinant mouse TNF-α (rTNF-α) stimulation *in vitro* was examined.

4.3.1 The expression of Notch target genes over time

The expression of *hes1* and *hey1* was first measured over a full time-course of 12 hours upon stimulation with rTNF-α (Figure 4.3), to confirm the link previously observed between TNF-α and the Notch signalling pathway.

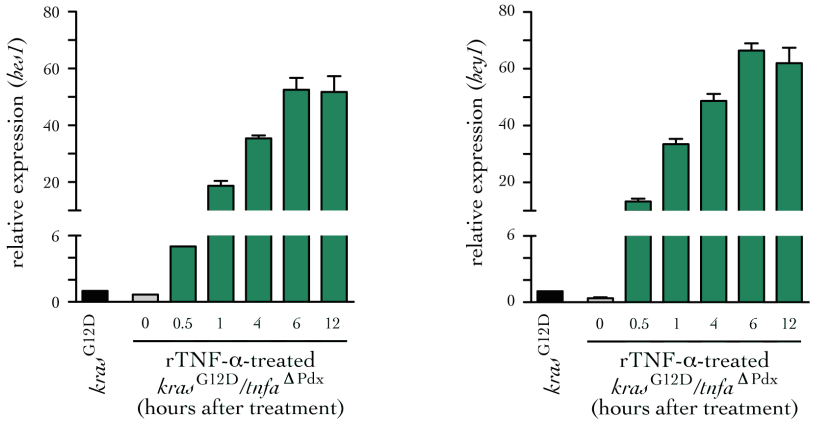

Figure 4.3: Time course of *hes1* and *hey1* expression upon rTNF-α stimulation

mRNA expression of *hes1* and *hey1* in cell lines derived from PanIN bearing *kras*^{G12D}/*tnfa*$^{\Delta Pdx}$ mice and stimulated with 1 ng/ml of rTNF-α over 12 hours. Relative expression was calculated by setting expression of untreated *kras*^{G12D} samples as 1. Data are shown as mean + SD of triplicate determinants and one representative experiment out of three is shown.

Upregulation of gene expression occurred within 30 minutes and reached a plateau between 6 to 12 hours after treatment. Detection of a significant increase in *hes1* expression after 30 minutes of stimulation with rTNF-α suggests that another intermediate protein is not involved in this process. The effects of rTNF-α stimulation were analysed after 6 hours for the other experiments desribed in this

thesis, as beyond this time point, the gene expression of *hes1* and *hey1* reaches a plateau.

4.3.2 Notch target genes are expressed upon stimulation with rTNF-α

On completion of the initial experiment described above, the expression profile of *hes1* and *hey1*, the main Notch target genes, as well as of other target genes (*batf*, *c-myc*, *tenascin-c* and *vegf*) was assesssed by qRT-PCR after rTNF-α stimulation in cells derived from PanIN bearing $kras^{G12D}$, $kras^{G12D}/ikk2^{\Delta Pdx}$ and $kras^{G12D}/tnfa^{\Delta Pdx}$ mice (Figure 4.4). The expression of each Notch target gene tested was increased in cells derived from $kras^{G12D}$ and $kras^{G12D}/tnfa^{\Delta Pdx}$ mice after rTNF-α stimulation. In contrast, rTNF-α failed to upregulate expression of these genes in cells derived from $kras^{G12D}/ikk2^{\Delta Pdx}$ mice.

HES1 and HEY1 protein levels were also analysed after rTNF-α stimulation in cell lines derived from PanIN bearing $kras^{G12D}$ mice (Figure 4.5). Immunofluorescent staining revealed basal Notch activity, demonstrated by nuclear location of the HES1 and HEY1 transcription factors. After stimulation with rTNF-α, HES1 and HEY1 protein expression was increased. In Figure 4.5, F-actin was stained in red in order to improve the visualisation of the cell outline.

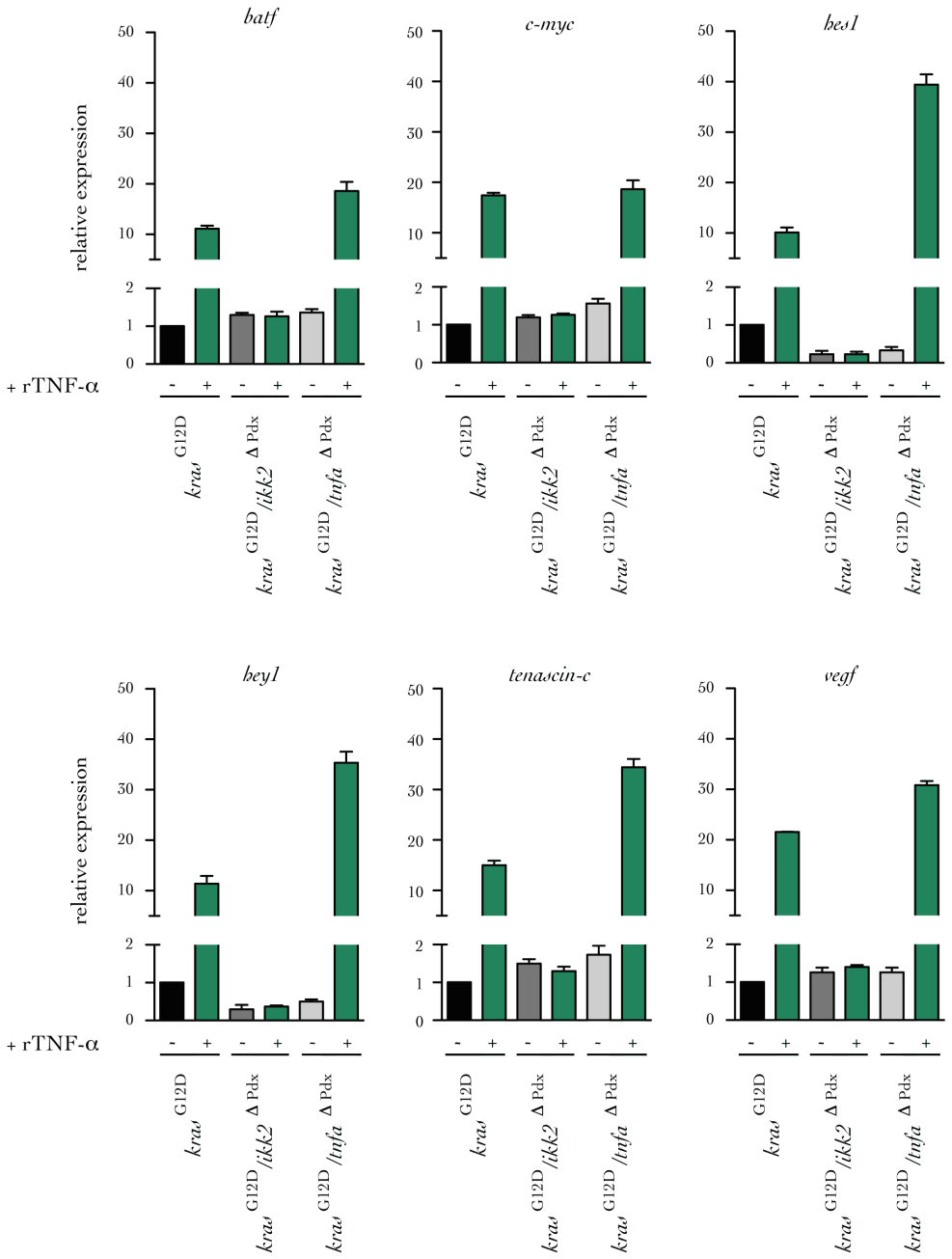

Figure 4.4: mRNA levels of Notch target genes in cell lines

Relative mRNA expression of *batf*, *c-myc*, *hes1*, *hey1*, *tenascin-c* and *vegf* in PanIN cell lines derived from the indicated mouse strains and stimulated with 1 ng/ml of rTNF-α for 6 hours. Relative expression was calculated by setting expression of untreated $kras^{G12D}$ samples as 1. Notch target genes are upregulated upon rTNF-α except in cells derived from $kras^{G12D}/ikk2^{\Delta Pdx}$ mice. Data are shown as mean + SD of triplicate determinants and one representative experiment out of three is shown.

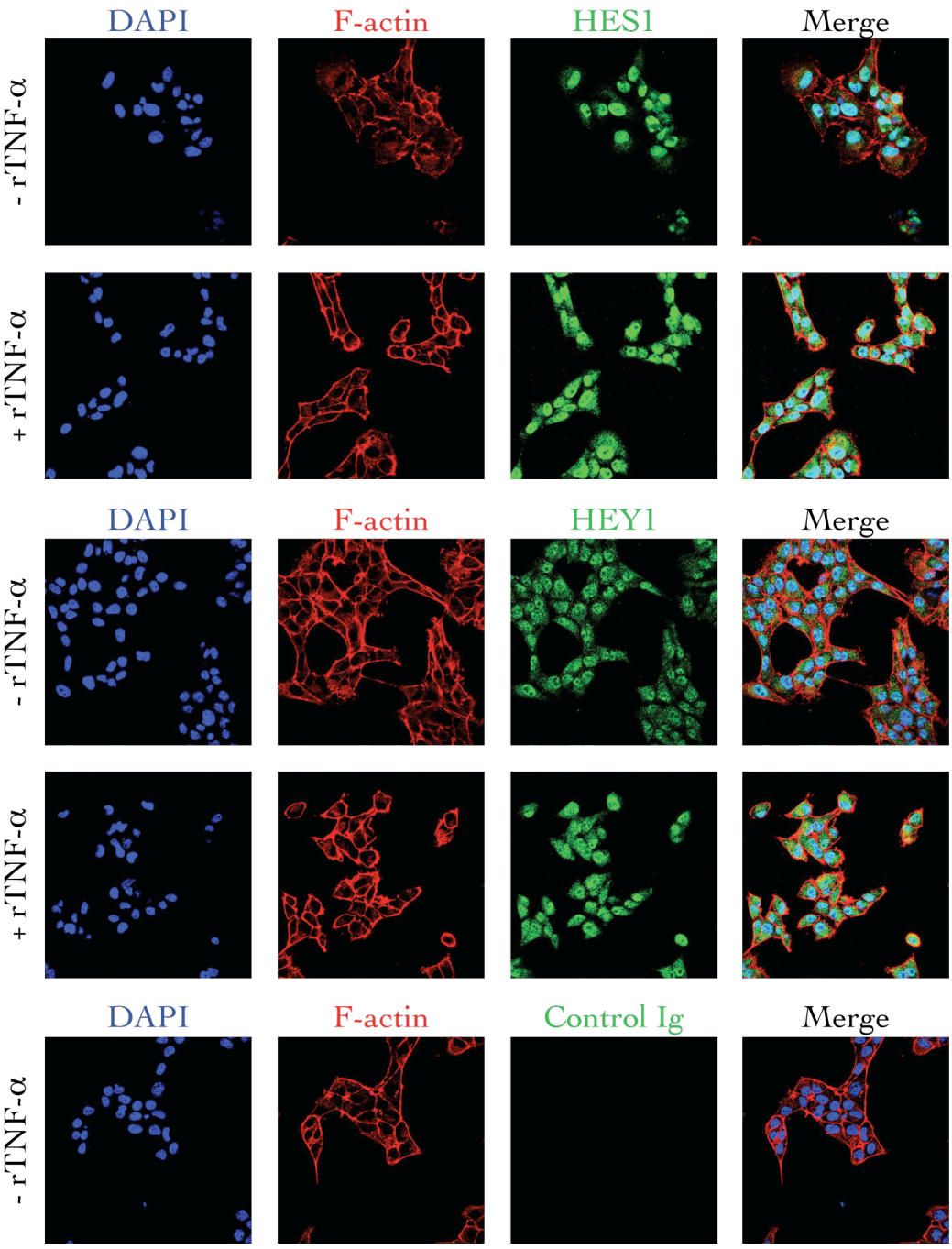

Figure 4.5: Immunofluorescent staining for HES1 and HEY1 in PanIN derived cell lines

Cell lines derived from PanIN bearing *kras*^{G12D} mice were stained by immunofluorescence for HES1 or HEY1 as well as F-actin and counterstained with DAPI. Cells were left unstimulated or were stimulated with 1 ng/ml of rTNF-α for 24 hours. Magnification X40. blue = DAPI, red = F-actin, green = HES1 or HEY1. HES1 and HEY1 expression is enhanced after rTNF-α stimulation. One representative experiment out of three performed is shown.

4.3.3 rTNF-α stimulation enhances the promoter activity of the *hes1* gene

To analyse TNF-α-induced *hes1* upregulation, the promoter activity of the *hes1* gene was studied in cell lines transiently transfected with a *hes1* luciferase reporter construct, allowing *luciferase* expression under the control of the *hes1* gene promoter (Takebayashi *et al.,* 1994) (Figure 4.6).

The stimulation of cells derived from PanIN bearing *kras*^{G12D}/*tnfa*$^{\Delta Pdx}$ mice with rTNF-α resulted in enhanced luciferase activity and consequently enhanced transcriptional activity of the *hes1* promoter (Figure 4.6). Similar activity was not observed after stimulating cells derived from PanIN bearing *kras*^{G12D}/*ikk2*$^{\Delta Pdx}$ mice (Figure 4.6).

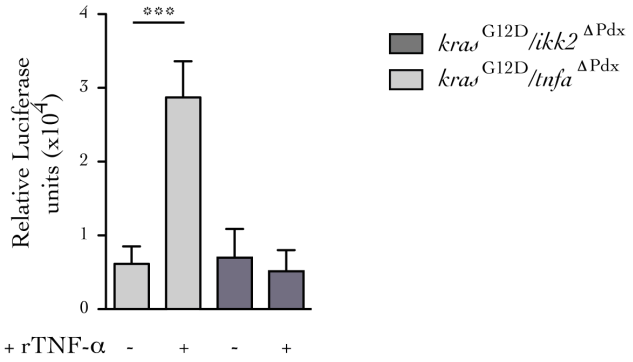

Figure 4.6: Transcriptional activity of the *hes1* promoter

hes1 luciferase reporter assay in cells derived from PanIN bearing *kras*^{G12D}/*tnfa*$^{\Delta Pdx}$ and *kras*^{G12D}/*ikk2*$^{\Delta Pdx}$ mice stimulated with 1 ng/ml of rTNF-α for 6 hours. rTNF-α induced activation of the *hes1* promoter in cells derived from *kras*^{G12D}/*tnfa*$^{\Delta Pdx}$ mice only. Results were normalised to firefly luciferase activity relative to internal control and expressed as mean + SD from triplicate transfections, ***p<0.001. One representative experiment out of three performed is shown.

In pre-malignant epithelial cells, IKK2 signalling is required for an increase in *hes1* promoter activity. The expression of other Notch target genes may be regulated in a similar manner.

4.3.4 rTNF-α stimulation does not increase the expression of Notch receptors and ligands

Notch receptors and ligands are both expressed in PanIN and PDAC cells. Several studies have shown that they can be upregulated following activation of different signalling pathways, in particular the NF-κB pathway (Bash *et al.,* 1999; Fung *et al.,* 2007; Monsalve *et al.,* 2006; Palaga *et al.,* 2008). However, in the context of pancreatic carcinogenesis, it has not been described whether or not the Notch pathway can be regulated by NF-κB signalling.

The next step was to assess whether the enhanced expression of Notch target genes observed upon stimulation with rTNF-α is due to an upregulation of Notch receptors and ligands. If more receptors and ligands are expressed, the signalling downstream of Notch would consequently be reinforced and this would explain the enhanced expression of Notch target genes.

In order to demonstrate the potential requirement of *de novo* protein synthesis for the induction of gene expression, cells derived from PanIN bearing *kras*^{G12D}*/tnfa*$^{\Delta Pdx}$ mice were treated with cycloheximide, an inhibitor of protein synthesis. *hes1* and *hey1* gene expression was measured by qRT-PCR with or without stimulation with rTNF-α (Figure 4.7). To validate the results from this experiment better, the expression levels of genes which are known to be induced by cyclohexamide, such as *c-myc* (Yokota *et al.,* 1995), should have also been measured by qRT-PCR.

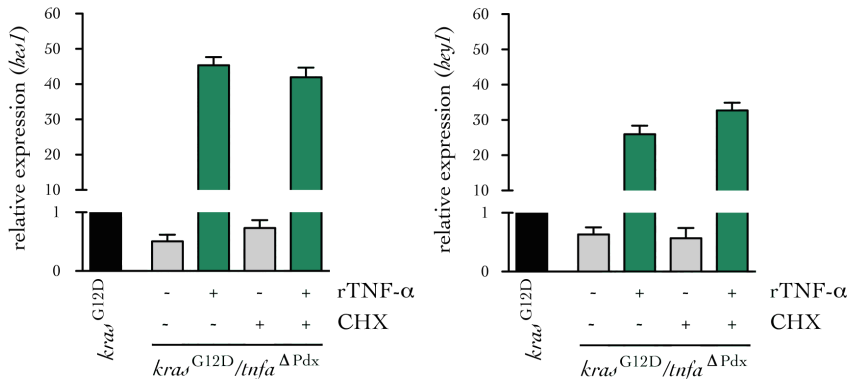

Figure 4.7: Effect of cycloheximide treatment on the expression of Notch target genes

mRNA expression of *hes1* and *hey1* in cell lines derived from PanIN bearing *kras*^{G12D}/*tnfa*$^{\Delta Pdx}$ mice and stimulated with 1 ng/ml of rTNF-α for 6 hours in the presence or absence of cycloheximide (CHX) at 15 μg/ml. The expression of Notch target genes is independent of *de novo* protein synthesis. Relative expression was calculated by setting expression of untreated *kras*^{G12D} samples as 1. Data are shown as mean + SD of triplicate determinants and one representative experiment out of three is shown.

As shown in Figure 4.7, stimulation with rTNF-α could induce and enhance *hes1* and *hey1* gene expression, independently of cycloheximide. *De novo* protein synthesis is therefore not essential for TNF-α-induced Notch target gene expression. The enhanced expression of Notch target genes observed upon stimulation with rTNF-α is independent of *de novo* protein synthesis and not due to an upregulation of the production of Notch receptors and ligands by the pancreatic epithelial cells. In addition, the levels of the Jagged1 and Dll4 Notch ligands were evaluated by flow cytometry and no differences were observed between the cell lines derived from PanIN bearing *kras*^{G12D}, *kras*^{G12D}/*tnfa*$^{\Delta Pdx}$ and *kras*^{G12D}/*ikk2*$^{\Delta Pdx}$ mice (personal communication Dr Eleni Maniati, Barts Cancer Institute, Queen Mary, University of London, London, UK).

The idea of a potential direct link between the TNF-α/IKK2 and the Notch pathways is supported by the fact that the upregulation of *hes1* and *hey1* is independent of new protein synthesis and because it occurs at an early time point after rTNF-α

stimulation (Figure 4.3). If an intermediate protein or signalling pathway was required, the upregulation of the Notch target genes upon rTNF-α stimulation would have been detected at later time points.

4.3.5 Canonical Notch signalling is required

The Notch pathway is initiated by proteolytic cleavage of NICD following receptor-ligand interactions. This cleavage is mediated by the γ-secretase activity of a multiprotein complex (Gordon *et al.,* 2008). Canonical Notch signal transduction occurs via the NICD/RBPjκ complex (Kopan and Ilagan 2009; Lai 2002). The requirement for canonical Notch signalling following TNF-α-induced upregulation of Notch target genes was investigated next. The effect of the synthetic γ-secretase inhibitor (GSI) L685458 (Shearman *et al.,* 2000) on the upregulation of expression of Notch target genes upon rTNF-α stimulation was assessed (Figure 4.8).

After blocking the Notch signalling pathway with L685458 at 5 μM for 6 hours, *hes1* and *hey1* expression were attenuated in rTNF-α-stimulated cells derived from PanIN bearing *kras*^{G12D}*/tnfa*$^{\Delta Pdx}$ mice. However, the transcription levels of *il1b*, *cox2* and *mmp13*, NF-κB target genes (Hiscott *et al.,* 1993; Liacini *et al.,* 2002; Mauviel 1993; Yamamoto *et al.,* 1995), remained unaffected (Figure 4.8). The upregulation of Notch target genes after stimulation with rTNF-α is therefore dependent on the activation of the Notch signalling pathway. This experiment demonstrates that an active Notch signalling pathway is required for *hes1* and *hey1* expression upon rTNF-α stimulation. As expected, gene expression levels of NF-κB target genes remain unaffected when inhibiting the Notch signalling pathway, especially upon rTNF-α stimulation which is the main activator of this signalling pathway.

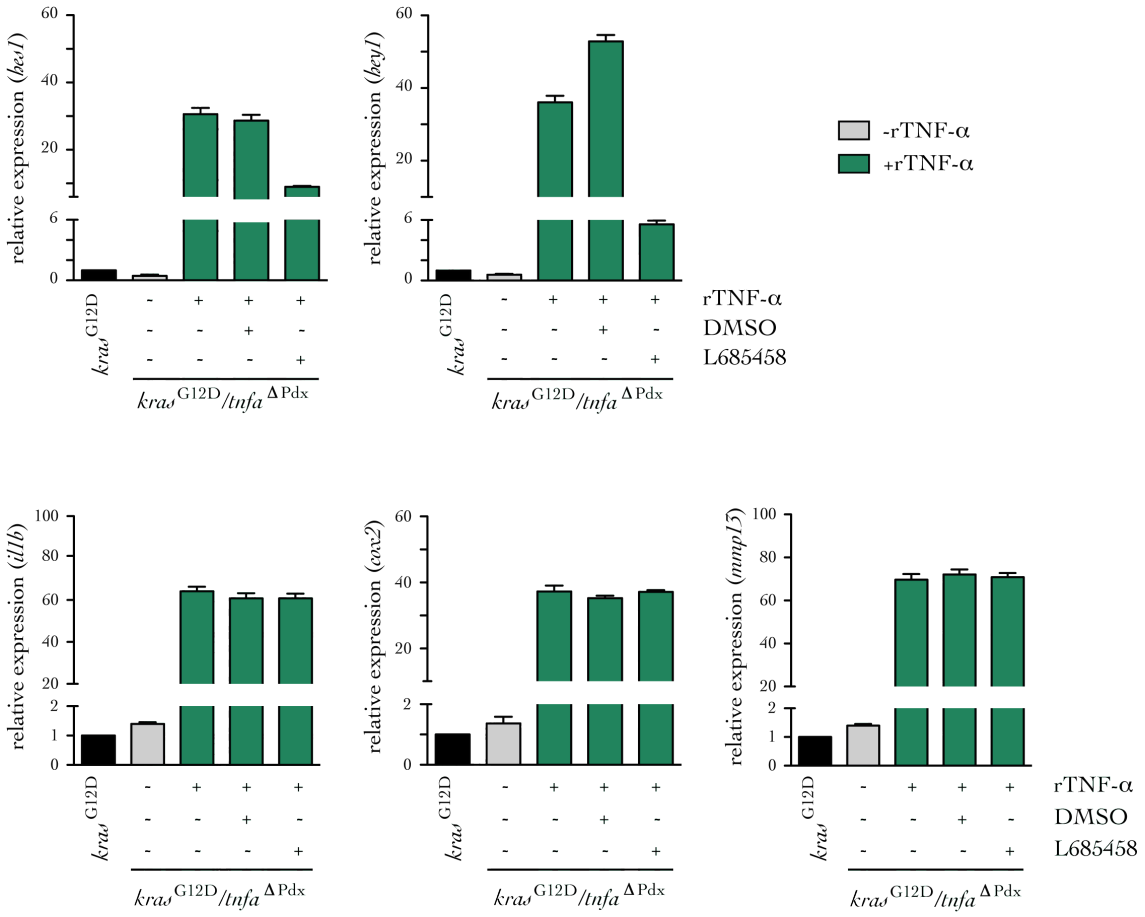

Figure 4.8: Effect of pharmacological inhibition of Notch signalling on the expression of TNF-α-induced Notch and NF-κB target genes

Relative mRNA expression of *hes1*, *hey1*, *il1b*, *cox2* and *mmp13* in cell lines derived from PanIN bearing *kras*^{G12D}/*tnfa*$^{\Delta Pdx}$ mice and stimulated with 1 ng/ml of rTNF-α for 6 hours in the presence or absence of the γ-secretase inhibitor L685458 (5 μM). Relative expression was calculated by setting expression of untreated *kras*^{G12D} samples as 1. Data are shown as mean + SD of triplicate determinants and one representative experiment out of three is shown.

The effects of maximal engagement of the Notch receptors on the expression levels of *hes1* and *hey1* were also explored. Cells derived from PanIN bearing *kras*^{G12D} mice were incubated with classical Notch ligands, either by treating the cultures with recombinant Jagged-2 or by performing some co-culture experiments with the OP9-DL1 cells, a bone-marrow-derived stromal cell line that ectopically expresses the Dll1 Notch ligand (Schmitt and Zuniga-Pflucker 2002). After 6 hours, *hes1* and *hey1* mRNA levels were evaluated by qRT-PCR (Figure 4.9).

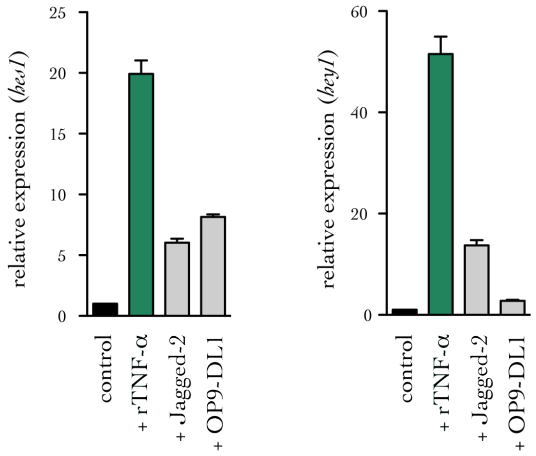

Figure 4.9: Expression of Notch target genes when maximally engaging Notch receptors

Relative mRNA expression of *hes1* and *hey1* in cell lines derived from PanIN bearing *kras*^{G12D}/*tnfa*$^{\Delta Pdx}$ mice and either treated with 1 ng/ml of rTNF-α, or 20 µg/ml of recombinant Jagged-2, or co-cultured with OP9-DL1 cells, all for 6 hours. Relative expression was calculated by setting expression of untreated *kras*^{G12D} samples as 1 (control). Data are shown as mean + SD of triplicate determinants and one representative experiment out of three is shown.

As shown in Figure 4.9, rTNF-α was more efficient at inducing the expression of *hes1* and *hey1* than ligand-mediated Notch activation of the pathway. As mentioned earlier, the cell lines tested already express the Notch ligands. The presence of high concentrations of Notch ligands, to saturate the Notch signalling pathway, slightly increases the expression of the Notch target genes *hes1* and *hey1*. However, rTNF-α stimulation induces a higher expression of these genes, suggesting that their expression is not only dependent on the Notch signalling pathway and that activation of the TNF-α/IKK2 signalling pathway also plays an important additional role.

The availability of the additional Notch ligands *in vitro* can be questioned, as stimulation with recombinant Jagged2 provides a soluble form of the ligand, and ligands and receptors normally involved in the activation of the Notch pathway are present on the cell surface. However, soluble forms of the ligands have also been shown to activate the pathway (D'Souza *et al.,* 2008). Moreover, even though OP9-

DL1 cells are not adherent cells per se, such immune cells tend to "stick" to the bottom of the plate when in culture and cell-cell contact is also probably facilitated by cellular projections, which have been shown to be enriched in Notch ligands (D'Souza *et al.,* 2008).

Finally, the requirement of canonical Notch signalling for TNF-α-mediated upregulation of *hes1* and *hey1* was further examined using siRNAs to knockdown the expression of *rbpj*. As mentioned earlier, RBPjκ is the nuclear transcription factor essential for canonical Notch target gene expression (Kopan and Ilagan 2009; Lai 2002) (Figure 4.10). siRNA technology was used to silence specific target genes. Three different commercially validated *rbpj* siRNAs and a non-targeting control were used to transfect cells derived from PanIN bearing $kras^{G12D}/tnfa^{\Delta Pdx}$ mice. The ability of each individual construct to inhibit *rbpj* expression was first assessed by checking mRNA levels by qRT-PCR (Figure 4.10 A) and protein levels by Western blot (Figure 4.10 B). Transfection with a single siRNA construct was sufficient to induce significant knockdown of the *rbpj* target gene.

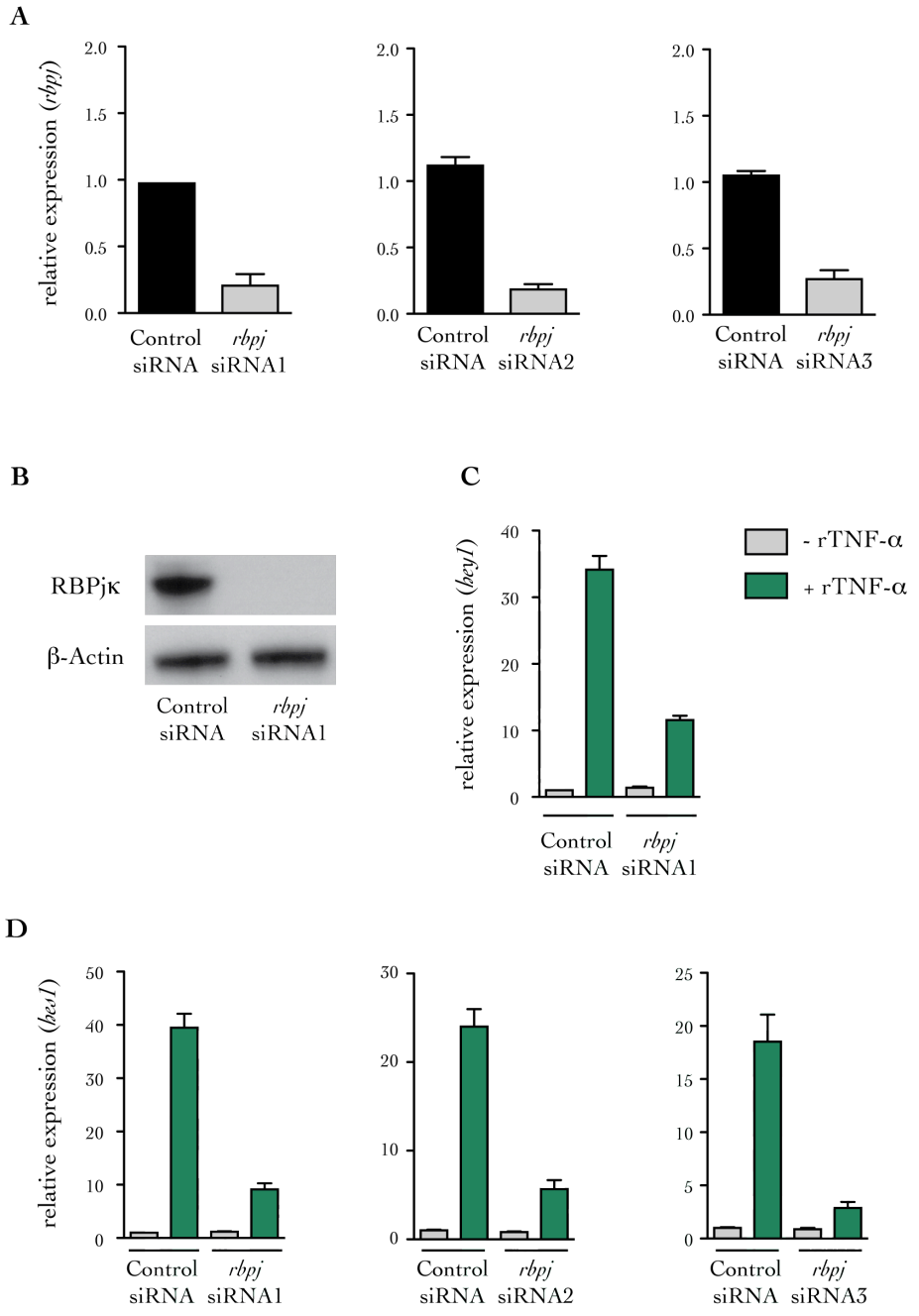

Figure 4.10: siRNA knockdown of *rbpj* in cell lines derived from PanIN bearing *kras*^{G12D}/*tnfa*$^{\Delta Pdx}$ mice

Cell lines derived from PanIN bearing *kras*^{G12D}/*tnfa*$^{\Delta Pdx}$ mice were transfected with *rbpj* specific siRNAs. *rbpj* knockdown was verified by (A) qRT-PCR and (B) Western blot. (C and D) 48 hours after transfection, cells were stimulated with 1 ng/ml of rTNF-α for 6 hours and expression of (C) *hey1* and (D) *hes1* was quantified by qRT-PCR. Relative expression was calculated by setting expression of *kras*^{G12D}/*tnfa*$^{\Delta Pdx}$ cells transfected with non-targeting siRNAs as 1. Expression of Notch target genes is RBPjκ-dependent. All data are shown as mean + SD of triplicate experiments and are representative of three independent experiments.

Cells derived from PanIN bearing *kraɔ*^{G12D}/*tnfa*$^{\Delta Pdx}$ mice were transfected with individual siRNA constructs and the expression levels of Notch target genes were assessed by qRT-PCR (Figure 4.10 C and D). The specific knockdown of *rbpj* resulted in a 4-fold decrease of *heɔ1* and *hey1* expression levels upon rTNF-α stimulation. In light of these data, it seems that the requirement of the NICD/RBPjκ complex is essential to induce *heɔ1* and *hey1* expression upon rTNF-α stimulation. The requirement of *rbpj* confirms the importance of canonical Notch signalling for the rTNF-α-induced Notch target gene expression, shown in Figure 4.8. However, downregulation of Notch target gene expression upon *rbpj* knockdown was expected, considering its essential role in canonical Notch signalling.

Taken together, the data presented in Figure 4.8, Figure 4.9 and Figure 4.10 demonstrate that the upregulation of the Notch target genes (*heɔ1* and *hey1*) after stimulation with rTNF-α is, in the context of *kraɔ*-mutant pancreatic carcinogenesis, dependent on canonical Notch signalling.

4.3.6 Activation of the Notch pathway is IKK2-dependent

To further investigate the role of induced TNF-α/IKK2 signalling in the activation of the Notch signalling pathway, siRNAs were used to knockdown the expression of different components of the IKK complex: IKK1, IKK2 and NEMO. Even though these three kinases share some homology, their role and function have shown to be different and context-specific (Hacker and Karin 2006).

The role of IKK2 was first explored by knocking down its expression (Figure 4.11). Three different commercially validated *ikk2* siRNAs and a non-targeting control were used to transfect cells derived from PanIN bearing *kras*^{G12D}/*tnfa*$^{\Delta Pdx}$ mice. After checking their specificity and efficiency at inhibiting *ikk2* gene expression by qRT-PCR (Figure 4.11 A) and Western blot (Figure 4.11 B), gene expression levels for *hes1* and *hey1* in response to rTNF-α stimulation were measured by qRT-PCR (Figure 4.11 C and D). Specific siRNA inhibition of *ikk2* resulted in a downregulation of *hes1* and *hey1* expression following rTNF-α treatment. This is consistent with previous observations that cells derived from PanIN bearing *kras*^{G12D}/*ikk2*$^{\Delta Pdx}$ mice lose the capacity to upregulate *hes1* and *hey1* upon rTNF-α stimulation (Figure 4.4).

The role of IKK1 was then investigated by knocking down its expression (Figure 4.12). Once again, the ability of each individual siRNA construct to inhibit *ikk1* expression was verified by qRT-PCR (Figure 4.12 A). Gene expression levels of *hes1* in response to rTNF-α stimulation were measured (Figure 4.12 B) and were similar whether *ikk1* was expressed or not.

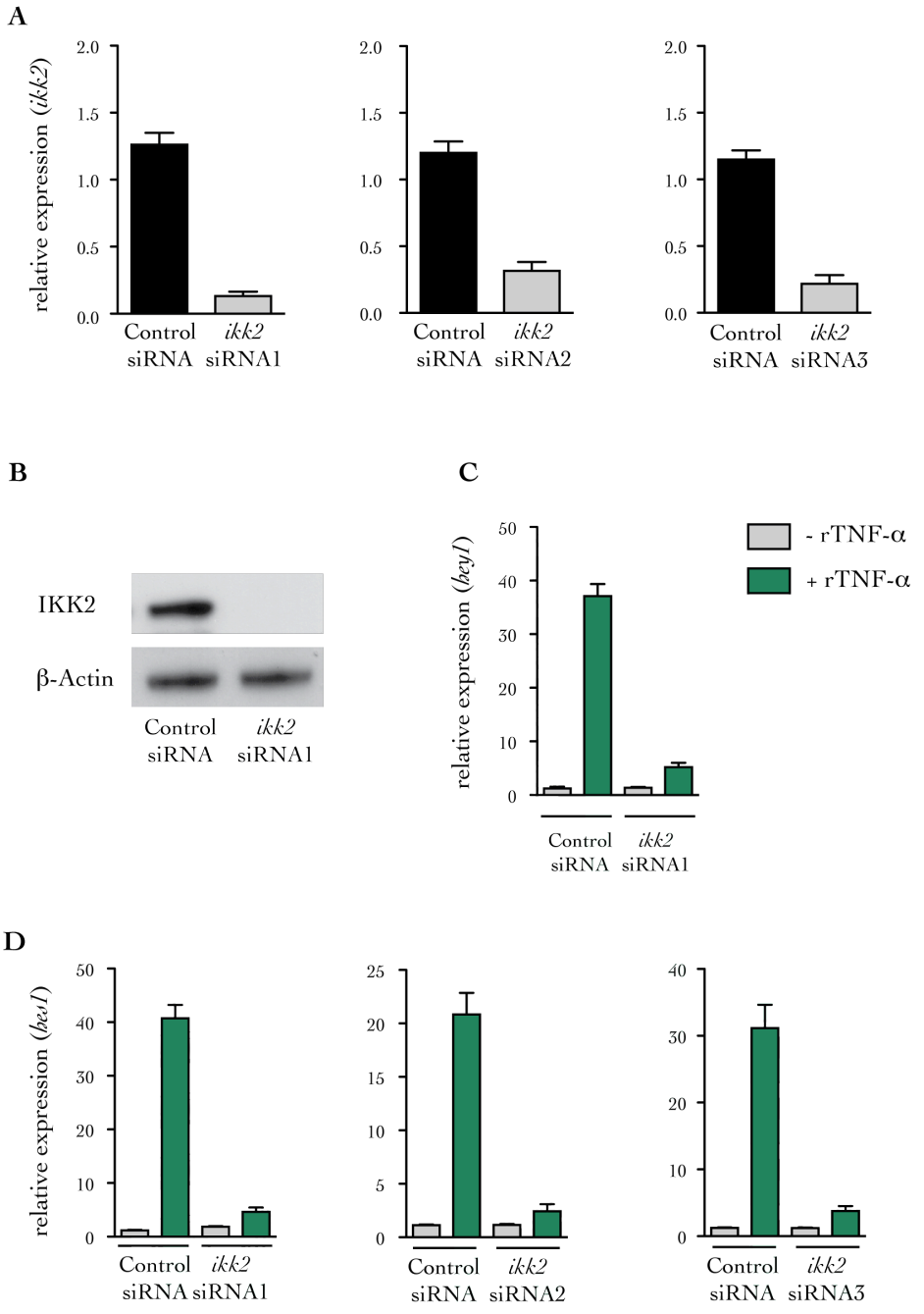

Figure 4.11: siRNA knockdown of *ikk2* in cell lines derived from PanIN bearing *kras*^{G12D}/*tnfa*$^{\Delta Pdx}$ mice

Cell lines derived from PanIN bearing *kras*^{G12D}/*tnfa*$^{\Delta Pdx}$ mice were transfected with *ikk2* specific siRNAs. *ikk2* knockdown was verified by (A) qRT-PCR and (B) Western blot. (C and D) 48 hours after transfection, cells were stimulated with 1 ng/ml of rTNF-α for 6 hours and expression of (C) *hey1* and (D) *hes1* was quantified by qRT-PCR. Relative expression was calculated by setting expression of *kras*^{G12D}/*tnfa*$^{\Delta Pdx}$ cells transfected with non-targeting siRNAs as 1. Expression of the Notch target genes is IKK2-dependent. All data are shown as mean + SD of triplicate determinants and are representative of three independent experiments.

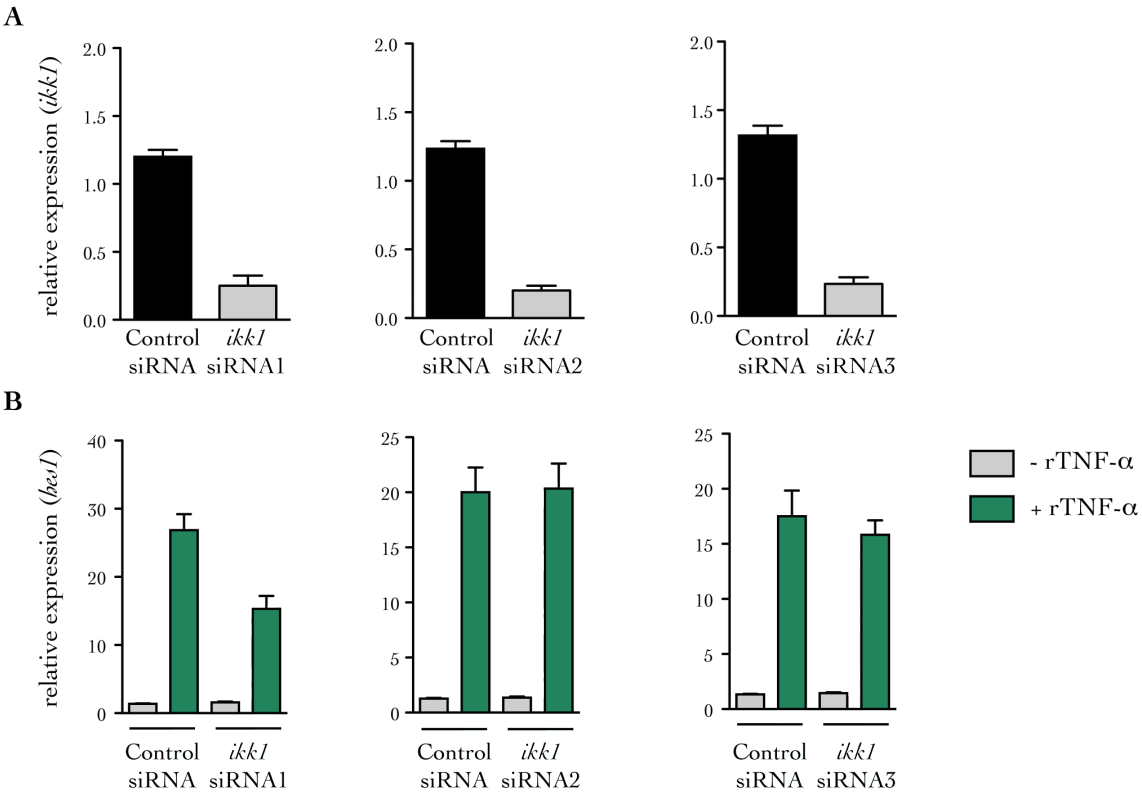

Figure 4.12: siRNA knockdown of *ikk1* in cell lines derived from PanIN bearing *kras*^{G12D}/*tnfa*$^{\Delta Pdx}$ mice

Cell lines derived from PanIN bearing *kras*^{G12D}/*tnfa*$^{\Delta Pdx}$ mice were transfected with *ikk1* specific siRNA. (A) *ikk1* knockdown was verified by qRT-PCR. (B) 48 hours after transfection, cells were stimulated with 1 ng/ml of rTNF-α for 6 hours and expression of *hes1* was quantified by qRT-PCR. Relative expression was calculated by setting expression of *kras*^{G12D}/*tnfa*$^{\Delta Pdx}$ cells transfected with non-targeting siRNAs as 1. Expression of the Notch target genes is IKK1-independent. All data are shown as mean + SD of triplicate determinants and are representative of three independent experiments.

Finally, the role of NEMO was studied (Figure 4.13). The three siRNA constructs used were able to silence the gene expression of *nemo* (Figure 4.13 A). Similarly to *ikk2* knockdown, *nemo* specific siRNA inhibition results in a downregulation of *hes1* and *hey1* expression following rTNF-α treatment (Figure 4.13 B).

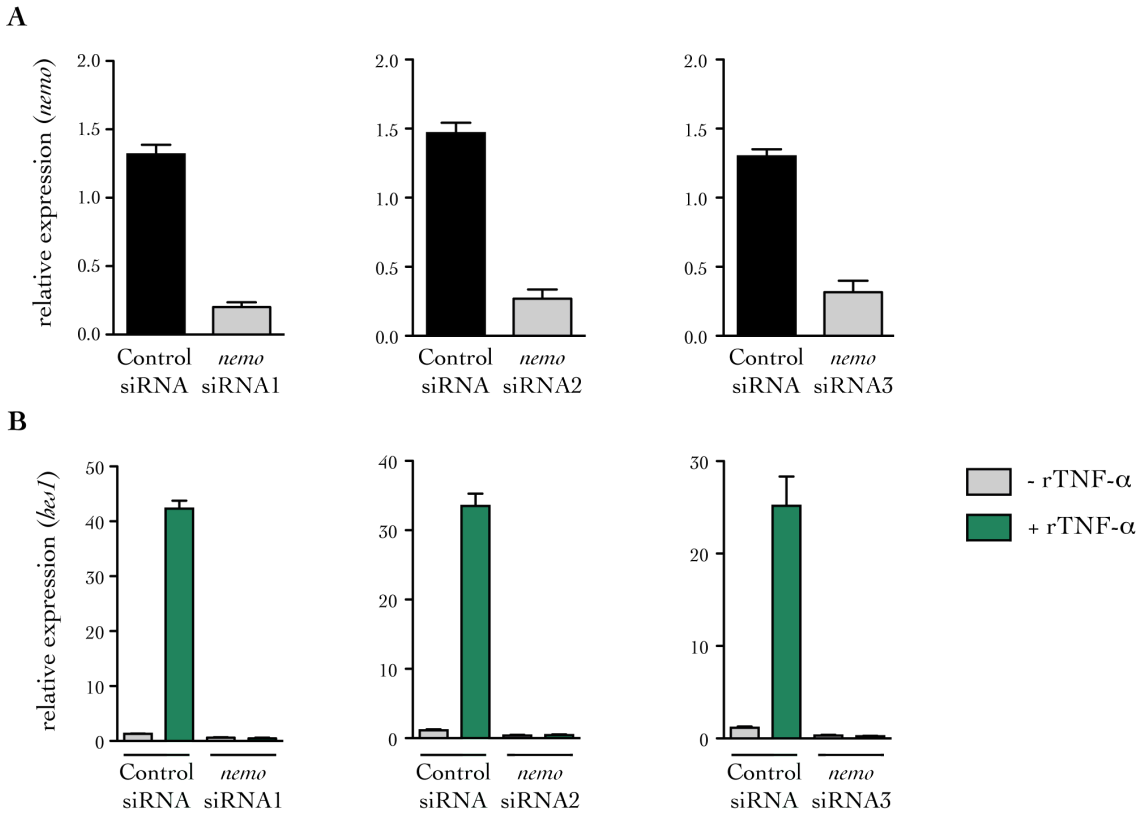

Figure 4.13: siRNA knockdown of *nemo* in cell lines derived from PanIN bearing *kras*^{G12D}/*tnfa*$^{\Delta Pdx}$ mice

Cell lines derived from PanIN bearing *kras*^{G12D}/*tnfa*$^{\Delta Pdx}$ mice were transfected with *nemo* specific siRNA. (A) *nemo* knockdown was verified by qRT-PCR. (B) 48 hours after transfection, cells were stimulated with 1 ng/ml of rTNF-α for 6 hours and expression of *hes1* was quantified by qRT-PCR. Relative expression was calculated by setting expression of *kras*^{G12D}/*tnfa*$^{\Delta Pdx}$ cells transfected with non-targeting siRNAs as 1. Expression of the Notch target genes is NEMO-dependent. All data are shown as mean + SD of triplicate determinants and are representative of three independent experiments.

To summarise this section, the upregulated expression of the Notch target genes (*hes1* and *hey1*) upon rTNF-α stimulation was demonstrated to be independent of IKK1 but dependent on the IKK2 and NEMO kinases.

4.4 Analysis of the crosstalk between NF-κB and Notch

In section 4.3, TNF-α-induced IKK2-dependent activation of the Notch pathway in *kras*-derived pancreatic epithelial cells was demonstrated. These data suggest a direct interaction downstream of the TNF-α/IKK2 and the Notch signalling pathways. This section will focus on further deciphering the mechanisms involved in this cooperation.

4.4.1 rTNF-α stimulation induces NICD cleavage

As described in Chapter 1, following receptor-ligand interaction, Notch signalling is initiated by proteolytic cleavage of the intracellular domain of Notch (NICD). Cleaved NICD translocates to the nucleus and along with the RBPjκ transcription factor forms a short-lived nuclear transcription complex, which mediates the expression of a number of genes including *hes1* and *hey1* (Gordon *et al.,* 2008).

Notch target genes are expressed in the $kras^{G12D}$ mouse model of pancreatic carcinogenesis (mRNA and protein levels - Figure 4.1 and Figure 4.2) and rTNF-α stimulation can increase their levels of expression *in vitro* (Figure 4.4 and Figure 4.5). Following these observations, the role of the activation of the NF-κB signalling pathway by stimulation with rTNF-α in the cleavage and release of NICD was investigated. NICD protein levels were measured by Western blot in cells derived from PanIN bearing $kras^{G12D}$ mice in the absence or presence of rTNF-α (Figure 4.14).

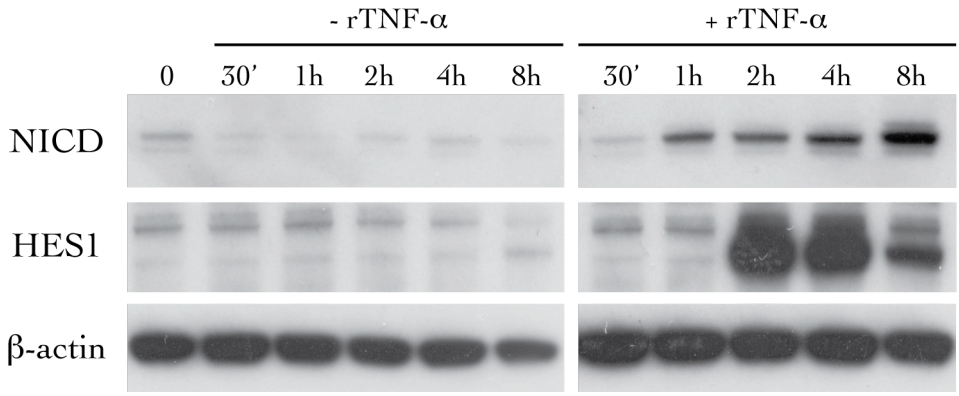

Figure 4.14: NICD and HES1 protein levels by Western blot in PanIN derived cells

Protein lysates from cell lines derived from PanIN bearing *kras*^{G12D} mice were analysed for NICD and HES1 expression with or without stimulation with rTNF-α at 1 ng/ml for the time indicated. rTNF-α stimulation increases HES1 protein levels from 2 hours of treatment but also the levels of NICD from 1 to 8 hours of treatment. β-actin was used as a loading control. One representative experiment out of two performed is shown.

Expression of Notch receptors and ligands in PanIN lesions and PDAC has previously been demonstrated (Mazur *et al.,* 2010a; Miyamoto *et al.,* 2003). Basal Notch activity, as evidenced by the expression of NICD and HES1 in cells derived from PanIN bearing *kras*^{G12D} mice, was detected (Figure 4.14). This is consistent with previous observations of Notch activity by others (Hingorani *et al.,* 2003) and in sections 4.2 and 4.3.2. Upon rTNF-α stimulation, a rapid increase in NICD and HES1 protein levels was observed (Figure 4.14).

Taken together, these *in vitro* data confirm previous *in vivo* observations that the Notch signalling pathway is activated in *kras*-mutant pancreatic adenocarcinoma and that rTNF-α can enhance Notch target gene expression. Moreover, the activation of the TNF-α/IKK2 signalling pathway contributes to an increase of NICD cleavage and release. These data suggest a cooperation between the TNF-α/IKK2 and the canonical Notch signalling pathways.

In section 3.4.5, it was demonstrated that *in vivo*, the production of TNF-α by the transformed pancreatic epithelial cells, rather than by the immune cells recruited on site, is critical for the early stages of PanIN promotion and progression, suggesting an autocrine role for this cytokine. However, in this experiment, transformed pancreatic epithelial cells derived from PanIN bearing *kras*^{G12D} mice were stimulated *in vitro* with rTNF-α, mimiking a paracrine source of the cytokine. This is because, as shown in Figure 4.14, autocrine TNF-α is not sufficient to induce significant HES1 protein expression. Treatment with rTNF-α was used to enhance the response, to identify the mechanisms involved in the upregulation of the expression of Notch target genes.

4.4.2 Interaction between NICD and IKK2 *in vitro*

Post-translational modifications of NICD have been demonstrated to play a critical role in its stabilisation and therefore in the control of the Notch pathway (Guarani *et al.,* 2011). To test whether IKK2 can directly phosphorylate NICD and contribute to Notch pathway upregulation by enhancing the stability or the proteolytic release of NICD, co-immunoprecipitation experiments were performed to identify a possible direct interaction between IKK2 and NICD.

pCR-FLAG-IKK2, pCR-FLAG-IKK2-KM and pDEST40-NICD-V5 plasmids were transfected into cells derived from PDAC bearing *kras*^{G12D} mice, allowing the overexpression of the protein fusion FLAG/IKK2, FLAG/IKK2-KM and NICD/V5 respectively. FLAG and V5 are peptide sequences used as a tag to facilitate the protein immunoprecipitation with high affinity antibodies. IKK2-KM is an inactive mutant protein in which a lysine residue in the ATP binding site of the kinase domain of the protein has been substituted by an alanine (K44A), therefore preventing ATP binding and phosphorylation of the IKK2 substrates (Nakano *et al.,* 1998).

Protein immunoprecipitations were performed with anti-FLAG or anti-V5 antibodies and presence of NICD or IKK2 was tested by Western blot to identify whether these two proteins interact. As a control to assess both the antibody specificity and success of precipitating protein complexes, the presence of FLAG or IKK2 and V5 or NICD was verified by Western blot after immunoprecipitation with anti-FLAG or anti-V5 antibodies respectively (Figure 4.15 A and B). As a positive control, protein complexes immunoprecipitated with anti-FLAG also contained IKK2 and similarly, the protein complexes immunoprecipitated with anti-V5 also included NICD.

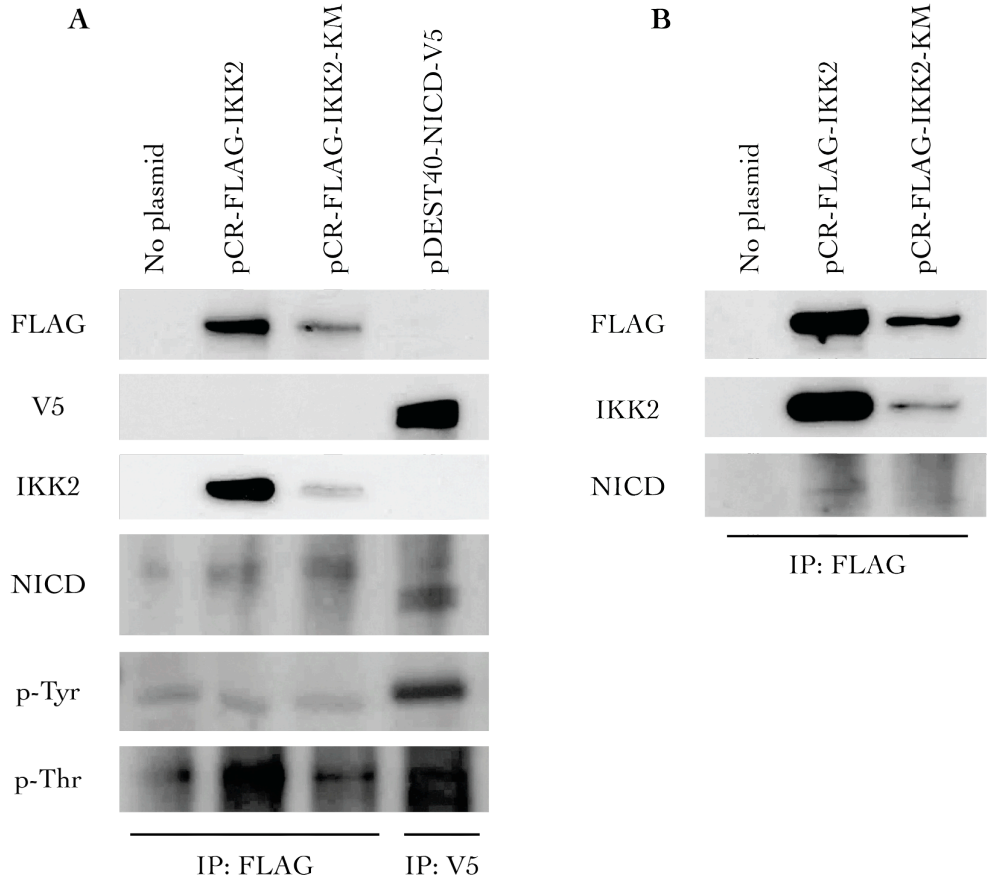

Figure 4.15: Protein levels by Western blot after co-immunoprecipitations in transfected cells

(A) Proteins from cells derived from PanIN bearing *kras*^{G12D} mice transfected with the pCR-FLAG-IKK2, pCR-FLAG-IKK2-KM and pDEST40-NICD-V5 plasmids were immunoprecipitated with an anti-FLAG or an anti-V5 antibody and immunoblotted with anti-FLAG, anti-V5, anti-IKK2, anti-NICD, anti-p-Tyr and anti-p-Thr antibodies. (B) Proteins from cells derived from PanIN bearing *kras*^{G12D} mice transfected with the pCR-FLAG-IKK2 or pCR-FLAG-IKK2-KM plasmids were immunoprecipitated with an anti-FLAG antibody and immunoblotted with anti-FLAG, anti-IKK2 and anti-NICD antibodies. One representative experiment out of two performed is shown.

Immunoblotting with an anti-NICD antibody seemed to reveal the presence of NICD in the immunocomplexes purified from cells transfected with the pCR-FLAG-IKK2 plasmid only (Figure 4.15 B). This is, to our knowledge, the first report suggesting a direct interaction between NICD and IKK2. It should be noted that the signal for NICD was weak and not always visible in the two experiments performed (one experiment is represented in Figure 4.15 A). This may be due to poor binding of the anti-NICD antibody. There is, however, a limited number of other commercially available clones that could have been tested.

To support and to try to confirm this result, the presence of phosphorylated residues was assessed by Western blot (Figure 4.15 A). The main target residues for phosphorylation are serine (Ser), threonine (Thr) and tyrosine (Tyr) (Bannister and Kouzarides 2011). However, no clear signal was obtained using an anti-phospho-serine antibody despite the number of different antibody clones tested (data not shown). Immunoblotting for phospho-threonin (p-Thr) residues did not show a specific pattern, however phospho-tyrosine (p-Tyr) residues were present in all precipitated samples, with an increased level in the immunocomplexes purified from cells transfected with the pDEST40-NICD-V5 plasmid (Figure 4.15 A). This may be due to the increased amount of NICD protein following transfection with the plasmid. These phosphorylated residues are likely to be part of NICD and not IKK2. It is well known now that the activation of the IKK2 kinase is triggered by the phosphorylation of two serine residues (Ser177/Ser181) (Delhase *et al.,* 1999) and not by the phosphoryation of tyrosine or threonine residues.

The lower levels observed of p-Tyr and p-Thr residues in the immunocomplexes purified from cells transfected with the pCR-FLAG-IKK2-KM plasmid are likely to

be due to the presence of the inactive form of the IKK2 kinase in the complex, thereby suggesting that these phosphorylation events are IKK2-mediated.

To confirm the co-immunoprecipitation of NICD and IKK2, but also to clarify whether phosphorylation events also occur, cells derived from PDAC bearing *kras*^{G12D} mice were transfected with the pCR-FLAG-IKK2, pCR-FLAG-IKK2-KM or pDEST40-NICD-V5 plasmids and proteins were immunoprecipitated with an anti-FLAG or an anti-V5 antibody. Immunocomplexes purified from these cells were analysed by mass spectrometry to identify the different protein partners co-immunoprecipitated. The purity of the samples after immunoprecipitation was first assessed by performing a Coomassie brilliant blue stain on the resolved proteins (Figure 4.16).

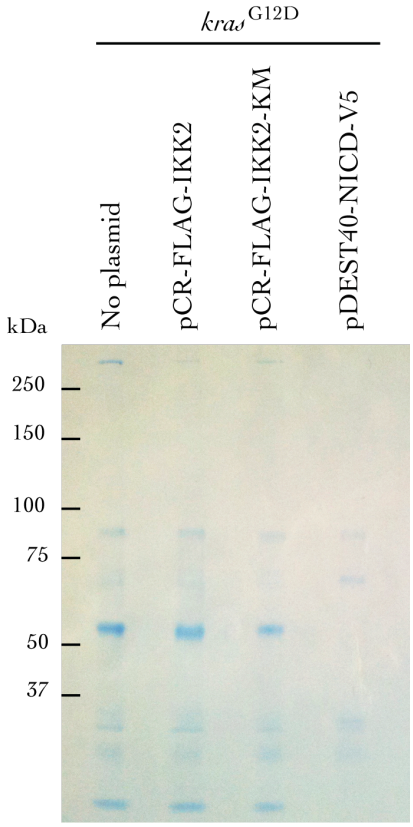

Figure 4.16: Coomassie brilliant blue staining of purified immunocomplexes

Cells derived from PDAC bearing *kras*^{G12D} mice were transfected with the pCR-FLAG-IKK2, pCR-FLAG-IKK2-KM or pDEST40-NICD-V5 plasmids and immunoprecipitated with an anti-FLAG or an anti-V5 antibody. Immunocomplexes were resolved on an SDS-NuPAGE® pre-cast 4-12 % w/v gradient bis tris gel by electrophoresis and proteins were stained with Coomassie brilliant blue.

The purity of the samples was satisfactory and immunocomplexes were once again resolved by electrophoresis but over a shorter distance. Lanes were cut out into 1 to 2 mm^3 cubes and sent for mass spectrometry analysis, which was performed by Dr Benjamin Thomas and Dr Fernando Martinez-Estrada, Central Proteomics Facility, Oxford University, Oxford, UK.

However, after mass spectrometry analysis, the proteins of interest could not be found (personal communication Dr Fernando Martinez-Estrada, Central Proteomics Facility, Oxford University, Oxford, UK). Even after immunoprecipitation using a very specific antibody against the FLAG or V5 tags, the proteins fused with the tag (IKK2 and NICD respectively) were not identified. The samples contained high levels of keratin, which could originate from the cell lines themselves, as they were epithelial cell lines, but also from contamination during sample preparation. However, due to time constraints, this experiment could not be repeated. Protein complexes were adequately immunoprecipitated as shown on Figure 4.15 but sample preparation and maybe the amount of starting material will need to be optimised to enhance the chances of detection of the proteins of interest by mass spectrometry.

4.4.3 Phosphorylation of histone H3 upon rTNF-α stimulation

As mentioned in section 4.3.6, the IKK2 kinase plays a critical role in the activation of the Notch signalling pathway in pancreatic cancer. To my knowledge, the classical Notch target gene *hes1* has so far not been shown to be regulated by an activated NF-κB signalling pathway (Bray 2006). The results from the co-immunoprecipitation experiments described in section 4.4.2 suggest a direct interaction between IKK2 and NICD, but subsequent experiments failed to confirm this interaction, possibly due to assay limitations. However, this remains a topic for further investigation in order to

explain the upregulated expression of the Notch target genes upon rTNF-α stimulation.

Another potential route downstream of IKK2 that could lead to *hes1* enhanced transcription could be IKK2-mediated histone modifiations, which would favour gene transcription. Activation of gene expression following histone modification, mainly through phosphorylation, acetylation or methylation, is a very well-described phenomenon (Bannister and Kouzarides 2011; Karlic *et al.,* 2010; Kouzarides 2007). Moreover, it has already been shown that IKK1 can phosphorylate histone H3, allowing the expression of NF-κB-regulated target genes (Anest *et al.,* 2003; Yamamoto *et al.,* 2003). The phosphorylation of histone H3 at serine 10 has been shown to control cell cycle progression and to be involved in gene transcription (Nowak and Corces 2004). To investigate whether IKK2 can phosphorylate histone H3 at serine 10, chromatin immunoprecipitation (ChIP) assays were carried out using an antibody directed against histone H3 (Figure 4.17) or against phospho-histone H3 (Ser10) (Figure 4.18). Immunoprecipitated DNA was analysed by qRT-PCR using *hes1* promoter-specific primers.

1 % of the sonicated chromatin was set aside as the input (representing the amount of chromatin used in the ChIP) and was not processed through the immunoprecipitation step. qRT-PCR with *hes1* promoter-specific primers was performed on the input and on the samples immunoprecipitated with histone H3 or phospho-histone H3 antibodies. The Ct values obtained for the 1 % input were adjusted to 100 %. This adjusted input is called ΔCt. The values for the percent recovery of the input were calculated using the formula $100 \times 2^{-\Delta Ct - Ct}$, where Ct represents the Ct value obtained for each sample.

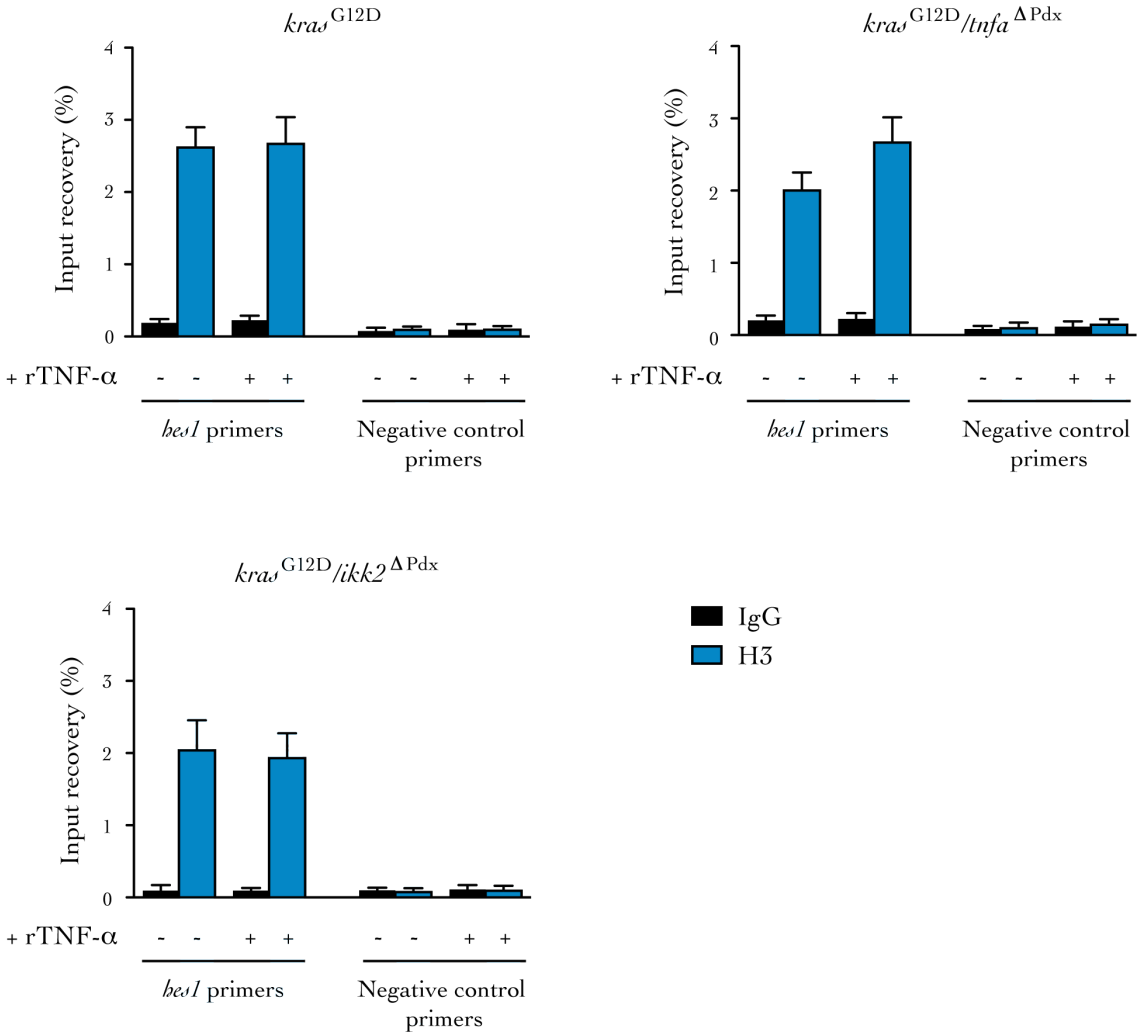

Figure 4.17: Chromatin immunoprecipitation of histone H3 to the *hes1* promoter

Cells derived from PanIN bearing *kras*^{G12D}, *kras*^{G12D}/*tnfa*$^{\Delta Pdx}$ and *kras*^{G12D}/*ikk2*$^{\Delta Pdx}$ mice were stimulated with rTNF-α (1 ng/ml) for 6 hours. ChIP assays were performed with anti-histone H3 antibody or anti-rabbit IgG antibody as a control. Immunoprecipitated DNA was analysed by qRT-PCR using *hes1* promoter-specific primers and compared with unstimulated cells. Results are shown as mean + SD of triplicate determinants and are representative of three independent experiments.

A high percentage of the recovery of the input indicates that the samples were enriched with the *hes1* target gene. Histone H3 occupies the *hes1* promoter locus in cells derived from PanIN bearing *kras*^{G12D}, *kras*^{G12D}/*ikk2*$^{\Delta Pdx}$ and *kras*^{G12D}/*tnfa*$^{\Delta Pdx}$ mice in presence or absence of rTNF-α stimulation (Figure 4.17).

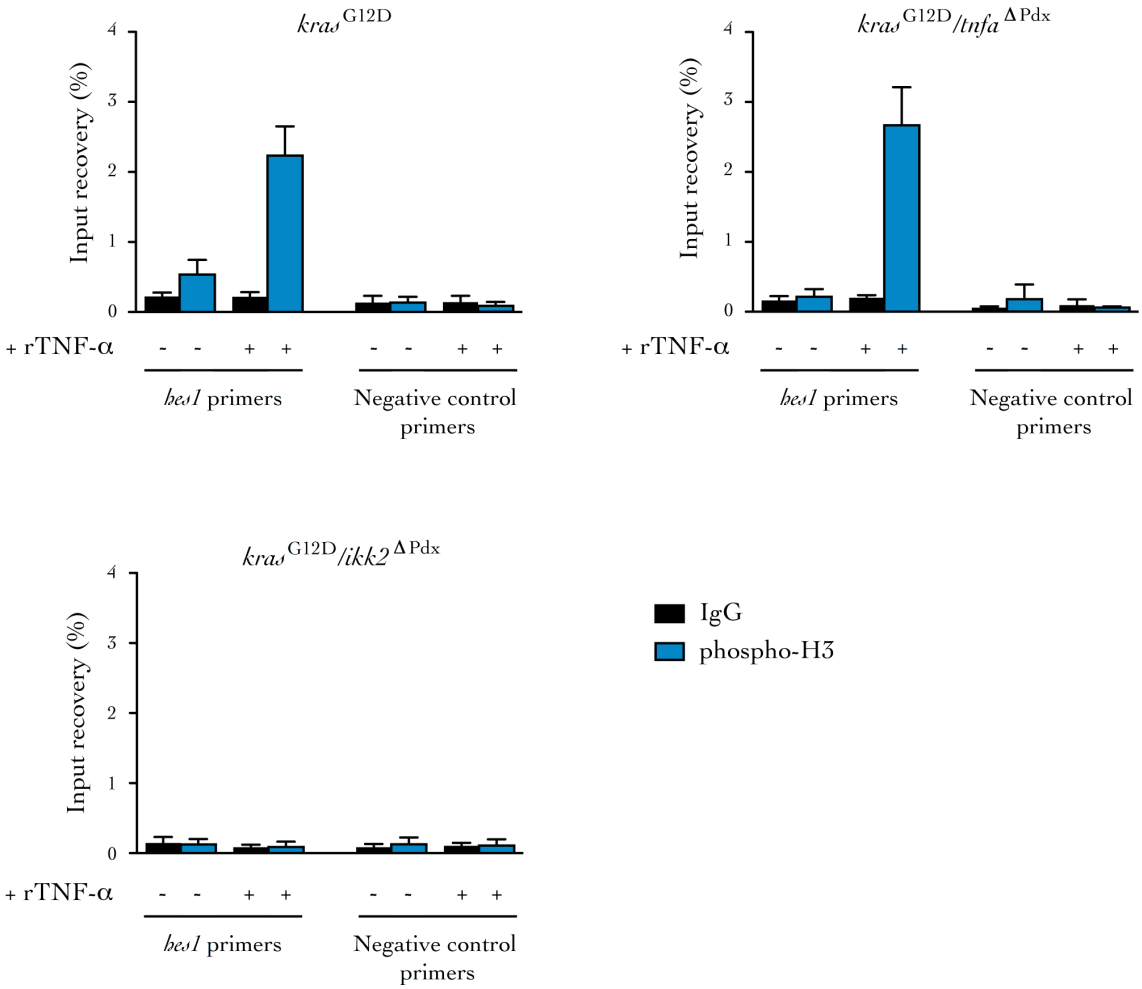

Figure 4.18: Chromatin immunoprecipitation of phospho-histone H3 (Ser10) to the *hes1* promoter

Cells derived from PanIN bearing *kras*^{G12D}, *kras*^{G12D}/*tnfa*$^{\Delta Pdx}$ and *kras*^{G12D}/*ikk2*$^{\Delta Pdx}$ mice were stimulated with rTNF-α (1 ng/ml) for 6 hours. ChIP assays were performed with anti-phospho-histone H3 (Ser10) antibody or anti-rabbit IgG antibody as a control. Immunoprecipitated DNA was analysed by qRT-PCR using *hes1* promoter-specific primers and compared with unstimulated cells. Results are shown as mean + SD of triplicate determinants and are representative of three independent experiments.

However, phosphorylated histone H3 on Ser10 was detected at the *hes1* promoter locus only when cells derived from PanIN bearing *kras*^{G12D} and *kras*^{G12D}/*tnfa*$^{\Delta Pdx}$ mice were stimulated with rTNF-α. This phosphorylation was abolished in cells derived from PanIN bearing *kras*^{G12D}/*ikk2*$^{\Delta Pdx}$ mice (Figure 4.18).

Taken together, these results show that activation of the TNF-α/IKK2 signalling pathway via rTNF-α stimulation can induce the phosphorylation of the histone H3 already present at the *hes1* promoter locus, which possibly enhances the trancriptional activity of a classical Notch target gene. IKK2 appears to be essential for the phosphorylation of the Ser10 residue on histone H3 at the *hes1* promoter locus.

Data described in this section show that IKK2 is involved in the phosphorylation of histone H3 on Ser10, which leads to the upregulation of the transcription of Notch target genes upon rTNF-α stimulation. However, little is known about a nuclear role for IKK2 and how this kinase would translocate to the nucleus. This would provide important information and would contribute to explain how the nuclear histone protein H3 is phosphorylated. Otherwise, intermediate protein partners will need to be characterised in order to identify another possible kinase downstream of IKK2 with a known nuclear role.

4.5 Discussion and conclusion

In this chapter, the cooperation between the TNF-α/IKK2 and the Notch signalling pathways in the pancreatic cancer models used was examined.

The pancreases of PanIN bearing *kras*^{G12D} mice presented an active Notch signalling pathway (demonstrated by Notch target gene and protein expression levels in Figure 4.1 and Figure 4.2) whereas for PanIN bearing *kras*^{G12D}/*tnfa*$^{\Delta Pdx}$ and *kras*^{G12D}/*ikk2*$^{\Delta Pdx}$ mice, this activation was respectively reduced or abolished. Immunofluorescent data for HES1 and HEY1 after the stimulation of the cells derived from PanIN bearing *kras*^{G12D} mice with rTNF-α *in vitro* (Figure 4.5) showed a higher ratio for nuclear location compared with cytoplasmic location, attesting the activation of the Notch pathway. Similar results were also obtained at the gene expression level after stimulating the corresponding cell lines with rTNF-α (Figure 4.4). The downregulation of the HES1 protein in *kras*^{G12D}/*ikk2*$^{\Delta Pdx}$ mice suggests a cooperation between the NF-κB and the Notch signalling pathways. It should be noted that in different cell types and settings, the expression of *hes1* has also been demonstrated to be regulated by Notch-independent mechanisms involving the RAS/RAF/MAPK and/or the JNK signalling pathways (Curry *et al.,* 2006; Katoh 2007; Stockhausen *et al.,* 2005). The data and findings described in this chapter do not exclude that, in pancreatic epithelial cells, *hes1* expression may be regulated by other signalling pathways.

Activation of TNF-α/IKK2 signalling leads to an upregulated transcriptional expression of the classical Notch target genes *hes1* and *hey1* (Figure 4.3). siRNA experiments showed that this upregulation requires canonical Notch signalling and is IKK2-dependent (Figure 4.8 to Figure 4.13). The knockdown of NEMO also affects

the upregulation of *hes1* but its role was not further investigated. More importantly, further analysis of the mechanisms involved reveal that TNF-α stimulation enhances NICD release (Figure 4.14) and additionally that IKK2 induces the phosphorylation of histone H3 at the *hes1* promoter locus, therefore activating the transcription of this Notch target gene (Figure 4.17 and Figure 4.18).

Chromatin remodelling is important in regulating the initiation of the transcription process. Histones are assembled into nucleosomes around which the DNA is tightly packed and ordered, forming the chromatin. Chromatin structure can be more or less condensed, depending on the phase of the cell cycle (Li and Reinberg 2011). For example, to allow the transcription machinery to access the DNA strand, the chromatin needs to be opened. These changes in chromatin organisation are mainly regulated by histone modifications (Bannister and Kouzarides 2011).

Histone proteins can often be acetylated, phosphorylated or methylated. Several histone modifications, particularly on histone H3, are involved in the activation of gene transcription (Bannister and Kouzarides 2011; Berger 2007; Kouzarides 2007; Li *et al.,* 2007). For example, acetylation of specific residues on histone H3 (Lys56) contributes to chromatin disassembly (Williams *et al.,* 2008). The hyperacetylated status of histone H3 in general also allows transcriptional activation through decondensation of the chromatin (Schubeler *et al.,* 2000). Methylation of arginine (Arg) and lysine (Lys) residues is also associated with gene activation; Arg17 on histone H3 (Bauer *et al.,* 2002) or Lys9 on histone H3 (Vakoc *et al.,* 2005). Phosphorylation of histone H3 on Ser10 also correlates with the activation of gene transcription in *Drosophila melanogaster* (Nowak and Corces 2000) and mouse fibroblasts (Strelkov and Davie 2002). Phosphorylated histone H3 on Ser10 is also a

marker for mitosis (Goto *et al.,* 1999; Hendzel *et al.,* 1997). The phosphorylation of histone H3 on Ser28 was recently shown to increase the transcription of the RNA polymerase III target genes, usually involved in the translation of proteins required for cell proliferation (Zhang *et al.,* 2011). A combination of phosphorylation and acetylation of histone H3 in response to EGF-stimulation has been shown to induce *c-fos* and *c-jun* gene transcription (activated via the MAPK/ERK pathway) and lysine methylation has also recently been proven to be involved in this process (Cheung *et al.,* 2000; Edmunds *et al.,* 2008).

There is therefore a huge complexity and diversity in histone modifications for gene activation. These modifications are not only involved in controlling and regulating transcription, but they have also been shown to be involved in other cellular processes such as chromosome condensation and DNA repair or replication (Kouzarides 2007).

MSK1, MSK2 (Davie 2003; Soloaga *et al.,* 2003) and IKK1 (Anest et al., 2003; Yamamoto et al., 2003) have been shown to be the kinases responsible for histone H3 phosphorylation on Ser10. These data lead to particular interest in IKK1 as they suggested a new unidentified nuclear role for this protein and a new regulatory process for NF-κB-activated genes. However, the main question remains of how these modifying proteins (kinases, acetylases and methylases) are recruited into the nucleus. Only few examples have been described, such as the discovery of a DNA-binding site in the well-studied kinase ERK (Hu *et al.,* 2009). Modifying proteins can also translocate into the nucleus in association with transcription factors or their coactivators.

This chapter attempts to identify whether IKK2 can directly interact with NICD and whether this interaction can contribute to the upregulation of the Notch target genes observed by either enhancing the proteolytic release of the NICD or its stability. The second hypothesis tested a potential role for IKK2 in enhancing Notch target gene transcription via histone modifications, inducing chromatin remodelling at the *hes1* gene locus and finally leading to the increased gene transcription observed throughout the experiments performed. The potential mechanisms described are represented in a simplified version in the Figure 4.19 below.

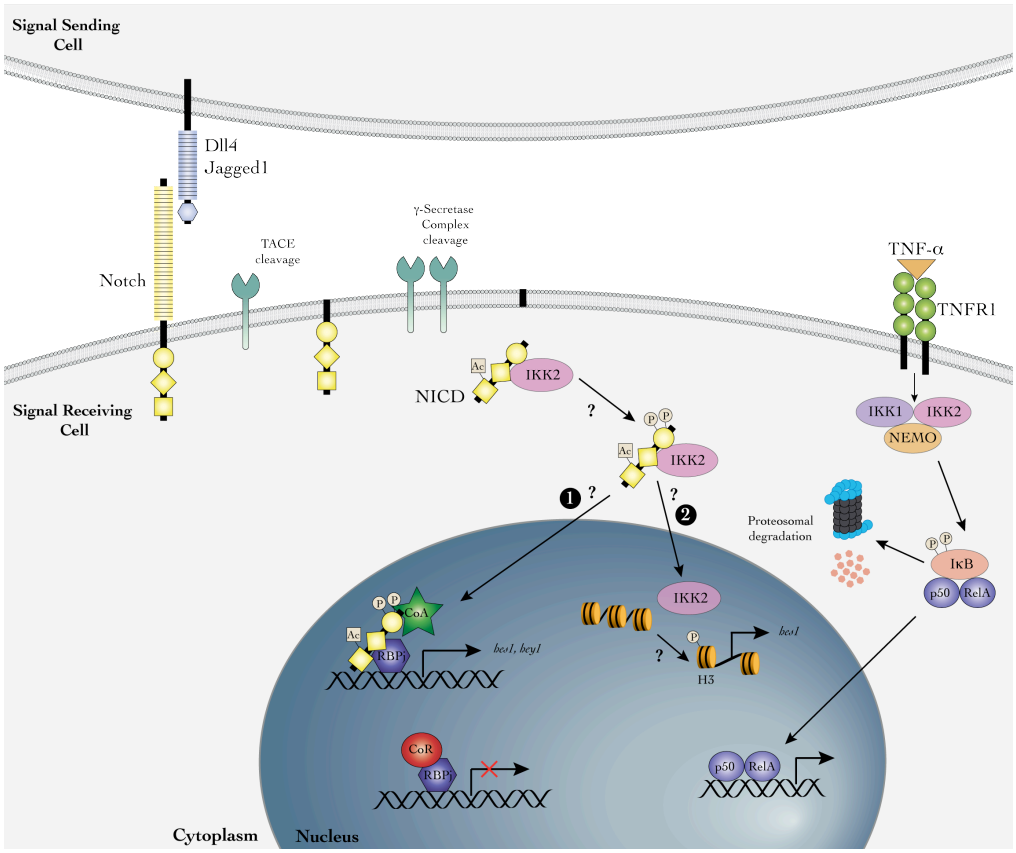

Figure 4.19: The link between the IKK2 and the Notch signalling pathways

Activation of the NF-κB signalling pathway upon TNF-α stimulation activates IKK2 and leads to an upregulation of the expression of the Notch target genes. Two hypotheses were tested: 1) whether IKK2 can interact with NICD and phosphorylate some NICD residues therefore favouring the translocation of NICD into the nucleus for an enhanced activation of the pathway or 2) whether activated-IKK2 can directly or indirectly induce histone phosphorylation, favouring transcriptional activity.

Activation of the transcription of Notch target genes upon rTNF-α stimulation occurs following histone H3 modification (phosphorylation on Ser10) at the *hes1* promoter locus and requires the IKK2 kinase (Figure 4.17 and Figure 4.18). A direct interaction between IKK2 and NICD was demonstrated (Figure 4.15), but additional experiments need to be performed to confirm this novel interaction.

Further experiments also need to be performed to show whether IKK2 can localise at the nucleus in cells derived from PanIN and PDAC bearing *kras*^{G12D} mice and stimulated with rTNF-α. Immunofluorescent staining and/or nuclear and cytoplasmic protein extraction to identify IKK2 by Western blot would provide preliminary insights on a possible nuclear location. Using bioinformatics, it would also be interesting to screen for potential non-identified nuclear translocation domains or DNA-binding sites within the IKK2 protein.

If a direct interaction between IKK2 and NICD occurs, it may indicate that this association can facilitate and mediate the translocation of IKK2 into the nucleus to induce histone modification or that IKK2 can directly phosphorylate NICD in the cytoplasm. It has recently been shown that post-translational modifications of NICD (such as acetylation) have an impact on its stabilisation and therefore on Notch target gene responses (Guarani *et al.,* 2011).

Phosphoproteomics technology could be used to identify the presence of phosphate groups on NICD and whether stimulation with rTNF-α induces significant changes in their numbers. Another possible route for further investigation would be to perform labelling experiments using phosphorus-32 (^{32}P) to study NICD phosphorylation upon rTNF-α stimulation. As phosphorylation is known to be an

important regulatory mechanism involved in many cellular processes (Johnson 2009), these experiments can indicate whether phosphorylation of NICD induces its stabilisation. In this case, a more stable NICD protein would contribute to explain the upregulation of the expression of the Notch target genes observed. However, phosphorylation of NICD in the C-terminal region is known to target it for ubiquitination and proteasomal degradation (Fryer *et al.,* 2004; Tsunematsu *et al.,* 2004).

It is possible that the TNF-α/IKK2/NF-κB signalling pathway had an effect upstream of NICD and could, for example, affect the activity of the enzymatic complexes involved in the release of NICD. The data shown in Figure 4.14 indicate that more NICD was released upon rTNF-α stimulation. An interesting question would be whether this stimulation can enhance the activity of the TACE and/or the γ-secretase complex. The activity of these enzymes can be measured by incubating cell membrane fractions with specific fluorogenic peptide probes and their substrate and using fluorescence resonance energy transfer (FRET) for example.

Another point of possible regulation following rTNF-α stimulation would be that the stability of the NICD protein is increased, either by some additional translational modifications such as acetylation or by modifying its proteosomal degradation. Acetylated residues can be identified using specific antibodies after co-immunoprecipitation and inhibition of the proteasome can be performed *in vitro* using the natural compound lactacystin or the synthetic peptide MG132.

A direct crosstalk between the TNF-α/IKK2 and the Notch signalling pathways is described in this chapter, showing that TNF-α can increase *hes1* gene expression.

HES1 can activate its own expression by binding to N-box sequences within its own promoter region (Takebayashi *et al.,* 1994) and this could contribute to the creation of a positive feedback loop leading to increased HES1 levels in pancreatic cancer cells. Moreover, HES1 is also known to promote inflammation. The effects of induced *hes1* expression on inflammatory processes in pancreatic carcinogenesis is investigated in the next chapter.

CHAPTER FIVE: HES1 AND INFLAMMATION

5.1 Introduction

The previous chapter describes how the TNF-α/IKK2 and the Notch signalling pathways cooperate in the context of *kras*-mutant pancreatic carcinogenesis and the potential mechanisms involved in the upregulation of the expression of the Notch target gene *hes1* upon TNF-α stimulation.

Basic helix-loop-helix (bHLH) genes, such as *hes1*, are the main regulators of the different developmental processes during embryogenesis and are highly conserved in multicellular organisms (Skinner *et al.,* 2010). The *hes1* gene is mostly involved in the differentiation processes of a variety of different cell types, mainly regulating neural development and segregation of the endocrine and exocrine compartments of the pancreas (Kageyama *et al.,* 2000). HES1 is a transcription factor, more particularly a transcription repressor, which functions as a homodimer or a heterodimer (Kageyama *et al.,* 2000), binding to N- and E-box sequences (CACNAG or CANGTG respectively) with high and low affinities respectively (Jarriault *et al.,* 1995; Sasai *et al.,* 1992). This transcription factor negatively regulates the expression of genes containing E-box and/or RBPj sites within their promoters (Fischer and Gessler 2007; Iso *et al.,* 2003; Tanigaki and Honjo 2007; Tun *et al.,* 1994).

Interestingly, HES1 has been shown to bind to E-box sequences within the promoter region of the peroxisome proliferator-activated receptor gamma (*pparg*) gene and this binding acts as a negative regulator for the *pparg* gene as it suppresses its expression (Herzig *et al.,* 2003). PPAR-γ is a ligand-dependent transcription factor, which regulates immunity and inflammatory processes (Glass and Saijo 2010). To further investigate the link between epithelial cell intrinsic inflammation and the Notch signalling pathway in pre-malignant pancreatic cells, the regulation of *pparg* gene

expression in the context of *kras*-induced pancreatic carcinogenesis is explored in the present chapter.

The PPAR-γ nuclear receptor has been shown to be activated by a variety of lipid ligands and to regulate fatty acid metabolism (Evans *et al.,* 2004; Kliewer *et al.,* 2001). Natural and synthetic ligands for PPAR-γ include prostaglandins (PG), such as PGJ2 (Forman *et al.,* 1995; Kliewer *et al.,* 1995), antidiabetic agents from the thiazolidinedione class (TZD) (Lehmann *et al.,* 1995) and non-steroidal anti-inflammatory drugs (Lehmann *et al.,* 1997). PPAR-γ receptors, also called adopted orphan receptor for non-steroidal ligands, form a heterodimer with a retinoid X receptor and bind to hormone response elements (HRE) within the promoter region of the target genes, in the presence or absence of their ligands (Glass and Saijo 2010).

The anti-inflammatory role of PPAR-γ agonists has been demonstrated by a reduction in the production of inflammatory cytokines by monocytes, therefore suggesting that PPAR-γ is a transcriptional repressor of inflammatory genes (Jiang *et al.,* 1998). The classical IL-12 production by macrophages upon LPS stimulation is inhibited by treatment with an oxidised low density lipoprotein. This inhibition has been shown to be related to modifications in the interactions between NF-κB and the DNA, but also to a direct interaction between NF-κB and PPAR-γ (Chung *et al.,* 2000). Recently, this receptor has also been shown to inhibit the differentiation of a subset of T helper cells (Th17) which are involved in autoimmune diseases (Klotz *et al.,* 2009). Finally, its role in anti-inflammation has been described in a model for colitis where PPAR-γ ligands can reduce the levels of cytokine production and this is related to an inhibition of the NF-κB transcription factor (Su *et al.,* 1999).

The hypothesis tested in this chapter was whether the HES1 upregulation observed in pre-malignant pancreatic cells following TNF-α stimulation leads to the suppression of *pparg* gene expression, which would in turn have an effect on inflammatory gene expression, therefore contributing to a sustained pro-inflammatory profile for the pre-malignant cells.

5.2 Link between HES1 and PPAR-γ in pancreatic cancer

5.2.1 Gene expression levels of *pparg*

The expression of the nuclear receptor *pparg* was evaluated in the pancreases of the three mouse models studied at 2 and 5 months of age (Figure 5.1).

As shown in Figure 5.1, at 2 months of age, *pparg* mRNA expression levels were upregulated in the pancreases of *kras*^{G12D}/*ikk2*$^{\Delta Pdx}$ and *kras*^{G12D}/*tnfa*$^{\Delta Pdx}$ mice compared with *kras*^{G12D} mice. However, by 5 months of age, *pparg* expression remained significantly elevated in the pancreases of *kras*^{G12D}/*ikk2*$^{\Delta Pdx}$ mice only.

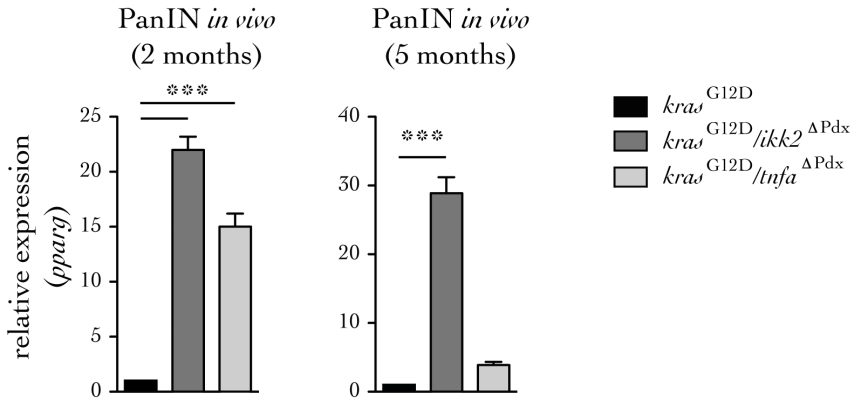

Figure 5.1: Nuclear receptor *pparg* gene expression *in vivo*

Relative mRNA expression of *pparg* in the pancreases of 2- and 5-month old *kras*^{G12D}/*ikk2*$^{\Delta Pdx}$ and *kras*^{G12D}/*tnfa*$^{\Delta Pdx}$ mice. Relative expression was calculated by setting expression of the pancreases of *kras*^{G12D} mice as 1. Data are shown as mean + SD of duplicate experiments, ***p<0.001, n=6.

The profile of *pparg* gene expression was also examined in the cell lines derived from PanIN bearing *kras*^{G12D}, *kras*^{G12D}/*tnfa*$^{\Delta Pdx}$ and *kras*^{G12D}/*ikk2*$^{\Delta Pdx}$ mice upon stimulation with rTNF-α (Figure 5.2).

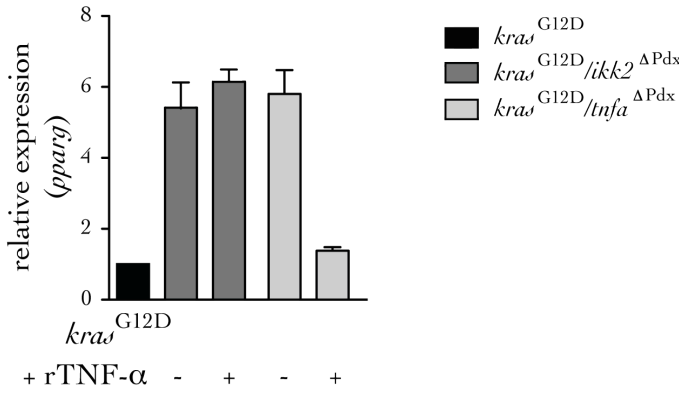

Figure 5.2: Nuclear receptor *pparg* gene expression upon rTNF-α stimulation *in vitro*

Relative mRNA expression of *pparg* in cell lines derived from PanIN bearing *kras*^{G12D}/*ikk2*$^{\Delta Pdx}$ and *kras*^{G12D}/*tnfa*$^{\Delta Pdx}$ mice, stimulated with 1 ng/ml of rTNF-α for 6 hours. Relative expression was calculated by setting expression of untreated *kras*^{G12D} samples as 1. Data are shown as mean + SD of triplicate determinants and one representative experiment out of two performed is shown.

After rTNF-α stimulation, cell lines derived from PanIN bearing *kras*^{G12D}/*tnfa*$^{\Delta Pdx}$ mice had reduced *pparg* mRNA expression levels. However, rTNF-α stimulation in cell lines derived from PanIN bearing *kras*^{G12D}/*ikk2*$^{\Delta Pdx}$ mice had no impact on the previously observed upregulation.

The gene expression profile observed for *pparg* in the pancreases of the different mouse models is inversely correlated with the gene expression profile for *hes1* (see Figure 4.1): high expression levels of *hes1* in *kras*^{G12D} mice are associated with low levels of *pparg* and vice versa in the *kras*^{G12D}/*tnfa*$^{\Delta Pdx}$ and *kras*^{G12D}/*ikk2*$^{\Delta Pdx}$ mice.

5.2.2 Expression of *pparg* is inhibited by HES1

As mentioned earlier, HES1 has been demonstrated to negatively regulate the expression of *pparg* in hepatocytes (Herzig *et al.,* 2003). To investigate whether this also occurs in pancreatic cancer cells, the effect of *hes1* specific siRNA knockdown in cells derived from PanIN bearing *kras*^{G12D} mice was investigated.

Three different commercially validated *hes1* siRNAs and a non-targeting control were used to transfect cells derived from PanIN bearing *kras*^{G12D} mice. Their specificity and efficiency in inhibiting *hes1* gene expression and HES1 protein production were assessed by qRT-PCR and Western blot (Figure 5.3).

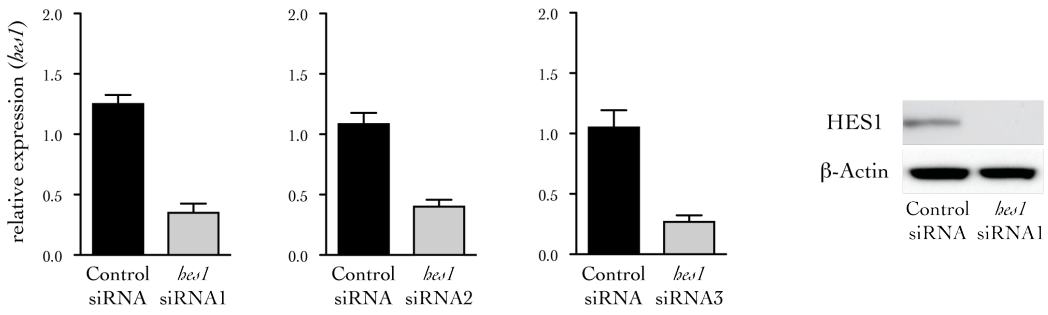

Figure 5.3: siRNA knockdown of *hes1* in cell lines derived from PanIN bearing *kras*^{G12D} mice

Cell lines derived from PanIN bearing *kras*^{G12D} mice were transfected wih *hes1* specific siRNA. *hes1* knockdown was verified by qRT-PCR and Western blot. Data are shown as mean + SD of triplicate determinants and are representative of three independent experiments.

To directly evaluate the impact of *hes1* knockdown, gene expression levels for *pparg* were measured and are shown in Figure 5.4.

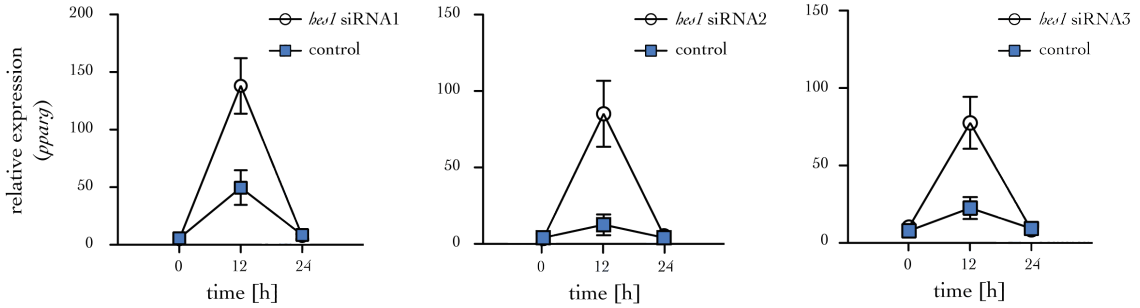

Figure 5.4: Gene expression levels for *pparg* following *hes1* knockdown

Cell lines derived from PanIN bearing $kras^{G12D}$ mice were transfected wih *hes1* specific siRNA or non-targeting control siRNAs. *pparg* gene expression was quantified by qRT-PCR. Data are shown as mean ± SD of triplicate determinants and are representative of three independent experiments.

Specific *hes1* knockdown results in a robust upregulation of *pparg* gene expression, indicating that HES1 can negatively regulate this transcription factor in cells derived from pancreatic PanIN lesions.

Expression of *cebpa*, a corepressor of inflammatory genes whose expression is also regulated by PPAR-γ (Li *et al.,* 2010; Zuo *et al.,* 2006), was also assessed and significantly upregulated after *hes1* knockdown (Figure 5.5).

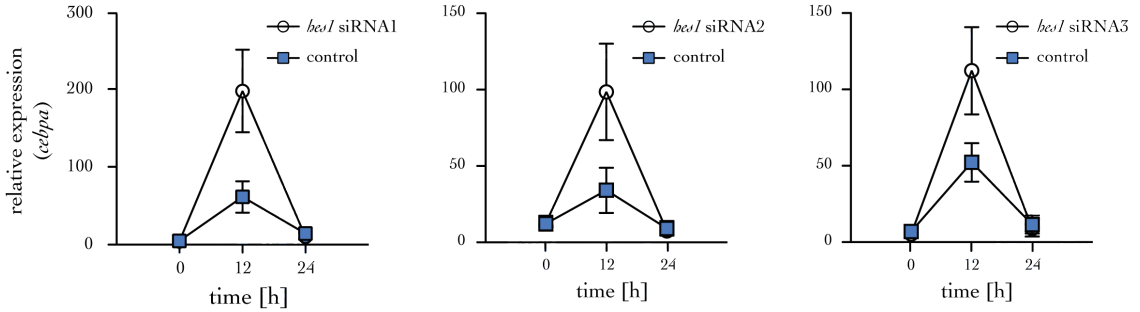

Figure 5.5: Gene expression levels for *cebpa* following *hes1* knockdown

Cell lines derived from PanIN bearing $kras^{G12D}$ mice were transfected wih *hes1* specific siRNA or non-targeting control siRNAs. *cebpa* gene expression was quantified by qRT-PCR. Data are shown as mean ± SD of triplicate determinants and are representative of three independent experiments.

To further investigate the effects of HES1 on the activity of the *pparg* promoter, cells derived from PanIN bearing *kras*^{G12D} and *kras*^{G12D}/*tnfa*$^{\Delta Pdx}$ mice were cotransfected with a *hes1* expression plasmid or a control vector with a *pparg* luciferase reporter construct (Figure 5.6).

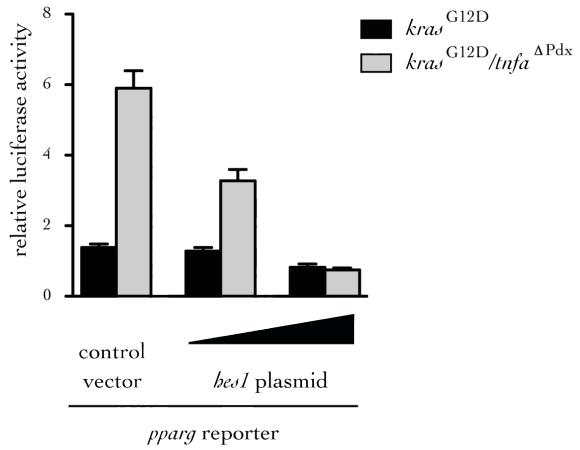

Figure 5.6: Effects of HES1 on the activity of the *pparg* promoter

Cells derived from PanIN bearing *kras*^{G12D} and *kras*^{G12D}/*tnfa*$^{\Delta Pdx}$ mice were cotransfected with a *hes1* expression plasmid or a control vector and a *pparg* luciferase reporter construct. Luciferase activity was analysed 24 hours post-transfection. Data are shown as mean + SD from duplicate transfections and are representative of three independent experiments.

As shown in Figure 5.6, luciferase activity was significantly increased in cells derived from PanIN bearing *kras*^{G12D}/*tnfa*$^{\Delta Pdx}$ mice cotransfected with the control vector and the *pparg* luciferase reporter construct compared with cells derived from PanIN bearing *kras*^{G12D} mice. Cells were generated from 2-month old PanIN bearing mice and have a *hes1* profile similar to that observed in Figure 4.4 (lower expression of *hes1* in cells derived from PanIN bearing *kras*^{G12D}/*tnfa*$^{\Delta Pdx}$ mice compared with cells derived from PanIN bearing *kras*^{G12D} mice). This is in agreement with the results presented in Figure 5.2, with high expression of *pparg* in cells derived from PanIN bearing *kras*^{G12D}/*tnfa*$^{\Delta Pdx}$ mice in absence of rTNF-α stimulation. However, when cotransfecting the cells with the *hes1* plasmid, luciferase activity decreases in a dose dependent manner. These results confirm the negative regulation of *pparg* expression by HES1 previously observed in Figure 5.4.

5.2.3 HES1 is present at the *pparg* promoter

HES1 has already been shown to bind to the promoter region of the *pparg* gene in hepatocytes (Herzig *et al.,* 2003). To investigate whether similar binding occurs in pancreatic cells, ChIP assays were carried out using an antibody directed against HES1 (Figure 5.7). Immunoprecipitated DNA was analysed by qRT-PCR using *pparg* promoter-specific primers and input recovery calculation is explained in section 4.4.3.

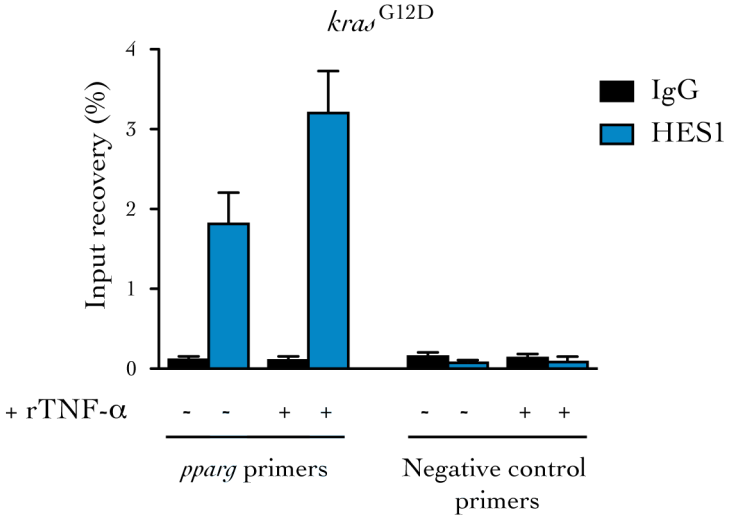

Figure 5.7: Chromatin immunoprecipitation of HES1 to the *pparg* promoter

Cells derived from PanIN bearing *kras*^{G12D} mice were stimulated with rTNF-α at 1 ng/ml for 6 hours. ChIP assays were performed with anti-HES1 antibody or anti-rabbit IgG antibody as a control. Immunoprecipitated DNA was analysed by qRT-PCR using *pparg* promoter-specific primers. Results are shown as mean + SD of triplicate determinants and are representative of three independent experiments.

In Figure 5.7, a high percentage of the recovery of the input indicates that the samples immunoprecipitated with anti-HES1 antibody are enriched in the *pparg* target gene. HES1 was found to bind to the *pparg* promoter locus in cells derived from PanIN bearing *kras*^{G12D} mice in the presence or absence of rTNF-α stimulation, in agreement with another study (Herzig *et al.,* 2003). A higher percentage of the recovery of the input upon rTNF-α stimulation was observed which is in agreement with HES1 production being upregulated in these conditions.

5.3 Discussion and conclusion

Pre-malignant epithelial pancreatic cells constitutively secrete the TNF-α cytokine which, in an autocrine manner, can upregulate and increase *hes1* gene expression and HES1 protein production. This chapter describes and investigates the role and the effects of these amplified levels of HES1 in the context of pancreatic cancer.

Interaction between HES1 and the *pparg* promoter has been demonstrated in hepatic cells (Herzig *et al.,* 2003) and similar data in pancreatic cancer cells were described in this chapter. HES1 can bind to the *pparg* promoter and negatively regulate its expression (Figure 5.4, Figure 5.6 and Figure 5.7).

The CEBP and PPAR transcription factors have initially been described to be involved in the adipogenesis process (Farmer 2006; Rosen and MacDougald 2006). In this context of adipocyte differentiation, a crosstalk and a crossregulation between CEBP-α and PPAR-γ has been suggested more than ten years ago (Wu *et al.,* 1995; Wu *et al.,* 1999), but the full mechanism has only been described recently. CEBP-β can bind to the *cebpa* promoter and inhibit its activity when associated to an histone deacetylase complex. PPAR-γ can target this complex to the proteasome, therefore releasing the inhibition and allowing *cebpa* expression (Salma *et al.,* 2006; Zuo *et al.,* 2006).

The expression of *pparg* is not only restricted to the adipose tissue and does not only play a role in lipid metabolism. PPAR-γ is also produced in rat pancreatic acinar cells and its activation with prostaglandin can induce apoptosis (Masamune *et al.,* 2002). This apoptotic role, in addition to its anti-inflammatory role has also been observed in

endothelial cells and macrophages (Bishop-Bailey and Hla 1999; Chinetti *et al.,* 1998).

PPAR-γ ligands have also been demonstrated to have an effect on different tumour cell lines with inhibition of tumour growth *in vivo* of prostate cancer cells as well as induction of necrosis *in vitro* (Kubota *et al.,* 1998) and a reduction in tumour growth in xenograft models with human colon cancer cells (Sarraf *et al.,* 1998).

The gene expression levels of *pparg* in the pancreases of the mouse models studied during this thesis correlate with the progression of the disease: *kras*^{G12D} mice have a high tumour incidence and do not express *pparg*; *kras*^{G12D}*/tnfa*$^{\Delta Pdx}$ mice have a similar but delayed pattern in disease progression compared with *kras*^{G12D} mice and this is also reflected by a shift from high to low *pparg* expression between 3 and 5 months of age; *kras*^{G12D}*/ikk2*$^{\Delta Pdx}$ mice have a significantly lower tumour incidence, but higher expression of this transcription factor (Figure 3.5 and Figure 5.1). It seems that TNF-α secreted by the pre-malignant epithelial cells leads to HES1 production in *kras*^{G12D} and *kras*^{G12D}*/tnfa*$^{\Delta Pdx}$ mice, which allows *pparg* suppression. This can retain an inflammatory profile for the pre-malignant cells at the early stages of the disease, and therefore enhance PanIN progression and PDAC development.

Considering the previously described anti-inflammatory role of PPAR-γ, the next and final chapter of this thesis will investigate the effects of anti-inflammatory agents, such as PPAR-γ ligands, in pancreatic cancer progression *in vivo*.

CHAPTER SIX: INFLAMMATION AND TUMOUR PROGRESSION IN PANCREATIC CANCER

6.1 Introduction

The previous chapter describes how TNF-α-induced upregulation of HES1 in pancreatic cancer leads to *pparg* suppression and examines the potential mechanisms involved in this regulation.

Prostaglandins (PG), such as PGJ2, are the main natural ligands for PPAR-γ, but synthetic ligands belonging to the thiazolidinediones (TZD) medication class are also effective. These TZD agonists (rosiglitazone, pioglitazone and troglitazone) are mostly used for the treatment of type II diabetes mellitus, to restore an anti-inflammatory response (Nosjean and Boutin 2002).

In colon cancer cell lines, PPAR-γ ligands can reduce the levels of cytokine production by inhibiting NF-κB activation, representing ideal candidates for the restoration of anti-inflammatory signalling pathways in inflammatory bowel disease (Su *et al.,* 1999). A similar mechanism has been highlited when inhibiting TNF-α in mice with chronic colitis (Han *et al.,* 2007). The natural ligand PGJ2 has been shown to be able to inhibit IKK (Rossi *et al.,* 2000) and a physical and direct interaction has been demonstrated between PPAR-γ and NF-κB (Chung *et al.,* 2000). One mechanism by which PPAR-γ ligands repress the expression of inflammatory genes controlled by NF-κB has been shown in a mouse leukemic monocyte macrophage cell line. It involves SUMOylation of the PPAR-γ ligand binding domain, which induces its translocation to the nucleus and in particular its interaction with corepressor proteins present at the promoter region of inflammatory genes. The presence of PPAR-γ therefore represses the removal of these corepressors, which is required to allow the activation of gene transcription (Pascual *et al.,* 2005).

PPAR-γ is also expressed in pancreatic acinar cells (Masamune *et al.,* 2002) and anti-inflammatory effects of PPAR-γ agonists on caerulein-induced pancreatitis have been investigated (Lee *et al.,* 2003; Wan *et al.,* 2008). The IL-6 expression and apoptotic cell death induced after caerulein treatment of rat pancreatic acinar cells is inhibited if the cells have previously been transfected with IκB mutant gene or *hras* mutant gene, demonstrating a role for the NF-κB and the MAPK signalling pathways in these processes (Lee *et al.,* 2003). Further analysis using the same cell line shows that treating the cells with a PPAR-γ agonist has several effects on the components of the NF-κB signalling pathway. Caerulein treatment induces Rel A DNA binding activity and increases its level of expression, which are both inhibited upon incubation with PPAR-γ ligand. Moreover, the phosphorylation-dependent proteolytic degradation of IκB required for NF-κB activation is induced by caerulein and inhibited when treating the cells with a PPAR-γ ligand. Furthermore, the activation of the IKK complex involved in the phosphorylation of IκB is decreased in the presence of the PPAR-γ agonist and finally, nuclear accumulation of NF-κB heterodimers is also reduced upon treatment with a PPAR-γ ligand (Wan *et al.,* 2008).

In conclusion, the PPAR-γ nuclear receptor plays a major role in suppressing inflammation in different models, including colitis and pancreatitis, by repressing inflammatory gene expression induced by other classes of transcription factors such as NF-κB (Blanquart *et al.,* 2003).

The interplay between TNF-α/IKK2, Notch and PPAR-γ observed and described in the previous chapters was suggested to retain the pre-malignant cells in a state of constitutive production of pro-inflammatory cytokines and chemokines and to promote tumour growth in *kras*^{G12D} and *kras*^{G12D}/*tnfa*$^{\Delta Pdx}$ mice.

In this chapter, pharmacological inhibitors were used to evaluate whether targeting Notch signalling *in vivo* can influence the inflammatory profile of the pre-malignant cells at the tumour site. A PPAR-γ ligand was also tested to investigate whether restoring anti-inflammaotry signals in *kras*^{G12D} mice can modify and reduce PanIN progression.

6.2 Inhibition of the Notch and the NF-κB signalling pathways

The impact of the inhibition of the Notch or the NF-κB signalling pathways on *hes1* expression was assessed *in vitro*. Cells derived from PanIN bearing *kras*^{G12D}/*tnfa*$^{\Delta Pdx}$ mice were treated with the γ-secretase inhibitor (GSI) L685458 (Shearman *et al.,* 2000) at 5 μM for 6 hours or the synthetic inhibitor Bay11-7082 at 1 μM for 6 hours (Figure 6.1). This compound inhibits the phosphorylation of IκB in an irreversible manner, therefore preventing the release of NF-κB, which remains sequestered in the cytoplasm without being able to induce the expression of its target genes upon activation (Pierce *et al.,* 1997).

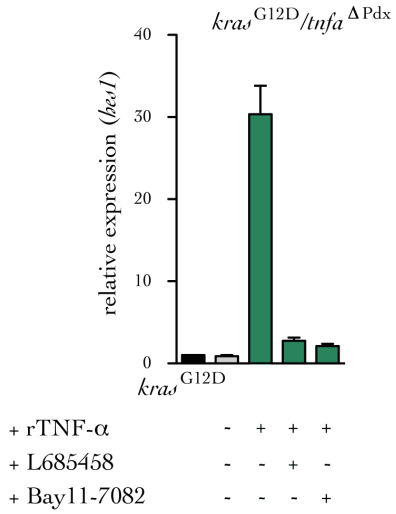

Figure 6.1: Changes in *hes1* expression levels upon inhibition of the Notch or the NF-κB signalling pathways *in vitro*

Relative mRNA expression of *hes1* in cell lines derived from PanIN bearing *kras*^{G12D}/*tnfa*$^{\Delta Pdx}$ mice and stimulated with 1 ng/ml of rTNF-α for 6 hours in the presence or absence of L685458 (5 μM) or Bay11-7082 (1 μM). Relative expression was calculated by setting expression of untreated *kras*^{G12D} samples as 1. Data are shown as mean + SD of triplicate determinants and one representative experiment out of three performed is shown.

As shown in Figure 6.1, in the presence of rTNF-α, both inhibitors were able to block *hes1* gene expression. These data confirm that canonical Notch signalling is essential in the upregulation of *hes1* expression and also that the NF-κB signalling pathway regulates *hes1* gene expression. Inhibition of either of these pathways is sufficient to prevent *hes1* expression upon rTNF-α stimulation.

To confirm these observations, pharmacological inhibition of these pathways was performed *in vivo* in *kras*^{G12D} mice and compared with untreated *kras*, *kras*^{G12D} and *kras*^{G12D}/*ikk2*$^{\Delta Pdx}$ mice (Figure 6.2).

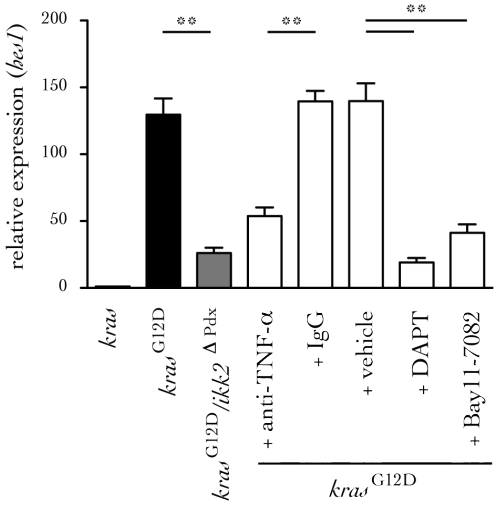

Figure 6.2: Changes in *hes1* expression levels upon inhibition of the Notch or the NF-κB signalling pathways *in vivo*

Relative mRNA expression of *hes1* in the pancreases of 5-month old untreated *kras*^{G12D}, *kras*^{G12D}/*ikk2*$^{\Delta Pdx}$ mice and of age-matched *kras*^{G12D} mice treated with anti-TNF-α (10 mg/kg/day), control IgG (10 mg/kg/day), DAPT (100 mg/kg/day), Bay11-7082 (10 mg/kg/day) or the vehicle control for seven days. Relative expression was calculated by setting expression of untreated *kras Cre* negative mice as 1. Data are shown as mean + SD of duplicate experiments, n=6, **p<0.01.

Inhibition of the Notch signalling pathway *in vivo* was achieved using the γ-secretase inhibitor DAPT (Dovey *et al.,* 2001), and of the NF-κB signalling pathway by using either an anti-murine-TNF-α antibody or the synthetic inhibitor Bay11-7082, which blocks the TNF-α-induced phosphorylation of IκB, therefore preventing NF-κB

nuclear translocation (Pierce *et al.,* 1997). The use of DAPT was favoured over L685458 because this inhibitor is commonly used *in vivo* as opposed to L685458 and also for cost reasons.

As already mentioned, *hes1* gene expression is upregulated in the pancreases of *kras*^{G12D} mice and reduced in the pancreases of *kras*^{G12D}/*ikk2*$^{\Delta Pdx}$ mice. However, this increased expression is abolished if the *kras*^{G12D} mice are treated with anti-TNF-α, DAPT or Bay11-7082. These *in vivo* data are in agreement with the previous *in vitro* data (Figure 6.1), reinforcing the hypothesis that NF-κB signalling is important for the gene expression of the Notch target gene *hes1*.

Cell lines derived from the treated or untreated *kras*^{G12D} mice, described in Figure 6.2, were established and mRNA and protein levels of the TNF-α cytokine were evaluated after culture *in vitro* for 24 hours (Figure 6.3).

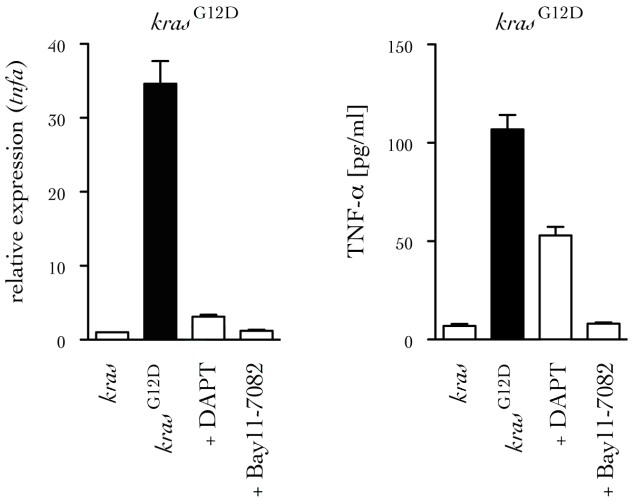

Figure 6.3: TNF-α cytokine levels

Relative mRNA expression of *tnfa* and protein levels of secreted TNF-α in cells derived from PanIN bearing *kras*^{G12D} mice treated or untreated with DAPT or Bay11-7082 measured by qRT-PCR and ELISA respectively. Relative expression was calculated by setting expression of untreated *kras Cre* negative mice as 1. Data are shown as mean + SD of triplicate experiments and are representative of three independent experiments.

Reduced *tnfa* gene expression and TNF-α cytokine production were observed in pancreatic cells derived from *kras*^{G12D} mice treated with both inhibitors, DAPT or Bay11-7082.

These results confirm that Bay11-7082 is efficiently blocking the NF-κB signalling pathway as shown by the downregulation of *tnfa* gene expression and TNF-α production and that a similar effect is obtained upon treatment with a GSI inhibitor. Considering all the data described so far, a reduction in TNF-α levels can lead to a reduction in HES1 production and therefore an upregulation of *pparg* expression. These inhibitors can consequently be used to restore the expression of anti-inflammatory proteins, which would provide a less inflamed environment and potentially delay or prevent PanIN progression. To test this hypothesis, the inflammatory status of the pancreases in different conditions was investigated in section 6.3.

6.3 Inflammatory status of the pancreas after DAPT treatment

The interplay between the TNF-α/IKK2 and the Notch signalling pathways, associated with a downregulation of the anti-inflammatory nuclear receptor PPAR-γ in *kras*^{G12D} and *kras*^{G12D}/*tnfa*$^{\Delta Pdx}$ mice, was shown in the previous chapters. This cooperation was inhibited using DAPT to treat *kras*^{G12D} mice and the effects on the production of inflammatory cytokines and chemokines by the pancreatic cells was evaluated. Protein levels in the pancreases of untreated or DAPT-treated *kras*^{G12D} mice were measured with cytokine and chemokine arrays and normalised to data obtained for wild type mice (Figure 6.4).

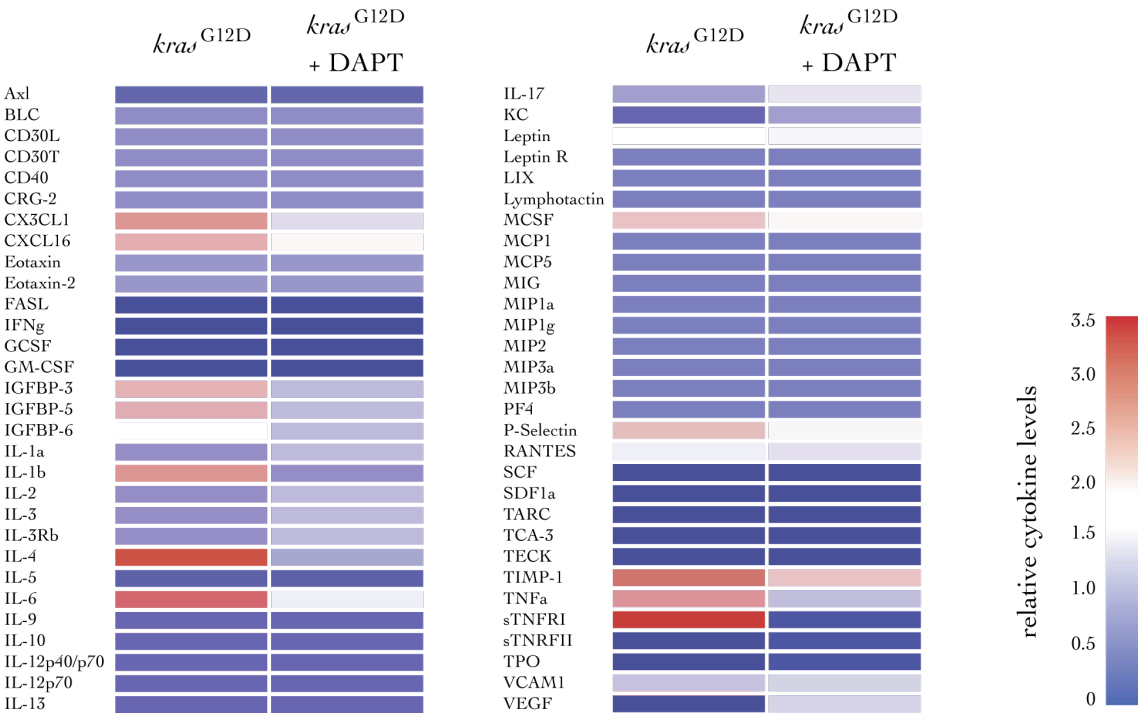

Figure 6.4: Cytokines and chemokines array data

Cytokine and chemokine levels in the pancreases of PanIN bearing *kras*^{G12D} mice at 5 months of age and treated or untreated with DAPT (intraperitoneally at 100 mg/kg/day for seven days, n=5) measured by protein array. The data is represented graphically as normalised to the signal intensity obtained for wild type mice.

The pancreases of untreated *kras*^{G12D} mice were previously shown to express high *hes1* mRNA and HES1 protein levels (Figure 4.1 and Figure 4.2), but also low gene

expression levels for *pparg* (see section 5.2.1). High levels of inflammatory cytokines such as IL-1β, IL-6 and TNF-α in the pancreases of *kras*^{G12D} mice confirm the inflammatory signature of the PanIN lesions. The cytokine array data reveal that *kras*^{G12D} mice treated with DAPT have lower levels of pro-inflammatory cytokines and chemokines, compared with untreated *kras*^{G12D} mice (Figure 6.4). Namely, the production levels of the cytokines/chemokines CX3CL1, CXCL16, IGFBP3, IGFBP5, IL-1β, IL-4, IL-6, MCSF, TIMP1, TNF-α and sTNFRI were reduced in treated animals. However, the production of VEGF was increased upon DAPT treatment and this is in contradiction with the mRNA level results presented in Figure 4.1. The expression of this Notch target gene was reduced in the pancreases of PanIN bearing *kras*^{G12D}/*ikk2*$^{\Delta Pdx}$ mice compared with PanIN bearing *kras*^{G12D} mice. Due to time constraints, this discrepancy was not further investigated but it could result from a dual regulation of *vegf* expression by the Notch and NF-κB signalling pathways.

To further investigate the impact of the Notch signalling pathway on the inflammatory state of the pre-malignant epithelial cells, *kras*^{G12D} mice carrying the *ROSA26-LSL-EYFP* allele were used. The *ROSA26-LSL-EYFP* mice allow the visualisation of *Cre* activity *in vivo* (Srinivas *et al.,* 2001). The *ROSA26* locus is ubiquitously expressed and the *eyfp* gene (coding for the enhanced yellow fluorescent protein) was inserted under the control of the promoter of this gene, but with an upstream STOP cassette flanked by two *loxP* sites (LSL). *eyfp* gene expression occurs in *ROSA26* and *Cre* expressing cells. After crossing the *kras*^{G12D} mice with the *ROSA26-LSL-EYFP* mice, the expression of *eyfp* was therefore concomitant to the oncogenic expression of the mutated *kras* allele in *pdx1* positive cells. It was then possible to sort the EYFP positive cells by fluorescence-activated cell sorting

(FACS), which was performed by Dr Guglielmo Rosignoli, Barts Cancer Institute, Queen Mary, University of London, London, UK.

Cohorts of *kras*^{G12D} mice (n=12) were treated or untreated with DAPT and the EYFP positive cells were isolated by FACS and analysed for cytokine gene expression levels (Figure 6.5). Expression of mutated *kras* was confirmed by PCR on the EYFP positive sorted cells (unpublished data from Dr Thorsten Hagemann's group, Barts Cancer Institute, Queen Mary, University of London, London, UK).

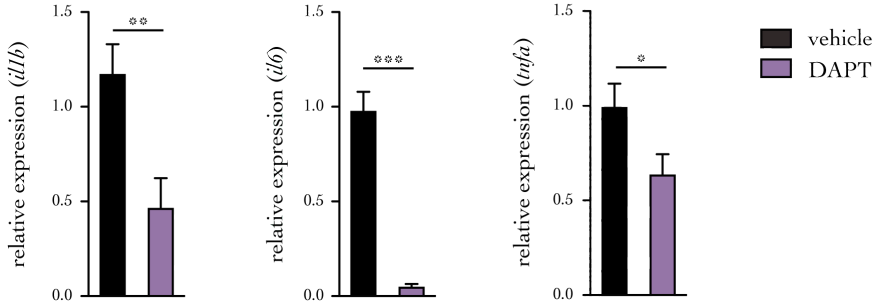

Figure 6.5: Cytokine gene expression levels upon DAPT treatment in *kras*^{G12D} mice

Relative mRNA expression of *il1b*, *il6* and *tnfa* in FACS sorted EYFP positive cells from PanIN bearing *kras*^{G12D} mice treated or untreated for one week with DAPT (100 mg/kg/day). Data are shown as mean + SD of duplicate experiments, *p<0.05, **p<0.01, ***p<0.001, n=12.

mRNA level analysis of the sorted cells showed a significant reduction in *il1b, il6* and *tnfa* gene expression levels in the pancreases of PanIN bearing *kras*^{G12D} mice treated with DAPT. This is in agreement with the protein data from the cytokine and chemokine array (Figure 6.4) and confirms the capacity of a Notch inhibitor to reduce cytokine and chemokine expression, mediated by *pparg* expression, in pre-malignant pancreatic epithelial cells derived from *kras*^{G12D} mice.

6.4 Effects of rosaglitazone treatment on the progression of pancreatic cancer

Using Notch inhibitors *in vivo* may have adverse effects, as this pathway is known to be involved in the development of many organs and at different stages (Bolos *et al.,* 2007; Roy *et al.,* 2007). Rather than inhibiting this pathway to restore *pparg* expression, PPAR-γ ligands, known to have anti-inflammatory properties (see section 6.1), can be used to re-activate anti-inflammatory reactions.

Rosiglitazone, a TZD compound, has been approved for the treatment of type II diabetes mellitus in humans. This non-insulin-dependent diabetes is characterised by high levels of glucose in the blood due to insulin resistance. This hormone is produced by the β-cells of the pancreas in large quantities and fat and muscle cells are not sensitive to this hormone, reducing their glucose uptake. These TZD agents reduce insulin resistance (Berger and Moller 2002; Berger *et al.,* 2005; Kota *et al.,* 2005b; Michalik *et al.,* 2006). In addition, these PPAR-γ agonists also have anti-inflammatory properties with effects on different models of inflammatory diseases such as colitis or pancreatitis (Cuzzocrea *et al.,* 2004; Ivashchenko *et al.,* 2007; Plutzky 2003; Straus *et al.,* 2000; Straus and Glass 2007).

The effects of rosiglitazone on PanIN development and pancreatic cancer progression were evaluated *in vivo* using the *kras*^{G12D} mice. A cohort of 40 *kras*^{G12D} mice was monitored for nearly two years while being treated with 3 mg/kg/day of rosiglitazone, which was added to their daily diet (Appendix F). Mice were sacrificed when they developed any signs of distress or reached the UK Home Office limits. For each mouse, tumour incidence and histology grade were evaluated, but also the sites of metastasis (liver or lung), the presence of peritoneal disease, ascites, skin

lesions (such as papilloma) and biliary obstruction. The body weight of the mice was monitored weekly over a period of 20 weeks and no difference was found between treated and untreated groups (Figure 6.6).

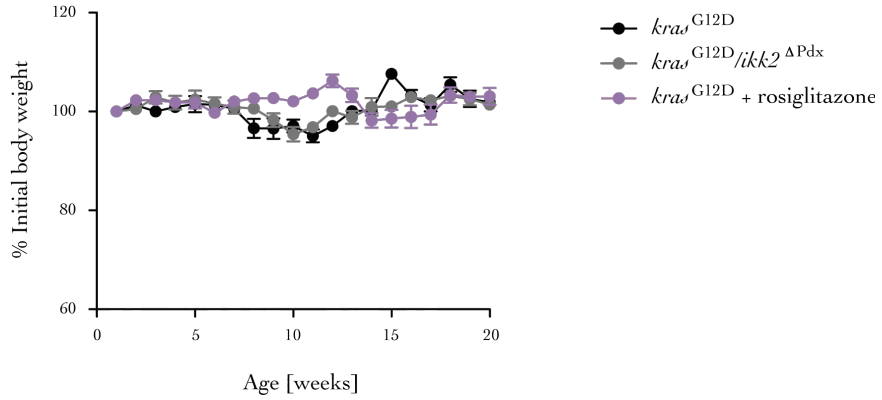

Figure 6.6: Body weight monitoring upon rosiglitazone treatment

The percentage of the initial body weight was assessed weekly for *kras*, *kras/ikk2*, *kras*^{G12D} and *kras*^{G12D}*/ikk2*$^{\Delta Pdx}$ mice. Data are shown as mean ± SD, n = 10.

As explained previously (see section 3.4.3), the proportion of the pancreas occupied by PanIN lesions and their stage were histologically assessed in *kras*^{G12D} treated or left untreated with rosiglitazone (Figure 6.7). PanIN progression was significantly delayed in rosiglitazone treated *kras*^{G12D} mice compared with the untreated controls ($p<0.01$, n=12).

This PPAR-γ agonist appears to be sufficient to reduce PanIN progression and development when the anti-inflammatory responses associated with the *pparg* gene expression are activated.

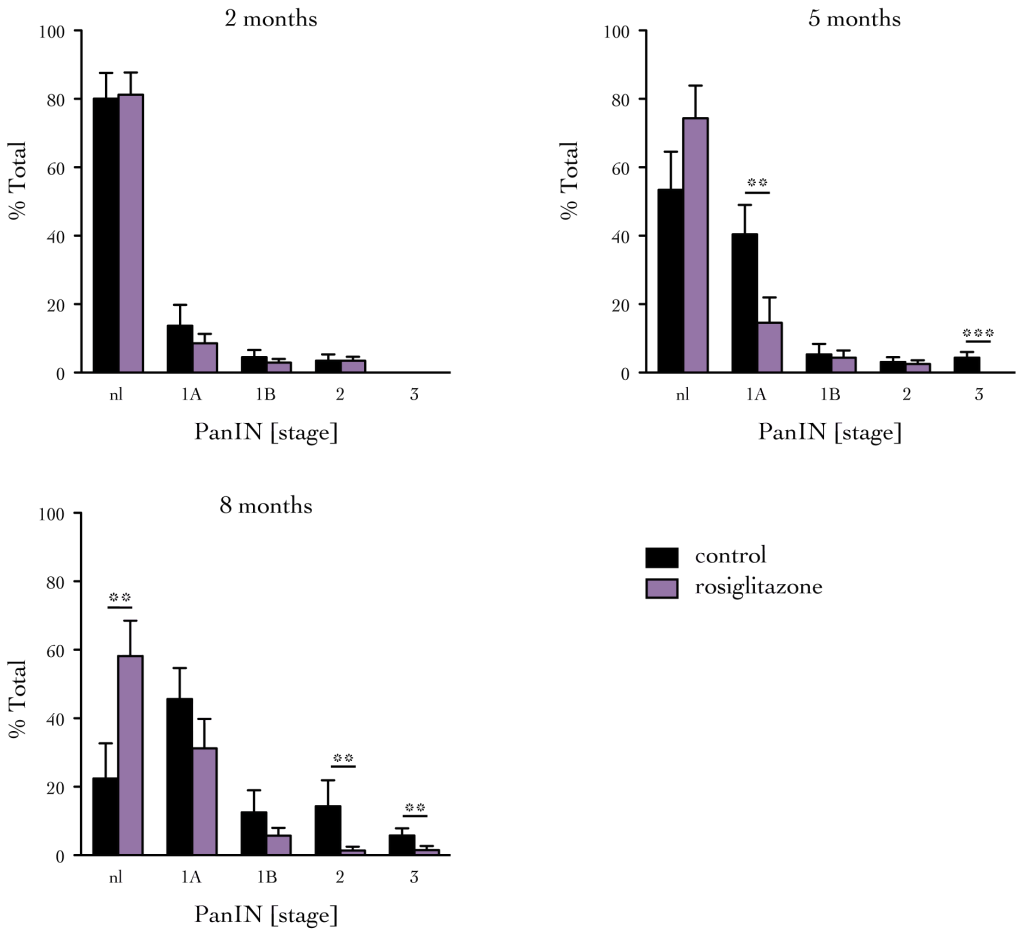

Figure 6.7: Proportion of the pancreas occupied by PanIN lesions

Quantification of the proportion of the pancreas occupied by normal tissue (nl, no lesion) and PanIN lesions in *kras*^{G12D} mice treated with rosiglitazone (3 mg/kg/day) compared with untreated controls. Frequency and grade of the lesions were assessed at 2, 5 and 8 months of age. Data are shown as mean + SD, **p<0.01, ***p<0.001, n=12.

Tumour incidence and histology grade were also evaluated in the *kras*^{G12D} mice treated with rosiglitazone and compared with the previous data from *kras*^{G12D} and *kras*^{G12D}*/ikk2*$^{\Delta Pdx}$ mice (Figure 6.8).

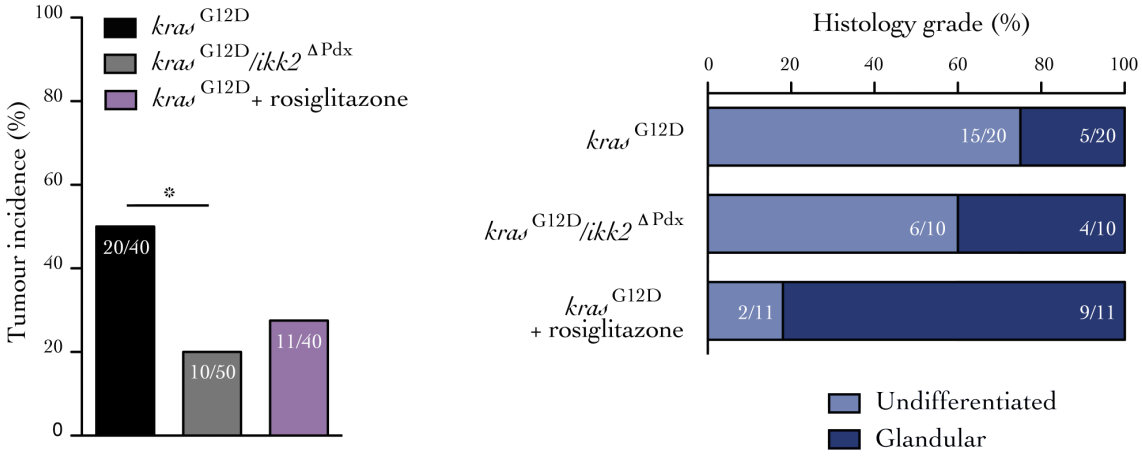

Figure 6.8: Tumour incidence and histology grade

Tumour incidence and histology grade in rosiglitazone-treated *kras*^{G12D} (n=40) mice (3 mg/kg/day) compared with untreated *kras*^{G12D} (n=40) and *kras*^{G12D}/*ikk2*$^{\Delta Pdx}$ (n=50) mice, *p<0.05. Respectively, 50 % and 20 % of *kras*^{G12D} and of *kras*^{G12D}/*ikk2*$^{\Delta Pdx}$ mice developed PDAC, while tumour incidence was reduced to 27.5 % in *kras*^{G12D} (n=40) mice treated with rosiglitazone. The number of mice presenting undifferentiated tumours was also reduced after treatment with rosiglitazone.

Figure 6.8 shows that *kras*^{G12D} and *kras*^{G12D}/*ikk2*$^{\Delta Pdx}$ mice presented a 50 % and 20 % tumour incidence respectively. After treatment with rosiglitazone, tumour incidence in *kras*^{G12D} mice was reduced compared with the untreated *kras*^{G12D} mice (11/40 and 20/40 respectively). However, this reduction was not significant as opposed to the difference between *kras*^{G12D} and *kras*^{G12D}/*ikk2*$^{\Delta Pdx}$ mice. Histology grade also showed a reduction in the number of PDAC presented with undifferentiated tumours, confirming the delay in PanIN progression. In addition, the frequency of liver metastasis was also reduced in *kras*^{G12D} mice treated with rosiglitazone (63.6 %) compared with the untreated *kras*^{G12D} mice (75 %) (Figure 6.9). As previously observed and discussed between *kras*^{G12D} and *kras*^{G12D}/*ikk2*$^{\Delta Pdx}$ mice, no significant effects on histological grade and metastatic potential were observed.

Deletion of *ikk2* is sufficient to significantly delay PDAC development and similar effects can be achieved by treating the mice with rosiglitazone, a PPAR-γ agonist.

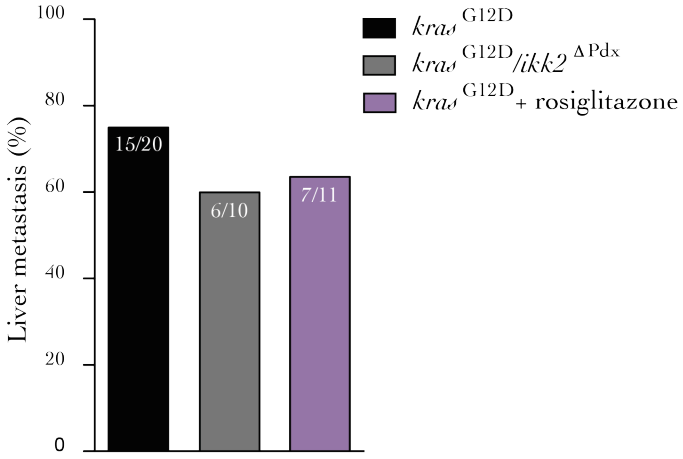

Figure 6.9: Liver metastasis

Liver metastasis in rosiglitazone-treated *kras*^{G12D} (n=40) mice (3 mg/kg/day) was reduced to a similar level than *kras*^{G12D}/*ikk2*$^{\Delta Pdx}$ (n=50) mice, compared with untreated *kras*^{G12D} (n=40).

To investigate whether rosiglitazone affects the infiltration of inflammatory cells at the tumour site, the pancreases of *kras*^{G12D} mice were analysed by flow cytometry for infiltrating macrophages, which are typically present in the pancreas of diseased animals (Figure 6.10).

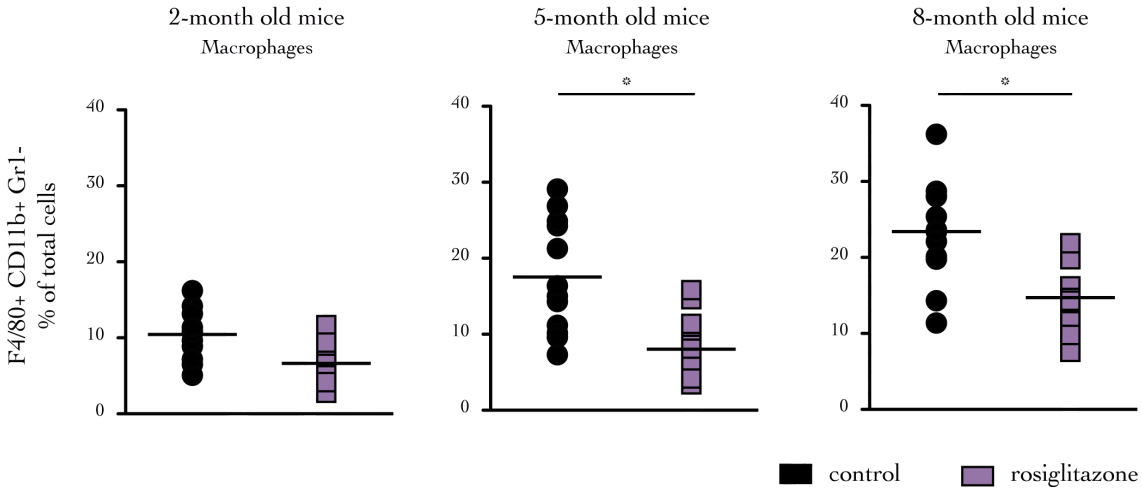

Figure 6.10: Macrophage infiltrate

Percentage of F4/80^{+}CD11b^{+}Gr1^{-} cells in the pancreases of 2, 5 and 8-month old *kras*^{G12D} mice treated with rosiglitazone (3 mg/kg/day) or untreated measured by flow cytometry. Each individual data point represents an individual mouse and mean values are depicted by horizontal lines, *p<0.05, n=10.

Previous data show that macrophages and neutrophils do not infiltrate the pancreases of *kras*^{G12D}/*ikk2*$^{\Delta Pdx}$ mice (see section 3.4.5.1), and this is consistent with a lower inflamed state. In a similar manner, as shown in Figure 6.10, there was a reduction in the frequency of macrophages infiltrating the pancreases of rosiglitazone treated animals. This reduction is significant at 5 and 8 months of age. These data further support an anti-inflammatory effect of rosiglitazone treatment on *kras*^{G12D} mice.

6.5 Discussion and conclusion

To summarise, the data presented in this chapter show that pharmacological inhibition of the Notch or the NF-κB signalling pathways can inhibit *hes1* gene expression upon treatment with two different Notch signalling inhibitors (DAPT and L685458) and two NF-κB signalling pathways inhibitors (Bay11-7082 and anti-TNF-α antibody). In addition, the treatment of $kras^{G12D}$ mice with DAPT has an anti-inflammatory effect in their pancreases by reducing cytokine and chemokine production (Figure 6.4).

Activation of the PPAR-γ anti-inflammatory responses by treating the $kras^{G12D}$ mice with rosiglitazone, similar to the effects of DAPT treatment, reduces the immune infiltrate into the pancreas and significantly delays PanIN progression. It would be interesting to evaluate cytokine and chemokine expression and production in the pancreas of rosiglitazone treated mice to confirm the ability of this PPAR-γ ligand to reduce pancreatic inflammation.

One limitation of the route of administration chosen for rosiglitazone is that its incorporation into the rodent's diet prevents monitoring of the exact amount of drug absorbed by the animals. However, daily administration of a natural PPAR-γ ligand, such as PGJ2, by oral gavage or intravenous injections over two years would not have been feasible and is also not authorised under Home Office regulations. In addition, PGJ2 cannot be incorporated into the rodent's diet. The use of rosiglitazone, a synthetic PPAR-γ ligand, added to the daily diet of the mice was then favoured. Rosiglitazone is an anti-diabetic drug and can therefore modify the mouse's daily food absorption. However, no significant change in the weight of the animals was observed, suggesting that this compound does not influence their usual diet.

Another member of the TZD class compounds (pioglitazone or troglitazone) could have potentially been used.

Natural and synthetic PPAR-γ ligands have proven to be effective in reducing the inflammation process in mouse models of caerulein-induced acute pancreatitis (Ivashchenko *et al.,* 2007; Konturek *et al.,* 2005; Rollins *et al.,* 2006; Weber and Adler 2001) but also in chronic pancreatitis models (Shimizu *et al.,* 2002). This attenuation of inflammation is associated with suppression of NF-κB activation (Wan *et al.,* 2008). The effects of rosiglitazone on the delayed PanIN progression observed in the *kras*^{G12D} treated mice may therefore be due to a suppression of the NF-κB signalling pathway.

Two TZD compounds (rosiglitazone and pioglitazone) have been shown to inhibit human pancreatic cancer cell invasiveness (Galli *et al.,* 2004) and growth *in vitro* (Elnemr *et al.,* 2000). The natural ligand PGJ2 is also able to inhibit the invasion of human pancreatic cancer cells (Sawai *et al.,* 2006). The first anti-tumour effects of activating PPAR-γ with small molecules *in vivo* have been observed on orthotopic xenograft models with human colorectal tumour cell lines and thyroid tumour cell lines in nude mice (Shimazaki *et al.,* 2008). Additional orthotopic xenograft models inoculating human pancreatic cancer cell lines into nude mice showed that rosiglitazone can suppress tumour progression by inhibiting angiogenesis (Dong *et al.,* 2009). However, little has previously been described regarding a role for PPAR-γ agonists in the context of spontaneous genetic mouse models of cancer, such as *kras*^{G12D} mice. In addition, orthotopic xenograft models do not allow the study of the role of the tumour microenvironment in tumour progression and development, which is not the case in genetic mouse models (Richmond and Su 2008).

Nevertheless, the hypothesis tested whether an anti-inflammatory response can inhibit PanIN progression and PDAC development was verified *in vivo* upon rosiglitazone treatment.

In addition to anti-inflammatory properties, rosiglitazone is also an anti-diabetic drug which reduces glucose concentration in the blood (Kahn *et al.,* 2006). Metformin, another glucose lowering drug, has been studied in patients suffering from type II diabetes and reduces the risk of developing pancreatic cancer by 62 % (Li and Abbruzzese 2010). Due to the increased risk for diabetic patients to develop pancreatic cancer (see section 1.2.3) and considering the clinical data obtained upon metformin treatment, a prophylactic treatment with rosiglitazone in a specific subset of diabetic patients may provide a protective effect against pancreatic cancer.

CHAPTER SEVEN: CONCLUSIONS AND FUTURE PLANS

Many cancers are driven by oncogenic expression of *RAS*, but this pathway represents a difficult molecular target as it is also expressed in normal cells. Studies reveal that drug combinations targeting additional molecules which are also abnormally expressed by malignant cells or by the surrounding microenvironment might be an alternative (De Raedt *et al.,* 2011). Oncogenic *KRAS* has a tumour-promoting role through activation of the NF-κB signalling pathway (see section 1.3.2.2) but it has also been recently demonstrated that it contributes to the cellular metabolism switch observed in cancer cells (Gaglio *et al.,* 2011). Tumours use glycolysis to produce ATP rather than the classic oxidative phophorylation metabolism, even in the presence of oxygen. This process, also known as the "Warburg effect", contributes to cancer progression and has been described as an emerging hallmark of cancer (Hanahan and Weinberg 2011; Warburg 1956).

KRAS mutations are characteristic of human pancreatic cancer, which remains a cancer with one of the poorest survival rates due to late diagnosis, a high frequency of relapse in curative setting of surgery and ineffective therapies. Great efforts are being carried out in order to further understand the mechanisms involved during its development. For this, genetic mouse models that mimic the human disease have been useful in understanding the mechanisms during pancreatic carcinogenesis (Hingorani *et al.,* 2003; Ijichi 2011). In this thesis, two variants of pancreatic cancer mouse models were generated: *kraɔ*^{G12D}/*ikk2*$^{\Delta Pdx}$ and *kraɔ*^{G12D}/*tnfa*$^{\Delta Pdx}$ mice. These mice were used to study the role of the TNF-α/IKK2 signalling pathway on the early stages of *kraɔ*-driven pancreatic carcinogenesis. The development of PanIN lesions is delayed in young *kraɔ*^{G12D}/*tnfa*$^{\Delta Pdx}$ mice compared with *kraɔ*^{G12D} mice and contrasts with the profound reduction in the frequency of the high-grade PanIN lesions observed in *kraɔ*^{G12D}/*ikk2*$^{\Delta Pdx}$ mice compared with *kraɔ*^{G12D} mice (Figure 3.5 and Figure

3.10). This demonstrates that genetic inactivation of *ikk2* delays the progression of malignant epithelial cell lesions towards higher-grade PanIN lesions and PDAC.

The role of IKK2 in carcinogenesis is context- and cell type-dependent. This kinase is required for the development of lung adenocarcinoma, induced by oncogenic *kras* and associated with activation of the NF-κB signalling pathway (Basseres *et al.,* 2010; Meylan *et al.,* 2009). In a spontaneous mouse model of skin carcinogenesis, characterised by mutant *kras* expression and inactivation of a tumour suppressor gene, genetic deletion of *ikk2* impairs the development of melanoma (Yang *et al.,* 2010). In the setting of inflammation-induced carcinogenesis (colitis-associated cancer), *ikk2* deletion reduces tumour growth and incidence (Greten *et al.,* 2004). Mice with a genetic inactivation of *ikk2* in hepatocytes alone are more susceptible to chemically-induced hepatocarcinogenesis, suggesting a protective role for this kinase in the setting of liver carcinogenesis (Maeda *et al.,* 2005). However, in the same study, it has been shown that deletion of *ikk2* in hepatocytes and macrophages can reduce chemically-induced hepatocarcinogenesis (Maeda *et al.,* 2005).

In the context of cancer-associated inflammation, activation of inflammatory signalling pathways can have two origins: inflammatory conditions (intrinsic pathway) or genetic alterations such as oncogene activation (extrinsic pathway) (see section 1.1.3) (Mantovani *et al.,* 2008). The intrinsic network of inflammatory mediators can act in an autocrine and/or paracrine manner on the malignant cells and/or on the surrounding stroma, to further enhance the activation of these pathways and to activate and stimulate different cellular processes, such as cell proliferation and migration (Grivennikov *et al.,* 2010). The main inflammatory signalling pathways involved are the NF-κB pathway, activated by TNF-α or IL-1

cytokines and inducing the secretion of mainly TNF-α and IL-6 and the STAT3 signalling pathway, activated by IL-6 (Grivennikov and Karin 2010; Naugler and Karin 2008). This inflammatory microenvironment can contribute to tumour initiation and progression. Cooperation between pro-inflammatory cytokines, transcription factors and oncogenic mutations are well described in the literature (see section 1.3.2.2). Oncogenic *ras* induces the secretion of IL-6, a highly inflammatory and angiogenic cytokine, which when inhibited contributes to slowing down the progression of cancers associated with *ras* mutations (Ancrile *et al.,* 2007). The activation of another oncoprotein, Src, which contributes to cellular transformation of normal breast cells, can induce an inflammatory response in breast cancer cells characterised by IL-6 production (Iliopoulos *et al.,* 2009). The IL-6 signalling pathway is a potential link between inflammation and cancer (Naugler and Karin 2008).

The TNF-α cytokine in the tumour microenvironment can be secreted by the tumour infiltrating immune cells or by the malignant cells. In the $kras^{G12D}$ mouse model of pancreatic cancer, the immune reaction is well described and shows that inflammatory immune cells, mainly macrophages and neutrophils, progressively infiltrate the pancreas as the disease progresses (Clark *et al.,* 2007). The results presented in Figure 3.16 are in agreement with this study and the $kras^{G12D}/ikk2^{\Delta Pdx}$ mice generated present a reduction of the infiltrating immune cells (macrophages and neutrophils) at the tumour site. Pancreatic cells with a genetic deletion for *ikk2* have an impaired NF-κB signalling, which normally controls the production of inflammatory mediators involved in the recruitment of immune cells (Grivennikov *et al.,* 2010). In addition, the delayed PanIN progression observed in $kras^{G12D}/tnfa^{\Delta Pdx}$ mice is suggested to be due to the TNF-α secretion by the recruited immune cells

(Figure 3.18). To further assess the impact of inhibiting the TNF-α/IKK2 pathway, it would have been interesting to determine the profile of the inflammatory cytokines and chemokines within the pancreases of the different mouse models generated. MSD assays or cytokine array technologies could have been used and considering the data summarised in this thesis, a reduction in the inflammatory cytokines such as TNF-α and IL-6 in the pancreases of the *kraʂ*^{G12D}*/ikk2*$^{\Delta Pdx}$ mice should be expected.

PanIN and PDAC cell lines generated from *kraʂ*^{G12D} mice constitutively secrete TNF-α, showing NF-κB activation upon oncogenic *kraʂ* expression. Constitutive secretion of TNF-α by ovarian epithelial cancer cells has previously been shown to sustain a network of inflammatory molecules and to promote invasion and neovascularisation of ovarian tumours *in vivo* (Balkwill 2009; Kulbe *et al.,* 2007; Kulbe *et al.,* 2011). A similar effect is possibly occurring in the pancreatic tumour microenvironment. In the early stages of the carcinogenic process, TNF-α secreted by the pre-malignant cells is critical for their growth, while at later stages, an influx of immune cells constitutes the major source of this cytokine. This is supported by the delayed pattern of pancreatic cancer progression observed in *kraʂ*^{G12D}*/tnfa*$^{\Delta Pdx}$ mice, where the absence of TNF-α production by the pre-malignant epithelial cells is compensated once the immune cells secreting this cytokine infiltrate the pancreas, in response to other cytokines such as CCL2 and CSF1. However, in *kraʂ*^{G12D}*/ikk2*$^{\Delta Pdx}$ mice, this compensation does not occur, as the recruitment of inflammatory cells is impaired (see Figure 3.16).

In *kraʂ*^{G12D}*/ikk2*$^{\Delta Pdx}$ mice, genetic deletion of *ikk2* correlates with a decrease in the expression of the classical Notch target genes *heʂ1* and *hey1* (Figure 4.1 and Figure 4.2). This observation is in agreement with the scientific literature, which shows that

Notch signalling is reactivated during pancreatic carcinogenesis and which suggests oncogenic properties in this context. In *kras*-mutant pancreatic carcinogenesis, activation of Notch signalling can cooperate with oncogenic *kras* promoting faster PanIN lesions formation (De La *et al.,* 2008). In addition to mutated *kras*, when an inflammatory environment is provided following chemically-induced pancreatitis, the development of PanIN lesions is accelerated (Carriere *et al.,* 2007; Guerra *et al.,* 2007). In response to inflammatory insult, the Notch and Hedgehog signalling pathways, which are normally expressed during pancreatic development, are transiently reactivated for pancreatic regeneration (Fendrich *et al.,* 2008; Jensen *et al.,* 2005; Siveke *et al.,* 2008). However, when oncogenic *kras* is expressed their reactivation is not transient but persists throughout time and during PanIN development (Morris *et al.,* 2010a). A separate line of evidence shows that even though Notch signalling is overexpressed in pancreatic carcinogenesis, Notch2 inhibition, as opposed to that of Notch1, can stop PanIN progression, therefore suggesting a tumour suppressive role (Mazur *et al.,* 2010a).

Stimulation of pre-malignant pancreatic epithelial cells with TNF-α *in vitro* induces an upregulation of *hes1* and *hey1* (Figure 4.4 and Figure 4.5). This upregulation is independent of *de novo* protein synthesis, requires canonical Notch signalling and is dependent of IKK2 (see sections 4.2 and 4.3). These data suggest that activation of NF-κB signalling can synergise with basal Notch signals to induce maximal expression of the Notch target genes during pancreatic carcinogenesis.

Activation of the NF-κB signalling pathway upon Notch signalling is well described in various types of cancer: constitutive activation of Notch results in NF-κB pathway activation in T cell leukaemia (Vilimas *et al.,* 2007) or cervical cancer (Song *et al.,*

2008). Another group has demonstrated that the Notch/HES1 signalling pathway sustains the NF-κB pathway activation by repressing the deubiquitinase CYLD, a negative IKK complex regulator (Espinosa *et al.,* 2010). However, interactions by NF-κB to Notch signalling are less well described and the results described in this thesis suggest a novel cooperation between these two signalling pathways in the context of *kras*-driven pancreatic carcinogenesis.

The effect of a cancer-related inflammatory microenvironment on the activation of the Notch signalling pathway has also recently been demonstrated in human high-grade serous ovarian cancer. A "TNF network", including TNF-α, CXCL12 and IL-6, produced by ovarian cancer cells has been described to have different paracrine actions contributing to tumour growth. Inhibition of these cytokines is associated with a reduction in Notch signalling (Kulbe *et al.,* 2011). This work reinforces the data presented in this thesis, showing that inflammatory and developmental signalling pathways can cooperate during carcinogenesis.

The effects of stimulating malignant epithelial cells with rTNF-α *in vitro* on the Notch target genes' expression occurs at the transcription level: IKK2 can mediate the phosphorylation of histone H3 (Figure 4.17 and Figure 4.18), which is a modification often associated with transcriptional activation (Anest *et al.,* 2003; Yamamoto *et al.,* 2003). Kinases, such as IKK1, are able to translocate to the nucleus to phosphorylate histone proteins, contributing to transcriptional regulation (Anest *et al.,* 2003; Baek 2011). IKK2 may act in a similar manner. However, IKK2 nuclear location was not demonstrated in this thesis and could have been shown by performing immunofluorescent staining or cytosolic and nuclear protein extraction in pre-malignant pancreatic epithelial cells stimulated with rTNF-α. To explain a potential

IKK2 nuclear location, it would be interesting to find out whether this kinase possesses an unknown DNA-binding site or whether it can interact with NICD, which will then allow its nuclear translocation. However, the experiments performed so far have not confirmed a physical interaction between these two proteins. This needs to be repeated in the future as it was only performed once and sample preparation for mass spectrometry analysis should be optimised. These additional experiments would help to provide supplementary information regarding a complete and more detailed mechanism to explain the transcriptional activation of the *hes1* gene locus upon TNF-α stimulation.

Another study shows that the NEMO-like kinase (NLK) negatively regulates the Notch signalling pathway by interacting and phosphorylating NICD. This phosphorylation impairs the binding of NICD to the coactivators required for its role in transcriptional activation. However, this mechanism has been shown in neurogenesis in zebrafish embryos (Ishitani *et al.,* 2010). This study shows how NICD post-translational modifications, such as phopshorylation, are important in regulating the activity of the pathway, as it is the case with acetylation (Guarani *et al.,* 2011). Considering the existence of such phenomena, it would be interesting to investigate further whether IKK2 can interact and modify NICD in the context of *kras*-driven pancreatic cancer.

The crosstalk between NF-κB and Notch signalling is mediated by IKK2 and HES1, which in turn can repress the expression of the anti-inflammatory nuclear receptor *pparg* by binding its promoter region (Figure 5.2, Figure 5.6 and Figure 5.7). PPAR-γ is a transcriptional repressor, which binds to DNA to repress the transcription of inflammatory genes. This repression has been demonstrated to be an important

mechanism by which cells can regulate inflammatory responses and homeostasis (Glass and Saijo 2010). The cooperation between activated NF-κB and Notch signalling and repression of the *pparg* gene provides an inflammatory context in which expression of inflammatory genes is sustained. This leads to a constitutive production of inflammatory mediators and chemokines by the transformed cells, retaining them in an inflammatory state, which favours pancreatic cancer progression.

Pharmacological inhibition of the Notch pathway in *kras*^{G12D} mice using DAPT, a γ-secretase inhibitor, results in a reduction of *hes1* gene expression (Figure 6.2), an attenuated expression of genes coding for different cytokines (Figure 6.3 and Figure 6.5) and a reduction in cytokine production in the pancreases of the treated mice (Figure 6.4). Inhibition of the Notch pathway has already been shown to significantly attenuate the development of PanIN lesions towards PDAC (Plentz *et al.,* 2009). To corroborate this, additional gene expression analysis should be performed to confirm that Notch inhibition could also restore *pparg* gene expression, which would partially explain the reduction in cytokine production.

Restoring an anti-inflammatory profile in the tumour microenvironment by re-activating the PPAR-γ receptor can reduce the frequency of the PanIN lesions and their progression into invasive carcinoma (Figure 6.7). This is associated with a reduction of the macrophage infiltrate (Figure 6.10). Such effects were observed after using rosiglitazone to treat *kras*^{G12D} mice. This PPAR-γ ligand, like most synthetic ligands, induces conformational changes to the receptor allowing it to effectively repress gene expression (Zoete *et al.,* 2007). In the *kras*^{G12D} mice, *pparg* expression is repressed (Figure 5.1), but this nuclear receptor is already present prior to cell transformation, providing a basal level of this protein in the nucleus.

Activating this receptor with the TZD agonist may be sufficient to inhibit the expression of inflammatory genes.

PPAR-γ ligands, and rosiglitazone in particular, have an anti-inflammatory effect in many mouse models of acute and chronic inflammation, such as inflammatory bowel disease (Dubuquoy *et al.,* 2006), arthritis (Cuzzocrea *et al.,* 2003; Shiojiri *et al.,* 2002) or caerulein-induced pancreatitis (Cuzzocrea *et al.,* 2004; Ivashchenko *et al.,* 2007). They appear to reduce chemokine expression in LPS-induced macrophages and to impair lymphocyte recruitment to the site of inflammation (Straus and Glass 2007).

The PPAR-γ nuclear receptor does not only play a role in inflammation but it can also affect adipocyte differentiation and glucose metabolism (Kota *et al.,* 2005a). TZD drugs are originally used for the treatment of type II diabetes as they have an insulin-sensitising action (Nosjean and Boutin 2002). Moreover, other glucose-lowering drugs, such as metformin, are used to treat patients with type II diabetes mellitus and also reduce the risk for these individuals to develop cancer (Currie *et al.,* 2009; Evans *et al.,* 2005; Phielix *et al.,* 2011). The effects of rosiglitazone on the prevention of cancer incidence are not significant and additional clinical studies need to be performed, as so far most of the trials have been conducted upon metformin treatment (Monami *et al.,* 2008).

Data in this thesis suggest that a TNF-α/HES1 mechanism of *pparg* inhibition operates in pre-malignant pancreatic epithelial cells, therefore sustaining an inflamed state which contributes to the formation of PanIN lesions and to the progression of pancreatic cancer (Figure 7.1).

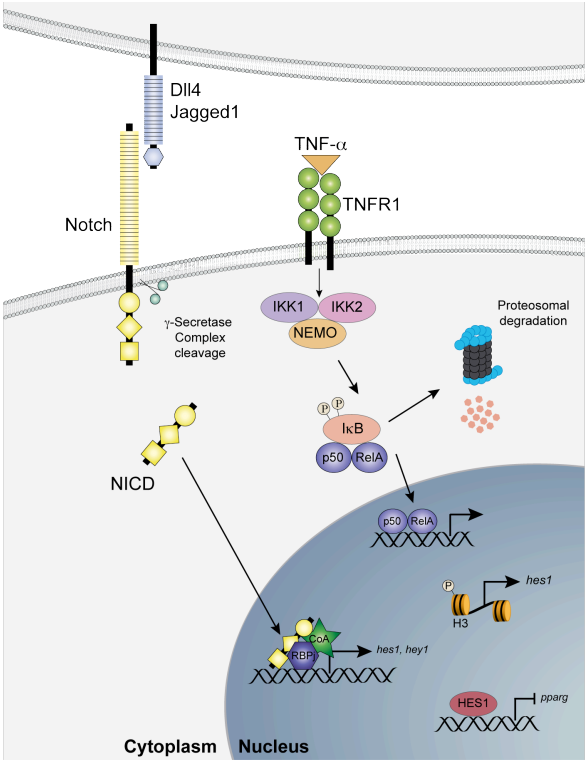

Figure 7.1: TNF-α/IKK2 is suggested to cooperate with Notch to sustain an inflammatory environment favouring pancreatic carcinogenesis

In the *kras*^{G12D} genetic mouse model of pancreatic carcinogenesis, activation of IKK2 upon TNF-α stimulation induces the expression of the classical Notch target genes. This overexpression is mediated by phosphorylation of the H3 histone at the *hes1* locus. HES1 represses *pparg* gene expression, therefore allowing expression of inflammatory genes. This inflamed microenvironment is sustained and contributes to pancreatic cancer progression.

The use of PPAR-γ ligands, such as rosiglitazone, can potentially provide a protective effect and/or reduce pancreatic carcinogenesis. However, in order to effectively use such compounds in human patients, it is important to be able to clearly identify the patients presenting higher risk of developing pancreatic cancer and to improve early methods of diagnosis.

The data presented in this thesis highlight the involvement of inflammatory signalling pathways as well as the role of the tumour microenvironment in pancreatic cancer development, revealing potential new key molecular targets to assist current treatments.

REFERENCES

Adamek, H. E., J. Albert, H. Breer, M. Weitz, D. Schilling and J. F. Riemann (2000). "Pancreatic cancer detection with magnetic resonance cholangiopancreatography and endoscopic retrograde cholangiopancreatography: a prospective controlled study." Lancet **356**(9225): 190-193.

Aggarwal, B. B., S. Shishodia, S. K. Sandur, M. K. Pandey and G. Sethi (2006). "Inflammation and cancer: how hot is the link?" Biochemical pharmacology **72**(11): 1605-1621.

Aguirre, A. J., N. Bardeesy, M. Sinha, L. Lopez, D. A. Tuveson, J. Horner, M. S. Redston and R. A. DePinho (2003). "Activated Kras and Ink4a/Arf deficiency cooperate to produce metastatic pancreatic ductal adenocarcinoma." Genes Dev **17**(24): 3112-3126.

Akiyama, H., J. E. Kim, K. Nakashima, G. Balmes, N. Iwai, J. M. Deng, Z. Zhang, J. F. Martin, R. R. Behringer, T. Nakamura and B. de Crombrugghe (2005). "Osteo-chondroprogenitor cells are derived from Sox9 expressing precursors." Proceedings of the National Academy of Sciences of the United States of America **102**(41): 14665-14670.

Albini, A. and M. B. Sporn (2007). "The tumour microenvironment as a target for chemoprevention." Nature reviews. Cancer **7**(2): 139-147.

Alcamo, E., J. P. Mizgerd, B. H. Horwitz, R. Bronson, A. A. Beg, M. Scott, C. M. Doerschuk, R. O. Hynes and D. Baltimore (2001). "Targeted mutation of TNF receptor I rescues the RelA-deficient mouse and reveals a critical role for NF-kappa B in leukocyte recruitment." Journal of immunology **167**(3): 1592-1600.

Allenspach, E. J., I. Maillard, J. C. Aster and W. S. Pear (2002). "Notch signaling in cancer." Cancer biology & therapy **1**(5): 466-476.

Amikura, K., M. Kobari and S. Matsuno (1995). "The time of occurrence of liver metastasis in carcinoma of the pancreas." International journal of pancreatology : official journal of the International Association of Pancreatology **17**(2): 139-146.

Ancrile, B., K. H. Lim and C. M. Counter (2007). "Oncogenic Ras-induced secretion of IL6 is required for tumorigenesis." Genes Dev **21**(14): 1714-1719.

Anest, V., J. L. Hanson, P. C. Cogswell, K. A. Steinbrecher, B. D. Strahl and A. S. Baldwin (2003). "A nucleosomal function for IkappaB kinase-alpha in NF-kappaB-dependent gene expression." Nature **423**(6940): 659-663.

Angeli, F., G. Koumakis, M. C. Chen, S. Kumar and J. G. Delinassios (2009). "Role of Stromal Fibroblasts in Cancer: Promoting or Impeding?" Tumour Biol **30**(3): 109-120.

Apelqvist, A., H. Li, L. Sommer, P. Beatus, D. J. Anderson, T. Honjo, M. Hrabe de Angelis, U. Lendahl and H. Edlund (1999). "Notch signalling controls pancreatic cell differentiation." Nature **400**(6747): 877-881.

Apte, M. V., S. Park, P. A. Phillips, N. Santucci, D. Goldstein, R. K. Kumar, G. A. Ramm, M. Buchler, H. Friess, J. A. McCarroll, G. Keogh, N. Merrett, R. Pirola and

J. S. Wilson (2004). "Desmoplastic reaction in pancreatic cancer: role of pancreatic stellate cells." Pancreas **29**(3): 179-187.

Apte, R. N., Y. Krelin, X. Song, S. Dotan, E. Recih, M. Elkabets, Y. Carmi, T. Dvorkin, R. M. White, L. Gayvoronsky, S. Segal and E. Voronov (2006). "Effects of micro-environment- and malignant cell-derived interleukin-1 in carcinogenesis, tumour invasiveness and tumour-host interactions." European journal of cancer **42**(6): 751-759.

Arlt, A., A. Gehrz, S. Muerkoster, J. Vorndamm, M. L. Kruse, U. R. Folsch and H. Schafer (2003). "Role of NF-kappaB and Akt/PI3K in the resistance of pancreatic carcinoma cell lines against gemcitabine-induced cell death." Oncogene **22**(21): 3243-3251.

Arlt, A., J. Vorndamm, M. Breitenbroich, U. R. Folsch, H. Kalthoff, W. E. Schmidt and H. Schafer (2001). "Inhibition of NF-kappaB sensitizes human pancreatic carcinoma cells to apoptosis induced by etoposide (VP16) or doxorubicin." Oncogene **20**(7): 859-868.

Arlt, A., J. Vorndamm, S. Muerkoster, H. Yu, W. E. Schmidt, U. R. Folsch and H. Schafer (2002). "Autocrine production of interleukin 1beta confers constitutive nuclear factor kappaB activity and chemoresistance in pancreatic carcinoma cell lines." Cancer research **62**(3): 910-916.

Artavanis-Tsakonas, S., M. D. Rand and R. J. Lake (1999). "Notch signaling: cell fate control and signal integration in development." Science **284**(5415): 770-776.

Assmann, A., C. Hinault and R. N. Kulkarni (2009). "Growth factor control of pancreatic islet regeneration and function." Pediatric diabetes **10**(1): 14-32.

Baek, S. H. (2011). "When signaling kinases meet histones and histone modifiers in the nucleus." Mol Cell **42**(3): 274-284.

Bailey, J. M., B. J. Swanson, T. Hamada, J. P. Eggers, P. K. Singh, T. Caffery, M. M. Ouellette and M. A. Hollingsworth (2008). "Sonic hedgehog promotes desmoplasia in pancreatic cancer." Clin Cancer Res **14**(19): 5995-6004.

Balkwill, F. (2002). "Tumor necrosis factor or tumor promoting factor?" Cytokine & growth factor reviews **13**(2): 135-141.

Balkwill, F. (2006). "TNF-alpha in promotion and progression of cancer." Cancer Metastasis Rev **25**(3): 409-416.

Balkwill, F. (2009). "Tumour necrosis factor and cancer." Nature reviews. Cancer **9**(5): 361-371.

Balkwill, F., K. A. Charles and A. Mantovani (2005). "Smoldering and polarized inflammation in the initiation and promotion of malignant disease." Cancer Cell **7**(3): 211-217.

Balkwill, F. and A. Mantovani (2001). "Inflammation and cancer: back to Virchow?" Lancet **357**(9255): 539-545.

Balkwill, F. R., A. Lee, G. Aldam, E. Moodie, J. A. Thomas, J. Tavernier and W. Fiers (1986). "Human tumor xenografts treated with recombinant human tumor necrosis factor alone or in combination with interferons." Cancer research **46**(8): 3990-3993.

Bannister, A. J. and T. Kouzarides (2011). "Regulation of chromatin by histone modifications." Cell research **21**(3): 381-395.

Bao, Y., D. Spiegelman, R. Li, E. Giovannucci, C. S. Fuchs and D. S. Michaud (2010). "History of peptic ulcer disease and pancreatic cancer risk in men." Gastroenterology **138**(2): 541-549.

Bardeesy, N., K. H. Cheng, J. H. Berger, G. C. Chu, J. Pahler, P. Olson, A. F. Hezel, J. Horner, G. Y. Lauwers, D. Hanahan and R. A. DePinho (2006). "Smad4 is dispensable for normal pancreas development yet critical in progression and tumor biology of pancreas cancer." Genes & development **20**(22): 3130-3146.

Bardeesy, N. and R. A. DePinho (2002). "Pancreatic cancer biology and genetics." Nature reviews. Cancer **2**(12): 897-909.

Bash, J., W. X. Zong, S. Banga, A. Rivera, D. W. Ballard, Y. Ron and C. Gelinas (1999). "Rel/NF-kappaB can trigger the Notch signaling pathway by inducing the expression of Jagged1, a ligand for Notch receptors." EMBO J **18**(10): 2803-2811.

Basseres, D. S. and A. S. Baldwin (2006). "Nuclear factor-kappaB and inhibitor of kappaB kinase pathways in oncogenic initiation and progression." Oncogene **25**(51): 6817-6830.

Basseres, D. S., A. Ebbs, E. Levantini and A. S. Baldwin (2010). "Requirement of the NF-kappaB subunit p65/RelA for K-Ras-induced lung tumorigenesis." Cancer Res **70**(9): 3537-3546.

Bauer, U. M., S. Daujat, S. J. Nielsen, K. Nightingale and T. Kouzarides (2002). "Methylation at arginine 17 of histone H3 is linked to gene activation." EMBO reports **3**(1): 39-44.

Beatty, G. L., E. G. Chiorean, M. P. Fishman, B. Saboury, U. R. Teitelbaum, W. Sun, R. D. Huhn, W. Song, D. Li, L. L. Sharp, D. A. Torigian, P. J. O'Dwyer and R. H. Vonderheide (2011). "CD40 agonists alter tumor stroma and show efficacy against pancreatic carcinoma in mice and humans." Science **331**(6024): 1612-1616.

Beg, A. A., W. C. Sha, R. T. Bronson, S. Ghosh and D. Baltimore (1995). "Embryonic lethality and liver degeneration in mice lacking the RelA component of NF-kappa B." Nature **376**(6536): 167-170.

Ben-Neriah, Y. and M. Karin (2011). "Inflammation meets cancer, with NF-kappaB as the matchmaker." Nature immunology **12**(8): 715-723.

Berechid, B. E., G. Thinakaran, P. C. Wong, S. S. Sisodia and J. S. Nye (1999). "Lack of requirement for presenilin1 in Notch1 signaling." Curr Biol **9**(24): 1493-1496.

Berger, J. and D. E. Moller (2002). "The mechanisms of action of PPARs." Annual review of medicine **53**: 409-435.

Berger, J. P., T. E. Akiyama and P. T. Meinke (2005). "PPARs: therapeutic targets for metabolic disease." Trends in pharmacological sciences **26**(5): 244-251.

Berger, S. L. (2007). "The complex language of chromatin regulation during transcription." Nature **447**(7143): 407-412.

Berlin, J. D., P. Catalano, J. P. Thomas, J. W. Kugler, D. G. Haller and A. B. Benson, 3rd (2002). "Phase III study of gemcitabine in combination with fluorouracil versus gemcitabine alone in patients with advanced pancreatic carcinoma: Eastern Cooperative Oncology Group Trial E2297." Journal of clinical oncology : official journal of the American Society of Clinical Oncology **20**(15): 3270-3275.

Bhat-Nakshatri, P., T. R. Newton, R. Goulet, Jr. and H. Nakshatri (1998). "NF-kappaB activation and interleukin 6 production in fibroblasts by estrogen receptor-negative breast cancer cell-derived interleukin 1alpha." Proceedings of the National Academy of Sciences of the United States of America **95**(12): 6971-6976.

Bielesz, B., Y. Sirin, H. Si, T. Niranjan, A. Gruenwald, S. Ahn, H. Kato, J. Pullman, M. Gessler, V. H. Haase and K. Susztak (2010). "Epithelial Notch signaling regulates interstitial fibrosis development in the kidneys of mice and humans." The Journal of clinical investigation **120**(11): 4040-4054.

Bishop-Bailey, D. and T. Hla (1999). "Endothelial cell apoptosis induced by the peroxisome proliferator-activated receptor (PPAR) ligand 15-deoxy-Delta12, 14-prostaglandin J2." The Journal of biological chemistry **274**(24): 17042-17048.

Biswas, D. K., Q. Shi, S. Baily, I. Strickland, S. Ghosh, A. B. Pardee and J. D. Iglehart (2004). "NF-kappa B activation in human breast cancer specimens and its role in cell proliferation and apoptosis." Proceedings of the National Academy of Sciences of the United States of America **101**(27): 10137-10142.

Biswas, S. K. and A. Mantovani (2010). "Macrophage plasticity and interaction with lymphocyte subsets: cancer as a paradigm." Nature immunology **11**(10): 889-896.

Bivona, T. G., H. Hieronymus, J. Parker, K. Chang, M. Taron, R. Rosell, P. Moonsamy, K. Dahlman, V. A. Miller, C. Costa, G. Hannon and C. L. Sawyers (2011). "FAS and NF-kappaB signalling modulate dependence of lung cancers on mutant EGFR." Nature **471**(7339): 523-526.

Blanquart, C., O. Barbier, J. C. Fruchart, B. Staels and C. Glineur (2003). "Peroxisome proliferator-activated receptors: regulation of transcriptional activities and roles in inflammation." The Journal of steroid biochemistry and molecular biology **85**(2-5): 267-273.

Blokzijl, A., C. Dahlqvist, E. Reissmann, A. Falk, A. Moliner, U. Lendahl and C. F. Ibanez (2003). "Cross-talk between the Notch and TGF-beta signaling pathways mediated by interaction of the Notch intracellular domain with Smad3." The Journal of cell biology **163**(4): 723-728.

Bolos, V., J. Grego-Bessa and J. L. de la Pompa (2007). "Notch signaling in development and cancer." Endocrine reviews **28**(3): 339-363.

Bonizzi, G. and M. Karin (2004). "The two NF-kappaB activation pathways and their role in innate and adaptive immunity." Trends Immunol **25**(6): 280-288.

Borggrefe, T. and F. Oswald (2009). "The Notch signaling pathway: transcriptional regulation at Notch target genes." Cellular and molecular life sciences : CMLS **66**(10): 1631-1646.

Bramhall, S. R., J. Schulz, J. Nemunaitis, P. D. Brown, M. Baillet and J. A. Buckels (2002). "A double-blind placebo-controlled, randomised study comparing gemcitabine and marimastat with gemcitabine and placebo as first line therapy in patients with advanced pancreatic cancer." British journal of cancer **87**(2): 161-167.

Brand, R. E., B. M. Nolen, H. J. Zeh, P. J. Allen, M. A. Eloubeidi, M. Goldberg, E. Elton, J. P. Arnoletti, J. D. Christein, S. M. Vickers, C. J. Langmead, D. P. Landsittel, D. C. Whitcomb, W. E. Grizzle and A. E. Lokshin (2011). "Serum biomarker panels for the detection of pancreatic cancer." Clin Cancer Res **17**(4): 805-816.

Bray, S. J. (2006). "Notch signalling: a simple pathway becomes complex." Nature reviews. Molecular cell biology **7**(9): 678-689.

Brembeck, F. H., F. S. Schreiber, T. B. Deramaudt, L. Craig, B. Rhoades, G. Swain, P. Grippo, D. A. Stoffers, D. G. Silberg and A. K. Rustgi (2003). "The mutant K-ras oncogene causes pancreatic periductal lymphocytic infiltration and gastric mucous neck cell hyperplasia in transgenic mice." Cancer research **63**(9): 2005-2009.

Brissova, M., M. Shiota, W. E. Nicholson, M. Gannon, S. M. Knobel, D. W. Piston, C. V. Wright and A. C. Powers (2002). "Reduction in pancreatic transcription factor PDX-1 impairs glucose-stimulated insulin secretion." The Journal of biological chemistry **277**(13): 11225-11232.

Brittan, M., T. Hunt, R. Jeffery, R. Poulsom, S. J. Forbes, K. Hodivala-Dilke, J. Goldman, M. R. Alison and N. A. Wright (2002). "Bone marrow derivation of pericryptal myofibroblasts in the mouse and human small intestine and colon." Gut **50**(6): 752-757.

Burris, H. A., 3rd, M. J. Moore, J. Andersen, M. R. Green, M. L. Rothenberg, M. R. Modiano, M. C. Cripps, R. K. Portenoy, A. M. Storniolo, P. Tarassoff, R. Nelson, F. A. Dorr, C. D. Stephens and D. D. Von Hoff (1997). "Improvements in survival and clinical benefit with gemcitabine as first-line therapy for patients with advanced pancreas cancer: a randomized trial." Journal of clinical oncology : official journal of the American Society of Clinical Oncology **15**(6): 2403-2413.

Cano, D. A., M. Hebrok and M. Zenker (2007). "Pancreatic development and disease." Gastroenterology **132**(2): 745-762.

Carriere, C., E. S. Seeley, T. Goetze, D. S. Longnecker and M. Korc (2007). "The Nestin progenitor lineage is the compartment of origin for pancreatic intraepithelial

neoplasia." Proceedings of the National Academy of Sciences of the United States of America **104**(11): 4437-4442.

Cascinu, S., M. Falconi, V. Valentini and S. Jelic (2010). "Pancreatic cancer: ESMO Clinical Practice Guidelines for diagnosis, treatment and follow-up." Annals of oncology : official journal of the European Society for Medical Oncology / ESMO **21 Suppl 5**: v55-58.

Castellano, E. and J. Downward (2011). "RAS Interaction with PI3K: More Than Just Another Effector Pathway." Genes & cancer **2**(3): 261-274.

Catalano, C., A. Laghi, F. Fraioli, F. Pediconi, A. Napoli, M. Danti, I. Reitano and R. Passariello (2003). "Pancreatic carcinoma: the role of high-resolution multislice spiral CT in the diagnosis and assessment of resectability." European radiology **13**(1): 149-156.

Chadwick, N., L. Zeef, V. Portillo, C. Fennessy, F. Warrander, S. Hoyle and A. M. Buckle (2009). "Identification of novel Notch target genes in T cell leukaemia." Molecular cancer **8**: 35.

Chen, Z. J., L. Parent and T. Maniatis (1996). "Site-specific phosphorylation of IkappaBalpha by a novel ubiquitination-dependent protein kinase activity." Cell **84**(6): 853-862.

Cheng, H. T. and R. Kopan (2005). "The role of Notch signaling in specification of podocyte and proximal tubules within the developing mouse kidney." Kidney international **68**(5): 1951-1952.

Cheng, P., A. Zlobin, V. Volgina, S. Gottipati, B. Osborne, E. J. Simel, L. Miele and D. I. Gabrilovich (2001). "Notch-1 regulates NF-kappaB activity in hemopoietic progenitor cells." Journal of immunology **167**(8): 4458-4467.

Cheung, P., K. G. Tanner, W. L. Cheung, P. Sassone-Corsi, J. M. Denu and C. D. Allis (2000). "Synergistic coupling of histone H3 phosphorylation and acetylation in response to epidermal growth factor stimulation." Molecular cell **5**(6): 905-915.

Chinetti, G., S. Griglio, M. Antonucci, I. P. Torra, P. Delerive, Z. Majd, J. C. Fruchart, J. Chapman, J. Najib and B. Staels (1998). "Activation of proliferator-activated receptors alpha and gamma induces apoptosis of human monocyte-derived macrophages." The Journal of biological chemistry **273**(40): 25573-25580.

Chou, C. H., L. H. Wei, M. L. Kuo, Y. J. Huang, K. P. Lai, C. A. Chen and C. Y. Hsieh (2005). "Up-regulation of interleukin-6 in human ovarian cancer cell via a Gi/PI3K-Akt/NF-kappaB pathway by lysophosphatidic acid, an ovarian cancer-activating factor." Carcinogenesis **26**(1): 45-52.

Chung, S. W., B. Y. Kang, S. H. Kim, Y. K. Pak, D. Cho, G. Trinchieri and T. S. Kim (2000). "Oxidized low density lipoprotein inhibits interleukin-12 production in lipopolysaccharide-activated mouse macrophages via direct interactions between peroxisome proliferator-activated receptor-gamma and nuclear factor-kappa B." The Journal of biological chemistry **275**(42): 32681-32687.

Clark, C. E., S. R. Hingorani, R. Mick, C. Combs, D. A. Tuveson and R. H. Vonderheide (2007). "Dynamics of the immune reaction to pancreatic cancer from inception to invasion." Cancer Res **67**(19): 9518-9527.

Conroy, T., F. Desseigne, M. Ychou, O. Bouche, R. Guimbaud, Y. Becouarn, A. Adenis, J. L. Raoul, S. Gourgou-Bourgade, C. de la Fouchardiere, J. Bennouna, J. B. Bachet, F. Khemissa-Akouz, D. Pere-Verge, C. Delbaldo, E. Assenat, B. Chauffert, P. Michel, C. Montoto-Grillot and M. Ducreux (2011). "FOLFIRINOX versus gemcitabine for metastatic pancreatic cancer." The New England journal of medicine **364**(19): 1817-1825.

Cordero, J. B., J. P. Macagno, R. K. Stefanatos, K. E. Strathdee, R. L. Cagan and M. Vidal (2010). "Oncogenic Ras diverts a host TNF tumor suppressor activity into tumor promoter." Developmental cell **18**(6): 999-1011.

Coussens, L. M. and Z. Werb (2002). "Inflammation and cancer." Nature **420**(6917): 860-867.

Couzin-Frankel, J. (2010). "Immune therapy steps up the attack." Science **330**(6003): 440-443.

Cunningham, D., I. Chau, D. D. Stocken, J. W. Valle, D. Smith, W. Steward, P. G. Harper, J. Dunn, C. Tudur-Smith, J. West, S. Falk, A. Crellin, F. Adab, J. Thompson, P. Leonard, J. Ostrowski, M. Eatock, W. Scheithauer, R. Herrmann and J. P. Neoptolemos (2009). "Phase III randomized comparison of gemcitabine versus gemcitabine plus capecitabine in patients with advanced pancreatic cancer." Journal of clinical oncology : official journal of the American Society of Clinical Oncology **27**(33): 5513-5518.

Currie, C. J., C. D. Poole and E. A. Gale (2009). "The influence of glucose-lowering therapies on cancer risk in type 2 diabetes." Diabetologia **52**(9): 1766-1777.

Curry, C. L., L. L. Reed, B. J. Nickoloff, L. Miele and K. E. Foreman (2006). "Notch-independent regulation of Hes-1 expression by c-Jun N-terminal kinase signaling in human endothelial cells." Laboratory investigation; a journal of technical methods and pathology **86**(8): 842-852.

Cuzzocrea, S., E. Mazzon, L. Dugo, N. S. Patel, I. Serraino, R. Di Paola, T. Genovese, D. Britti, M. De Maio, A. P. Caputi and C. Thiemermann (2003). "Reduction in the evolution of murine type II collagen-induced arthritis by treatment with rosiglitazone, a ligand of the peroxisome proliferator-activated receptor gamma." Arthritis and rheumatism **48**(12): 3544-3556.

Cuzzocrea, S., B. Pisano, L. Dugo, A. Ianaro, D. Britti, N. S. Patel, R. Di Paola, T. Genovese, M. Di Rosa, A. P. Caputi and C. Thiemermann (2004). "Rosiglitazone, a ligand of the peroxisome proliferator-activated receptor-gamma, reduces acute pancreatitis induced by cerulein." Intensive care medicine **30**(5): 951-956.

D'Souza, B., A. Miyamoto and G. Weinmaster (2008). "The many facets of Notch ligands." Oncogene **27**(38): 5148-5167.

Dahlqvist, C., A. Blokzijl, G. Chapman, A. Falk, K. Dannaeus, C. F. Ibanez and U. Lendahl (2003). "Functional Notch signaling is required for BMP4-induced inhibition of myogenic differentiation." Development **130**(24): 6089-6099.

Dajee, M., M. Lazarov, J. Y. Zhang, T. Cai, C. L. Green, A. J. Russell, M. P. Marinkovich, S. Tao, Q. Lin, Y. Kubo and P. A. Khavari (2003). "NF-kappaB blockade and oncogenic Ras trigger invasive human epidermal neoplasia." Nature **421**(6923): 639-643.

Danielian, P. S., R. White, S. A. Hoare, S. E. Fawell and M. G. Parker (1993). "Identification of residues in the estrogen receptor that confer differential sensitivity to estrogen and hydroxytamoxifen." Mol Endocrinol **7**(2): 232-240.

Davie, J. R. (2003). "MSK1 and MSK2 mediate mitogen- and stress-induced phosphorylation of histone H3: a controversy resolved." Science's STKE : signal transduction knowledge environment **2003**(195): PE33.

Day, J. D., J. A. Digiuseppe, C. Yeo, M. Lai-Goldman, S. M. Anderson, S. N. Goodman, S. E. Kern and R. H. Hruban (1996). "Immunohistochemical evaluation of HER-2/neu expression in pancreatic adenocarcinoma and pancreatic intraepithelial neoplasms." Human pathology **27**(2): 119-124.

De La, O. J., L. L. Emerson, J. L. Goodman, S. C. Froebe, B. E. Illum, A. B. Curtis and L. C. Murtaugh (2008). "Notch and Kras reprogram pancreatic acinar cells to ductal intraepithelial neoplasia." Proc Natl Acad Sci U S A **105**(48): 18907-18912.

De La, O. J. and L. C. Murtaugh (2009). "Notch and Kras in pancreatic cancer: at the crossroads of mutation, differentiation and signaling." Cell Cycle **8**(12): 1860-1864.

De Raedt, T., Z. Walton, J. L. Yecies, D. Li, Y. Chen, C. F. Malone, O. Maertens, S. M. Jeong, R. T. Bronson, V. Lebleu, R. Kalluri, E. Normant, M. C. Haigis, B. D. Manning, K. K. Wong, K. F. Macleod and K. Cichowski (2011). "Exploiting cancer cell vulnerabilities to develop a combination therapy for ras-driven tumors." Cancer Cell **20**(3): 400-413.

Delacour, A., V. Nepote, A. Trumpp and P. L. Herrera (2004). "Nestin expression in pancreatic exocrine cell lineages." Mechanisms of development **121**(1): 3-14.

Delhase, M., M. Hayakawa, Y. Chen and M. Karin (1999). "Positive and negative regulation of IkappaB kinase activity through IKKbeta subunit phosphorylation." Science **284**(5412): 309-313.

Demarest, R. M., N. Dahmane and A. J. Capobianco (2011). "Notch is oncogenic dominant in T-cell acute lymphoblastic leukemia." Blood **117**(10): 2901-2909.

Deng, Y., X. Ren, L. Yang, Y. Lin and X. Wu (2003). "A JNK-dependent pathway is required for TNFalpha-induced apoptosis." Cell **115**(1): 61-70.

Desai, B. M., J. Oliver-Krasinski, D. D. De Leon, C. Farzad, N. Hong, S. D. Leach and D. A. Stoffers (2007). "Preexisting pancreatic acinar cells contribute to acinar

cell, but not islet beta cell, regeneration." The Journal of clinical investigation **117**(4): 971-977.

Desmouliere, A., C. Guyot and G. Gabbiani (2004). "The stroma reaction myofibroblast: a key player in the control of tumor cell behavior." Int J Dev Biol **48**(5-6): 509-517.

Dighe, A. S., E. Richards, L. J. Old and R. D. Schreiber (1994). "Enhanced in vivo growth and resistance to rejection of tumor cells expressing dominant negative IFN gamma receptors." Immunity **1**(6): 447-456.

DiGiuseppe, J. A., R. H. Hruban, G. J. Offerhaus, M. J. Clement, F. M. van den Berg, J. L. Cameron and A. D. van Mansfeld (1994). "Detection of K-ras mutations in mucinous pancreatic duct hyperplasia from a patient with a family history of pancreatic carcinoma." Am J Pathol **144**(5): 889-895.

Direkze, N. C., K. Hodivala-Dilke, R. Jeffery, T. Hunt, R. Poulsom, D. Oukrif, M. R. Alison and N. A. Wright (2004). "Bone marrow contribution to tumor-associated myofibroblasts and fibroblasts." Cancer Res **64**(23): 8492-8495.

Dong, J., J. Grunstein, M. Tejada, F. Peale, G. Frantz, W. C. Liang, W. Bai, L. Yu, J. Kowalski, X. Liang, G. Fuh, H. P. Gerber and N. Ferrara (2004). "VEGF-null cells require PDGFR alpha signaling-mediated stromal fibroblast recruitment for tumorigenesis." EMBO J **23**(14): 2800-2810.

Dong, Y. W., X. P. Wang and K. Wu (2009). "Suppression of pancreatic carcinoma growth by activating peroxisome proliferator-activated receptor gamma involves angiogenesis inhibition." World journal of gastroenterology : WJG **15**(4): 441-448.

Dovey, H. F., V. John, J. P. Anderson, L. Z. Chen, P. de Saint Andrieu, L. Y. Fang, S. B. Freedman, B. Folmer, E. Goldbach, E. J. Holsztynska, K. L. Hu, K. L. Johnson-Wood, S. L. Kennedy, D. Kholodenko, J. E. Knops, L. H. Latimer, M. Lee, Z. Liao, I. M. Lieberburg, R. N. Motter, L. C. Mutter, J. Nietz, K. P. Quinn, K. L. Sacchi, P. A. Seubert, G. M. Shopp, E. D. Thorsett, J. S. Tung, J. Wu, S. Yang, C. T. Yin, D. B. Schenk, P. C. May, L. D. Altstiel, M. H. Bender, L. N. Boggs, T. C. Britton, J. C. Clemens, D. L. Czilli, D. K. Dieckman-McGinty, J. J. Droste, K. S. Fuson, B. D. Gitter, P. A. Hyslop, E. M. Johnstone, W. Y. Li, S. P. Little, T. E. Mabry, F. D. Miller and J. E. Audia (2001). "Functional gamma-secretase inhibitors reduce beta-amyloid peptide levels in brain." Journal of neurochemistry **76**(1): 173-181.

Dror, V., V. Nguyen, P. Walia, T. B. Kalynyak, J. A. Hill and J. D. Johnson (2007). "Notch signalling suppresses apoptosis in adult human and mouse pancreatic islet cells." Diabetologia **50**(12): 2504-2515.

Druker, B. J. (2008). "Translation of the Philadelphia chromosome into therapy for CML." Blood **112**(13): 4808-4817.

Dubuquoy, L., C. Rousseaux, X. Thuru, L. Peyrin-Biroulet, O. Romano, P. Chavatte, M. Chamaillard and P. Desreumaux (2006). "PPARgamma as a new therapeutic target in inflammatory bowel diseases." Gut **55**(9): 1341-1349.

Dunn, G. P., L. J. Old and R. D. Schreiber (2004). "The three Es of cancer immunoediting." Annual review of immunology **22**: 329-360.

Dvorak, H. F. (1986). "Tumors: wounds that do not heal. Similarities between tumor stroma generation and wound healing." The New England journal of medicine **315**(26): 1650-1659.

Dvorak, H. F., V. M. Weaver, T. D. Tlsty and G. Bergers (2011). "Tumor microenvironment and progression." Journal of surgical oncology **103**(6): 468-474.

Edmunds, J. W., L. C. Mahadevan and A. L. Clayton (2008). "Dynamic histone H3 methylation during gene induction: HYPB/Setd2 mediates all H3K36 trimethylation." The EMBO journal **27**(2): 406-420.

Egberts, J. H., V. Cloosters, A. Noack, B. Schniewind, L. Thon, S. Klose, B. Kettler, C. von Forstner, C. Kneitz, J. Tepel, D. Adam, H. Wajant, H. Kalthoff and A. Trauzold (2008). "Anti-tumor necrosis factor therapy inhibits pancreatic tumor growth and metastasis." Cancer research **68**(5): 1443-1450.

El-Omar, E. M., M. Carrington, W. H. Chow, K. E. McColl, J. H. Bream, H. A. Young, J. Herrera, J. Lissowska, C. C. Yuan, N. Rothman, G. Lanyon, M. Martin, J. F. Fraumeni, Jr. and C. S. Rabkin (2000). "Interleukin-1 polymorphisms associated with increased risk of gastric cancer." Nature **404**(6776): 398-402.

Elaraj, D. M., D. M. Weinreich, S. Varghese, M. Puhlmann, S. M. Hewitt, N. M. Carroll, E. D. Feldman, E. M. Turner and H. R. Alexander (2006). "The role of interleukin 1 in growth and metastasis of human cancer xenografts." Clinical cancer research : an official journal of the American Association for Cancer Research **12**(4): 1088-1096.

Ellisen, L. W., J. Bird, D. C. West, A. L. Soreng, T. C. Reynolds, S. D. Smith and J. Sklar (1991). "TAN-1, the human homolog of the Drosophila notch gene, is broken by chromosomal translocations in T lymphoblastic neoplasms." Cell **66**(4): 649-661.

Elnemr, A., T. Ohta, K. Iwata, I. Ninomia, S. Fushida, G. Nishimura, H. Kitagawa, M. Kayahara, M. Yamamoto, T. Terada and K. Miwa (2000). "PPARgamma ligand (thiazolidinedione) induces growth arrest and differentiation markers of human pancreatic cancer cells." International journal of oncology **17**(6): 1157-1164.

Erez, N., M. Truitt, P. Olson, S. T. Arron and D. Hanahan (2010). "Cancer-Associated Fibroblasts Are Activated in Incipient Neoplasia to Orchestrate Tumor-Promoting Inflammation in an NF-kappaB-Dependent Manner." Cancer Cell **17**(2): 135-147.

Esni, F., D. A. Stoffers, T. Takeuchi and S. D. Leach (2004). "Origin of exocrine pancreatic cells from nestin-positive precursors in developing mouse pancreas." Mechanisms of development **121**(1): 15-25.

Espinosa, L., S. Cathelin, T. D'Altri, T. Trimarchi, A. Statnikov, J. Guiu, V. Rodilla, J. Ingles-Esteve, J. Nomdedeu, B. Bellosillo, C. Besses, O. Abdel-Wahab, N. Kucine, S. C. Sun, G. Song, C. C. Mullighan, R. L. Levine, K. Rajewsky, I. Aifantis

and A. Bigas (2010). "The Notch/Hes1 pathway sustains NF-kappaB activation through CYLD repression in T cell leukemia." Cancer Cell **18**(3): 268-281.

Esposito, I., M. Menicagli, N. Funel, F. Bergmann, U. Boggi, F. Mosca, G. Bevilacqua and D. Campani (2004). "Inflammatory cells contribute to the generation of an angiogenic phenotype in pancreatic ductal adenocarcinoma." Journal of clinical pathology **57**(6): 630-636.

Evans, J. M., L. A. Donnelly, A. M. Emslie-Smith, D. R. Alessi and A. D. Morris (2005). "Metformin and reduced risk of cancer in diabetic patients." BMJ **330**(7503): 1304-1305.

Evans, R. M., G. D. Barish and Y. X. Wang (2004). "PPARs and the complex journey to obesity." Nature medicine **10**(4): 355-361.

Fabbri, G., S. Rasi, D. Rossi, V. Trifonov, H. Khiabanian, J. Ma, A. Grunn, M. Fangazio, D. Capello, S. Monti, S. Cresta, E. Gargiulo, F. Forconi, A. Guarini, L. Arcaini, M. Paulli, L. Laurenti, L. M. Larocca, R. Marasca, V. Gattei, D. Oscier, F. Bertoni, C. G. Mullighan, R. Foa, L. Pasqualucci, R. Rabadan, R. Dalla-Favera and G. Gaidano (2011). "Analysis of the chronic lymphocytic leukemia coding genome: role of NOTCH1 mutational activation." The Journal of experimental medicine **208**(7): 1389-1401.

Farmer, S. R. (2006). "Transcriptional control of adipocyte formation." Cell metabolism **4**(4): 263-273.

Farrow, B., D. Albo and D. H. Berger (2008). "The role of the tumor microenvironment in the progression of pancreatic cancer." The Journal of surgical research **149**(2): 319-328.

Feldmann, G., R. Beaty, R. H. Hruban and A. Maitra (2007). "Molecular genetics of pancreatic intraepithelial neoplasia." J Hepatobiliary Pancreat Surg **14**(3): 224-232.

Fendrich, V., F. Esni, M. V. Garay, G. Feldmann, N. Habbe, J. N. Jensen, Y. Dor, D. Stoffers, J. Jensen, S. D. Leach and A. Maitra (2008). "Hedgehog signaling is required for effective regeneration of exocrine pancreas." Gastroenterology **135**(2): 621-631.

Ferlay, J., H. R. Shin, F. Bray, D. Forman, C. Mathers and D. M. Parkin (2010). "Estimates of worldwide burden of cancer in 2008: GLOBOCAN 2008." International journal of cancer. Journal international du cancer **127**(12): 2893-2917.

Finco, T. S., J. K. Westwick, J. L. Norris, A. A. Beg, C. J. Der and A. S. Baldwin, Jr. (1997). "Oncogenic Ha-Ras-induced signaling activates NF-kappaB transcriptional activity, which is required for cellular transformation." The Journal of biological chemistry **272**(39): 24113-24116.

Finkelman, F. D., A. Svetic, I. Gresser, C. Snapper, J. Holmes, P. P. Trotta, I. M. Katona and W. C. Gause (1991). "Regulation by interferon alpha of immunoglobulin isotype selection and lymphokine production in mice." The Journal of experimental medicine **174**(5): 1179-1188.

Fire, A., S. Xu, M. K. Montgomery, S. A. Kostas, S. E. Driver and C. C. Mello (1998). "Potent and specific genetic interference by double-stranded RNA in Caenorhabditis elegans." Nature **391**(6669): 806-811.

Fischer, A. and M. Gessler (2007). "Delta-Notch--and then? Protein interactions and proposed modes of repression by Hes and Hey bHLH factors." Nucleic Acids Res **35**(14): 4583-4596.

Fjallskog, M. L., M. H. Lejonklou, K. E. Oberg, B. K. Eriksson and E. T. Janson (2003). "Expression of molecular targets for tyrosine kinase receptor antagonists in malignant endocrine pancreatic tumors." Clinical cancer research : an official journal of the American Association for Cancer Research **9**(4): 1469-1473.

Foell, J., B. Hewes and R. S. Mittler (2007). "T cell costimulatory and inhibitory receptors as therapeutic targets for inducing anti-tumor immunity." Current cancer drug targets **7**(1): 55-70.

Fong, C. H., M. Bebien, A. Didierlaurent, R. Nebauer, T. Hussell, D. Broide, M. Karin and T. Lawrence (2008). "An antiinflammatory role for IKKbeta through the inhibition of "classical" macrophage activation." J Exp Med **205**(6): 1269-1276.

Fong, L. and E. J. Small (2008). "Anti-cytotoxic T-lymphocyte antigen-4 antibody: the first in an emerging class of immunomodulatory antibodies for cancer treatment." Journal of clinical oncology : official journal of the American Society of Clinical Oncology **26**(32): 5275-5283.

Forman, B. M., P. Tontonoz, J. Chen, R. P. Brun, B. M. Spiegelman and R. M. Evans (1995). "15-Deoxy-delta 12, 14-prostaglandin J2 is a ligand for the adipocyte determination factor PPAR gamma." Cell **83**(5): 803-812.

Fridman, W. H., J. Galon, F. Pages, E. Tartour, C. Sautes-Fridman and G. Kroemer (2011). "Prognostic and predictive impact of intra- and peritumoral immune infiltrates." Cancer research **71**(17): 5601-5605.

Friess, H., J. Kleeff, M. Korc and M. W. Buchler (1999). "Molecular aspects of pancreatic cancer and future perspectives." Digestive surgery **16**(4): 281-290.

Fryer, C. J., J. B. White and K. A. Jones (2004). "Mastermind recruits CycC:CDK8 to phosphorylate the Notch ICD and coordinate activation with turnover." Molecular cell **16**(4): 509-520.

Fryer, R. A., B. Barlett, C. Galustian and A. G. Dalgleish (2011). "Mechanisms underlying gemcitabine resistance in pancreatic cancer and sensitisation by the iMiD lenalidomide." Anticancer research **31**(11): 3747-3756.

Fujikura, J., K. Hosoda, H. Iwakura, T. Tomita, M. Noguchi, H. Masuzaki, K. Tanigaki, D. Yabe, T. Honjo and K. Nakao (2006). "Notch/Rbp-j signaling prevents premature endocrine and ductal cell differentiation in the pancreas." Cell Metab **3**(1): 59-65.

Fujioka, S., G. M. Sclabas, C. Schmidt, W. A. Frederick, Q. G. Dong, J. L. Abbruzzese, D. B. Evans, C. Baker and P. J. Chiao (2003a). "Function of nuclear

factor kappaB in pancreatic cancer metastasis." Clinical cancer research : an official journal of the American Association for Cancer Research **9**(1): 346-354.

Fujioka, S., G. M. Sclabas, C. Schmidt, J. Niu, W. A. Frederick, Q. G. Dong, J. L. Abbruzzese, D. B. Evans, C. Baker and P. J. Chiao (2003b). "Inhibition of constitutive NF-kappa B activity by I kappa B alpha M suppresses tumorigenesis." Oncogene **22**(9): 1365-1370.

Fung, E., S. M. Tang, J. P. Canner, K. Morishige, J. F. Arboleda-Velasquez, A. A. Cardoso, N. Carlesso, J. C. Aster and M. Aikawa (2007). "Delta-like 4 induces notch signaling in macrophages: implications for inflammation." Circulation **115**(23): 2948-2956.

Gaglio, D., C. M. Metallo, P. A. Gameiro, K. Hiller, L. S. Danna, C. Balestrieri, L. Alberghina, G. Stephanopoulos and F. Chiaradonna (2011). "Oncogenic K-Ras decouples glucose and glutamine metabolism to support cancer cell growth." Molecular systems biology **7**: 523.

Galli, A., E. Ceni, D. W. Crabb, T. Mello, R. Salzano, C. Grappone, S. Milani, E. Surrenti, C. Surrenti and A. Casini (2004). "Antidiabetic thiazolidinediones inhibit invasiveness of pancreatic cancer cells via PPARgamma independent mechanisms." Gut **53**(11): 1688-1697.

Galmarini, C. M., M. L. Clarke, L. Jordheim, C. L. Santos, E. Cros, J. R. Mackey and C. Dumontet (2004). "Resistance to gemcitabine in a human follicular lymphoma cell line is due to partial deletion of the deoxycytidine kinase gene." BMC pharmacology **4**: 8.

Gandini, S., A. B. Lowenfels, E. M. Jaffee, T. D. Armstrong and P. Maisonneuve (2005). "Allergies and the risk of pancreatic cancer: a meta-analysis with review of epidemiology and biological mechanisms." Cancer epidemiology, biomarkers & prevention : a publication of the American Association for Cancer Research, cosponsored by the American Society of Preventive Oncology **14**(8): 1908-1916.

Gao, Q., S. J. Qiu, J. Fan, J. Zhou, X. Y. Wang, Y. S. Xiao, Y. Xu, Y. W. Li and Z. Y. Tang (2007a). "Intratumoral balance of regulatory and cytotoxic T cells is associated with prognosis of hepatocellular carcinoma after resection." Journal of clinical oncology : official journal of the American Society of Clinical Oncology **25**(18): 2586-2593.

Gao, S. P., K. G. Mark, K. Leslie, W. Pao, N. Motoi, W. L. Gerald, W. D. Travis, W. Bornmann, D. Veach, B. Clarkson and J. F. Bromberg (2007b). "Mutations in the EGFR kinase domain mediate STAT3 activation via IL-6 production in human lung adenocarcinomas." The Journal of clinical investigation **117**(12): 3846-3856.

Garber, K. (2007). "Notch emerges as new cancer drug target." Journal of the National Cancer Institute **99**(17): 1284-1285.

Garber, K. (2010). "Stromal depletion goes on trial in pancreatic cancer." J Natl Cancer Inst **102**(7): 448-450.

Georgia, S. and A. Bhushan (2004). "Beta cell replication is the primary mechanism for maintaining postnatal beta cell mass." The Journal of clinical investigation **114**(7): 963-968.

Georgia, S. and A. Bhushan (2006). "p27 Regulates the transition of beta-cells from quiescence to proliferation." Diabetes **55**(11): 2950-2956.

Gerondakis, S., M. Grossmann, Y. Nakamura, T. Pohl and R. Grumont (1999). "Genetic approaches in mice to understand Rel/NF-kappaB and IkappaB function: transgenics and knockouts." Oncogene **18**(49): 6888-6895.

Ghiringhelli, F., C. Menard, M. Terme, C. Flament, J. Taieb, N. Chaput, P. E. Puig, S. Novault, B. Escudier, E. Vivier, A. Lecesne, C. Robert, J. Y. Blay, J. Bernard, S. Caillat-Zucman, A. Freitas, T. Tursz, O. Wagner-Ballon, C. Capron, W. Vainchencker, F. Martin and L. Zitvogel (2005). "CD4+CD25+ regulatory T cells inhibit natural killer cell functions in a transforming growth factor-beta-dependent manner." The Journal of experimental medicine **202**(8): 1075-1085.

Glass, C. K. and K. Saijo (2010). "Nuclear receptor transrepression pathways that regulate inflammation in macrophages and T cells." Nature reviews. Immunology **10**(5): 365-376.

Goggins, M., R. H. Hruban and S. E. Kern (2000). "BRCA2 is inactivated late in the development of pancreatic intraepithelial neoplasia: evidence and implications." The American journal of pathology **156**(5): 1767-1771.

Goldner, J. (1938). "A modification of the masson trichrome technique for routine laboratory purposes." The American journal of pathology **14**(2): 237-243.

Goldstein, J. C., F. Rodier, J. C. Garbe, M. R. Stampfer and J. Campisi (2005). "Caspase-independent cytochrome c release is a sensitive measure of low-level apoptosis in cell culture models." Aging cell **4**(4): 217-222.

Gomez, G., E. W. Englander, G. Wang and G. H. Greeley, Jr. (2004). "Increased expression of hypoxia-inducible factor-1alpha, p48, and the Notch signaling cascade during acute pancreatitis in mice." Pancreas **28**(1): 58-64.

Gordon, W. R., K. L. Arnett and S. C. Blacklow (2008). "The molecular logic of Notch signaling--a structural and biochemical perspective." J Cell Sci **121**(Pt 19): 3109-3119.

Goto, H., Y. Tomono, K. Ajiro, H. Kosako, M. Fujita, M. Sakurai, K. Okawa, A. Iwamatsu, T. Okigaki, T. Takahashi and M. Inagaki (1999). "Identification of a novel phosphorylation site on histone H3 coupled with mitotic chromosome condensation." The Journal of biological chemistry **274**(36): 25543-25549.

Greer, J. B. and D. C. Whitcomb (2009). "Inflammation and pancreatic cancer: an evidence-based review." Current opinion in pharmacology **9**(4): 411-418.

Greten, F. R., L. Eckmann, T. F. Greten, J. M. Park, Z. W. Li, L. J. Egan, M. F. Kagnoff and M. Karin (2004). "IKKbeta links inflammation and tumorigenesis in a mouse model of colitis-associated cancer." Cell **118**(3): 285-296.

Gridley, T. (1997). "Notch signaling in vertebrate development and disease." Molecular and cellular neurosciences **9**(2): 103-108.

Grippo, P. J., P. S. Nowlin, M. J. Demeure, D. S. Longnecker and E. P. Sandgren (2003). "Preinvasive pancreatic neoplasia of ductal phenotype induced by acinar cell targeting of mutant Kras in transgenic mice." Cancer research **63**(9): 2016-2019.

Grivennikov, S. I., F. R. Greten and M. Karin (2010). "Immunity, inflammation, and cancer." Cell **140**(6): 883-899.

Grivennikov, S. I. and M. Karin (2010). "Dangerous liaisons: STAT3 and NF-kappaB collaboration and crosstalk in cancer." Cytokine Growth Factor Rev **21**(1): 11-19.

Grivennikov, S. I., A. V. Tumanov, D. J. Liepinsh, A. A. Kruglov, B. I. Marakusha, A. N. Shakhov, T. Murakami, L. N. Drutskaya, I. Forster, B. E. Clausen, L. Tessarollo, B. Ryffel, D. V. Kuprash and S. A. Nedospasov (2005). "Distinct and nonredundant in vivo functions of TNF produced by t cells and macrophages/neutrophils: protective and deleterious effects." Immunity **22**(1): 93-104.

Gu, H., J. D. Marth, P. C. Orban, H. Mossmann and K. Rajewsky (1994). "Deletion of a DNA polymerase beta gene segment in T cells using cell type-specific gene targeting." Science **265**(5168): 103-106.

Guarani, V., G. Deflorian, C. A. Franco, M. Kruger, L. K. Phng, K. Bentley, L. Toussaint, F. Dequiedt, R. Mostoslavsky, M. H. Schmidt, B. Zimmermann, R. P. Brandes, M. Mione, C. H. Westphal, T. Braun, A. M. Zeiher, H. Gerhardt, S. Dimmeler and M. Potente (2011). "Acetylation-dependent regulation of endothelial Notch signalling by the SIRT1 deacetylase." Nature **473**(7346): 234-238.

Guerra, C., M. Collado, C. Navas, A. J. Schuhmacher, I. Hernandez-Porras, M. Canamero, M. Rodriguez-Justo, M. Serrano and M. Barbacid (2011). "Pancreatitis-induced inflammation contributes to pancreatic cancer by inhibiting oncogene-induced senescence." Cancer Cell **19**(6): 728-739.

Guerra, C., A. J. Schuhmacher, M. Canamero, P. J. Grippo, L. Verdaguer, L. Perez-Gallego, P. Dubus, E. P. Sandgren and M. Barbacid (2007). "Chronic pancreatitis is essential for induction of pancreatic ductal adenocarcinoma by K-Ras oncogenes in adult mice." Cancer Cell **11**(3): 291-302.

Habbe, N., G. Shi, R. A. Meguid, V. Fendrich, F. Esni, H. Chen, G. Feldmann, D. A. Stoffers, S. F. Konieczny, S. D. Leach and A. Maitra (2008). "Spontaneous induction of murine pancreatic intraepithelial neoplasia (mPanIN) by acinar cell targeting of oncogenic Kras in adult mice." Proceedings of the National Academy of Sciences of the United States of America **105**(48): 18913-18918.

Hacker, H. and M. Karin (2006). "Regulation and function of IKK and IKK-related kinases." Science's STKE : signal transduction knowledge environment **2006**(357): re13.

Hagemann, T., S. K. Biswas, T. Lawrence, A. Sica and C. E. Lewis (2009). "Regulation of macrophage function in tumors: the multifaceted role of NF-kappaB." Blood **113**(14): 3139-3146.

Hagemann, T., T. Lawrence, I. McNeish, K. A. Charles, H. Kulbe, R. G. Thompson, S. C. Robinson and F. R. Balkwill (2008). ""Re-educating" tumor-associated macrophages by targeting NF-kappaB." J Exp Med **205**(6): 1261-1268.

Hagemann, T., J. Wilson, F. Burke, H. Kulbe, N. F. Li, A. Pluddemann, K. Charles, S. Gordon and F. R. Balkwill (2006). "Ovarian cancer cells polarize macrophages toward a tumor-associated phenotype." Journal of immunology **176**(8): 5023-5032.

Hagemann, T., J. Wilson, H. Kulbe, N. F. Li, D. A. Leinster, K. Charles, F. Klemm, T. Pukrop, C. Binder and F. R. Balkwill (2005). "Macrophages induce invasiveness of epithelial cancer cells via NF-kappa B and JNK." J Immunol **175**(2): 1197-1205.

Hald, J., J. P. Hjorth, M. S. German, O. D. Madsen, P. Serup and J. Jensen (2003). "Activated Notch1 prevents differentiation of pancreatic acinar cells and attenuate endocrine development." Developmental biology **260**(2): 426-437.

Hale, M. A., H. Kagami, L. Shi, A. M. Holland, H. P. Elsasser, R. E. Hammer and R. J. MacDonald (2005). "The homeodomain protein PDX1 is required at mid-pancreatic development for the formation of the exocrine pancreas." Developmental biology **286**(1): 225-237.

Halfdanarson, T. R., J. Rubin, M. B. Farnell, C. S. Grant and G. M. Petersen (2008). "Pancreatic endocrine neoplasms: epidemiology and prognosis of pancreatic endocrine tumors." Endocrine-related cancer **15**(2): 409-427.

Hallam, S., M. Escorcio-Correia, R. Soper, A. Schultheiss and T. Hagemann (2009). "Activated macrophages in the tumour microenvironment-dancing to the tune of TLR and NF-kappaB." The Journal of pathology **219**(2): 143-152.

Hamacher, R., R. M. Schmid, D. Saur and G. Schneider (2008). "Apoptotic pathways in pancreatic ductal adenocarcinoma." Molecular cancer **7**: 64.

Hammer, R. E., G. H. Swift, D. M. Ornitz, C. J. Quaife, R. D. Palmiter, R. L. Brinster and R. J. MacDonald (1987). "The rat elastase I regulatory element is an enhancer that directs correct cell specificity and developmental onset of expression in transgenic mice." Molecular and cellular biology **7**(8): 2956-2967.

Han, S. S., H. Yun, D. J. Son, V. S. Tompkins, L. Peng, S. T. Chung, J. S. Kim, E. S. Park and S. Janz (2010). "NF-kappaB/STAT3/PI3K signaling crosstalk in iMyc E mu B lymphoma." Molecular cancer **9**: 97.

Han, X., N. Benight, B. Osuntokun, K. Loesch, S. J. Frank and L. A. Denson (2007). "Tumour necrosis factor alpha blockade induces an anti-inflammatory growth hormone signalling pathway in experimental colitis." Gut **56**(1): 73-81.

Hanahan, D. and R. A. Weinberg (2000). "The hallmarks of cancer." Cell **100**(1): 57-70.

Hanahan, D. and R. A. Weinberg (2011). "Hallmarks of cancer: the next generation." Cell **144**(5): 646-674.

Hassan, M. M., M. L. Bondy, R. A. Wolff, J. L. Abbruzzese, J. N. Vauthey, P. W. Pisters, D. B. Evans, R. Khan, T. H. Chou, R. Lenzi, L. Jiao and D. Li (2007). "Risk factors for pancreatic cancer: case-control study." The American journal of gastroenterology **102**(12): 2696-2707.

Hausen, H. Z. (2006). Infections causing human cancer, Wiley-VCH.

Hayden, M. S. and S. Ghosh (2004). "Signaling to NF-kappaB." Genes & development **18**(18): 2195-2224.

Heintz, N., H. L. Sive and R. G. Roeder (1983). "Regulation of human histone gene expression: kinetics of accumulation and changes in the rate of synthesis and in the half-lives of individual histone mRNAs during the HeLa cell cycle." Molecular and cellular biology **3**(4): 539-550.

Hemminki, K., X. Li, J. Sundquist and K. Sundquist (2008). "Cancer risks in ulcerative colitis patients." International journal of cancer. Journal international du cancer **123**(6): 1417-1421.

Hemminki, K., X. Li, J. Sundquist and K. Sundquist (2009). "Cancer risks in Crohn disease patients." Annals of oncology : official journal of the European Society for Medical Oncology / ESMO **20**(3): 574-580.

Hendzel, M. J., Y. Wei, M. A. Mancini, A. Van Hooser, T. Ranalli, B. R. Brinkley, D. P. Bazett-Jones and C. D. Allis (1997). "Mitosis-specific phosphorylation of histone H3 initiates primarily within pericentromeric heterochromatin during G2 and spreads in an ordered fashion coincident with mitotic chromosome condensation." Chromosoma **106**(6): 348-360.

Herrera, P. L. (2002). "Defining the cell lineages of the islets of Langerhans using transgenic mice." The International journal of developmental biology **46**(1): 97-103.

Herzig, S., S. Hedrick, I. Morantte, S. H. Koo, F. Galimi and M. Montminy (2003). "CREB controls hepatic lipid metabolism through nuclear hormone receptor PPAR-gamma." Nature **426**(6963): 190-193.

Hezel, A. F., A. C. Kimmelman, B. Z. Stanger, N. Bardeesy and R. A. Depinho (2006). "Genetics and biology of pancreatic ductal adenocarcinoma." Genes & development **20**(10): 1218-1249.

Hingorani, S. R., E. F. Petricoin, A. Maitra, V. Rajapakse, C. King, M. A. Jacobetz, S. Ross, T. P. Conrads, T. D. Veenstra, B. A. Hitt, Y. Kawaguchi, D. Johann, L. A. Liotta, H. C. Crawford, M. E. Putt, T. Jacks, C. V. Wright, R. H. Hruban, A. M. Lowy and D. A. Tuveson (2003). "Preinvasive and invasive ductal pancreatic cancer and its early detection in the mouse." Cancer Cell **4**(6): 437-450.

Hingorani, S. R., L. Wang, A. S. Multani, C. Combs, T. B. Deramaudt, R. H. Hruban, A. K. Rustgi, S. Chang and D. A. Tuveson (2005). "Trp53R172H and

KrasG12D cooperate to promote chromosomal instability and widely metastatic pancreatic ductal adenocarcinoma in mice." Cancer Cell **7**(5): 469-483.

Hiraoka, N., K. Onozato, T. Kosuge and S. Hirohashi (2006). "Prevalence of FOXP3+ regulatory T cells increases during the progression of pancreatic ductal adenocarcinoma and its premalignant lesions." Clinical cancer research : an official journal of the American Association for Cancer Research **12**(18): 5423-5434.

Hiscott, J., J. Marois, J. Garoufalis, M. D'Addario, A. Roulston, I. Kwan, N. Pepin, J. Lacoste, H. Nguyen, G. Bensi and et al. (1993). "Characterization of a functional NF-kappa B site in the human interleukin 1 beta promoter: evidence for a positive autoregulatory loop." Molecular and cellular biology **13**(10): 6231-6240.

Holcomb, B., M. Yip-Schneider and C. M. Schmidt (2008). "The role of nuclear factor kappaB in pancreatic cancer and the clinical applications of targeted therapy." Pancreas **36**(3): 225-235.

Hong, S. M., C. M. Heaphy, C. Shi, S. H. Eo, H. Cho, A. K. Meeker, J. R. Eshleman, R. H. Hruban and M. Goggins (2011). "Telomeres are shortened in acinar-to-ductal metaplasia lesions associated with pancreatic intraepithelial neoplasia but not in isolated acinar-to-ductal metaplasias." Modern pathology : an official journal of the United States and Canadian Academy of Pathology, Inc **24**(2): 256-266.

Hruban, R. H., N. V. Adsay, J. Albores-Saavedra, C. Compton, E. S. Garrett, S. N. Goodman, S. E. Kern, D. S. Klimstra, G. Kloppel, D. S. Longnecker, J. Luttges and G. J. Offerhaus (2001). "Pancreatic intraepithelial neoplasia: a new nomenclature and classification system for pancreatic duct lesions." Am J Surg Pathol **25**(5): 579-586.

Hruban, R. H., A. Maitra and M. Goggins (2008). "Update on pancreatic intraepithelial neoplasia." International journal of clinical and experimental pathology **1**(4): 306-316.

Hu, S., Z. Xie, A. Onishi, X. Yu, L. Jiang, J. Lin, H. S. Rho, C. Woodard, H. Wang, J. S. Jeong, S. Long, X. He, H. Wade, S. Blackshaw, J. Qian and H. Zhu (2009). "Profiling the human protein-DNA interactome reveals ERK2 as a transcriptional repressor of interferon signaling." Cell **139**(3): 610-622.

Hug, H., M. Costas, P. Staeheli, M. Aebi and C. Weissmann (1988). "Organization of the murine Mx gene and characterization of its interferon- and virus-inducible promoter." Molecular and cellular biology **8**(8): 3065-3079.

Huxley, R., A. Ansary-Moghaddam, A. Berrington de Gonzalez, F. Barzi and M. Woodward (2005). "Type-II diabetes and pancreatic cancer: a meta-analysis of 36 studies." British journal of cancer **92**(11): 2076-2083.

Hwang, R. F., T. Moore, T. Arumugam, V. Ramachandran, K. D. Amos, A. Rivera, B. Ji, D. B. Evans and C. D. Logsdon (2008). "Cancer-associated stromal fibroblasts promote pancreatic tumor progression." Cancer Res **68**(3): 918-926.

Ide, T., Y. Kitajima, A. Miyoshi, T. Ohtsuka, M. Mitsuno, K. Ohtaka, Y. Koga and K. Miyazaki (2006). "Tumor-stromal cell interaction under hypoxia increases the invasiveness of pancreatic cancer cells through the hepatocyte growth factor/c-Met pathway." International journal of cancer. Journal international du cancer **119**(12): 2750-2759.

Ijichi, H. (2011). "Genetically-engineered mouse models for pancreatic cancer: Advances and current limitations." World J Clin Oncol **2**(5): 195-202.

Ijichi, H., A. Chytil, A. E. Gorska, M. E. Aakre, B. Bierie, M. Tada, D. Mohri, K. Miyabayashi, Y. Asaoka, S. Maeda, T. Ikenoue, K. Tateishi, C. V. Wright, K. Koike, M. Omata and H. L. Moses (2011). "Inhibiting Cxcr2 disrupts tumor-stromal interactions and improves survival in a mouse model of pancreatic ductal adenocarcinoma." The Journal of clinical investigation **121**(10): 4106-4117.

Ijichi, H., A. Chytil, A. E. Gorska, M. E. Aakre, Y. Fujitani, S. Fujitani, C. V. Wright and H. L. Moses (2006). "Aggressive pancreatic ductal adenocarcinoma in mice caused by pancreas-specific blockade of transforming growth factor-beta signaling in cooperation with active Kras expression." Genes & development **20**(22): 3147-3160.

Iliopoulos, D., H. A. Hirsch and K. Struhl (2009). "An epigenetic switch involving NF-kappaB, Lin28, Let-7 MicroRNA, and IL6 links inflammation to cell transformation." Cell **139**(4): 693-706.

Iodice, S., S. Gandini, P. Maisonneuve and A. B. Lowenfels (2008). "Tobacco and the risk of pancreatic cancer: a review and meta-analysis." Langenbeck's archives of surgery / Deutsche Gesellschaft fur Chirurgie **393**(4): 535-545.

Ishitani, T., T. Hirao, M. Suzuki, M. Isoda, S. Ishitani, K. Harigaya, M. Kitagawa, K. Matsumoto and M. Itoh (2010). "Nemo-like kinase suppresses Notch signalling by interfering with formation of the Notch active transcriptional complex." Nature cell biology **12**(3): 278-285.

Ishiwata, T., Y. Matsuda and Z. Naito (2011). "Nestin in gastrointestinal and other cancers: effects on cells and tumor angiogenesis." World journal of gastroenterology : WJG **17**(4): 409-418.

Iso, T., L. Kedes and Y. Hamamori (2003). "HES and HERP families: multiple effectors of the Notch signaling pathway." J Cell Physiol **194**(3): 237-255.

Itoh, F., S. Itoh, M. J. Goumans, G. Valdimarsdottir, T. Iso, G. P. Dotto, Y. Hamamori, L. Kedes, M. Kato and P. ten Dijke Pt (2004). "Synergy and antagonism between Notch and BMP receptor signaling pathways in endothelial cells." The EMBO journal **23**(3): 541-551.

Ivashchenko, C. Y., S. Z. Duan, M. G. Usher and R. M. Mortensen (2007). "PPAR-gamma knockout in pancreatic epithelial cells abolishes the inhibitory effect of rosiglitazone on caerulein-induced acute pancreatitis." American journal of physiology. Gastrointestinal and liver physiology **293**(1): G319-326.

Izeradjene, K., C. Combs, M. Best, A. Gopinathan, A. Wagner, W. M. Grady, C. X. Deng, R. H. Hruban, N. V. Adsay, D. A. Tuveson and S. R. Hingorani (2007).

"Kras(G12D) and Smad4/Dpc4 haploinsufficiency cooperate to induce mucinous cystic neoplasms and invasive adenocarcinoma of the pancreas." Cancer Cell **11**(3): 229-243.

Jacobs, E. J., S. J. Chanock, C. S. Fuchs, A. Lacroix, R. R. McWilliams, E. Steplowski, R. Z. Stolzenberg-Solomon, A. A. Arslan, H. B. Bueno-de-Mesquita, M. Gross, K. Helzlsouer, G. Petersen, W. Zheng, I. Agalliu, N. E. Allen, L. Amundadottir, M. C. Boutron-Ruault, J. E. Buring, F. Canzian, S. Clipp, M. Dorronsoro, J. M. Gaziano, E. L. Giovannucci, S. E. Hankinson, P. Hartge, R. N. Hoover, D. J. Hunter, K. B. Jacobs, M. Jenab, P. Kraft, C. Kooperberg, S. M. Lynch, M. Sund, J. B. Mendelsohn, T. Mouw, C. C. Newton, K. Overvad, D. Palli, P. H. Peeters, A. Rajkovic, X. O. Shu, G. Thomas, G. S. Tobias, D. Trichopoulos, J. Virtamo, J. Wactawski-Wende, B. M. Wolpin, K. Yu and A. Zeleniuch-Jacquotte (2010). "Family history of cancer and risk of pancreatic cancer: a pooled analysis from the Pancreatic Cancer Cohort Consortium (PanScan)." International journal of cancer. Journal international du cancer **127**(6): 1421-1428.

Jarriault, S., C. Brou, F. Logeat, E. H. Schroeter, R. Kopan and A. Israel (1995). "Signalling downstream of activated mammalian Notch." Nature **377**(6547): 355-358.

Jensen, J., E. E. Pedersen, P. Galante, J. Hald, R. S. Heller, M. Ishibashi, R. Kageyama, F. Guillemot, P. Serup and O. D. Madsen (2000). "Control of endodermal endocrine development by Hes-1." Nature genetics **24**(1): 36-44.

Jensen, J. N., E. Cameron, M. V. Garay, T. W. Starkey, R. Gianani and J. Jensen (2005). "Recapitulation of elements of embryonic development in adult mouse pancreatic regeneration." Gastroenterology **128**(3): 728-741.

Jiang, C., A. T. Ting and B. Seed (1998). "PPAR-gamma agonists inhibit production of monocyte inflammatory cytokines." Nature **391**(6662): 82-86.

Johansen, L. M., C. D. Deppmann, K. D. Erickson, W. F. Coffin, 3rd, T. M. Thornton, S. E. Humphrey, J. M. Martin and E. J. Taparowsky (2003). "EBNA2 and activated Notch induce expression of BATF." Journal of virology **77**(10): 6029-6040.

Johansson, M., D. G. Denardo and L. M. Coussens (2008). "Polarized immune responses differentially regulate cancer development." Immunological reviews **222**: 145-154.

Johnson, C. L., A. S. Kowalik, N. Rajakumar and C. L. Pin (2004). "Mist1 is necessary for the establishment of granule organization in serous exocrine cells of the gastrointestinal tract." Mechanisms of development **121**(3): 261-272.

Johnson, L., K. Mercer, D. Greenbaum, R. T. Bronson, D. Crowley, D. A. Tuveson and T. Jacks (2001). "Somatic activation of the K-ras oncogene causes early onset lung cancer in mice." Nature **410**(6832): 1111-1116.

Johnson, L. N. (2009). "The regulation of protein phosphorylation." Biochemical Society transactions **37**(Pt 4): 627-641.

Jonsson, J., L. Carlsson, T. Edlund and H. Edlund (1994). "Insulin-promoter-factor 1 is required for pancreas development in mice." Nature **371**(6498): 606-609.

Joyce, J. A. and J. W. Pollard (2009). "Microenvironmental regulation of metastasis." Nature reviews. Cancer **9**(4): 239-252.

Kageyama, R., T. Ohtsuka and K. Tomita (2000). "The bHLH gene Hes1 regulates differentiation of multiple cell types." Molecules and cells **10**(1): 1-7.

Kahn, S. E., S. M. Haffner, M. A. Heise, W. H. Herman, R. R. Holman, N. P. Jones, B. G. Kravitz, J. M. Lachin, M. C. O'Neill, B. Zinman and G. Viberti (2006). "Glycemic durability of rosiglitazone, metformin, or glyburide monotherapy." The New England journal of medicine **355**(23): 2427-2443.

Kalluri, R. and M. Zeisberg (2006). "Fibroblasts in cancer." Nat Rev Cancer **6**(5): 392-401.

Kalser, M. H., J. Barkin and J. M. MacIntyre (1985). "Pancreatic cancer. Assessment of prognosis by clinical presentation." Cancer **56**(2): 397-402.

Kamata, H., S. Honda, S. Maeda, L. Chang, H. Hirata and M. Karin (2005). "Reactive oxygen species promote TNFalpha-induced death and sustained JNK activation by inhibiting MAP kinase phosphatases." Cell **120**(5): 649-661.

Kamb, A., N. A. Gruis, J. Weaver-Feldhaus, Q. Liu, K. Harshman, S. V. Tavtigian, E. Stockert, R. S. Day, 3rd, B. E. Johnson and M. H. Skolnick (1994). "A cell cycle regulator potentially involved in genesis of many tumor types." Science **264**(5157): 436-440.

Kanda, K., H. M. Hu, L. Zhang, J. Grandchamps and L. M. Boxer (2000). "NF-kappa B activity is required for the deregulation of c-myc expression by the immunoglobulin heavy chain enhancer." The Journal of biological chemistry **275**(41): 32338-32346.

Kaplan, D. H., V. Shankaran, A. S. Dighe, E. Stockert, M. Aguet, L. J. Old and R. D. Schreiber (1998). "Demonstration of an interferon gamma-dependent tumor surveillance system in immunocompetent mice." Proceedings of the National Academy of Sciences of the United States of America **95**(13): 7556-7561.

Karlic, R., H. R. Chung, J. Lasserre, K. Vlahovicek and M. Vingron (2010). "Histone modification levels are predictive for gene expression." Proceedings of the National Academy of Sciences of the United States of America **107**(7): 2926-2931.

Karpoff, H. M., D. S. Klimstra, M. F. Brennan and K. C. Conlon (2001). "Results of total pancreatectomy for adenocarcinoma of the pancreas." Archives of surgery **136**(1): 44-47; discussion 48.

Katoh, M. (2007). "Integrative genomic analyses on HES/HEY family: Notch-independent HES1, HES3 transcription in undifferentiated ES cells, and Notch-dependent HES1, HES5, HEY1, HEY2, HEYL transcription in fetal tissues, adult tissues, or cancer." International journal of oncology **31**(2): 461-466.

Kawaguchi, Y., B. Cooper, M. Gannon, M. Ray, R. J. MacDonald and C. V. Wright (2002). "The role of the transcriptional regulator Ptf1a in converting intestinal to pancreatic progenitors." Nature genetics **32**(1): 128-134.

Kayahara, M., T. Nagakawa, K. Ueno, T. Ohta, T. Takeda and I. Miyazaki (1993). "An evaluation of radical resection for pancreatic cancer based on the mode of recurrence as determined by autopsy and diagnostic imaging." Cancer **72**(7): 2118-2123.

Kempermann, G., H. G. Kuhn and F. H. Gage (1997a). "Genetic influence on neurogenesis in the dentate gyrus of adult mice." Proceedings of the National Academy of Sciences of the United States of America **94**(19): 10409-10414.

Kempermann, G., H. G. Kuhn and F. H. Gage (1997b). "More hippocampal neurons in adult mice living in an enriched environment." Nature **386**(6624): 493-495.

Kent, J., S. C. Wheatley, J. E. Andrews, A. H. Sinclair and P. Koopman (1996). "A male-specific role for SOX9 in vertebrate sex determination." Development **122**(9): 2813-2822.

Kim, B. Y., R. B. Gaynor, K. Song, A. Dritschilo and M. Jung (2002). "Constitutive activation of NF-kappaB in Ki-ras-transformed prostate epithelial cells." Oncogene **21**(29): 4490-4497.

Kim, J. E., K. T. Lee, J. K. Lee, S. W. Paik, J. C. Rhee and K. W. Choi (2004). "Clinical usefulness of carbohydrate antigen 19-9 as a screening test for pancreatic cancer in an asymptomatic population." Journal of gastroenterology and hepatology **19**(2): 182-186.

Klein, W. M., R. H. Hruban, A. J. Klein-Szanto and R. E. Wilentz (2002). "Direct correlation between proliferative activity and dysplasia in pancreatic intraepithelial neoplasia (PanIN): additional evidence for a recently proposed model of progression." Modern pathology : an official journal of the United States and Canadian Academy of Pathology, Inc **15**(4): 441-447.

Kliewer, S. A., J. M. Lenhard, T. M. Willson, I. Patel, D. C. Morris and J. M. Lehmann (1995). "A prostaglandin J2 metabolite binds peroxisome proliferator-activated receptor gamma and promotes adipocyte differentiation." Cell **83**(5): 813-819.

Kliewer, S. A., H. E. Xu, M. H. Lambert and T. M. Willson (2001). "Peroxisome proliferator-activated receptors: from genes to physiology." Recent progress in hormone research **56**: 239-263.

Klotz, L., S. Burgdorf, I. Dani, K. Saijo, J. Flossdorf, S. Hucke, J. Alferink, N. Nowak, M. Beyer, G. Mayer, B. Langhans, T. Klockgether, A. Waisman, G. Eberl, J. Schultze, M. Famulok, W. Kolanus, C. Glass, C. Kurts and P. A. Knolle (2009). "The nuclear receptor PPAR gamma selectively inhibits Th17 differentiation in a T cell-intrinsic fashion and suppresses CNS autoimmunity." The Journal of experimental medicine **206**(10): 2079-2089.

Knight, B., G. C. Yeoh, K. L. Husk, T. Ly, L. J. Abraham, C. Yu, J. A. Rhim and N. Fausto (2000). "Impaired preneoplastic changes and liver tumor formation in tumor necrosis factor receptor type 1 knockout mice." The Journal of experimental medicine **192**(12): 1809-1818.

Kojima, K., S. M. Vickers, N. V. Adsay, N. C. Jhala, H. G. Kim, T. R. Schoeb, W. E. Grizzle and C. A. Klug (2007). "Inactivation of Smad4 accelerates Kras(G12D)-mediated pancreatic neoplasia." Cancer research **67**(17): 8121-8130.

Konturek, P. C., A. Dembinski, Z. Warzecha, G. Burnat, P. Ceranowicz, E. G. Hahn, M. Dembinski, R. Tomaszewska and S. J. Konturek (2005). "Pioglitazone, a specific ligand of peroxisome proliferator-activated receptor-gamma, protects pancreas against acute cerulein-induced pancreatitis." World journal of gastroenterology : WJG **11**(40): 6322-6329.

Kopan, R. and M. X. Ilagan (2009). "The canonical Notch signaling pathway: unfolding the activation mechanism." Cell **137**(2): 216-233.

Kota, B. P., T. H. Huang and B. D. Roufogalis (2005a). "An overview on biological mechanisms of PPARs." Pharmacol Res **51**(2): 85-94.

Kota, B. P., T. H. Huang and B. D. Roufogalis (2005b). "An overview on biological mechanisms of PPARs." Pharmacological research : the official journal of the Italian Pharmacological Society **51**(2): 85-94.

Koukourakis, M. I., A. Giatromanolaki, A. L. Harris and E. Sivridis (2006). "Comparison of metabolic pathways between cancer cells and stromal cells in colorectal carcinomas: a metabolic survival role for tumor-associated stroma." Cancer Res **66**(2): 632-637.

Kouzarides, T. (2007). "Chromatin modifications and their function." Cell **128**(4): 693-705.

Kraman, M., P. J. Bambrough, J. N. Arnold, E. W. Roberts, L. Magiera, J. O. Jones, A. Gopinathan, D. A. Tuveson and D. T. Fearon (2010). "Suppression of antitumor immunity by stromal cells expressing fibroblast activation protein-alpha." Science **330**(6005): 827-830.

Krapp, A., M. Knofler, B. Ledermann, K. Burki, C. Berney, N. Zoerkler, O. Hagenbuchle and P. K. Wellauer (1998). "The bHLH protein PTF1-p48 is essential for the formation of the exocrine and the correct spatial organization of the endocrine pancreas." Genes & development **12**(23): 3752-3763.

Krummel, M. F. and J. P. Allison (1995). "CD28 and CTLA-4 have opposing effects on the response of T cells to stimulation." The Journal of experimental medicine **182**(2): 459-465.

Kubben, F. J., A. Peeters-Haesevoets, L. G. Engels, C. G. Baeten, B. Schutte, J. W. Arends, R. W. Stockbrugger and G. H. Blijham (1994). "Proliferating cell nuclear antigen (PCNA): a new marker to study human colonic cell proliferation." Gut **35**(4): 530-535.

Kubota, T., K. Koshizuka, E. A. Williamson, H. Asou, J. W. Said, S. Holden, I. Miyoshi and H. P. Koeffler (1998). "Ligand for peroxisome proliferator-activated receptor gamma (troglitazone) has potent antitumor effect against human prostate cancer both in vitro and in vivo." Cancer research **58**(15): 3344-3352.

Kuhn, R., F. Schwenk, M. Aguet and K. Rajewsky (1995). "Inducible gene targeting in mice." Science **269**(5229): 1427-1429.

Kulbe, H., P. Chakravarty, D. A. Leinster, K. A. Charles, J. Kwong, R. G. Thompson, J. I. Coward, T. Schioppa, S. C. Robinson, W. M. Gallagher, L. Galletta, M. A. Salako, J. F. Smyth, T. Hagemann, D. J. Brennan, D. D. Bowtell and F. R. Balkwill (2011). "A dynamic inflammatory cytokine network in the human ovarian cancer microenvironment." Cancer research.

Kulbe, H., R. Thompson, J. L. Wilson, S. Robinson, T. Hagemann, R. Fatah, D. Gould, A. Ayhan and F. Balkwill (2007). "The inflammatory cytokine tumor necrosis factor-alpha generates an autocrine tumor-promoting network in epithelial ovarian cancer cells." Cancer Res **67**(2): 585-592.

Kuper, H., H. O. Adami and D. Trichopoulos (2000). "Infections as a major preventable cause of human cancer." Journal of internal medicine **248**(3): 171-183.

Kushner, J. A., M. A. Ciemerych, E. Sicinska, L. M. Wartschow, M. Teta, S. Y. Long, P. Sicinski and M. F. White (2005). "Cyclins D2 and D1 are essential for postnatal pancreatic beta-cell growth." Molecular and cellular biology **25**(9): 3752-3762.

Kwak, E. L., J. Jankowski, S. P. Thayer, G. Y. Lauwers, B. W. Brannigan, P. L. Harris, R. A. Okimoto, S. M. Haserlat, D. R. Driscoll, D. Ferry, B. Muir, J. Settleman, C. S. Fuchs, M. H. Kulke, D. P. Ryan, J. W. Clark, D. C. Sgroi, D. A. Haber and D. W. Bell (2006). "Epidermal growth factor receptor kinase domain mutations in esophageal and pancreatic adenocarcinomas." Clinical cancer research : an official journal of the American Association for Cancer Research **12**(14 Pt 1): 4283-4287.

Lai, E. C. (2002). "Keeping a good pathway down: transcriptional repression of Notch pathway target genes by CSL proteins." EMBO reports **3**(9): 840-845.

Lammert, E., J. Brown and D. A. Melton (2000). "Notch gene expression during pancreatic organogenesis." Mechanisms of development **94**(1-2): 199-203.

Le, X., Q. Shi, B. Wang, Q. Xiong, C. Qian, Z. Peng, X. C. Li, H. Tang, J. L. Abbruzzese and K. Xie (2000). "Molecular regulation of constitutive expression of interleukin-8 in human pancreatic adenocarcinoma." Journal of interferon & cytokine research : the official journal of the International Society for Interferon and Cytokine Research **20**(11): 935-946.

Lee, J., J. Seo, H. Kim, J. B. Chung and K. H. Kim (2003). "Signal transduction of cerulein-induced cytokine expression and apoptosis in pancreatic acinar cells." Annals of the New York Academy of Sciences **1010**: 104-108.

Lefebvre, V., W. Huang, V. R. Harley, P. N. Goodfellow and B. de Crombrugghe (1997). "SOX9 is a potent activator of the chondrocyte-specific enhancer of the pro alpha1(II) collagen gene." Molecular and cellular biology **17**(4): 2336-2346.

Lehmann, J. M., J. M. Lenhard, B. B. Oliver, G. M. Ringold and S. A. Kliewer (1997). "Peroxisome proliferator-activated receptors alpha and gamma are activated by indomethacin and other non-steroidal anti-inflammatory drugs." The Journal of biological chemistry **272**(6): 3406-3410.

Lehmann, J. M., L. B. Moore, T. A. Smith-Oliver, W. O. Wilkison, T. M. Willson and S. A. Kliewer (1995). "An antidiabetic thiazolidinedione is a high affinity ligand for peroxisome proliferator-activated receptor gamma (PPAR gamma)." The Journal of biological chemistry **270**(22): 12953-12956.

Lesina, M., M. U. Kurkowski, K. Ludes, S. Rose-John, M. Treiber, G. Kloppel, A. Yoshimura, W. Reindl, B. Sipos, S. Akira, R. M. Schmid and H. Algul (2011). "Stat3/Socs3 activation by IL-6 transsignaling promotes progression of pancreatic intraepithelial neoplasia and development of pancreatic cancer." Cancer Cell **19**(4): 456-469.

Lewis, A. M., S. Varghese, H. Xu and H. R. Alexander (2006). "Interleukin-1 and cancer progression: the emerging role of interleukin-1 receptor antagonist as a novel therapeutic agent in cancer treatment." Journal of translational medicine **4**: 48.

Lewis, C. E. and J. W. Pollard (2006). "Distinct role of macrophages in different tumor microenvironments." Cancer research **66**(2): 605-612.

Li, B., M. Carey and J. L. Workman (2007). "The role of chromatin during transcription." Cell **128**(4): 707-719.

Li, B. and J. H. Wang (2009). "Fibroblasts and myofibroblasts in wound healing: Force generation and measurement." J Tissue Viability.

Li, D. and J. L. Abbruzzese (2010). "New strategies in pancreatic cancer: emerging epidemiologic and therapeutic concepts." Clinical cancer research : an official journal of the American Association for Cancer Research **16**(17): 4313-4318.

Li, G. and D. Reinberg (2011). "Chromatin higher-order structures and gene regulation." Current opinion in genetics & development **21**(2): 175-186.

Li, H. X., L. Xiao, C. Wang, J. L. Gao and Y. G. Zhai (2010). "Review: Epigenetic regulation of adipocyte differentiation and adipogenesis." Journal of Zhejiang University. Science. B **11**(10): 784-791.

Li, Q., D. Van Antwerp, F. Mercurio, K. F. Lee and I. M. Verma (1999). "Severe liver degeneration in mice lacking the IkappaB kinase 2 gene." Science **284**(5412): 321-325.

Li, Z. W., S. A. Omori, T. Labuda, M. Karin and R. C. Rickert (2003). "IKK beta is required for peripheral B cell survival and proliferation." J Immunol **170**(9): 4630-4637.

Liacini, A., J. Sylvester, W. Q. Li and M. Zafarullah (2002). "Inhibition of interleukin-1-stimulated MAP kinases, activating protein-1 (AP-1) and nuclear factor kappa B (NF-kappa B) transcription factors down-regulates matrix metalloproteinase gene expression in articular chondrocytes." Matrix biology : journal of the International Society for Matrix Biology **21**(3): 251-262.

Lioubinski, O., M. Muller, M. Wegner and M. Sander (2003). "Expression of Sox transcription factors in the developing mouse pancreas." Developmental dynamics : an official publication of the American Association of Anatomists **227**(3): 402-408.

Lobry, C., P. Oh and I. Aifantis (2011). "Oncogenic and tumor suppressor functions of Notch in cancer: it's NOTCH what you think." The Journal of experimental medicine **208**(10): 1931-1935.

Logunov, D. Y., D. V. Scheblyakov, O. V. Zubkova, M. M. Shmarov, I. V. Rakovskaya, K. V. Gurova, N. D. Tararova, L. G. Burdelya, B. S. Naroditsky, A. L. Ginzburg and A. V. Gudkov (2008). "Mycoplasma infection suppresses p53, activates NF-kappaB and cooperates with oncogenic Ras in rodent fibroblast transformation." Oncogene **27**(33): 4521-4531.

Lopez Hanninen, E., H. Amthauer, N. Hosten, J. Ricke, M. Bohmig, J. Langrehr, R. Hintze, P. Neuhaus, B. Wiedenmann, S. Rosewicz and R. Felix (2002). "Prospective evaluation of pancreatic tumors: accuracy of MR imaging with MR cholangiopancreatography and MR angiography." Radiology **224**(1): 34-41.

LoRusso, P. M., C. M. Rudin, J. C. Reddy, R. Tibes, G. J. Weiss, M. J. Borad, C. L. Hann, J. R. Brahmer, I. Chang, W. C. Darbonne, R. A. Graham, K. L. Zerivitz, J. A. Low and D. D. Von Hoff (2011). "Phase I trial of hedgehog pathway inhibitor vismodegib (GDC-0449) in patients with refractory, locally advanced or metastatic solid tumors." Clinical cancer research : an official journal of the American Association for Cancer Research **17**(8): 2502-2511.

Lowenfels, A. B., P. Maisonneuve, E. P. DiMagno, Y. Elitsur, L. K. Gates, Jr., J. Perrault and D. C. Whitcomb (1997). "Hereditary pancreatitis and the risk of pancreatic cancer. International Hereditary Pancreatitis Study Group." Journal of the National Cancer Institute **89**(6): 442-446.

Lu, T., S. S. Sathe, S. M. Swiatkowski, C. V. Hampole and G. R. Stark (2004). "Secretion of cytokines and growth factors as a general cause of constitutive NFkappaB activation in cancer." Oncogene **23**(12): 2138-2145.

Lu, T. and G. R. Stark (2004). "Cytokine overexpression and constitutive NFkappaB in cancer." Cell cycle **3**(9): 1114-1117.

Lu, Z., Y. Li, A. Takwi, B. Li, J. Zhang, D. J. Conklin, K. H. Young and R. Martin (2011). "miR-301a as an NF-kappaB activator in pancreatic cancer cells." EMBO J **30**(1): 57-67.

Luo, J. L., W. Tan, J. M. Ricono, O. Korchynskyi, M. Zhang, S. L. Gonias, D. A. Cheresh and M. Karin (2007). "Nuclear cytokine-activated IKKalpha controls prostate cancer metastasis by repressing Maspin." Nature **446**(7136): 690-694.

Luttges, J., H. Galehdari, V. Brocker, I. Schwarte-Waldhoff, D. Henne-Bruns, G. Kloppel, W. Schmiegel and S. A. Hahn (2001). "Allelic loss is often the first hit in the biallelic inactivation of the p53 and DPC4 genes during pancreatic carcinogenesis." The American journal of pathology **158**(5): 1677-1683.

Luttges, J., S. Neumann, R. Jesnowski, V. Borries, M. Lohr and G. Kloppel (2003). "Lack of apoptosis in PanIN-1 and PanIN-2 lesions associated with pancreatic ductal adenocarcinoma is not dependent on K-ras status." Pancreas **27**(3): e57-62.

Maeda, S., H. Kamata, J. L. Luo, H. Leffert and M. Karin (2005). "IKKbeta couples hepatocyte death to cytokine-driven compensatory proliferation that promotes chemical hepatocarcinogenesis." Cell **121**(7): 977-990.

Mahadevan, D. and D. D. Von Hoff (2007). "Tumor-stroma interactions in pancreatic ductal adenocarcinoma." Molecular cancer therapeutics **6**(4): 1186-1197.

Maitra, A., N. V. Adsay, P. Argani, C. Iacobuzio-Donahue, A. De Marzo, J. L. Cameron, C. J. Yeo and R. H. Hruban (2003). "Multicomponent analysis of the pancreatic adenocarcinoma progression model using a pancreatic intraepithelial neoplasia tissue microarray." Modern pathology : an official journal of the United States and Canadian Academy of Pathology, Inc **16**(9): 902-912.

Maliekal, T. T., J. Bajaj, V. Giri, D. Subramanyam and S. Krishna (2008). "The role of Notch signaling in human cervical cancer: implications for solid tumors." Oncogene **27**(38): 5110-5114.

Malka, D., P. Hammel, F. Maire, P. Rufat, I. Madeira, F. Pessione, P. Levy and P. Ruszniewski (2002). "Risk of pancreatic adenocarcinoma in chronic pancreatitis." Gut **51**(6): 849-852.

Maniati, E., R. Soper and T. Hagemann (2010). "Up for Mischief? IL-17/Th17 in the tumour microenvironment." Oncogene **29**(42): 5653-5662.

Mantovani, A. (2009). "Cancer: Inflaming metastasis." Nature **457**(7225): 36-37.

Mantovani, A., P. Allavena, A. Sica and F. Balkwill (2008). "Cancer-related inflammation." Nature **454**(7203): 436-444.

Mantovani, A., G. Germano, F. Marchesi, M. Locatelli and S. K. Biswas (2011). "Cancer-promoting tumor-associated macrophages: new vistas and open questions." European journal of immunology **41**(9): 2522-2525.

Mantovani, A., T. Schioppa, C. Porta, P. Allavena and A. Sica (2006). "Role of tumor-associated macrophages in tumor progression and invasion." Cancer metastasis reviews **25**(3): 315-322.

Martin, S. J., C. P. Reutelingsperger, A. J. McGahon, J. A. Rader, R. C. van Schie, D. M. LaFace and D. R. Green (1995). "Early redistribution of plasma membrane phosphatidylserine is a general feature of apoptosis regardless of the initiating stimulus: inhibition by overexpression of Bcl-2 and Abl." The Journal of experimental medicine **182**(5): 1545-1556.

Martinez Arias, A., V. Zecchini and K. Brennan (2002). "CSL-independent Notch signalling: a checkpoint in cell fate decisions during development?" Current opinion in genetics & development **12**(5): 524-533.

Masamune, A., K. Satoh, Y. Sakai, M. Yoshida, A. Satoh and T. Shimosegawa (2002). "Ligands of peroxisome proliferator-activated receptor-gamma induce apoptosis in AR42J cells." Pancreas **24**(2): 130-138.

Massague, J., J. Seoane and D. Wotton (2005). "Smad transcription factors." Genes & development **19**(23): 2783-2810.

Mathers, J. C. (2007). "Overview of genes, diet and cancer." Genes & nutrition **2**(1): 67-70.

Matsuno, K., R. J. Diederich, M. J. Go, C. M. Blaumueller and S. Artavanis-Tsakonas (1995). "Deltex acts as a positive regulator of Notch signaling through interactions with the Notch ankyrin repeats." Development **121**(8): 2633-2644.

Mattioni, T., J. F. Louvion and D. Picard (1994). "Regulation of protein activities by fusion to steroid binding domains." Methods in cell biology **43 Pt A**: 335-352.

Mauviel, A. (1993). "Cytokine regulation of metalloproteinase gene expression." Journal of cellular biochemistry **53**(4): 288-295.

Mazumder, S., D. Plesca and A. Almasan (2008). "Caspase-3 activation is a critical determinant of genotoxic stress-induced apoptosis." Methods in molecular biology **414**: 13-21.

Mazur, P. K., H. Einwachter, M. Lee, B. Sipos, H. Nakhai, R. Rad, U. Zimber-Strobl, L. J. Strobl, F. Radtke, G. Kloppel, R. M. Schmid and J. T. Siveke (2010a). "Notch2 is required for progression of pancreatic intraepithelial neoplasia and development of pancreatic ductal adenocarcinoma." Proc Natl Acad Sci U S A **107**(30): 13438-13443.

Mazur, P. K., B. M. Gruner, H. Nakhai, B. Sipos, U. Zimber-Strobl, L. J. Strobl, F. Radtke, R. M. Schmid and J. T. Siveke (2010b). "Identification of epidermal Pdx1 expression discloses different roles of Notch1 and Notch2 in murine Kras(G12D)-induced skin carcinogenesis in vivo." PloS one **5**(10): e13578.

Melisi, D., J. Niu, Z. Chang, Q. Xia, B. Peng, S. Ishiyama, D. B. Evans and P. J. Chiao (2009). "Secreted interleukin-1alpha induces a metastatic phenotype in pancreatic cancer by sustaining a constitutive activation of nuclear factor-kappaB." Molecular cancer research : MCR **7**(5): 624-633.

Metzger, D., J. Clifford, H. Chiba and P. Chambon (1995). "Conditional site-specific recombination in mammalian cells using a ligand-dependent chimeric Cre recombinase." Proc Natl Acad Sci U S A **92**(15): 6991-6995.

Meylan, E., A. L. Dooley, D. M. Feldser, L. Shen, E. Turk, C. Ouyang and T. Jacks (2009). "Requirement for NF-kappaB signalling in a mouse model of lung adenocarcinoma." Nature **462**(7269): 104-107.

Michalik, L., J. Auwerx, J. P. Berger, V. K. Chatterjee, C. K. Glass, F. J. Gonzalez, P. A. Grimaldi, T. Kadowaki, M. A. Lazar, S. O'Rahilly, C. N. Palmer, J. Plutzky, J. K. Reddy, B. M. Spiegelman, B. Staels and W. Wahli (2006). "International Union of Pharmacology. LXI. Peroxisome proliferator-activated receptors." Pharmacological reviews **58**(4): 726-741.

Minniti, S., C. Bruno, C. Biasiutti, D. Tonel, A. Falzone, M. Falconi and C. Procacci (2003). "Sonography versus helical CT in identification and staging of pancreatic ductal adenocarcinoma." Journal of clinical ultrasound : JCU **31**(4): 175-182.

Miyachi, K., M. J. Fritzler and E. M. Tan (1978). "Autoantibody to a nuclear antigen in proliferating cells." Journal of immunology **121**(6): 2228-2234.

Miyahara, Y., K. Odunsi, W. Chen, G. Peng, J. Matsuzaki and R. F. Wang (2008). "Generation and regulation of human CD4+ IL-17-producing T cells in ovarian cancer." Proceedings of the National Academy of Sciences of the United States of America **105**(40): 15505-15510.

Miyamoto, Y., A. Maitra, B. Ghosh, U. Zechner, P. Argani, C. A. Iacobuzio-Donahue, V. Sriuranpong, T. Iso, I. M. Meszoely, M. S. Wolfe, R. H. Hruban, D. W. Ball, R. M. Schmid and S. D. Leach (2003). "Notch mediates TGF alpha-induced changes in epithelial differentiation during pancreatic tumorigenesis." Cancer Cell **3**(6): 565-576.

Monami, M., C. Lamanna, N. Marchionni and E. Mannucci (2008). "Rosiglitazone and risk of cancer: a meta-analysis of randomized clinical trials." Diabetes care **31**(7): 1455-1460.

Monsalve, E., M. A. Perez, A. Rubio, M. J. Ruiz-Hidalgo, V. Baladron, J. J. Garcia-Ramirez, J. C. Gomez, J. Laborda and M. J. Diaz-Guerra (2006). "Notch-1 up-regulation and signaling following macrophage activation modulates gene expression patterns known to affect antigen-presenting capacity and cytotoxic activity." J Immunol **176**(9): 5362-5373.

Montagut, C. and J. Settleman (2009). "Targeting the RAF-MEK-ERK pathway in cancer therapy." Cancer letters **283**(2): 125-134.

Moore, M. J., D. Goldstein, J. Hamm, A. Figer, J. R. Hecht, S. Gallinger, H. J. Au, P. Murawa, D. Walde, R. A. Wolff, D. Campos, R. Lim, K. Ding, G. Clark, T. Voskoglou-Nomikos, M. Ptasynski and W. Parulekar (2007). "Erlotinib plus gemcitabine compared with gemcitabine alone in patients with advanced pancreatic cancer: a phase III trial of the National Cancer Institute of Canada Clinical Trials Group." Journal of clinical oncology : official journal of the American Society of Clinical Oncology **25**(15): 1960-1966.

Moore, R. J., D. M. Owens, G. Stamp, C. Arnott, F. Burke, N. East, H. Holdsworth, L. Turner, B. Rollins, M. Pasparakis, G. Kollias and F. Balkwill (1999). "Mice deficient in tumor necrosis factor-alpha are resistant to skin carcinogenesis." Nat Med **5**(7): 828-831.

Morais da Silva, S., A. Hacker, V. Harley, P. Goodfellow, A. Swain and R. Lovell-Badge (1996). "Sox9 expression during gonadal development implies a conserved

role for the gene in testis differentiation in mammals and birds." Nature genetics **14**(1): 62-68.

Moran, S. T., A. Cariappa, H. Liu, B. Muir, D. Sgroi, C. Boboila and S. Pillai (2007). "Synergism between NF-kappa B1/p50 and Notch2 during the development of marginal zone B lymphocytes." Journal of immunology **179**(1): 195-200.

Morris, J. P. t., D. A. Cano, S. Sekine, S. C. Wang and M. Hebrok (2010a). "Beta-catenin blocks Kras-dependent reprogramming of acini into pancreatic cancer precursor lesions in mice." J Clin Invest **120**(2): 508-520.

Morris, J. P. t. and M. Hebrok (2009). "It's a free for all--insulin-positive cells join the group of potential progenitors for pancreatic ductal adenocarcinoma." Cancer Cell **16**(5): 359-361.

Morris, J. P. t., S. C. Wang and M. Hebrok (2010b). "KRAS, Hedgehog, Wnt and the twisted developmental biology of pancreatic ductal adenocarcinoma." Nat Rev Cancer **10**(10): 683-695.

Moskaluk, C. A., R. H. Hruban and S. E. Kern (1997). "p16 and K-ras gene mutations in the intraductal precursors of human pancreatic adenocarcinoma." Cancer research **57**(11): 2140-2143.

Mueller, M. M. and N. E. Fusenig (2004). "Friends or foes - bipolar effects of the tumour stroma in cancer." Nat Rev Cancer **4**(11): 839-849.

Muerkoster, S., A. Arlt, M. Witt, A. Gehrz, S. Haye, C. March, F. Grohmann, K. Wegehenkel, H. Kalthoff, U. R. Folsch and H. Schafer (2003). "Usage of the NF-kappaB inhibitor sulfasalazine as sensitizing agent in combined chemotherapy of pancreatic cancer." International journal of cancer. Journal international du cancer **104**(4): 469-476.

Muerkoster, S., K. Wegehenkel, A. Arlt, M. Witt, B. Sipos, M. L. Kruse, T. Sebens, G. Kloppel, H. Kalthoff, U. R. Folsch and H. Schafer (2004). "Tumor stroma interactions induce chemoresistance in pancreatic ductal carcinoma cells involving increased secretion and paracrine effects of nitric oxide and interleukin-1beta." Cancer research **64**(4): 1331-1337.

Mullendore, M. E., J. B. Koorstra, Y. M. Li, G. J. Offerhaus, X. Fan, C. M. Henderson, W. Matsui, C. G. Eberhart, A. Maitra and G. Feldmann (2009). "Ligand-dependent Notch signaling is involved in tumor initiation and tumor maintenance in pancreatic cancer." Clinical cancer research : an official journal of the American Association for Cancer Research **15**(7): 2291-2301.

Murtaugh, L. C., B. Z. Stanger, K. M. Kwan and D. A. Melton (2003). "Notch signaling controls multiple steps of pancreatic differentiation." Proceedings of the National Academy of Sciences of the United States of America **100**(25): 14920-14925.

Muskhelishvili, L., J. R. Latendresse, R. L. Kodell and E. B. Henderson (2003). "Evaluation of cell proliferation in rat tissues with BrdU, PCNA, Ki-67(MIB-5) immunohistochemistry and in situ hybridization for histone mRNA." The journal of

histochemistry and cytochemistry : official journal of the Histochemistry Society **51**(12): 1681-1688.

Mysliwiec, P. and M. J. Boucher (2009). "Targeting Notch signaling in pancreatic cancer patients--rationale for new therapy." Advances in medical sciences **54**(2): 136-142.

Nakano, H., M. Shindo, S. Sakon, S. Nishinaka, M. Mihara, H. Yagita and K. Okumura (1998). "Differential regulation of IkappaB kinase alpha and beta by two upstream kinases, NF-kappaB-inducing kinase and mitogen-activated protein kinase/ERK kinase kinase-1." Proc Natl Acad Sci U S A **95**(7): 3537-3542.

Naugler, W. E. and M. Karin (2008). "The wolf in sheep's clothing: the role of interleukin-6 in immunity, inflammation and cancer." Trends Mol Med **14**(3): 109-119.

Neesse, A., P. Michl, K. K. Frese, C. Feig, N. Cook, M. A. Jacobetz, M. P. Lolkema, M. Buchholz, K. P. Olive, T. M. Gress and D. A. Tuveson (2010). "Stromal biology and therapy in pancreatic cancer." Gut.

Neri, A., C. C. Chang, L. Lombardi, M. Salina, P. Corradini, A. T. Maiolo, R. S. Chaganti and R. Dalla-Favera (1991). "B cell lymphoma-associated chromosomal translocation involves candidate oncogene lyt-10, homologous to NF-kappa B p50." Cell **67**(6): 1075-1087.

Ngo, V. N., R. M. Young, R. Schmitz, S. Jhavar, W. Xiao, K. H. Lim, H. Kohlhammer, W. Xu, Y. Yang, H. Zhao, A. L. Shaffer, P. Romesser, G. Wright, J. Powell, A. Rosenwald, H. K. Muller-Hermelink, G. Ott, R. D. Gascoyne, J. M. Connors, L. M. Rimsza, E. Campo, E. S. Jaffe, J. Delabie, E. B. Smeland, R. I. Fisher, R. M. Braziel, R. R. Tubbs, J. R. Cook, D. D. Weisenburger, W. C. Chan and L. M. Staudt (2011). "Oncogenically active MYD88 mutations in human lymphoma." Nature **470**(7332): 115-119.

Nicolas, M., A. Wolfer, K. Raj, J. A. Kummer, P. Mill, M. van Noort, C. C. Hui, H. Clevers, G. P. Dotto and F. Radtke (2003). "Notch1 functions as a tumor suppressor in mouse skin." Nature genetics **33**(3): 416-421.

Nieuwenhuijsen, B. W., Y. Huang, Y. Wang, F. Ramirez, G. Kalgaonkar and K. H. Young (2003). "A dual luciferase multiplexed high-throughput screening platform for protein-protein interactions." Journal of biomolecular screening **8**(6): 676-684.

Niu, J., Z. Li, B. Peng and P. J. Chiao (2004). "Identification of an autoregulatory feedback pathway involving interleukin-1alpha in induction of constitutive NF-kappaB activation in pancreatic cancer cells." The Journal of biological chemistry **279**(16): 16452-16462.

Nosjean, O. and J. A. Boutin (2002). "Natural ligands of PPARgamma: are prostaglandin J(2) derivatives really playing the part?" Cellular signalling **14**(7): 573-583.

Nowak, S. J. and V. G. Corces (2000). "Phosphorylation of histone H3 correlates with transcriptionally active loci." Genes & development **14**(23): 3003-3013.

Nowak, S. J. and V. G. Corces (2004). "Phosphorylation of histone H3: a balancing act between chromosome condensation and transcriptional activation." Trends in genetics : TIG **20**(4): 214-220.

Nowakowski, R. S., S. B. Lewin and M. W. Miller (1989). "Bromodeoxyuridine immunohistochemical determination of the lengths of the cell cycle and the DNA-synthetic phase for an anatomically defined population." Journal of neurocytology **18**(3): 311-318.

O'Hagan, R. C. and J. Heyer (2011). "KRAS Mouse Models: Modeling Cancer Harboring KRAS Mutations." Genes Cancer **2**(3): 335-343.

Oberhammer, F., J. W. Wilson, C. Dive, I. D. Morris, J. A. Hickman, A. E. Wakeling, P. R. Walker and M. Sikorska (1993). "Apoptotic death in epithelial cells: cleavage of DNA to 300 and/or 50 kb fragments prior to or in the absence of internucleosomal fragmentation." The EMBO journal **12**(9): 3679-3684.

Oeckinghaus, A., M. S. Hayden and S. Ghosh (2011). "Crosstalk in NF-kappaB signaling pathways." Nature immunology **12**(8): 695-708.

Offield, M. F., T. L. Jetton, P. A. Labosky, M. Ray, R. W. Stein, M. A. Magnuson, B. L. Hogan and C. V. Wright (1996). "PDX-1 is required for pancreatic outgrowth and differentiation of the rostral duodenum." Development **122**(3): 983-995.

Okusaka, T., S. Okada, H. Ueno, M. Ikeda, K. Shimada, J. Yamamoto, T. Kosuge, S. Yamasaki, N. Fukushima and M. Sakamoto (2001). "Abdominal pain in patients with resectable pancreatic cancer with reference to clinicopathologic findings." Pancreas **22**(3): 279-284.

Olive, K. P., M. A. Jacobetz, C. J. Davidson, A. Gopinathan, D. McIntyre, D. Honess, B. Madhu, M. A. Goldgraben, M. E. Caldwell, D. Allard, K. K. Frese, G. Denicola, C. Feig, C. Combs, S. P. Winter, H. Ireland-Zecchini, S. Reichelt, W. J. Howat, A. Chang, M. Dhara, L. Wang, F. Ruckert, R. Grutzmann, C. Pilarsky, K. Izeradjene, S. R. Hingorani, P. Huang, S. E. Davies, W. Plunkett, M. Egorin, R. H. Hruban, N. Whitebread, K. McGovern, J. Adams, C. Iacobuzio-Donahue, J. Griffiths and D. A. Tuveson (2009). "Inhibition of Hedgehog signaling enhances delivery of chemotherapy in a mouse model of pancreatic cancer." Science **324**(5933): 1457-1461.

Oliveira-Cunha, M., W. G. Newman and A. K. Siriwardena (2011). "Epidermal Growth Factor Receptor in Pancreatic Cancer." Cancers **3**(2): 1513-1526.

Olson, P. and D. Hanahan (2009). "Cancer. Breaching the cancer fortress." Science **324**(5933): 1400-1401.

Orban, P. C., D. Chui and J. D. Marth (1992). "Tissue- and site-specific DNA recombination in transgenic mice." Proceedings of the National Academy of Sciences of the United States of America **89**(15): 6861-6865.

Ordentlich, P., A. Lin, C. P. Shen, C. Blaumueller, K. Matsuno, S. Artavanis-Tsakonas and T. Kadesch (1998). "Notch inhibition of E47 supports the existence of a novel signaling pathway." Molecular and cellular biology **18**(4): 2230-2239.

Orimo, A. and R. A. Weinberg (2006). "Stromal fibroblasts in cancer: a novel tumor-promoting cell type." Cell Cycle **5**(15): 1597-1601.

Ornitz, D. M., R. E. Hammer, A. Messing, R. D. Palmiter and R. L. Brinster (1987). "Pancreatic neoplasia induced by SV40 T-antigen expression in acinar cells of transgenic mice." Science **238**(4824): 188-193.

Ostman, A. and M. Augsten (2009). "Cancer-associated fibroblasts and tumor growth - bystanders turning into key players." Curr Opin Genet Dev.

Ostrand-Rosenberg, S. (2008). "Immune surveillance: a balance between protumor and antitumor immunity." Current opinion in genetics & development **18**(1): 11-18.

Ottenhof, N. A., A. N. Milne, F. H. Morsink, P. Drillenburg, F. J. Ten Kate, A. Maitra and G. J. Offerhaus (2009). "Pancreatic intraepithelial neoplasia and pancreatic tumorigenesis: of mice and men." Archives of pathology & laboratory medicine **133**(3): 375-381.

Paget, S. (1989). "The distribution of secondary growths in cancer of the breast. 1889." Cancer metastasis reviews **8**(2): 98-101.

Pahl, H. L. (1999). "Activators and target genes of Rel/NF-kappaB transcription factors." Oncogene **18**(49): 6853-6866.

Palaga, T., C. Buranaruk, S. Rengpipat, A. H. Fauq, T. E. Golde, S. H. Kaufmann and B. A. Osborne (2008). "Notch signaling is activated by TLR stimulation and regulates macrophage functions." Eur J Immunol **38**(1): 174-183.

Palomero, T., W. K. Lim, D. T. Odom, M. L. Sulis, P. J. Real, A. Margolin, K. C. Barnes, J. O'Neil, D. Neuberg, A. P. Weng, J. C. Aster, F. Sigaux, J. Soulier, A. T. Look, R. A. Young, A. Califano and A. A. Ferrando (2006). "NOTCH1 directly regulates c-MYC and activates a feed-forward-loop transcriptional network promoting leukemic cell growth." Proceedings of the National Academy of Sciences of the United States of America **103**(48): 18261-18266.

Pan, Z. G. and B. Wang (2007). "Anaplastic carcinoma of the pancreas associated with a mucinous cystic adenocarcinoma. A case report and review of the literature." JOP : Journal of the pancreas **8**(6): 775-782.

Pasca di Magliano, M., A. V. Biankin, P. W. Heiser, D. A. Cano, P. J. Gutierrez, T. Deramaudt, D. Segara, A. C. Dawson, J. G. Kench, S. M. Henshall, R. L. Sutherland, A. Dlugosz, A. K. Rustgi and M. Hebrok (2007). "Common activation of canonical Wnt signaling in pancreatic adenocarcinoma." PLoS ONE **2**(11): e1155.

Pasca di Magliano, M., S. Sekine, A. Ermilov, J. Ferris, A. A. Dlugosz and M. Hebrok (2006). "Hedgehog/Ras interactions regulate early stages of pancreatic cancer." Genes Dev **20**(22): 3161-3173.

Pascual, G., A. L. Fong, S. Ogawa, A. Gamliel, A. C. Li, V. Perissi, D. W. Rose, T. M. Willson, M. G. Rosenfeld and C. K. Glass (2005). "A SUMOylation-dependent pathway mediates transrepression of inflammatory response genes by PPAR-gamma." Nature **437**(7059): 759-763.

Pasparakis, M., L. Alexopoulou, V. Episkopou and G. Kollias (1996). "Immune and inflammatory responses in TNF alpha-deficient mice: a critical requirement for TNF alpha in the formation of primary B cell follicles, follicular dendritic cell networks and germinal centers, and in the maturation of the humoral immune response." The Journal of experimental medicine **184**(4): 1397-1411.

Permuth-Wey, J. and K. M. Egan (2009). "Family history is a significant risk factor for pancreatic cancer: results from a systematic review and meta-analysis." Familial cancer **8**(2): 109-117.

Phielix, E., J. Szendroedi and M. Roden (2011). "The role of metformin and thiazolidinediones in the regulation of hepatic glucose metabolism and its clinical impact." Trends in pharmacological sciences **32**(10): 607-616.

Philip, M., D. A. Rowley and H. Schreiber (2004). "Inflammation as a tumor promoter in cancer induction." Semin Cancer Biol **14**(6): 433-439.

Pierce, J. W., R. Schoenleber, G. Jesmok, J. Best, S. A. Moore, T. Collins and M. E. Gerritsen (1997). "Novel inhibitors of cytokine-induced IkappaBalpha phosphorylation and endothelial cell adhesion molecule expression show anti-inflammatory effects in vivo." The Journal of biological chemistry **272**(34): 21096-21103.

Pietras, K. and A. Ostman (2010). "Hallmarks of cancer: interactions with the tumor stroma." Exp Cell Res **316**(8): 1324-1331.

Pikarsky, E., R. M. Porat, I. Stein, R. Abramovitch, S. Amit, S. Kasem, E. Gutkovich-Pyest, S. Urieli-Shoval, E. Galun and Y. Ben-Neriah (2004). "NF-kappaB functions as a tumour promoter in inflammation-associated cancer." Nature **431**(7007): 461-466.

Pin, C. L., A. C. Bonvissuto and S. F. Konieczny (2000). "Mist1 expression is a common link among serous exocrine cells exhibiting regulated exocytosis." The Anatomical record **259**(2): 157-167.

Piper, K., S. G. Ball, J. W. Keeling, S. Mansoor, D. I. Wilson and N. A. Hanley (2002). "Novel SOX9 expression during human pancreas development correlates to abnormalities in Campomelic dysplasia." Mechanisms of development **116**(1-2): 223-226.

Plentz, R., J. S. Park, A. D. Rhim, D. Abravanel, A. F. Hezel, S. V. Sharma, S. Gurumurthy, V. Deshpande, C. Kenific, J. Settleman, P. K. Majumder, B. Z. Stanger and N. Bardeesy (2009). "Inhibition of gamma-secretase activity inhibits tumor progression in a mouse model of pancreatic ductal adenocarcinoma." Gastroenterology **136**(5): 1741-1749 e1746.

Plunkett, W., P. Huang and V. Gandhi (1995). "Preclinical characteristics of gemcitabine." Anti-cancer drugs **6 Suppl 6**: 7-13.

Plutzky, J. (2003). "The potential role of peroxisome proliferator-activated receptors on inflammation in type 2 diabetes mellitus and atherosclerosis." The American journal of cardiology **92**(4A): 34J-41J.

Porta, C., E. Riboldi and A. Sica (2011). "Mechanisms linking pathogens-associated inflammation and cancer." Cancer letters **305**(2): 250-262.

Prives, C. and V. Gottifredi (2008). "The p21 and PCNA partnership: a new twist for an old plot." Cell cycle **7**(24): 3840-3846.

Puente, X. S., M. Pinyol, V. Quesada, L. Conde, G. R. Ordonez, N. Villamor, G. Escaramis, P. Jares, S. Bea, M. Gonzalez-Diaz, L. Bassaganyas, T. Baumann, M. Juan, M. Lopez-Guerra, D. Colomer, J. M. Tubio, C. Lopez, A. Navarro, C. Tornador, M. Aymerich, M. Rozman, J. M. Hernandez, D. A. Puente, J. M. Freije, G. Velasco, A. Gutierrez-Fernandez, D. Costa, A. Carrio, S. Guijarro, A. Enjuanes, L. Hernandez, J. Yague, P. Nicolas, C. M. Romeo-Casabona, H. Himmelbauer, E. Castillo, J. C. Dohm, S. de Sanjose, M. A. Piris, E. de Alava, J. San Miguel, R. Royo, J. L. Gelpi, D. Torrents, M. Orozco, D. G. Pisano, A. Valencia, R. Guigo, M. Bayes, S. Heath, M. Gut, P. Klatt, J. Marshall, K. Raine, L. A. Stebbings, P. A. Futreal, M. R. Stratton, P. J. Campbell, I. Gut, A. Lopez-Guillermo, X. Estivill, E. Montserrat, C. Lopez-Otin and E. Campo (2011). "Whole-genome sequencing identifies recurrent mutations in chronic lymphocytic leukaemia." Nature **475**(7354): 101-105.

Qian, B. Z. and J. W. Pollard (2010). "Macrophage diversity enhances tumor progression and metastasis." Cell **141**(1): 39-51.

Quaife, C. J., C. A. Pinkert, D. M. Ornitz, R. D. Palmiter and R. L. Brinster (1987). "Pancreatic neoplasia induced by ras expression in acinar cells of transgenic mice." Cell **48**(6): 1023-1034.

Quesada, I., E. Tuduri, C. Ripoll and A. Nadal (2008). "Physiology of the pancreatic alpha-cell and glucagon secretion: role in glucose homeostasis and diabetes." The Journal of endocrinology **199**(1): 5-19.

Rachet, B., C. Maringe, U. Nur, M. Quaresma, A. Shah, L. M. Woods, L. Ellis, S. Walters, D. Forman, J. Steward and M. P. Coleman (2009). "Population-based cancer survival trends in England and Wales up to 2007: an assessment of the NHS cancer plan for England." The lancet oncology **10**(4): 351-369.

Radisky, D. C., P. A. Kenny and M. J. Bissell (2007). "Fibrosis and cancer: do myofibroblasts come also from epithelial cells via EMT?" J Cell Biochem **101**(4): 830-839.

Rakoff-Nahoum, S. (2006). "Why cancer and inflammation?" The Yale journal of biology and medicine **79**(3-4): 123-130.

Ramain, P., K. Khechumian, L. Seugnet, N. Arbogast, C. Ackermann and P. Heitzler (2001). "Novel Notch alleles reveal a Deltex-dependent pathway repressing neural fate." Current biology : CB **11**(22): 1729-1738.

Ranganathan, P., K. L. Weaver and A. J. Capobianco (2011). "Notch signalling in solid tumours: a little bit of everything but not all the time." Nature reviews. Cancer **11**(5): 338-351.

Reedijk, M., S. Odorcic, L. Chang, H. Zhang, N. Miller, D. R. McCready, G. Lockwood and S. E. Egan (2005). "High-level coexpression of JAG1 and NOTCH1 is observed in human breast cancer and is associated with poor overall survival." Cancer research **65**(18): 8530-8537.

Richmond, A. and Y. Su (2008). "Mouse xenograft models vs GEM models for human cancer therapeutics." Disease models & mechanisms **1**(2-3): 78-82.

Rocha Lima, C. M., M. R. Green, R. Rotche, W. H. Miller, Jr., G. M. Jeffrey, L. A. Cisar, A. Morganti, N. Orlando, G. Gruia and L. L. Miller (2004). "Irinotecan plus gemcitabine results in no survival advantage compared with gemcitabine monotherapy in patients with locally advanced or metastatic pancreatic cancer despite increased tumor response rate." Journal of clinical oncology : official journal of the American Society of Clinical Oncology **22**(18): 3776-3783.

Rollins, M. D., S. Sudarshan, M. A. Firpo, B. H. Etherington, B. J. Hart, H. H. Jackson, J. D. Jackson, L. L. Emerson, D. T. Yang, S. J. Mulvihill and R. E. Glasgow (2006). "Anti-inflammatory effects of PPAR-gamma agonists directly correlate with PPAR-gamma expression during acute pancreatitis." Journal of gastrointestinal surgery : official journal of the Society for Surgery of the Alimentary Tract **10**(8): 1120-1130.

Romagosa, C., S. Simonetti, L. Lopez-Vicente, A. Mazo, M. E. Lleonart, J. Castellvi and S. Ramon y Cajal (2011). "p16(Ink4a) overexpression in cancer: a tumor suppressor gene associated with senescence and high-grade tumors." Oncogene **30**(18): 2087-2097.

Rooman, I., N. De Medts, L. Baeyens, J. Lardon, S. De Breuck, H. Heimberg and L. Bouwens (2006). "Expression of the Notch signaling pathway and effect on exocrine cell proliferation in adult rat pancreas." The American journal of pathology **169**(4): 1206-1214.

Rosen, E. D. and O. A. MacDougald (2006). "Adipocyte differentiation from the inside out." Nature reviews. Molecular cell biology **7**(12): 885-896.

Rossi, A., P. Kapahi, G. Natoli, T. Takahashi, Y. Chen, M. Karin and M. G. Santoro (2000). "Anti-inflammatory cyclopentenone prostaglandins are direct inhibitors of IkappaB kinase." Nature **403**(6765): 103-108.

Roy, M., W. S. Pear and J. C. Aster (2007). "The multifaceted role of Notch in cancer." Current opinion in genetics & development **17**(1): 52-59.

Rudolph, D., W. C. Yeh, A. Wakeham, B. Rudolph, D. Nallainathan, J. Potter, A. J. Elia and T. W. Mak (2000). "Severe liver degeneration and lack of NF-kappaB

activation in NEMO/IKKgamma-deficient mice." Genes & development **14**(7): 854-862.

Ruffell, B., D. G. DeNardo, N. I. Affara and L. M. Coussens (2010). "Lymphocytes in cancer development: polarization towards pro-tumor immunity." Cytokine & growth factor reviews **21**(1): 3-10.

Saha, A., R. Kaul, M. Murakami and E. S. Robertson (2010). "Tumor viruses and cancer biology: Modulating signaling pathways for therapeutic intervention." Cancer biology & therapy **10**(10): 961-978.

Sakurai, T., S. Maeda, L. Chang and M. Karin (2006). "Loss of hepatic NF-kappa B activity enhances chemical hepatocarcinogenesis through sustained c-Jun N-terminal kinase 1 activation." Proceedings of the National Academy of Sciences of the United States of America **103**(28): 10544-10551.

Salma, N., H. Xiao and A. N. Imbalzano (2006). "Temporal recruitment of CCAAT/enhancer-binding proteins to early and late adipogenic promoters in vivo." Journal of molecular endocrinology **36**(1): 139-151.

Sansone, P., G. Storci, S. Tavolari, T. Guarnieri, C. Giovannini, M. Taffurelli, C. Ceccarelli, D. Santini, P. Paterini, K. B. Marcu, P. Chieco and M. Bonafe (2007). "IL-6 triggers malignant features in mammospheres from human ductal breast carcinoma and normal mammary gland." The Journal of clinical investigation **117**(12): 3988-4002.

Sarraf, P., E. Mueller, D. Jones, F. J. King, D. J. DeAngelo, J. B. Partridge, S. A. Holden, L. B. Chen, S. Singer, C. Fletcher and B. M. Spiegelman (1998). "Differentiation and reversal of malignant changes in colon cancer through PPARgamma." Nature medicine **4**(9): 1046-1052.

Sasai, Y., R. Kageyama, Y. Tagawa, R. Shigemoto and S. Nakanishi (1992). "Two mammalian helix-loop-helix factors structurally related to Drosophila hairy and Enhancer of split." Genes & development **6**(12B): 2620-2634.

Sato, N., N. Maehara and M. Goggins (2004). "Gene expression profiling of tumor-stromal interactions between pancreatic cancer cells and stromal fibroblasts." Cancer Res **64**(19): 6950-6956.

Sauer, B. (1987). "Functional expression of the cre-lox site-specific recombination system in the yeast Saccharomyces cerevisiae." Molecular and cellular biology **7**(6): 2087-2096.

Sauer, B. and N. Henderson (1988). "Site-specific DNA recombination in mammalian cells by the Cre recombinase of bacteriophage P1." Proceedings of the National Academy of Sciences of the United States of America **85**(14): 5166-5170.

Sawai, H., J. Liu, H. A. Reber, O. J. Hines and G. Eibl (2006). "Activation of peroxisome proliferator-activated receptor-gamma decreases pancreatic cancer cell invasion through modulation of the plasminogen activator system." Molecular cancer research : MCR **4**(3): 159-167.

Sawey, E. T., J. A. Johnson and H. C. Crawford (2007). "Matrix metalloproteinase 7 controls pancreatic acinar cell transdifferentiation by activating the Notch signaling pathway." Proceedings of the National Academy of Sciences of the United States of America **104**(49): 19327-19332.

Schmitt, T. M. and J. C. Zuniga-Pflucker (2002). "Induction of T cell development from hematopoietic progenitor cells by delta-like-1 in vitro." Immunity **17**(6): 749-756.

Schneider, G., A. Henrich, G. Greiner, V. Wolf, A. Lovas, M. Wieczorek, T. Wagner, S. Reichardt, A. von Werder, R. M. Schmid, F. Weih, T. Heinzel, D. Saur and O. H. Kramer (2010). "Cross talk between stimulated NF-kappaB and the tumor suppressor p53." Oncogene **29**(19): 2795-2806.

Schreiber, F. S., T. B. Deramaudt, T. B. Brunner, M. I. Boretti, K. J. Gooch, D. A. Stoffers, E. J. Bernhard and A. K. Rustgi (2004). "Successful growth and characterization of mouse pancreatic ductal cells: functional properties of the Ki-RAS(G12V) oncogene." Gastroenterology **127**(1): 250-260.

Schreiber, R. D., L. J. Old and M. J. Smyth (2011). "Cancer immunoediting: integrating immunity's roles in cancer suppression and promotion." Science **331**(6024): 1565-1570.

Schubeler, D., C. Francastel, D. M. Cimbora, A. Reik, D. I. Martin and M. Groudine (2000). "Nuclear localization and histone acetylation: a pathway for chromatin opening and transcriptional activation of the human beta-globin locus." Genes & development **14**(8): 940-950.

Schulz, T. J., M. Glaubitz, D. Kuhlow, R. Thierbach, M. Birringer, P. Steinberg, A. F. Pfeiffer and M. Ristow (2007). "Variable expression of Cre recombinase transgenes precludes reliable prediction of tissue-specific gene disruption by tail-biopsy genotyping." PloS one **2**(10): e1013.

Schwarzbich, M. A., M. Gutknecht, J. Salih, H. R. Salih, P. Brossart, S. M. Rittig and F. Grunebach (2012). "The immune inhibitory receptor osteoactivin is upregulated in monocyte-derived dendritic cells by BCR-ABL tyrosine kinase inhibitors." Cancer immunology, immunotherapy : CII **61**(2): 193-202.

Scian, M. J., K. E. Stagliano, M. A. Anderson, S. Hassan, M. Bowman, M. F. Miles, S. P. Deb and S. Deb (2005). "Tumor-derived p53 mutants induce NF-kappaB2 gene expression." Molecular and cellular biology **25**(22): 10097-10110.

Secchiero, P., E. Melloni, M. G. di Iasio, M. Tiribelli, E. Rimondi, F. Corallini, V. Gattei and G. Zauli (2009). "Nutlin-3 up-regulates the expression of Notch1 in both myeloid and lymphoid leukemic cells, as part of a negative feedback antiapoptotic mechanism." Blood **113**(18): 4300-4308.

Senftleben, U., Z. W. Li, V. Baud and M. Karin (2001). "IKKbeta is essential for protecting T cells from TNFalpha-induced apoptosis." Immunity **14**(3): 217-230.

Sethi, N. and Y. Kang (2011). "Notch signalling in cancer progression and bone metastasis." British journal of cancer.

Seymour, P. A., K. K. Freude, C. L. Dubois, H. P. Shih, N. A. Patel and M. Sander (2008). "A dosage-dependent requirement for Sox9 in pancreatic endocrine cell formation." Developmental biology **323**(1): 19-30.

Seymour, P. A., K. K. Freude, M. N. Tran, E. E. Mayes, J. Jensen, R. Kist, G. Scherer and M. Sander (2007). "SOX9 is required for maintenance of the pancreatic progenitor cell pool." Proceedings of the National Academy of Sciences of the United States of America **104**(6): 1865-1870.

Sfanos, K. S., T. C. Bruno, C. H. Maris, L. Xu, C. J. Thoburn, A. M. DeMarzo, A. K. Meeker, W. B. Isaacs and C. G. Drake (2008). "Phenotypic analysis of prostate-infiltrating lymphocytes reveals TH17 and Treg skewing." Clinical cancer research : an official journal of the American Association for Cancer Research **14**(11): 3254-3261.

Shah, S. A., M. W. Potter, T. P. McDade, R. Ricciardi, R. A. Perugini, P. J. Elliott, J. Adams and M. P. Callery (2001). "26S proteasome inhibition induces apoptosis and limits growth of human pancreatic cancer." Journal of cellular biochemistry **82**(1): 110-122.

Shankaran, V., H. Ikeda, A. T. Bruce, J. M. White, P. E. Swanson, L. J. Old and R. D. Schreiber (2001). "IFNgamma and lymphocytes prevent primary tumour development and shape tumour immunogenicity." Nature **410**(6832): 1107-1111.

Shao, H., L. Cai, J. M. Grichnik, A. S. Livingstone, O. C. Velazquez and Z. J. Liu (2011). "Activation of Notch1 signaling in stromal fibroblasts inhibits melanoma growth by upregulating WISP-1." Oncogene **30**(42): 4316-4326.

Sharma, C., K. M. Eltawil, P. D. Renfrew, M. J. Walsh and M. Molinari (2011a). "Advances in diagnosis, treatment and palliation of pancreatic carcinoma: 1990-2010." World journal of gastroenterology : WJG **17**(7): 867-897.

Sharma, P., K. Wagner, J. D. Wolchok and J. P. Allison (2011b). "Novel cancer immunotherapy agents with survival benefit: recent successes and next steps." Nature reviews. Cancer **11**(11): 805-812.

Sharma, V. M., J. A. Calvo, K. M. Draheim, L. A. Cunningham, N. Hermance, L. Beverly, V. Krishnamoorthy, M. Bhasin, A. J. Capobianco and M. A. Kelliher (2006). "Notch1 contributes to mouse T-cell leukemia by directly inducing the expression of c-myc." Molecular and cellular biology **26**(21): 8022-8031.

Shearman, M. S., D. Beher, E. E. Clarke, H. D. Lewis, T. Harrison, P. Hunt, A. Nadin, A. L. Smith, G. Stevenson and J. L. Castro (2000). "L-685,458, an aspartyl protease transition state mimic, is a potent inhibitor of amyloid beta-protein precursor gamma-secretase activity." Biochemistry **39**(30): 8698-8704.

Shen, M., P. Boffetta, J. H. Olsen, A. Andersen, K. Hemminki, E. Pukkala, E. Tracey, D. H. Brewster, M. L. McBride, V. Pompe-Kirn, E. V. Kliewer, J. M. Tonita, K. S. Chia, C. Martos, J. G. Jonasson, D. Colin, G. Scelo and P. Brennan (2006). "A pooled analysis of second primary pancreatic cancer." American journal of epidemiology **163**(6): 502-511.

Sherr, C. J. (2004). "Principles of tumor suppression." Cell **116**(2): 235-246.

Shevach, E. M., R. S. McHugh, C. A. Piccirillo and A. M. Thornton (2001). "Control of T-cell activation by CD4+ CD25+ suppressor T cells." Immunological reviews **182**: 58-67.

Shi, G., L. Zhu, Y. Sun, R. Bettencourt, B. Damsz, R. H. Hruban and S. F. Konieczny (2009). "Loss of the acinar-restricted transcription factor Mist1 accelerates Kras-induced pancreatic intraepithelial neoplasia." Gastroenterology **136**(4): 1368-1378.

Shih, V. F., R. Tsui, A. Caldwell and A. Hoffmann (2011). "A single NFkappaB system for both canonical and non-canonical signaling." Cell research **21**(1): 86-102.

Shimazaki, N., N. Togashi, M. Hanai, T. Isoyama, K. Wada, T. Fujita, K. Fujiwara and S. Kurakata (2008). "Anti-tumour activity of CS-7017, a selective peroxisome proliferator-activated receptor gamma agonist of thiazolidinedione class, in human tumour xenografts and a syngeneic tumour implant model." European journal of cancer **44**(12): 1734-1743.

Shimizu, K., K. Shiratori, N. Hayashi, M. Kobayashi, T. Fujiwara and H. Horikoshi (2002). "Thiazolidinedione derivatives as novel therapeutic agents to prevent the development of chronic pancreatitis." Pancreas **24**(2): 184-190.

Shiojiri, T., K. Wada, A. Nakajima, K. Katayama, A. Shibuya, C. Kudo, T. Kadowaki, T. Mayumi, Y. Yura and Y. Kamisaki (2002). "PPAR gamma ligands inhibit nitrotyrosine formation and inflammatory mediator expressions in adjuvant-induced rheumatoid arthritis mice." European journal of pharmacology **448**(2-3): 231-238.

Sica, A. (2010). "Role of tumour-associated macrophages in cancer-related inflammation." Experimental oncology **32**(3): 153-158.

Sivasankaran, B., M. Degen, A. Ghaffari, M. E. Hegi, M. F. Hamou, M. C. Ionescu, C. Zweifel, M. Tolnay, M. Wasner, S. Mergenthaler, A. R. Miserez, R. Kiss, M. M. Lino, A. Merlo, R. Chiquet-Ehrismann and J. L. Boulay (2009). "Tenascin-C is a novel RBPJkappa-induced target gene for Notch signaling in gliomas." Cancer research **69**(2): 458-465.

Siveke, J. T., C. Lubeseder-Martellato, M. Lee, P. K. Mazur, H. Nakhai, F. Radtke and R. M. Schmid (2008). "Notch signaling is required for exocrine regeneration after acute pancreatitis." Gastroenterology **134**(2): 544-555.

Skinner, M. K., A. Rawls, J. Wilson-Rawls and E. H. Roalson (2010). "Basic helix-loop-helix transcription factor gene family phylogenetics and nomenclature." Differentiation; research in biological diversity **80**(1): 1-8.

Soloaga, A., S. Thomson, G. R. Wiggin, N. Rampersaud, M. H. Dyson, C. A. Hazzalin, L. C. Mahadevan and J. S. Arthur (2003). "MSK2 and MSK1 mediate the mitogen- and stress-induced phosphorylation of histone H3 and HMG-14." The EMBO journal **22**(11): 2788-2797.

Solt, L. A., L. A. Madge, J. S. Orange and M. J. May (2007). "Interleukin-1-induced NF-kappaB activation is NEMO-dependent but does not require IKKbeta." The Journal of biological chemistry **282**(12): 8724-8733.

Song, L. L., Y. Peng, J. Yun, P. Rizzo, V. Chaturvedi, S. Weijzen, W. M. Kast, P. J. Stone, L. Santos, A. Loredo, U. Lendahl, G. Sonenshein, B. Osborne, J. Z. Qin, A. Pannuti, B. J. Nickoloff and L. Miele (2008). "Notch-1 associates with IKKalpha and regulates IKK activity in cervical cancer cells." Oncogene **27**(44): 5833-5844.

Soussi, T. and G. Lozano (2005). "p53 mutation heterogeneity in cancer." Biochemical and biophysical research communications **331**(3): 834-842.

Soussi, T. and K. G. Wiman (2007). "Shaping genetic alterations in human cancer: the p53 mutation paradigm." Cancer Cell **12**(4): 303-312.

Spaeth, E. L., J. L. Dembinski, A. K. Sasser, K. Watson, A. Klopp, B. Hall, M. Andreeff and F. Marini (2009). "Mesenchymal stem cell transition to tumor-associated fibroblasts contributes to fibrovascular network expansion and tumor progression." PloS one **4**(4): e4992.

Sparmann, A. and D. Bar-Sagi (2004). "Ras-induced interleukin-8 expression plays a critical role in tumor growth and angiogenesis." Cancer Cell **6**(5): 447-458.

Srinivas, S., T. Watanabe, C. S. Lin, C. M. William, Y. Tanabe, T. M. Jessell and F. Costantini (2001). "Cre reporter strains produced by targeted insertion of EYFP and ECFP into the ROSA26 locus." BMC developmental biology **1**: 4.

Staeheli, P., P. Danielson, O. Haller and J. G. Sutcliffe (1986). "Transcriptional activation of the mouse Mx gene by type I interferon." Molecular and cellular biology **6**(12): 4770-4774.

Steinberg, W. (1990). "The clinical utility of the CA 19-9 tumor-associated antigen." The American journal of gastroenterology **85**(4): 350-355.

Stevens, R. J., A. W. Roddam and V. Beral (2007). "Pancreatic cancer in type 1 and young-onset diabetes: systematic review and meta-analysis." British journal of cancer **96**(3): 507-509.

Stockhausen, M. T., J. Sjolund and H. Axelson (2005). "Regulation of the Notch target gene Hes-1 by TGFalpha induced Ras/MAPK signaling in human neuroblastoma cells." Experimental cell research **310**(1): 218-228.

Stolzenberg-Solomon, R. Z., B. I. Graubard, S. Chari, P. Limburg, P. R. Taylor, J. Virtamo and D. Albanes (2005). "Insulin, glucose, insulin resistance, and pancreatic cancer in male smokers." JAMA : the journal of the American Medical Association **294**(22): 2872-2878.

Strachan, T. and A. P. Read (1999). Human Molecular Genetics. New York.

Stramer, B. M., R. Mori and P. Martin (2007). "The inflammation-fibrosis link? A Jekyll and Hyde role for blood cells during wound repair." The Journal of investigative dermatology **127**(5): 1009-1017.

Straus, D. S. and C. K. Glass (2007). "Anti-inflammatory actions of PPAR ligands: new insights on cellular and molecular mechanisms." Trends Immunol **28**(12): 551-558.

Straus, D. S., G. Pascual, M. Li, J. S. Welch, M. Ricote, C. H. Hsiang, L. L. Sengchanthalangsy, G. Ghosh and C. K. Glass (2000). "15-deoxy-delta 12,14-prostaglandin J2 inhibits multiple steps in the NF-kappa B signaling pathway." Proc Natl Acad Sci U S A **97**(9): 4844-4849.

Strelkov, I. S. and J. R. Davie (2002). "Ser-10 phosphorylation of histone H3 and immediate early gene expression in oncogene-transformed mouse fibroblasts." Cancer research **62**(1): 75-78.

Strobl, L. J., H. Hofelmayr, G. Marschall, M. Brielmeier, G. W. Bornkamm and U. Zimber-Strobl (2000). "Activated Notch1 modulates gene expression in B cells similarly to Epstein-Barr viral nuclear antigen 2." Journal of virology **74**(4): 1727-1735.

Su, C. G., X. Wen, S. T. Bailey, W. Jiang, S. M. Rangwala, S. A. Keilbaugh, A. Flanigan, S. Murthy, M. A. Lazar and G. D. Wu (1999). "A novel therapy for colitis utilizing PPAR-gamma ligands to inhibit the epithelial inflammatory response." The Journal of clinical investigation **104**(4): 383-389.

Sugimoto, H., T. M. Mundel, M. W. Kieran and R. Kalluri (2006). "Identification of fibroblast heterogeneity in the tumor microenvironment." Cancer Biol Ther **5**(12): 1640-1646.

Sumimoto, H., F. Imabayashi, T. Iwata and Y. Kawakami (2006). "The BRAF-MAPK signaling pathway is essential for cancer-immune evasion in human melanoma cells." The Journal of experimental medicine **203**(7): 1651-1656.

Suzuki, K. and H. Matsubara (2011). "Recent advances in p53 research and cancer treatment." Journal of biomedicine & biotechnology **2011**: 978312.

Szlosarek, P. W., M. J. Grimshaw, H. Kulbe, J. L. Wilson, G. D. Wilbanks, F. Burke and F. R. Balkwill (2006). "Expression and regulation of tumor necrosis factor alpha in normal and malignant ovarian epithelium." Molecular cancer therapeutics **5**(2): 382-390.

Takebayashi, K., Y. Sasai, Y. Sakai, T. Watanabe, S. Nakanishi and R. Kageyama (1994). "Structure, chromosomal locus, and promoter analysis of the gene encoding the mouse helix-loop-helix factor HES-1. Negative autoregulation through the multiple N box elements." The Journal of biological chemistry **269**(7): 5150-5156.

Talmadge, J. E., H. Phillips, M. Schneider, T. Rowe, R. Pennington, O. Bowersox and B. Lenz (1988). "Immunomodulatory properties of recombinant murine and human tumor necrosis factor." Cancer research **48**(3): 544-550.

Talora, C., D. C. Sgroi, C. P. Crum and G. P. Dotto (2002). "Specific down-modulation of Notch1 signaling in cervical cancer cells is required for sustained HPV-E6/E7 expression and late steps of malignant transformation." Genes & development **16**(17): 2252-2263.

Tanigaki, K. and T. Honjo (2007). "Regulation of lymphocyte development by Notch signaling." Nat Immunol **8**(5): 451-456.

Tapia, J. A., G. M. Salido and A. Gonzalez (2010). "Ethanol consumption as inductor of pancreatitis." World journal of gastrointestinal pharmacology and therapeutics **1**(1): 3-8.

Teta, M., S. Y. Long, L. M. Wartschow, M. M. Rankin and J. A. Kushner (2005). "Very slow turnover of beta-cells in aged adult mice." Diabetes **54**(9): 2557-2567.

Thayer, S. P., M. P. di Magliano, P. W. Heiser, C. M. Nielsen, D. J. Roberts, G. Y. Lauwers, Y. P. Qi, S. Gysin, C. Fernandez-del Castillo, V. Yajnik, B. Antoniu, M. McMahon, A. L. Warshaw and M. Hebrok (2003). "Hedgehog is an early and late mediator of pancreatic cancer tumorigenesis." Nature **425**(6960): 851-856.

Thelu, J., P. Rossio and B. Favier (2002). "Notch signalling is linked to epidermal cell differentiation level in basal cell carcinoma, psoriasis and wound healing." BMC dermatology **2**: 7.

Tian, M., Y. Nishijima, M. L. Asp, M. B. Stout, P. J. Reiser and M. A. Belury (2010). "Cardiac alterations in cancer-induced cachexia in mice." International journal of oncology **37**(2): 347-353.

Tobita, K., H. Kijima, S. Dowaki, H. Kashiwagi, Y. Ohtani, Y. Oida, H. Yamazaki, M. Nakamura, Y. Ueyama, M. Tanaka, S. Inokuchi and H. Makuuchi (2003). "Epidermal growth factor receptor expression in human pancreatic cancer: Significance for liver metastasis." International journal of molecular medicine **11**(3): 305-309.

Tomasek, J. J., G. Gabbiani, B. Hinz, C. Chaponnier and R. A. Brown (2002). "Myofibroblasts and mechano-regulation of connective tissue remodelling." Nat Rev Mol Cell Biol **3**(5): 349-363.

Tsunematsu, R., K. Nakayama, Y. Oike, M. Nishiyama, N. Ishida, S. Hatakeyama, Y. Bessho, R. Kageyama, T. Suda and K. I. Nakayama (2004). "Mouse Fbw7/Sel-10/Cdc4 is required for notch degradation during vascular development." The Journal of biological chemistry **279**(10): 9417-9423.

Tun, T., Y. Hamaguchi, N. Matsunami, T. Furukawa, T. Honjo and M. Kawaichi (1994). "Recognition sequence of a highly conserved DNA binding protein RBP-J kappa." Nucleic acids research **22**(6): 965-971.

Tuveson, D. A., A. T. Shaw, N. A. Willis, D. P. Silver, E. L. Jackson, S. Chang, K. L. Mercer, R. Grochow, H. Hock, D. Crowley, S. R. Hingorani, T. Zaks, C. King, M. A. Jacobetz, L. Wang, R. T. Bronson, S. H. Orkin, R. A. DePinho and T. Jacks (2004). "Endogenous oncogenic K-ras(G12D) stimulates proliferation and widespread neoplastic and developmental defects." Cancer Cell **5**(4): 375-387.

Tuveson, D. A., L. Zhu, A. Gopinathan, N. A. Willis, L. Kachatrian, R. Grochow, C. L. Pin, N. Y. Mitin, E. J. Taparowsky, P. A. Gimotty, R. H. Hruban, T. Jacks and S. F. Konieczny (2006). "Mist1-KrasG12D knock-in mice develop mixed differentiation metastatic exocrine pancreatic carcinoma and hepatocellular carcinoma." Cancer research **66**(1): 242-247.

Vacca, A., M. P. Felli, R. Palermo, G. Di Mario, A. Calce, M. Di Giovine, L. Frati, A. Gulino and I. Screpanti (2006). "Notch3 and pre-TCR interaction unveils distinct NF-kappaB pathways in T-cell development and leukemia." The EMBO journal **25**(5): 1000-1008.

Vakoc, C. R., S. A. Mandat, B. A. Olenchock and G. A. Blobel (2005). "Histone H3 lysine 9 methylation and HP1gamma are associated with transcription elongation through mammalian chromatin." Molecular cell **19**(3): 381-391.

Van Cutsem, E., H. van de Velde, P. Karasek, H. Oettle, W. L. Vervenne, A. Szawlowski, P. Schoffski, S. Post, C. Verslype, H. Neumann, H. Safran, Y. Humblet, J. Perez Ruixo, Y. Ma and D. Von Hoff (2004). "Phase III trial of gemcitabine plus tipifarnib compared with gemcitabine plus placebo in advanced pancreatic cancer." Journal of clinical oncology : official journal of the American Society of Clinical Oncology **22**(8): 1430-1438.

van Heek, N. T., A. K. Meeker, S. E. Kern, C. J. Yeo, K. D. Lillemoe, J. L. Cameron, G. J. Offerhaus, J. L. Hicks, R. E. Wilentz, M. G. Goggins, A. M. De Marzo, R. H. Hruban and A. Maitra (2002). "Telomere shortening is nearly universal in pancreatic intraepithelial neoplasia." The American journal of pathology **161**(5): 1541-1547.

Vesely, M. D., M. H. Kershaw, R. D. Schreiber and M. J. Smyth (2011). "Natural innate and adaptive immunity to cancer." Annual review of immunology **29**: 235-271.

Viatour, P., U. Ehmer, L. A. Saddic, C. Dorrell, J. B. Andersen, C. Lin, A. F. Zmoos, P. K. Mazur, B. E. Schaffer, A. Ostermeier, H. Vogel, K. G. Sylvester, S. S. Thorgeirsson, M. Grompe and J. Sage (2011). "Notch signaling inhibits hepatocellular carcinoma following inactivation of the RB pathway." The Journal of experimental medicine **208**(10): 1963-1976.

Vilimas, T., J. Mascarenhas, T. Palomero, M. Mandal, S. Buonamici, F. Meng, B. Thompson, C. Spaulding, S. Macaroun, M. L. Alegre, B. L. Kee, A. Ferrando, L. Miele and I. Aifantis (2007). "Targeting the NF-kappaB signaling pathway in Notch1-induced T-cell leukemia." Nat Med **13**(1): 70-77.

Virchow, R. (1864). Die krankhaften Geschw√ºlste: dreissig Vorlesungen gehalten w√§hrend des Wintersemesters 1862-1863 an der Universit√§t zu Berlin, A. Hirschwald.

Vonderheide, R. H. (2007). "Prospect of targeting the CD40 pathway for cancer therapy." Clinical cancer research : an official journal of the American Association for Cancer Research **13**(4): 1083-1088.

Vrieling, A., H. B. Bueno-de-Mesquita, H. C. Boshuizen, D. S. Michaud, M. T. Severinsen, K. Overvad, A. Olsen, A. Tjonneland, F. Clavel-Chapelon, M. C. Boutron-Ruault, R. Kaaks, S. Rohrmann, H. Boeing, U. Nothlings, A. Trichopoulou, E. Moutsiou, V. Dilis, D. Palli, V. Krogh, S. Panico, R. Tumino, P. Vineis, C. H. van Gils, P. H. Peeters, E. Lund, I. T. Gram, L. Rodriguez, A. Agudo, N. Larranaga, M. J. Sanchez, C. Navarro, A. Barricarte, J. Manjer, B. Lindkvist, M. Sund, W. Ye, S. Bingham, K. T. Khaw, A. Roddam, T. Key, P. Boffetta, E. J. Duell, M. Jenab, V. Gallo and E. Riboli (2010). "Cigarette smoking, environmental tobacco smoke exposure and pancreatic cancer risk in the European Prospective Investigation into Cancer and Nutrition." International journal of cancer. Journal international du cancer **126**(10): 2394-2403.

Wan, H., Y. Yuan, A. Qian, Y. Sun and M. Qiao (2008). "Pioglitazone, a PPARgamma ligand, suppresses NFkappaB activation through inhibition of IkappaB kinase activation in cerulein-treated AR42J cells." Biomedicine & pharmacotherapy = Biomedecine & pharmacotherapie **62**(7): 466-472.

Wang, J., L. Shelly, L. Miele, R. Boykins, M. A. Norcross and E. Guan (2001). "Human Notch-1 inhibits NF-kappa B activity in the nucleus through a direct interaction involving a novel domain." Journal of immunology **167**(1): 289-295.

Wang, W., J. L. Abbruzzese, D. B. Evans, L. Larry, K. R. Cleary and P. J. Chiao (1999). "The nuclear factor-kappa B RelA transcription factor is constitutively activated in human pancreatic adenocarcinoma cells." Clinical cancer research : an official journal of the American Association for Cancer Research **5**(1): 119-127.

Wang, Z., Y. Li, D. Kong and F. H. Sarkar (2010). "The role of Notch signaling pathway in epithelial-mesenchymal transition (EMT) during development and tumor aggressiveness." Current drug targets **11**(6): 745-751.

Wang, Z., Y. Zhang, Y. Li, S. Banerjee, J. Liao and F. H. Sarkar (2006). "Down-regulation of Notch-1 contributes to cell growth inhibition and apoptosis in pancreatic cancer cells." Molecular cancer therapeutics **5**(3): 483-493.

Warburg, O. (1956). "On the origin of cancer cells." Science **123**(3191): 309-314.

Watanabe, M., A. Nobuta, J. Tanaka and M. Asaka (1996). "An effect of K-ras gene mutation on epidermal growth factor receptor signal transduction in PANC-1 pancreatic carcinoma cells." International journal of cancer. Journal international du cancer **67**(2): 264-268.

Weber, C. K. and G. Adler (2001). "Acute pancreatitis." Current opinion in gastroenterology **17**(5): 426-429.

Weber, J. S., O. Hamid, S. D. Chasalow, D. Y. Wu, S. M. Parker, S. Galbraith, S. Gnjatic and D. Berman (2011). "Ipilimumab Increases Activated T Cells and Enhances Humoral Immunity in Patients With Advanced Melanoma." Journal of immunotherapy.

Weeks, M. E., D. Hariharan, L. Petronijevic, T. P. Radon, H. J. Whiteman, H. M. Kocher, J. F. Timms, N. R. Lemoine and T. Crnogorac-Jurcevic (2008). "Analysis of

the urine proteome in patients with pancreatic ductal adenocarcinoma." Proteomics. Clinical applications **2**(7-8): 1047-1057.

Weng, A. P., J. M. Millholland, Y. Yashiro-Ohtani, M. L. Arcangeli, A. Lau, C. Wai, C. Del Bianco, C. G. Rodriguez, H. Sai, J. Tobias, Y. Li, M. S. Wolfe, C. Shachaf, D. Felsher, S. C. Blacklow, W. S. Pear and J. C. Aster (2006). "c-Myc is an important direct target of Notch1 in T-cell acute lymphoblastic leukemia/lymphoma." Genes & development **20**(15): 2096-2109.

Whitcomb, D. C., S. Applebaum and S. P. Martin (1999). "Hereditary pancreatitis and pancreatic carcinoma." Annals of the New York Academy of Sciences **880**: 201-209.

Whitfield, J. R. and L. Soucek (2011). "Tumor microenvironment: becoming sick of Myc." Cellular and molecular life sciences : CMLS.

Wickremasinghe, R. G., A. G. Prentice and A. J. Steele (2011). "p53 and Notch signaling in chronic lymphocytic leukemia: clues to identifying novel therapeutic strategies." Leukemia : official journal of the Leukemia Society of America, Leukemia Research Fund, U.K **25**(9): 1400-1407.

Wilentz, R. E., C. A. Iacobuzio-Donahue, P. Argani, D. M. McCarthy, J. L. Parsons, C. J. Yeo, S. E. Kern and R. H. Hruban (2000). "Loss of expression of Dpc4 in pancreatic intraepithelial neoplasia: evidence that DPC4 inactivation occurs late in neoplastic progression." Cancer research **60**(7): 2002-2006.

Williams, S. K., D. Truong and J. K. Tyler (2008). "Acetylation in the globular core of histone H3 on lysine-56 promotes chromatin disassembly during transcriptional activation." Proceedings of the National Academy of Sciences of the United States of America **105**(26): 9000-9005.

Willis, B. C., R. M. duBois and Z. Borok (2006). "Epithelial origin of myofibroblasts during fibrosis in the lung." Proc Am Thorac Soc **3**(4): 377-382.

Wright, E., M. R. Hargrave, J. Christiansen, L. Cooper, J. Kun, T. Evans, U. Gangadharan, A. Greenfield and P. Koopman (1995). "The Sry-related gene Sox9 is expressed during chondrogenesis in mouse embryos." Nature genetics **9**(1): 15-20.

Wu, Z., E. D. Rosen, R. Brun, S. Hauser, G. Adelmant, A. E. Troy, C. McKeon, G. J. Darlington and B. M. Spiegelman (1999). "Cross-regulation of C/EBP alpha and PPAR gamma controls the transcriptional pathway of adipogenesis and insulin sensitivity." Molecular cell **3**(2): 151-158.

Wu, Z., Y. Xie, N. L. Bucher and S. R. Farmer (1995). "Conditional ectopic expression of C/EBP beta in NIH-3T3 cells induces PPAR gamma and stimulates adipogenesis." Genes & development **9**(19): 2350-2363.

Xiong, H. Q., J. L. Abbruzzese, E. Lin, L. Wang, L. Zheng and K. Xie (2004). "NF-kappaB activity blockade impairs the angiogenic potential of human pancreatic cancer cells." International journal of cancer. Journal international du cancer **108**(2): 181-188.

Yamamoto, K., T. Arakawa, N. Ueda and S. Yamamoto (1995). "Transcriptional roles of nuclear factor kappa B and nuclear factor-interleukin-6 in the tumor necrosis factor alpha-dependent induction of cyclooxygenase-2 in MC3T3-E1 cells." The Journal of biological chemistry **270**(52): 31315-31320.

Yamamoto, N., S. Yamamoto, F. Inagaki, M. Kawaichi, A. Fukamizu, N. Kishi, K. Matsuno, K. Nakamura, G. Weinmaster, H. Okano and M. Nakafuku (2001). "Role of Deltex-1 as a transcriptional regulator downstream of the Notch receptor." The Journal of biological chemistry **276**(48): 45031-45040.

Yamamoto, Y., U. N. Verma, S. Prajapati, Y. T. Kwak and R. B. Gaynor (2003). "Histone H3 phosphorylation by IKK-alpha is critical for cytokine-induced gene expression." Nature **423**(6940): 655-659.

Yamamoto, Y., M. J. Yin and R. B. Gaynor (2000). "IkappaB kinase alpha (IKKalpha) regulation of IKKbeta kinase activity." Mol Cell Biol **20**(10): 3655-3666.

Yang, J., R. Splittgerber, F. E. Yull, S. Kantrow, G. D. Ayers, M. Karin and A. Richmond (2010). "Conditional ablation of Ikkb inhibits melanoma tumor development in mice." J Clin Invest **120**(7): 2563-2574.

Yokota, T., R. Kanamoto and S. Hayashi (1995). "c-myc mRNA is stabilized by deprivation of amino acids in primary cultured rat hepatocytes." Journal of nutritional science and vitaminology **41**(4): 455-463.

Yonezawa, S., M. Higashi, N. Yamada and M. Goto (2008). "Precursor lesions of pancreatic cancer." Gut and liver **2**(3): 137-154.

Yoshida, K. and Y. Miki (2004). "Role of BRCA1 and BRCA2 as regulators of DNA repair, transcription, and cell cycle in response to DNA damage." Cancer science **95**(11): 866-871.

Zabaleta, J. (2012). "Multifactorial etiology of gastric cancer." Methods in molecular biology **863**: 411-435.

Zagouras, P., S. Stifani, C. M. Blaumueller, M. L. Carcangiu and S. Artavanis-Tsakonas (1995). "Alterations in Notch signaling in neoplastic lesions of the human cervix." Proceedings of the National Academy of Sciences of the United States of America **92**(14): 6414-6418.

Zaynagetdinov, R., G. T. Stathopoulos, T. P. Sherrill, D. S. Cheng, A. G. McLoed, J. A. Ausborn, V. V. Polosukhin, L. Connelly, W. Zhou, B. Fingleton, R. S. Peebles, L. S. Prince, F. E. Yull and T. S. Blackwell (2011). "Epithelial nuclear factor-kappaB signaling promotes lung carcinogenesis via recruitment of regulatory T lymphocytes." Oncogene.

Zenz, T., A. Benner, H. Dohner and S. Stilgenbauer (2008). "Chronic lymphocytic leukemia and treatment resistance in cancer: the role of the p53 pathway." Cell cycle **7**(24): 3810-3814.

Zhang, J. P., J. Yan, J. Xu, X. H. Pang, M. S. Chen, L. Li, C. Wu, S. P. Li and L. Zheng (2009). "Increased intratumoral IL-17-producing cells correlate with poor survival in hepatocellular carcinoma patients." Journal of hepatology **50**(5): 980-989.

Zhang, Q., Q. Zhong, A. G. Evans, D. Levy and S. Zhong (2011). "Phosphorylation of histone H3 serine 28 modulates RNA polymerase III-dependent transcription." Oncogene.

Zhu, L., G. Shi, C. M. Schmidt, R. H. Hruban and S. F. Konieczny (2007). "Acinar cells contribute to the molecular heterogeneity of pancreatic intraepithelial neoplasia." The American journal of pathology **171**(1): 263-273.

Zoete, V., A. Grosdidier and O. Michielin (2007). "Peroxisome proliferator-activated receptor structures: ligand specificity, molecular switch and interactions with regulators." Biochim Biophys Acta **1771**(8): 915-925.

Zuo, Y., L. Qiang and S. R. Farmer (2006). "Activation of CCAAT/enhancer-binding protein (C/EBP) alpha expression by C/EBP beta during adipogenesis requires a peroxisome proliferator-activated receptor-gamma-associated repression of HDAC1 at the C/ebp alpha gene promoter." The Journal of biological chemistry **281**(12): 7960-7967.

APPENDICES

APPENDIX A: SOLUTIONS

Solutions are listed in alphabetical order. Unless indicated, the pH of buffers was adjusted using either 1 M NaOH or 1 M HCl and reagents were dissolved in deionised water.

Agarose Gel

1.2 % w/v agarose
4 % v/v GelRed™ Nucleic Acid Gel Stain
Dissolved in 1X TAE

Antibody dilution

3 % w/v BSA
0.01 % w/v sodium azide
Dissolved in 1X TBS/T 0.05 %

ChIP dilution buffer

16.7 mM Tris-HCl pH 8.1
1.2 mM EDTA
167 mM NaCl
1.1 % v/v Triton®-X-100
0.01 % w/v SDS

ChIP lysis buffer

5 µl 200X Protease inhibitor cocktail II (Millipore - 20-283)
Volume adjusted to 1 ml with PBS

ChIP SDS lysis buffer

50 mM Tris pH 8.1
10 mM EDTA
1 % w/v SDS

FACS buffer

1 % v/v FCS

0.01 % w/v sodium azide

Dissolved in PBS

Kinase buffer

20 mM Tris pH 7.5

1 mM EDTA

1 mM DTT (add just before use)

Loading buffer (6X) (DNA)

0.3 % w/v bromophenol blue

0.3 % w/v xylene cyanol

30 % v/v glycerol

Loading buffer (6X) (Protein)

350 mM Tris-HCl pH 6.8

30 % v/v glycerol

10 % w/v SDS

0.02 % w/v bromophenol blue

Before use, add 1 volume 1 M DTT to 2 volumes loading buffer

Once the DTT is added, store at - 20 °C

L. agar

15 mg/ml agar

Dissolved in lysogeny broth

Lysogeny broth (L. broth)

10 mg/ml typtone

5 mg/ml yeast extract

85 mM NaCl

Adjust to pH 7.4 and autoclave

Lysis buffer

50 mM Tris-HCl pH 7.5

250 mM NaCl

3 mM EDTA pH 8

3 mM EGTA pH 8

1 % v/v Triton®-X-100

0.5 % v/v igepal CA-630

10 % v/v glycerol

Add 1 Complete Mini Protease Inhibitor cocktail (Roche - 11836153001) per 10 ml of lysis buffer. This solution can be stored at - 20 °C.
Before use, add 10 µl of phosphatase inhibitor cocktail (Sigma Aldrich - P5726) per 1 ml of lysis buffer.

MOPS SDS running buffer (1X) (Electrophoresis)

50 ml 20X MOPS SDS running buffer (Invitrogen - NP0001)

Volume adjusted to 1 l with deionised water

Running buffer (10X) (Electrophoresis)

0.25 M Tris base

1.92 M glycine

1 % w/v SDS

Running buffer (1X) (Electrophoresis)

100 ml 10X running buffer

Volume adjusted to 1 l with deionised water

TAE (50X)

2 M Tris base

1 M acetic acid

50 mM EDTA

TAE (1X)

20 ml 50X TAE

Volume adjusted to 1 l with deionised water

TBS (10X)

200 mM Tris base

1.5 M NaCl

TBS/T 0.05 % (1X)

100 ml 10X TBS

500 µl Tween 20

Volume adjusted to 1 l with deionised water

Transfer buffer (10X) (Electrophoresis)

0.27 M Tris base

1.92 M glycine

Transfer buffer (1X) (Electrophoresis)

100 ml 10X transfer buffer

200 ml methanol

Volume adjusted to 1 l with deionised water

APPENDIX B: PLASMID MAPS

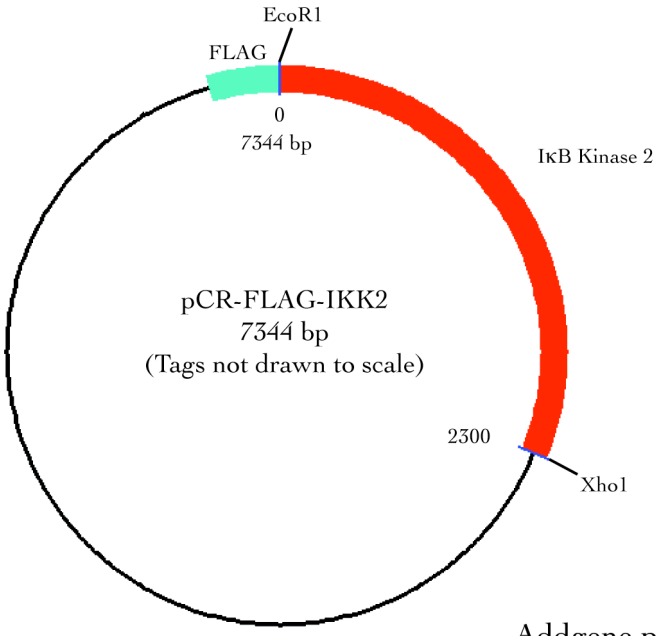

Addgene plasmid 15465
(Nakano *et al.,* 1998)

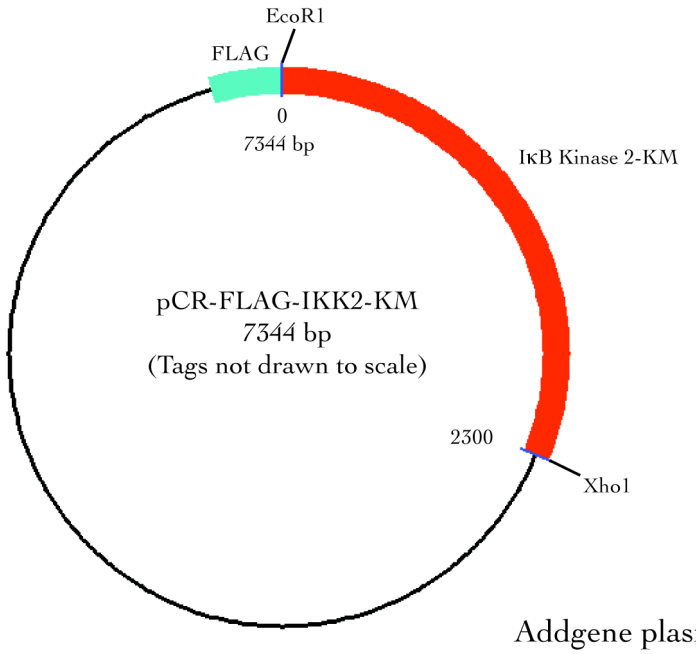

Addgene plasmid 15466
(Nakano *et al.,* 1998)

Downloaded and adapted from www.addgene.org

APPENDIX C: QUANTITATIVE RT-PCR ASSAYS

Gene	Species	Quencher	Reporter	Assay ID
b220	Mouse	TAMRA	FAM	Mm01293575_m1
batf	Mouse	TAMRA	FAM	Mm00479410_m1
cd208	Mouse	TAMRA	FAM	Mm00616604_m1
cd2r	Mouse	TAMRA	FAM	Mm00488928_m1
cd8a	Mouse	TAMRA	FAM	Mm01182108_m1
cebpa	Mouse	TAMRA	FAM	Mm00514283_s1
c-myc	Mouse	TAMRA	FAM	Mm00487804_m1
cox2	Mouse	TAMRA	FAM	Mm01307329_m1
cxcr1	Mouse	TAMRA	FAM	Mm00731329_s1
f4/80	Mouse	TAMRA	FAM	Mm00802529_m1
hes1	Mouse	TAMRA	FAM	Mm01342805_m1
hey1	Mouse	TAMRA	FAM	Mm00468865_m1
ikk1	Mouse	TAMRA	FAM	Mm01214283_m1
ikk2	Mouse	TAMRA	FAM	Mm01222249_m1
il1b	Mouse	TAMRA	FAM	Mm00434228_m1
il6	Mouse	TAMRA	FAM	Mm00446191_m1
mmp13	Mouse	TAMRA	FAM	Mm00439491_m1
nemo	Mouse	TAMRA	FAM	Mm00494928_g1
nk1.1	Mouse	TAMRA	FAM	Mm00824341_m1
pparg	Mouse	TAMRA	FAM	Mm00440945_m1
rbpj	Mouse	TAMRA	FAM	Mm03053645_s1
tenascin-c	Mouse	TAMRA	FAM	Mm00495662_m1
tnfa	Mouse	TAMRA	FAM	Mm00443258_m1
vegf	Mouse	TAMRA	FAM	Mm01204733_m1

Table describes the qRT-PCR assays used listing the gene, species, quencher, reporter and assay identification number (ID).

APPENDIX D: DISEASE SPECTRUM IN *KRAS*^{G12D} MICE

ID	Age (days)	PDAC	Histology	Liver	Lung	PD	Ascites	BO	Other
TH04-75	523	Y	undifferentiated	Y				Y	
TH04-81	514	Y	undifferentiated	Y		Y			LN
TH04-83	584								
TH04-111	408								
TH04-121	447	Y	undifferentiated	Y		Y			LN
TH04-122	432								
TH04-128	522	Y	undifferentiated	Y	Y				
TH04-175	167								
TH04-177	185								
TH04-190	224								
TH04-195	364	Y	glandular				Y	Y	
TH04-198	361	Y	glandular				Y	Y	
TH04-224	301	Y	undifferentiated	Y	Y				
TH04-230	254								
TH04-234	485								
TH04-236	203								
TH04-248	308								
TH04-249	388	Y	undifferentiated	Y		Y		Y	
TH04-255	365	Y	undifferentiated	Y	Y				
TH04-269	214	Y	undifferentiated	Y			Y		
TH04-271	394	Y	glandular					Y	
TH04-274	575	Y	undifferentiated	Y					
TH04-277	564								
TH04-294	467								
TH04-312	481	Y	undifferentiated	Y				Y	
TH04-318	348								
TH04-324	506	Y	undifferentiated	Y	Y				
TH04-328	407								
TH04-351	519								
TH04-361	522								
TH04-366	413	Y	glandular				Y	Y	
TH04-367	497								
TH04-372	463	Y	undifferentiated	Y			Y		
TH04-373	482	Y	undifferentiated	Y	Y			Y	
TH04-385	506	Y	undifferentiated	Y					
TH04-386	322								
TH04-387	471	Y	glandular					Y	
TH04-402	449	Y	undifferentiated	Y	Y			Y	
TH04-406	367								
TH04-425	308								
	Median 422.5	**50 %**	**75 % undif. 25 % gland.**	**37.5 %**	**15 %**	**7.5 %**	**12.5 %**	**25 %**	

Table describes the identification number (ID), age, presence or absence of PDAC, histology grade, liver and lung metastasis, peritoneal disease (PD), ascites and biliary obstruction (BO) for each mouse. Other sites of metastasis include the lymph nodes (LN).

APPENDIX E: DISEASE SPECTRUM IN *KRAS*^{G12D}/*IKK2*$^{\Delta Pdx}$ MICE

ID	Age (days)	PDAC	Histology	Liver	Lung	PD	Ascites	Skin	BO	Atrophy
TH03-35	526									Y
TH03-58	599									Y
TH03-59	517									Y
TH03-61	422	Y	glandular	Y	Y	Y			Y	
TH03-66	501									Y
TH03-67	449									Y
TH03-82	209							Y		
TH03-88	297							Y		
TH03-89	388									Y
TH03-115	436	Y	undifferentiated	Y	Y	Y				
TH03-131	587									Y
TH03-136	555									Y
TH03-148	475									Y
TH03-149	391									Y
TH03-167	155							Y		
TH03-177	422	Y	glandular	Y			Y			
TH03-181	448									Y
TH03-196	401									Y
TH03-197	412	Y	undifferentiated	Y	Y	Y			Y	
TH03-206	389	Y	undifferentiated							
TH03-207	455							Y		
TH03-213	438									Y
TH03-344	264							Y		
TH03-365	428									Y
TH03-374	417									Y
TH03-384	409	Y	galdular							
TH03-402	337									Y
TH03-404	316	Y	undifferentiated	Y	Y	Y	Y	Y	Y	
TH03-405	406									Y
TH03-416	472									Y
TH03-425	515									Y
TH03-431	411									Y
TH03-452	509	Y	undifferentiated	Y	Y		Y		Y	
TH03-497	377									Y
TH03-499	482	Y	undifferentiated		Y	Y			Y	
TH03-503	568									Y
TH03-509	263							Y		
TH03-515	174							Y		
TH03-518	248							Y		
TH03-522	315									
TH03-546	427									Y
TH03-551	482									Y
TH03-552	517									Y
TH03-568	268							Y		
TH03-574	216							Y		
TH03-681	498									Y
TH03-682	571									Y
TH03-693	501									Y
TH03-699	585	Y	glandular				Y		Y	Y
TH03-706	433							Y		
	Median 427.5	**20 %**	**60 % undif. 40 % gland.**	**12 %**	**12 %**	**10 %**	**8 %**	**24 %**	**12 %**	**58 %**

Table describes the identification number (ID), age, presence or absence of PDAC, histology grade, liver and lung metastasis, peritoneal disease (PD), ascites, skin lesions, biliary obstruction (BO) and atrophy for each mouse.

APPENDIX F: DISEASE SPECTRUM IN *KRAS*^{G12D} MICE TREATED WITH ROSIGLITAZONE

ID	Age (days)	PDAC	Histology	Liver	Lung	PD	Ascites	Skin	BO
CHS601-8	421								
CHS601-15	438								
CHS601-19	567								
CHS601-21	558	Y	glandular			Y	Y		Y
CHS601-25	621								
CHS601-27	521	Y	glandular	Y			Y		Y
CHS601-30	504	Y	glandular			Y			Y
CHS601-31	486								
CHS601-33	531								
CHS601-46	367								
CHS601-55	422								
CHS601-57	394	Y	undifferentiated	Y	Y				Y
CHS601-67	357	Y	glandular	Y					
CHS601-68	547	Y	glandular	Y			Y		Y
CHS601-69	555								
CHS601-79	501								
CHS601-80	408								
CHS601-83	486								
CHS601-84	433								
CHS601-92	567								
CHS601-96	555								
CHS601-99	537								
CHS601-108	521								
CHS601-116	482	Y	glandular			Y	Y		Y
CHS601-127	444								
CHS601-128	518								
CHS601-142	525	Y	glandular	Y					Y
CHS601-144	367								
CHS601-161	418								
CHS601-167	632								
CHS601-170	555	Y	undifferentiated	Y	Y				
CHS601-177	407								
CHS601-178	634								
CHS601-185	524	Y	glandular				Y		Y
CHS601-192	301								
CHS601-197	287								
CHS601-201	425								
CHS601-222	486								
CHS601-224	411	Y	glandular	Y				Y	
CHS601-229	518								
	Median 493.5	**27.5 %**	**18 % undif. 92 % gland.**	**17.5 %**	**5 %**	**7.5 %**	**12.5 %**	**2.5 %**	**2 %**

Table describes the identification number (ID), age, presence or absence of PDAC, histology grade, liver and lung metastasis, peritoneal disease (PD), ascites, skin lesions and biliary obstruction (BO) for each mouse.

PUBLICATION

Crosstalk between the canonical NF-κB and Notch signaling pathways inhibits Pparγ expression and promotes pancreatic cancer progression in mice

Eleni Maniati,[1] Maud Bossard,[1] Natalie Cook,[2] Juliana B. Candido,[1] Nia Emami-Shahri,[1] Sergei A. Nedospasov,[3,4] Frances R. Balkwill,[1] David A. Tuveson,[2] and Thorsten Hagemann[1]

[1]Centre for Cancer and Inflammation, Barts Cancer Institute, Queen Mary University of London, London, United Kingdom. [2]Cambridge Research Institute/CRUK, Cambridge, United Kingdom. [3]Laboratory of Molecular Immunology, Engelhardt Institute of Molecular Biology, Moscow, Russia. [4]German Rheumatism Research Center, a Leibniz Institute, Berlin, Germany.

The majority of human pancreatic cancers have activating mutations in the *KRAS* proto-oncogene. These mutations result in increased activity of the NF-κB pathway and the subsequent constitutive production of proinflammatory cytokines. Here, we show that inhibitor of κB kinase 2 (Ikk2), a component of the canonical NF-κB signaling pathway, synergizes with basal Notch signaling to upregulate transcription of primary Notch target genes, resulting in suppression of antiinflammatory protein expression and promotion of pancreatic carcinogenesis in mice. We found that in the *Kras*^{G12D}*Pdx1-cre* mouse model of pancreatic cancer, genetic deletion of *Ikk2* in initiated pre-malignant epithelial cells substantially delayed pancreatic oncogenesis and resulted in downregulation of the classical Notch target genes *Hes1* and *Hey1*. Tnf-α stimulated canonical NF-κB signaling and, in collaboration with basal Notch signals, induced optimal expression of Notch targets. Mechanistically, Tnf-α stimulation resulted in phosphorylation of histone H3 at the *Hes1* promoter, and this signal was lost with *Ikk2* deletion. Hes1 suppresses expression of *Pparg*, which encodes the antiinflammatory nuclear receptor Pparγ. Thus, crosstalk between Tnf-α/Ikk2 and Notch sustains the intrinsic inflammatory profile of transformed cells. These findings reveal what we believe to be a novel interaction between oncogenic inflammation and a major cell fate pathway and show how these pathways can cooperate to promote cancer progression.

Introduction

Cancer-related inflammation has been shown to be critically linked with malignant disease — either by being the initiating, extrinsic cause or by supporting the intrinsic microenvironment during tumor progression (1). Most solid tumors are characterized by an intrinsic tumor-promoting inflammatory response (1). Activation of proto-oncogenes such as *ras* and/or inactivation of tumor suppressors orchestrates a proinflammatory transcriptional program and constitutive production of inflammatory cytokines and chemokines that shape a tumor-promoting microenvironment. Oncogenes and tumor suppressor genes are, however, difficult molecular targets in cancer therapy (2). In contrast, inflammatory cytokines and signaling pathways affected by the genetic changes occurring in malignant diseases are attractive druggable targets.

Activating mutations of the *KRAS* proto-oncogene are found in more than 90% of pancreatic ductal adenocarcinomas (PDACs), the most prevalent form of pancreatic cancer (3). Histological and molecular studies have demonstrated that disease progression occurs through a series of preinvasive lesions, pancreatic intraepithelial neoplasias (PanINs), that progress into invasive carcinoma (4). Mouse models with pancreas-specific activation of oncogenic Kras display the full spectrum of PanINs and recapitulate the features of human PDAC (5, 6). NF-κB, a major transcription factor for inflammatory responses, is found activated in Kras-transformed epithelial cells (7, 8). NF-κB activation is regulated through the inhibitor of κB kinase (Ikk) complex, which consists of two catalytic subunits, Ikk1 and Ikk2 and the regulatory protein Ikk3 (or Nemo) (reviewed in ref. 9). During canonical NF-κB signaling, inflammatory stimuli including cytokines such as Tnf-α generate signals that converge at the Ikk complex, phosphorylating Ikk2, which in turn phosphorylates the inhibitory molecule inhibitor of κB (IκB), resulting in its proteasomal degradation. This releases the p65/p50 NF-κB heterodimer, allowing its nuclear translocation and promoter binding for inflammatory gene transcription. A series of studies has indicated a requirement of Ikk2 and p65 in both murine and human Kras-induced transformation of lung epithelial cells and in models of inflammation-induced carcinogenesis (7, 8, 10, 11). However, the implication of the pathway in pancreatic cancer has so far been unexplored.

Interestingly, in many types of cancer, including pancreatic cancer, the NF-κB and Notch pathways are activated (12–15). Classical activation of Notch signaling is triggered by ligation of Notch receptors and ligands. This leads to proteolytic cleavage of Notch and the release of the Notch intracellular domain (NICD). NICD subsequently translocates to the nucleus and binds to the DNA-binding protein Rbp-j. This interaction results in assembly of a transcriptional activation complex that drives the expression of Notch target genes (16). Among the best-characterized direct Notch target genes are the *Hes* and *Hey* families of transcriptional repressors. These genes are found to be upregulated in early PanINs

Authorship note: Eleni Maniati and Maud Bossard contributed equally to this work.
Conflict of interest: The authors have declared that no conflict of interest exists.
Citation for this article: *J Clin Invest.* 2011;121(12):4685–4699. doi:10.1172/JCI45797.

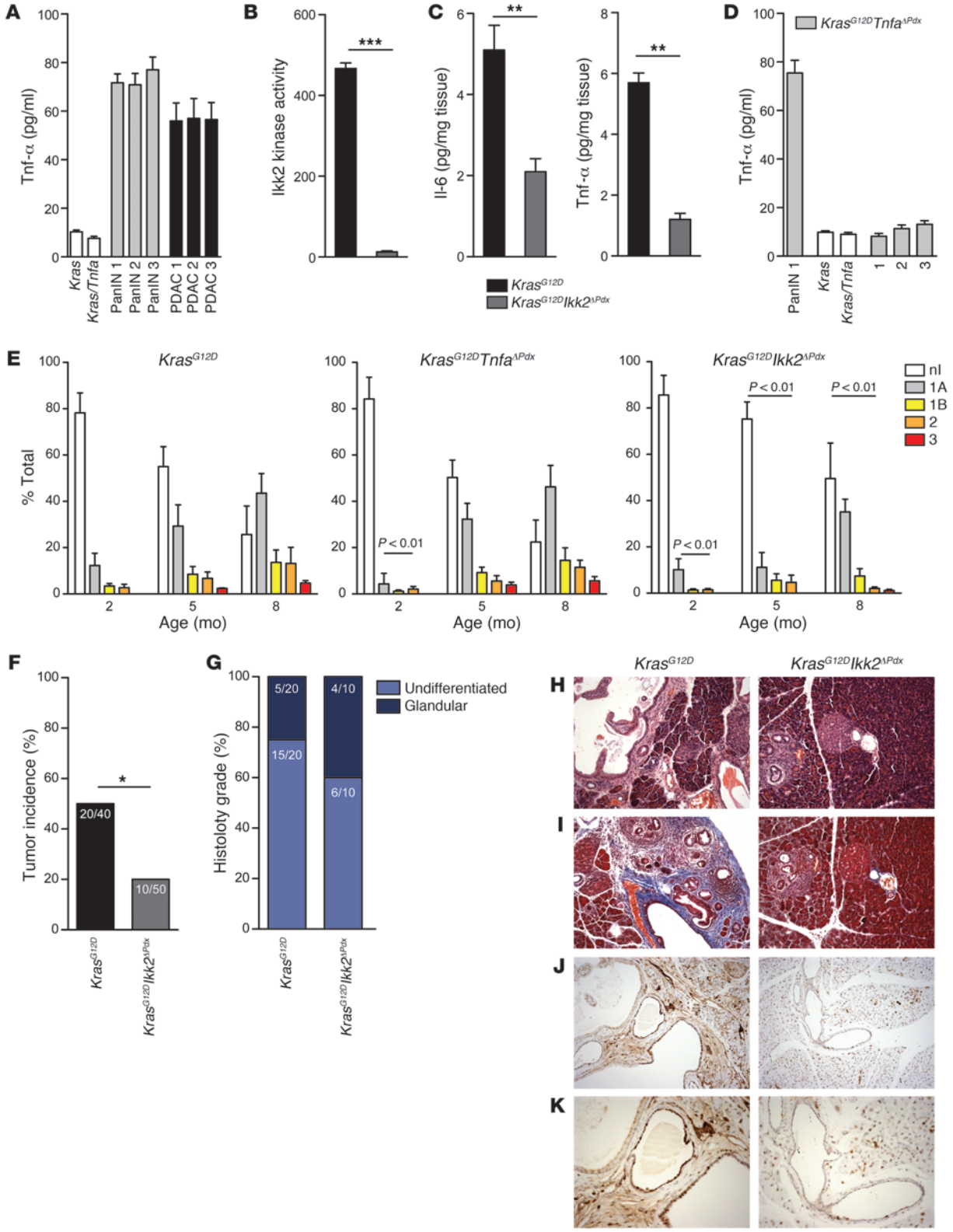
A
Tnf-α (pg/ml)
Kras
Kras/Tnfa
PanIN 1
PanIN 2
PanIN 3
PDAC 1
PDAC 2
PDAC 3
B
Ikk2 kinase activity
***
C
Il-6 (pg/mg tissue)
**
Tnf-α (pg/mg tissue)
**
KrasG12D
KrasG12DIkk2ΔPdx
D
KrasG12DTnfaΔPdx
Tnf-α (pg/ml)
PanIN 1
Kras
Kras/Tnfa
1
2
3
E
KrasG12D
KrasG12DTnfaΔPdx
KrasG12DIkk2ΔPdx
% Total
Age (mo)
P < 0.01
nl
1A
1B
2
3
F
Tumor incidence (%)
*
20/40
10/50
KrasG12D
KrasG12DIkk2ΔPdx
G
Histoloty grade (%)
5/20
15/20
4/10
6/10
Undifferentiated
Glandular
KrasG12D
KrasG12DIkk2ΔPdx
H
I
J
K
KrasG12D
KrasG12DIkk2ΔPdx

Figure 1
Genetic deletion of *Ikk2* inhibits PanIN progression. (**A**) Tnf-α secretion by ductal cell lines derived from $Kras^{G12D}$ PanIN- or PDAC-bearing mice measured by ELISA. Control cells were generated from *Kras* and *Kras*/*Tnfa* cre-negative pancreases. (**B**) Cellular Ikk2 kinase activity in cell lines derived from $Kras^{G12D}$ and $Kras^{G12D}Ikk2^{\Delta Pdx}$ mice. (**C**) Il-6 and Tnf-α secretion in pancreatic tissue of $Kras^{G12D}$ and $Kras^{G12D}Ikk2^{\Delta Pdx}$ mice. $n = 6$; $^{**}P < 0.01$, $^{***}P < 0.01$. (**D**) Tnf-α secretion by cell lines derived from $Kras^{G12D}$ (PanIN 1) or $Kras^{G12D}Tnfa^{\Delta Pdx}$ PanIN- or PDAC-bearing mice. Cre-negative *Kras* and *Kras*/*Tnfa* control cells were included. Data in **C** are shown as mean + SD of $n = 6$ mice, and data in **A**, **B**, and **D** are mean + SD of triplicate experiments. (**E**) Quantification of the proportion of pancreas occupied by PanIN lesions. Frequency and grade of the lesions was quantified at 2, 5, and 8 months of age. Data are shown as mean + SD; $P < 0.01$. nl, no lesion. (**F**) Tumor incidence and (**G**) histology grade in $Kras^{G12D}$ and $Kras^{G12D}Ikk2^{\Delta Pdx}$ mice. $^{*}P < 0.05$. (**H**–**K**) $Kras^{G12D}$ and $Kras^{G12D}Ikk2^{\Delta Pdx}$ 4-month old pancreases stained with (**H**) hematoxylin and eosin, (**I**) Masson's trichrome (blue, collagen; red, muscle fibers and cytoplasm; black, nuclei) and (**J** and **K**) anti-PCNA. Original magnification, ×10 (**H**–**J**), ×20 (**K**).

and throughout PDAC but not in normal pancreatic epithelium (5, 15). In the context of mutant Kras, Notch pathway activation has been shown to have a tumor-promoting role and has been implicated in mediating metaplasia of acinar to ductal epithelium, a critical process in pancreatic carcinogenesis (17–19).

In the present study we showed that genetic deletion of *Ikk2* in $Kras^{+/LSL\text{-}G12D}Pdx1\text{-}cre$ mice blocked the progression of PanIN lesions. We further demonstrated that Tnf-α stimulation of initiated pre-malignant epithelial cells via Ikk2 engaged with canonical Notch signaling to upregulate the expression of primary Notch target genes. The crosstalk between NF-κB and Notch downregulated Pparγ, a repressor of inflammatory gene expression and retained a constitutive production of proinflammatory mediators and cytokines by the transformed cells.

Results

Pancreas-specific deletion of Ikk2 blocks PanIN progression in $Kras^{G12D}$ mice. $Kras^{+/LSL\text{-}G12D}Pdx1\text{-}cre$ (abbreviated as $Kras^{G12D}$) mice express an endogenous oncogenic $Kras^{G12D}$ allele initially in pancreatic progenitors and later in the adult pancreas (5). We generated ductal epithelial cell lines from PanIN- and PDAC-bearing $Kras^{G12D}$ mice and identified constitutive secretion of Tnf-α (Figure 1A), similar to previous data indicating Tnf-α production by initiated pre-malignant ovarian epithelial cells (20). To determine the role of Ikk2/NF-κB signaling in formation and progression of PanINs, we generated $Kras^{+/LSL\text{-}G12D}Ikk2^{fl/fl}Pdx1\text{-}cre$ ($Kras^{G12D}Ikk2^{\Delta Pdx}$) mice. In parallel, we assessed the contribution of malignant cell–derived Tnf-α using $Kras^{+/LSL\text{-}G12D}Tnfa^{fl/fl}Pdx1\text{-}cre$ ($Kras^{G12D}Tnfa^{\Delta Pdx}$) mice.

The compound strains were generated by interbreeding C57BL/6 mice carrying floxed *Ikk2* or *Tnfa* alleles with the $Kras^{+/LSL\text{-}G12D}$ and *Pdx1-cre* strains (Supplemental Figure 1A; supplemental material available online with this article; doi:10.1172/JCI45797DS1). No gross pathology was observed in the pancreas of $Ikk2^{\Delta Pdx}$ or $Tnfa^{\Delta Pdx}$ mice (Supplemental Figure 1B). Activity of the Ikk complex was abolished in cells derived from $Kras^{G12D}Ikk2^{\Delta Pdx}$ mice, confirming excision of the *Ikk2* locus (Figure 1B). Secretion of Tnf-α and Il-6 in the pancreas was also significantly decreased ($P < 0.01$, $n = 6$, Figure 1C). Similarly, cell lines derived from PanIN- and PDAC-bearing $Kras^{G12D}Tnfa^{\Delta Pdx}$ mice secreted minimal levels of Tnf-α, confirming *Tnfa* inactivation (Figure 1D).

We assessed the development of PanIN lesions in cohorts ($n = 12$ per time point) of $Kras^{G12D}$, $Kras^{G12D}Ikk2^{\Delta Pdx}$, and $Kras^{G12D}Tnfa^{\Delta Pdx}$ mice at 2, 5, and 8 months of age. Histological assessment for the proportion of pancreas occupied by PanINs was carried out as previously described (4). *Ikk2* deletion in $Kras^{G12D}Ikk2^{\Delta Pdx}$ mice resulted in a profound decrease in the frequency of high-grade PanINs (PanINs 2 and 3) at all time points ($P < 0.01$; Figure 1E). Only low-grade PanINs were present in 5-month-old $Kras^{G12D}Ikk2^{\Delta Pdx}$ mice, while approximately 80% of the pancreatic parenchyma retained normal exocrine tissue. Even at 8 months of age, formation of grade 2 and 3 lesions was minimal, and the frequency of grade 1 PanINs was lower compared with both $Kras^{G12D}$ and $Kras^{G12D}Tnfa^{\Delta Pdx}$ mice ($P < 0.01$; Figure 1E).

Two-month-old $Kras^{G12D}Tnfa^{\Delta Pdx}$ mice exhibited a significant reduction in early PanIN lesions ($P < 0.01$, $n = 12$). However, by 5 months of age, PanINs had formed and progressed in a pattern similar to that in $Kras^{G12D}$ mice (Figure 1E). These results indicated that, in the context of mutant *Kras*, Ikk2 signaling was important for the development and progression of PanINs. Activation of the pathway by Tnf-α provided by the transformed epithelial cells was important early during the carcinogenic process. However, as the disease progressed, an influx of tumor-associated immune cells, primarily macrophages and neutrophils, compensated Tnf-α cytokine levels. To address the importance of the inflammatory infiltrate to compensate for the lack of inflammatory cytokines, we generated chimeras using *Mx1-cre* mice to target Tnf-α deletion in the leukocyte compartment (Supplemental Figure 2, A–D). Infiltration of these cells was minimal in $Kras^{G12D}Ikk2^{\Delta Pdx}$ pancreases, indicating that *Ikk2* inactivation impaired their capacity to attract other cell types (Supplemental Figure 2, A and B).

To assess whether *Ikk2* depletion affected PDAC development, we followed cohorts of 50 $Kras^{G12D}Ikk2^{\Delta Pdx}$ and 40 $Kras^{G12D}$ mice for nearly 2 years (Table 1 and Supplemental Table 1). Mice were sacrificed when they developed signs of distress. 20% of $Kras^{G12D}Ikk2^{\Delta Pdx}$ mice had PDAC, while there was a 50% tumor incidence in $Kras^{G12D}$ mice (Figure 1F). Interestingly, deletion of *Ikk2* changed the histopathological feature of the observed tumors, as shown by the ratio of undifferentiated to glandular morphology in these mice (Figure 1G) at end point (Table 1 and Supplemental Table 1).

Further histological analyses of $Kras^{G12D}Ikk2^{\Delta Pdx}$ pancreases showed a profound delay in stromal reaction (Figure 1, H and I). Proliferation of acinar cells was assessed by PCNA expression. As shown in Figure 1, J and K, there was a reduction in proliferating acinar cells in $Kras^{G12D}Ikk2^{\Delta Pdx}$ compared with $Kras^{G12D}$ pancreases. No difference was noted in the levels of apoptosis, measured by cleaved caspase-3 staining (data not shown). Collectively, these data indicated that PanIN progression and development of PDAC were dependent on epithelial *Ikk2* depletion.

Notch target genes Hes1 and Hey1 are downregulated in $Kras^{G12D}Ikk2^{\Delta Pdx}$ PanINs. The Notch pathway, normally quiescent in the adult pancreas, is found to be reactivated in pancreatic cancer throughout PanIN and PDAC development (15, 17, 21). We assessed the regulation of Notch downstream targets as indicators of disease development (5). In accordance with previous studies, we found that the classical Notch target genes *Hes1* and *Hey1* were expressed in $Kras^{G12D}$ PanIN-bearing mice (5). However, there was a substantial decrease in their expression in age-matched $Kras^{G12D}Tnfa^{\Delta Pdx}$ and $Kras^{G12D}Ikk2^{\Delta Pdx}$ mice (Figure 2A). The pancreases of $Kras^{G12D}Ikk2^{\Delta Pdx}$ showed decreased expression of *Igfr1*, *Vegf*, and *tenascin C*, all Notch target genes, while expression of *Myc* and the AP-1 family transcription factor *Batf* was not altered (Figure 2A). Inactivation of *Tnfa* had little impact on the expression levels of these genes. Immunofluorescence analysis

Table 1
Disease spectrum in *Kras^{G12D}Ikk2$^{\Delta Pdx}$* mice

ID	Age (d)	PDAC	Histology	Liver	Lung	PD	Ascites	Skin	BO	Atrophy
TH03-35	526	N		N	N	N	N	N	N	Y
TH03-58	599	N		N	N	N	N	N	N	Y
TH03-59	517	N		N	N	N	N	N	N	Y
TH03-61	422	Y	Glandular	Y	Y	Y	N	N	Y	
TH03-66	501	N		N	N	N	N	N	N	Y
TH03-67	449	N		N	N	N	N	N	N	Y
TH03-82	209	N		N	N	N	N	Y	N	
TH03-88	297	N		N	N	N	N	Y	N	
TH03-89	388	N		N	N	N	N	N	N	Y
TH03-115	436	Y	Undifferentiated	Y	Y	Y	N	N	N	
TH03-131	587	N		N	N	N	N	N	N	Y
TH03-136	555	N		N	N	N	N	N	N	Y
TH03-148	475	N		N	N	N	N	N	N	Y
TH03-149	391	N		N	N	N	N	N	N	Y
TH03-167	155	N		N	N	N	N	Y	N	
TH03-177	422	Y	Glandular	Y	N	N	Y	N	N	
TH03-181	448	N		N	N	N	N	N	N	Y
TH03-196	401	N		N	N	N	N	N	N	Y
TH03-197	412	Y	Undifferentiated	Y	Y	Y	N	N	Y	
TH03-206	389	Y	Undifferentiated	N	N	N	N	N	N	
TH03-207	455	N		N	N	N	N	Y	N	
TH03-213	438	N		N	N	N	N	N	N	Y
TH03-344	264	N		N	N	N	N	Y	N	
TH03-365	428	N		N	N	N	N	N	N	Y
TH03-374	417	N		N	N	N	N	N	N	Y
TH03-384	409	Y	Glandular	N	N	N	N	N	N	
TH03-402	337	N		N	N	N	N	N	N	Y
TH03-404	316	Y	Undifferentiated	Y	Y	Y	Y	Y	Y	
TH03-405	406	N		N	N	N	N	N	N	Y
TH03-416	472	N		N	N	N	N	N	N	Y
TH03-425	515	N		N	N	N	N	N	N	Y
TH03-431	411	N		N	N	N	N	N	N	Y
TH03-452	509	Y	Undifferentiated	Y	Y	N	Y	N	Y	
TH03-497	377	N		N	N	N	N	N	N	Y
TH03-499	482	Y	Undifferentiated	N	Y	Y	N	N	Y	
TH03-503	568	N		N	N	N	N	N	N	Y
TH03-509	263	N		N	N	N	N	Y	N	
TH03-515	174	N		N	N	N	N	Y	N	
TH03-518	248	N		N	N	N	N	Y	N	
TH03-522	315	N		N	N	N	N	N	N	
TH03-546	427	N		N	N	N	N	N	N	Y
TH03-551	482	N		N	N	N	N	N	N	Y
TH03-552	517	N		N	N	N	N	N	N	Y
TH03-568	268	N		N	N	N	N	Y	N	
TH03-574	216	N		N	N	N	N	Y	N	
TH03-681	498	N		N	N	N	N	N	N	Y
TH03-682	571	N		N	N	N	N	N	N	Y
TH03-693	501	N		N	N	N	N	N	N	Y
TH03-699	585	Y	Glandular	N	N	N	Y	N	Y	Y
TH03-706	433	N		N	N	N	N	Y	N	N
Median	427.5	20% Y	60% undifferentiated, 40% glandular	12%	12%	10%	8%	24%	12%	58%

PD, peritoneal disease; BO, biliary obstruction.

revealed Hes1-positive staining in PanIN lesions of 3-month-old *Kras^{G12D}* mice. Similar levels of Hes1 were found in *Kras^{G12D}Tnfa$^{\Delta Pdx}$* mice (Figure 2B). In contrast, Hes1 protein was minimal in age-matched *Kras^{G12D}Ikk2$^{\Delta Pdx}$* animals (Figure 2B). These results indicated concurrent activity of the classical NF-κB and Notch pathways.

To further dissect the interaction of the Tnf-α/Ikk2 and Notch signaling pathways, we examined the response of cell lines derived from *Kras^{G12D}*, *Kras^{G12D}Tnfa$^{\Delta Pdx}$* and *Kras^{G12D}Ikk2$^{\Delta Pdx}$* mice to recombinant Tnf-α (rTnf-α) stimulation in vitro. Basal Notch activity in *Kras^{G12D}* cell lines was demonstrated by nuclear localization of

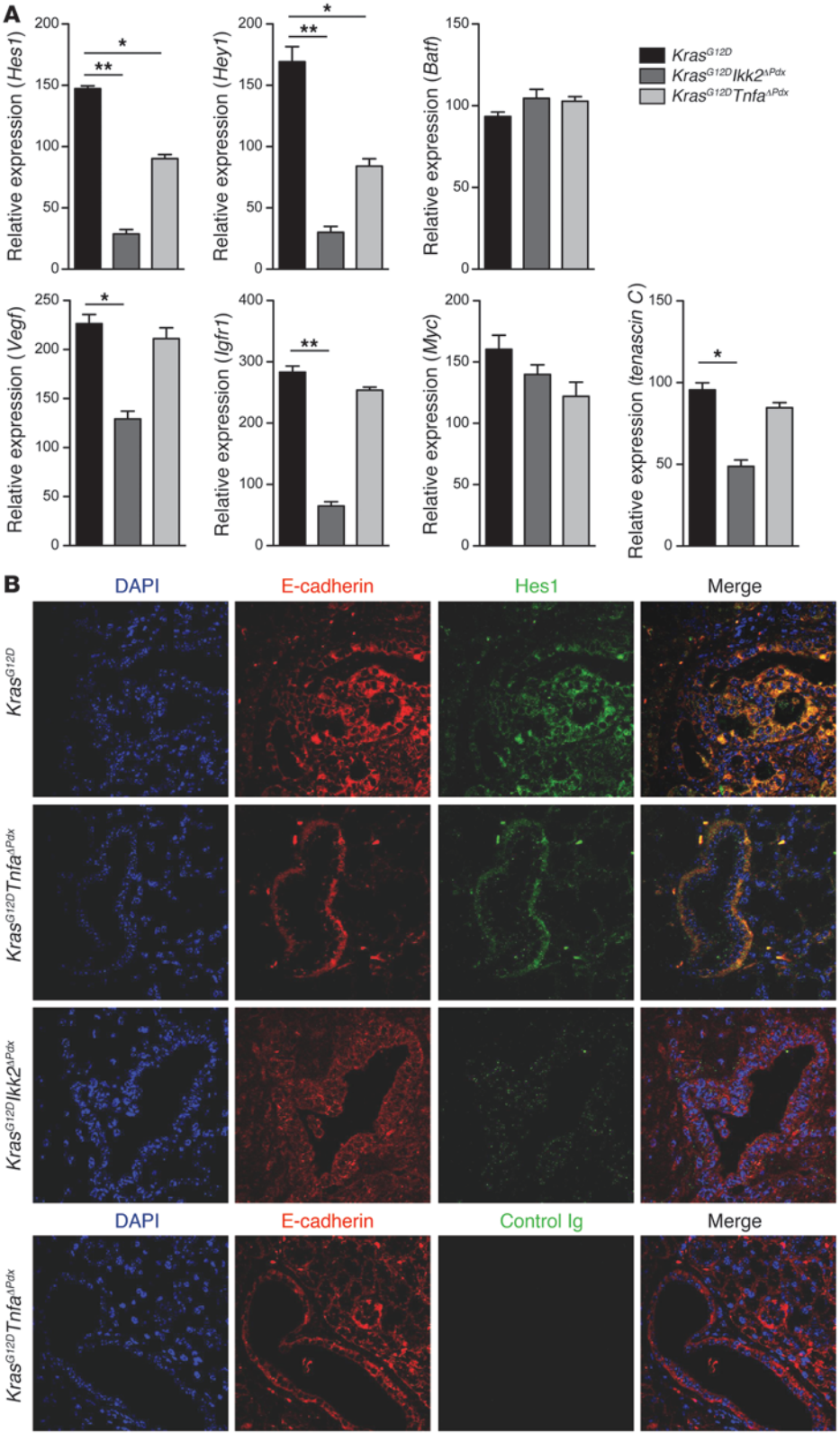

Figure 2
Molecular analysis of Notch and NF-κB target gene expression in *Kras*^{G12D} *Tnfa*$^{\Delta Pdx}$ and *Kras*^{G12D}*Ikk2*$^{\Delta Pdx}$ pancreases. (**A**) Relative mRNA expression of *Hes1*, *Hey1*, *Batf*, *Vegf*, *Igfr1*, *Myc*, and *tenascin C* in *Kras*^{G12D}*Tnfa*$^{\Delta Pdx}$ and *Kras*^{G12D}*Ikk2*$^{\Delta Pdx}$ 3-month PanIN-bearing pancreases was measured by real-time PCR. Data are shown as mean + SD; $n = 6$. $^{*}P < 0.05$, $^{**}P < 0.01$. The experiment was done in duplicate. (**B**) Immunofluorescence staining for Hes1 and E-cadherin in PanIN-bearing pancreases from *Kras*^{G12D}*Tnfa*$^{\Delta Pdx}$, *Kras*^{G12D}*Ikk2*$^{\Delta Pdx}$, and *Kras*^{G12D} mice at 3 months of age. Original magnification, ×40. Blue, DAPI; red, E-cadherin; green, Hes1.

Hes1 and low levels of cytoplasmic staining (Figure 3A). Stimulation with rTnf-α increased expression of both nuclear and cytoplasmic Hes1 protein (Figure 3A). The expression of *Hes1*, *Hey1*, as well as *Batf*, *Vegf*, *Igfr1*, *Myc*, and *tenascin C* was increased in *Kras*^{G12D} and *Kras*^{G12D}*Tnfa*$^{\Delta Pdx}$ cells after rTnf-α stimulation. In contrast, rTnf-α failed to upregulate expression of these genes in *Kras*^{G12D}*Ikk2*$^{\Delta Pdx}$ cells (Figure 3B and Supplemental Figure 3A). We next transiently transfected the cell lines with a *Hes1* luciferase reporter construct and

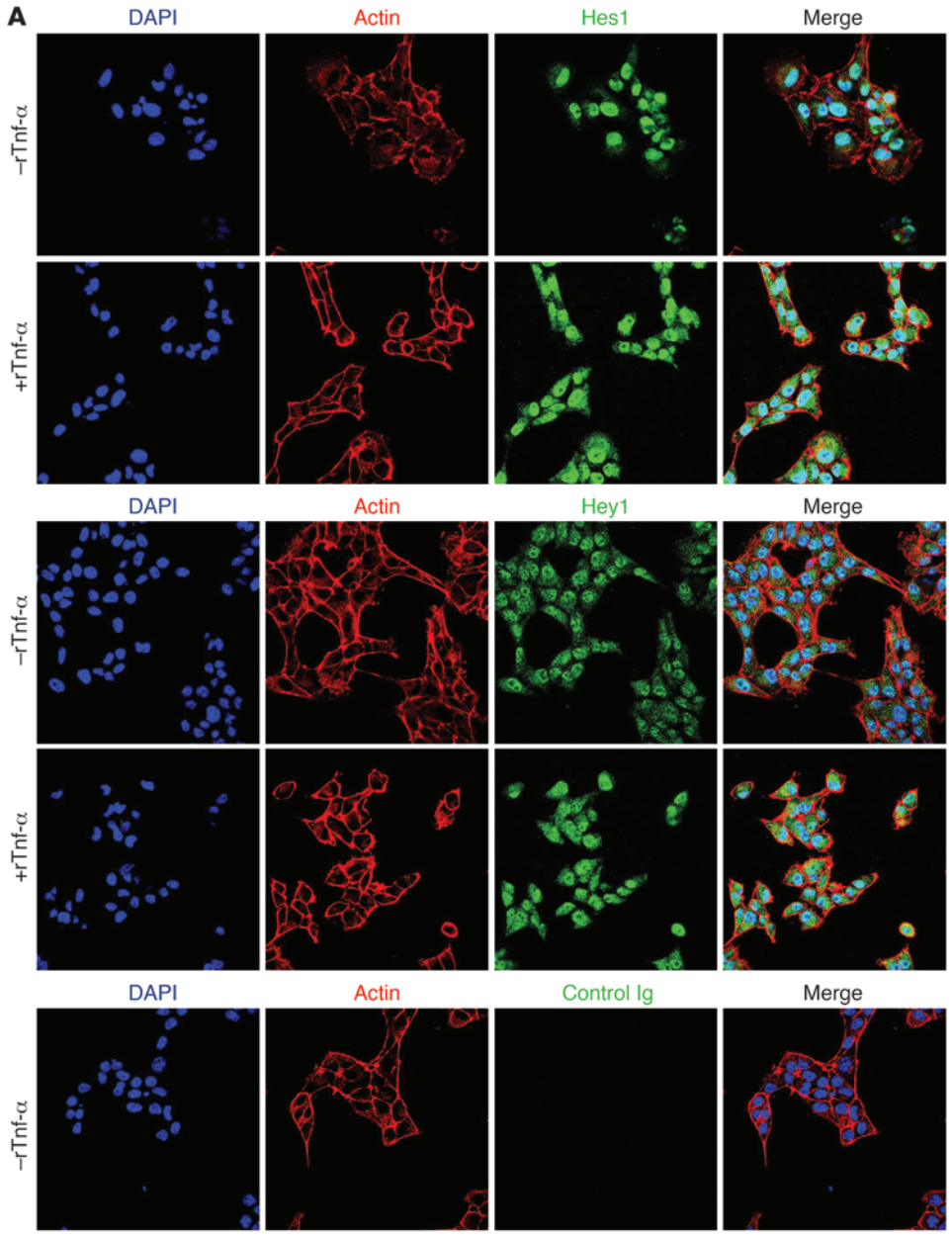
A
DAPI
Actin
Hes1
Merge
−rTnf-α
+rTnf-α
DAPI
Actin
Hey1
Merge
−rTnf-α
+rTnf-α
DAPI
Actin
Control Ig
Merge
−rTnf-α

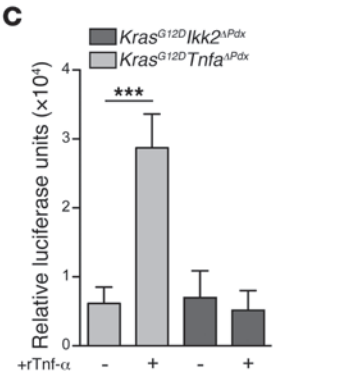
C
KrasG12DIkk2ΔPdx
KrasG12DTnfaΔPdx
Relative luciferase units (×10⁴)
***
+rTnf-α

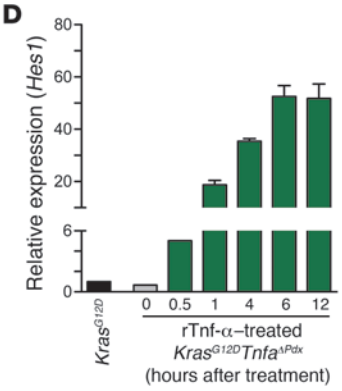
D
Relative expression (Hes1)
KrasG12D
rTnf-α–treated
KrasG12DTnfaΔPdx
(hours after treatment)

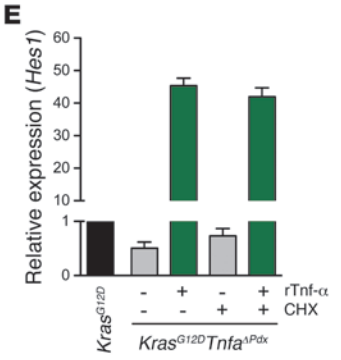
E
Relative expression (Hes1)
rTnf-α
CHX
KrasG12D
KrasG12DTnfaΔPdx

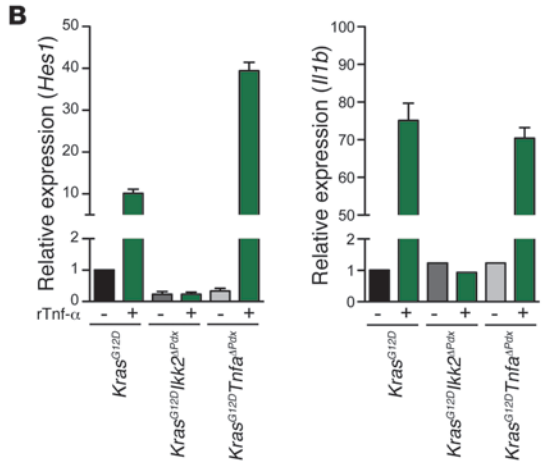
B
Relative expression (Hes1)
Relative expression (Il1b)
rTnf-α
KrasG12D
KrasG12DIkk2ΔPdx
KrasG12DTnfaΔPdx

Figure 3
Tnf-α–induced Notch and NF-κB target gene expression in PanIN cell lines. (**A**) Expression of *Hes1* and *Hey1* in $Kras^{G12D}$ PanIN cell lines was examined by immunofluorescence staining; cells were left unstimulated or were stimulated with 10 ng/ml rTnf-α for 24 hours. Original magnification, ×40. Blue, DAPI; red, actin; green, Hes1. One representative experiment of 3 performed is shown. (**B**) Relative mRNA expression of *Hes1* and *Il1b* in PanIN cell lines stimulated with 1 ng/ml rTnf-α for 6 hours. Relative expression was calculated by setting expression of untreated $Kras^{G12D}$ samples as 1. (**C**) *Hes1* luciferase reporter assay in $Kras^{G12D}Tnfa^{\Delta Pdx}$ and $Kras^{G12D}Ikk2^{\Delta Pdx}$ PanIN cell lines stimulated with 1 ng/ml rTnf-α for 6 hours. Results were normalized to firefly luciferase activity relative to internal control and are expressed as mean + SD from triplicate transfections. $^{***}P < 0.01$. One representative experiment of 3 performed is shown. (**D**) Kinetic analysis of *Hes1* mRNA expression in $Kras^{G12D}Tnfa^{\Delta Pdx}$ PanIN cell lines stimulated with 1 ng/ml rTnf-α. (**E**) $Kras^{G12D}Tnfa^{\Delta Pdx}$ PanIN cells were treated with 1 ng/ml rTnf-α in the presence or absence of 15 μg/ml cycloheximide (CHX). Expression of *Hes1* was quantified by real-time PCR. Relative expression was calculated by setting expression of untreated $Kras^{G12D}$ samples as 1. (**B**, **D**, and **E**) Data are shown as mean + SD of triplicate determinants, and 1 representative experiment of 3 is shown.

stimulated them with 1 ng/ml rTnf-α. This resulted in enhanced transcriptional activity of the *Hes1* promoter in $Kras^{G12D}Tnfa^{\Delta Pdx}$ but not in $Kras^{G12D}Ikk2^{\Delta Pdx}$ cells (Figure 3C). These results showed that in initiated pre-malignant epithelial cells Ikk2 signaling enhanced the expression of Notch target genes.

Activation of the NF-κB pathway is known to upregulate Notch receptors and ligands, both of which are found to be expressed on PanIN and PDAC cells (17, 22–26). However, an interaction downstream of the two pathways has not been described. We next assessed whether this enhanced expression of Notch target genes upon stimulation with rTnf-α was due to upregulation of Notch receptors and ligands, which would reinforce downstream signaling. We stimulated $Kras^{G12D}Tnfa^{\Delta Pdx}$ cell lines with rTnf-α over a full 12-hour time course and assessed mRNA expression of *Hes1* and *Hey1*. Upregulation of gene expression occurred within 30 minutes and reached a plateau between 6 and 12 hours after treatment (Figure 3D and Supplemental Figure 3B). This rapid upregulation of *Hes1* and *Hey1* was independent of new protein synthesis and suggested a direct interaction between the pathways (Figure 3E and Supplemental Figure 3C).

Tnf-α–induced Notch target gene expression requires canonical Notch signaling and Ikk2-mediated histone phosphorylation. We next sought to determine whether Tnf-α–induced upregulation of Notch target genes required canonical Notch signaling. This is initiated by proteolytic cleavage of NICD following receptor-ligand interactions, mediated by the γ-secretase activity of a multiprotein complex (27). Pharmacological inhibition of γ-secretase using the synthetic inhibitor L685458 resulted in attenuation of *Hes1* and *Hey1* expression in rTnf-α–stimulated $Kras^{G12D}Tnfa^{\Delta Pdx}$ PanIN cell lines (Figure 4A). While expression of both these genes was sensitive to L685458, transcription levels of *Il1b*, *Mmp13*, and *Cox2*, all NF-κB targets, remained unaffected (Supplemental Figure 4). We maximally engaged Notch receptors by stimulating $Kras^{G12D}$ cells with the classical Notch ligands Jagged-2 and Delta-like–1 (Dll1) and compared the levels of *Hes1* and *Hey1* expression with those after treatment with rTnf-α. rTnf-α induced higher *Hes1* and *Hey1* levels than ligand-mediated Notch activation of the pathway (Figure 4B).

We further examined the requirement of Notch signaling for Tnf-α–mediated upregulation of *Hes1* and *Hey1* using siRNA to knock down the expression of *Rbpj*, a nuclear transcription factor essential for Notch target gene expression. Transfection of $Kras^{G12D}Tnfa^{\Delta Pdx}$ cell lines with *Rbpj* siRNA resulted in a 4-fold decrease in *Hes1* and *Hey1* transcripts, confirming the requirement of NICD–Rbp-j interaction for upregulation of target gene expression (Figure 4C and Supplemental Figure 5A). Expression of the NF-κB targets *Il1b* and *Cox2* remained unaffected in *Rbpj*-knockdown cells (data not shown). Specific siRNA inhibition of *Ikk2* also resulted in a downregulation of *Hes1* and *Hey1* expression following rTnf-α treatment (Figure 4D and Supplemental Figure 5B). This was consistent with our previous observation that $Kras^{G12D}Ikk2^{\Delta Pdx}$ cell lines lost the capacity to upregulate *Hes1* and *Hey1* upon rTnf-α stimulation. Similarly, knockdown of *Nemo* blocked *Hes1* and *Hey1* expression (Supplemental Figure 5C), while knockdown of *Ikk1* (Supplemental Figure 5D) had no effect on *Hes1* or *Hey1* expression.

Hes1 expression is not known to be regulated by NF-κB (16). To investigate the pathways downstream of Ikk2 that lead to *Hes1* activation, we examined phosphorylation of histone H3 at serine 10, a histone modification that is induced by Ikk2 and is linked with recruitment of RNA polymerase II and transcriptional activation (28–30). We carried out ChIP and real-time PCR assays and showed that rTnf-α stimulation induced phosphorylation of histone H3 at serine 10 at the *Hes1* promoter (Figure 5). This inducible phosphorylation was abolished in $Kras^{G12D}Ikk2^{\Delta Pdx}$ cells (Figure 5). These results indicate a link between Tnf-α–stimulated Ikk2 signaling and the *Hes1* locus, whereby Tnf-α enhanced the transcriptional activity of a classical Notch target gene via Ikk2 by inducing histone H3 phosphorylation.

Tnf-α–induced crosstalk between NF-κB and Notch pathways leads to Hes1-mediated Pparγ inhibition. Hes1 is known to bind to the promoter region of the nuclear receptor Pparγ and suppress its expression (31). Pparγ represses inflammatory gene expression induced by other classes of transcription factors including NF-κB. We observed higher *Pparg* mRNA expression in 2-month-old $Kras^{G12D}Tnfa^{\Delta Pdx}$ and $Kras^{G12D}Ikk2^{\Delta Pdx}$ compared with $Kras^{G12D}$ pancreases (Figure 6A). However, by 5 months of age, expression of *Pparg* in $Kras^{G12D}Tnfa^{\Delta Pdx}$ was only marginally higher than in $Kras^{G12D}$ mice. In contrast, it remained elevated in $Kras^{G12D}Ikk2^{\Delta Pdx}$ pancreases (Figure 6A). Moreover, after rTnf-α stimulation, *Pparg* mRNA in $Kras^{G12D}Tnfa^{\Delta Pdx}$ cells decreased to levels similar to those in $Kras^{G12D}$ cells (Figure 6B). Binding of Hes1 to the *Pparg* promoter in $Kras^{G12D}$ cells was confirmed by ChIP (Figure 6C). These data indicated that Tnf-α–induced *Hes1* upregulation in initiated pre-malignant cells resulted in *Pparg* suppression.

We further examined the interplay between *Hes1* and *Pparg* using *Hes1*-specific siRNA to knock down *Hes1* expression in $Kras^{G12D}$ PanIN cell lines. This resulted in robust upregulation of *Pparg* expression, which indicates *Hes1*-mediated inhibition of *Pparg* transcription (Figure 6D and Supplemental Figure 6, A and B). Similarly, *Cebpa*, a transcription factor whose expression requires *Pparg*, was also negatively regulated by *Hes1* (Figure 6D and Supplemental Figure 6C).

Hes proteins suppress gene expression by a number of mechanisms that include binding to N boxes or suppressing E box–mediated transcription in promoters that contain tandem E boxes and Rbp-j sites (32–34). We investigated the mechanism by which Hes1 inhibits *Pparg* expression in our system by analyzing the effects of Hes1 on

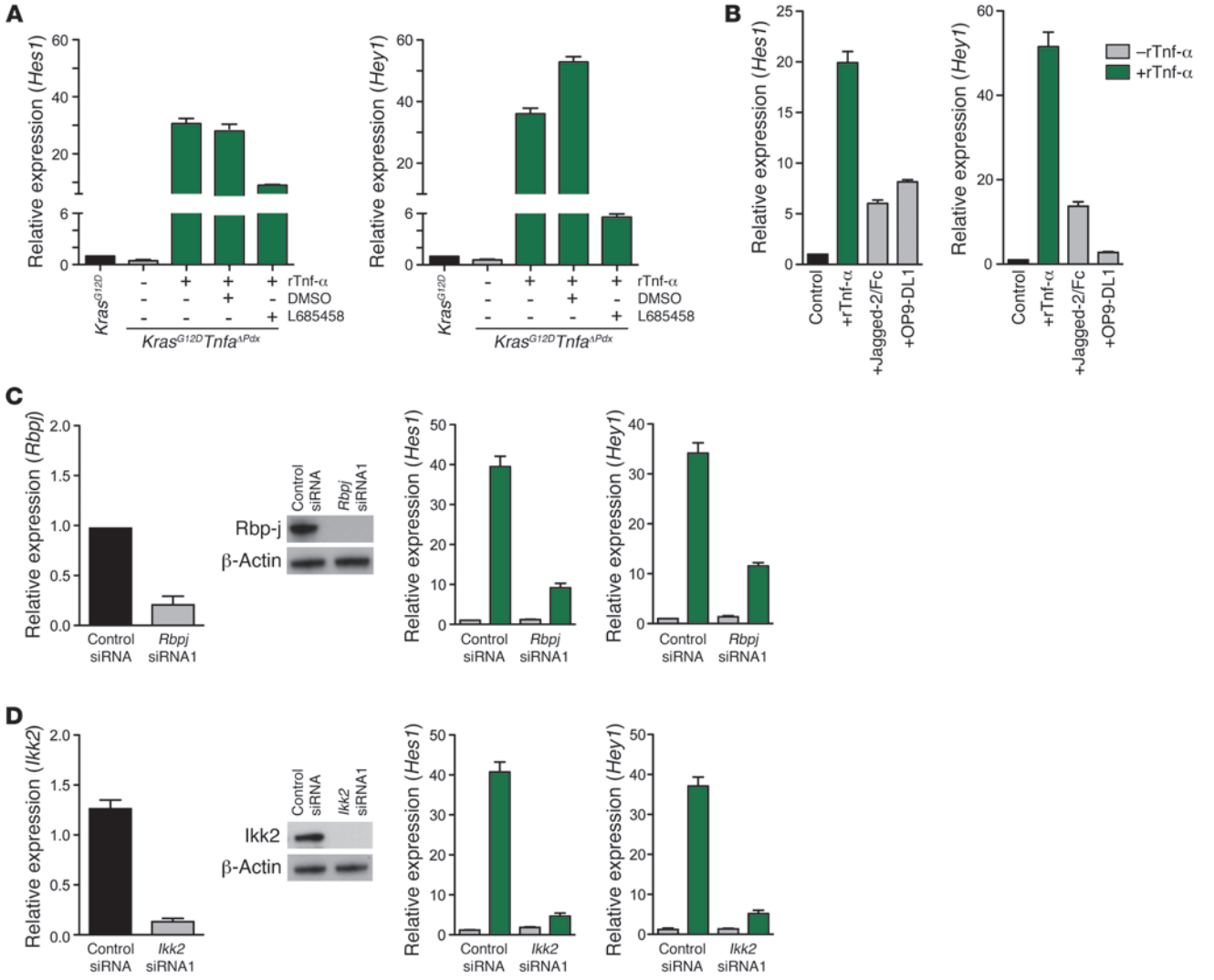

Figure 4

Tnf-α–induced Notch target gene expression requires expression of *Rbpj* and *Ikk2*. (**A**) Inhibition of *Hes1* and *Hey1* mRNA expression in Tnf-α–induced $Kras^{G12D}Tnfa^{\Delta Pdx}$ PanIN cells treated with the γ-secretase inhibitor L685458 (5 μM). Cells were stimulated with 1 ng/ml rTnf-α. (**B**) $Kras^{G12D}Tnfa^{\Delta Pdx}$ PanIN cells were treated with rTnf-α, 20 μg/ml Jagged-2/Fc, or cocultured with OP9-DL1 cells. Tnf-α was more efficient in inducing the expression of *Hes1* and *Hey1*. The results were normalized to values obtained from $Kras^{G12D}$ cells. (**C** and **D**) $Kras^{G12D}Tnfa^{\Delta Pdx}$ PanIN cell lines transfected with (**C**) *Rbpj*- or (**D**) *Ikk2*-specific siRNA. Forty-eight hours after transfection, cells were stimulated with 1 ng/ml rTnf-α for 6 hours, and expression of *Hes1* was quantified by real-time PCR. Nontargeting siRNA and/or unstimulated controls were included. Results were normalized to uninfected and unstimulated $Kras^{G12D}Tnfa^{\Delta Pdx}$ cells. All data are shown as mean + SD of triplicate determinants and are representative of 3 independent experiments.

the activity of a *Pparg* promoter–driven reporter gene. We confirmed, in transient transfection assays, that Hes1 suppressed expression of a *Pparg* promoter–driven reporter gene, in a dose-dependent manner (Figure 6E), through sequences from –1,500 to –160 that contain 6 E-box elements (31). A truncated E box sequence abrogated the ability of Hes1 to inhibit *Pparg* promoter activity (Figure 6F).

Pharmacological intervention in Notch and Pparγ signaling modulates the inflammatory profile of malignant cells and inhibits PanIN growth. Pharmacological inhibition of NF-κB or Notch signaling by anti–Tnf-α, the NF-κB inhibitor Bay11-7082, or the γ-secretase inhibitor DAPT could block the expression of *Hes1* in PanIN-bearing 5-month-old mice. As shown in Figure 7, each of these approaches inhibited *Hes1* in PanIN-bearing pancreases and reduced Tnf-α cytokine levels in $Kras^{G12D}$ cells ($P < 0.01$; Figure 7, A–C).

We hypothesized that this interplay between NF-κB and Notch signaling and a coordinated downregulation of *Pparg* acted as a forward feedback loop that sustains expression of inflammatory cytokines and chemokines by the transformed cells. To address this hypothesis, we treated $Kras^{G12D}$ mice with DAPT, a γ-secretase inhibitor. Cytokine arrays on whole pancreases of untreated and DAPT-treated mice revealed downregulation of proinflammatory cytokines and chemokines (Figure 7D). To further strengthen the impact of Notch signaling on the inflammatory state of the transformed cells, we used $Kras^{G12D}$ mice carrying the *Rosa26-LSL-Eyfp*

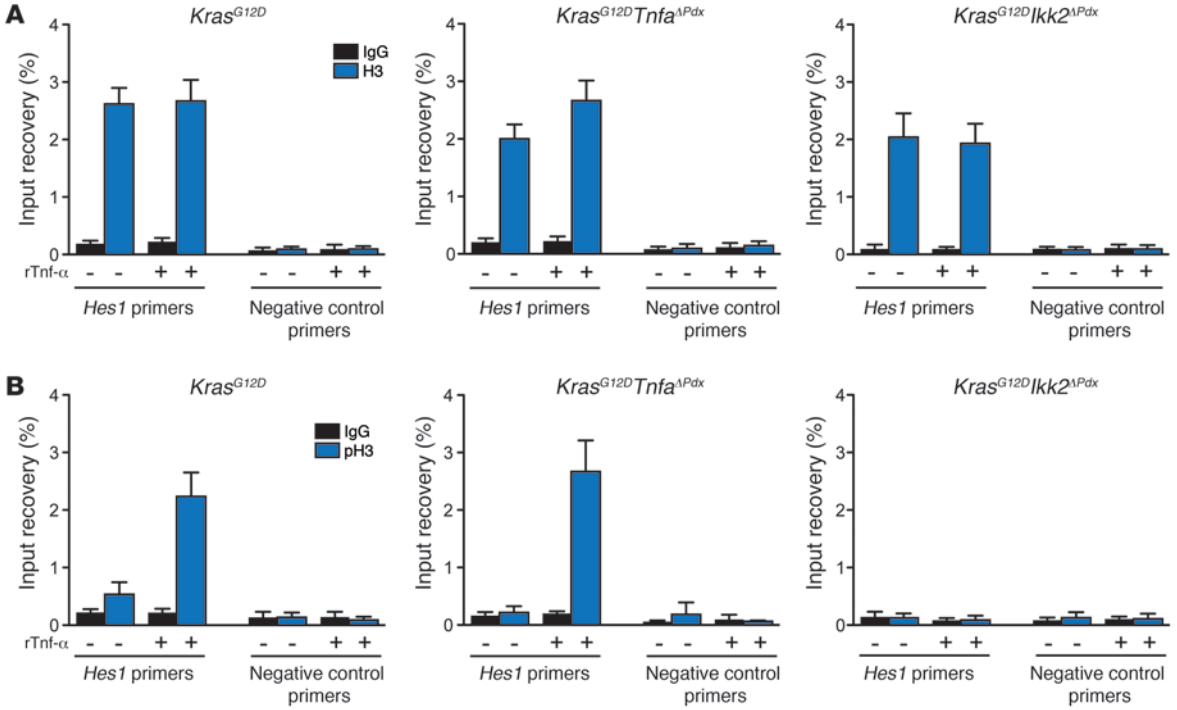

Figure 5
Tnf-α–induced Notch target gene expression is dependent on Ikk2 and chromatin remodeling. ChIP was performed on rTnf-α–treated *Kras*^{G12D}, *Kras*^{G12D}*Tnfa*$^{\Delta Pdx}$, and *Kras*^{G12D}*Ikk2*$^{\Delta Pdx}$ samples with anti–histone H3 (**A**) or anti–phospho–histone H3 at serine 10 (pH3) (**B**). Rabbit IgG was used as control. Precipitated DNA was measured by real-time PCR using primers specific for *Hes1*. Results are shown as mean + SD of triplicate determinants and are representative of 3 independent experiments.

allele. In these mice, *Eyfp* expression was confined to the *Kras*^{G12D}-expressing epithelial cell pool. Cohorts of $n = 12$ mice were treated with DAPT or vehicle, and the Eyfp-positive cells were isolated by FACS. Analysis of the sorted cells showed significant downregulation of *Tnfa* ($P < 0.05$), *Il6* ($P < 0.001$), and *Il1b* expression ($P < 0.01$) in the DAPT-treated group (Figure 7E).

We finally asked whether treatment with rosiglitazone, a Pparγ agonist with antiinflammatory properties in vivo, would influence PanIN development in *Kras*^{G12D} mice (35, 36). Mice were treated with 3 mg/kg/d rosiglitazone added to their daily diet, and cohorts of *Kras*^{G12D} mice were followed for nearly 2 years (Table 2). Progression of PanINs was significantly delayed in rosiglitazone-treated mice compared with the untreated controls ($P < 0.01$, $n = 12$, Figure 8A). Tumor incidence was 2-fold lower (11 of 40) compared with that in untreated mice, greater than that observed in the *Ikk2*-depleted *Kras*^{G12D}*Ikk2*$^{\Delta Pdx}$ animals (10 of 50) (Figure 8, B and C). Analysis of the macrophage infiltrate showed a reduction in the frequency of these cells in rosiglitazone-treated animals (Figure 8D). In total, these data suggest that modulation of tumor-associated inflammatory networks can inhibit PanIN progression and restrain stromal inflammatory components.

Discussion

The integrative interactions among proinflammatory cytokines, transcription factors, and oncogenic signaling pathways are currently the focus of extensive investigation. Here we demonstrated that in the context of Kras-driven pancreatic carcinogenesis, genetic inactivation of *Ikk2* blocked the progression of PanIN lesions. Depletion of *Ikk2* correlated with decreased expression of the classical Notch target genes *Hes1* and *Hey1*. Our further work showed that Tnf-α–induced activation of the NF-κB pathway in initiated pre-malignant epithelial cells cooperated with basal Notch signals to enhance the expression of Notch target genes, in an Ikk2-dependent manner. The interplay between Ikk2 and Notch, via the expression of *Hes1*, repressed the antiinflammatory nuclear receptor Pparγ and created a forward feedback loop that retained the transformed cells in an inflammatory state.

Ikk2 is essential for canonical activation of NF-κB and has been shown to be required for carcinogenesis both in settings where NF-κB activation is driven by *ras* mutations and in inflammation-induced cancer models (7, 8, 10, 11). However, the role of the Ikk2/NF-κB axis is context and cell type dependent; in certain settings, such as those observed in hepatocarcinogenesis, *Ikk2* depletion results in tumor promotion (37). Our data demonstrated that in the context of Kras-driven pancreatic carcinogenesis, genetic deletion of *Ikk2* blocked the progression of malignant epithelial cell lesions.

Activation of NF-κB is known to regulate a number of cellular processes, including a malignant cell–intrinsic network of inflammatory cytokines and chemokines (38). These act in an autocrine and paracrine manner both on the malignant cells and on the surrounding stroma and induce the activity of a number of oncogenic transcription factors, including Stat3 and AP-1 as well as NF-κB itself (10, 11, 20, 39, 40). With deletion of *Ikk2* in initiated pre-malignant epithelial cells, an array of inflammatory cytokines and chemokines at the tumor site was significantly downregulated, and recruitment of macrophages and neutrophils was profoundly decreased (Supplemental Figure 2 and data not shown). Cell-autonomous processes such as proliferation were also affected,

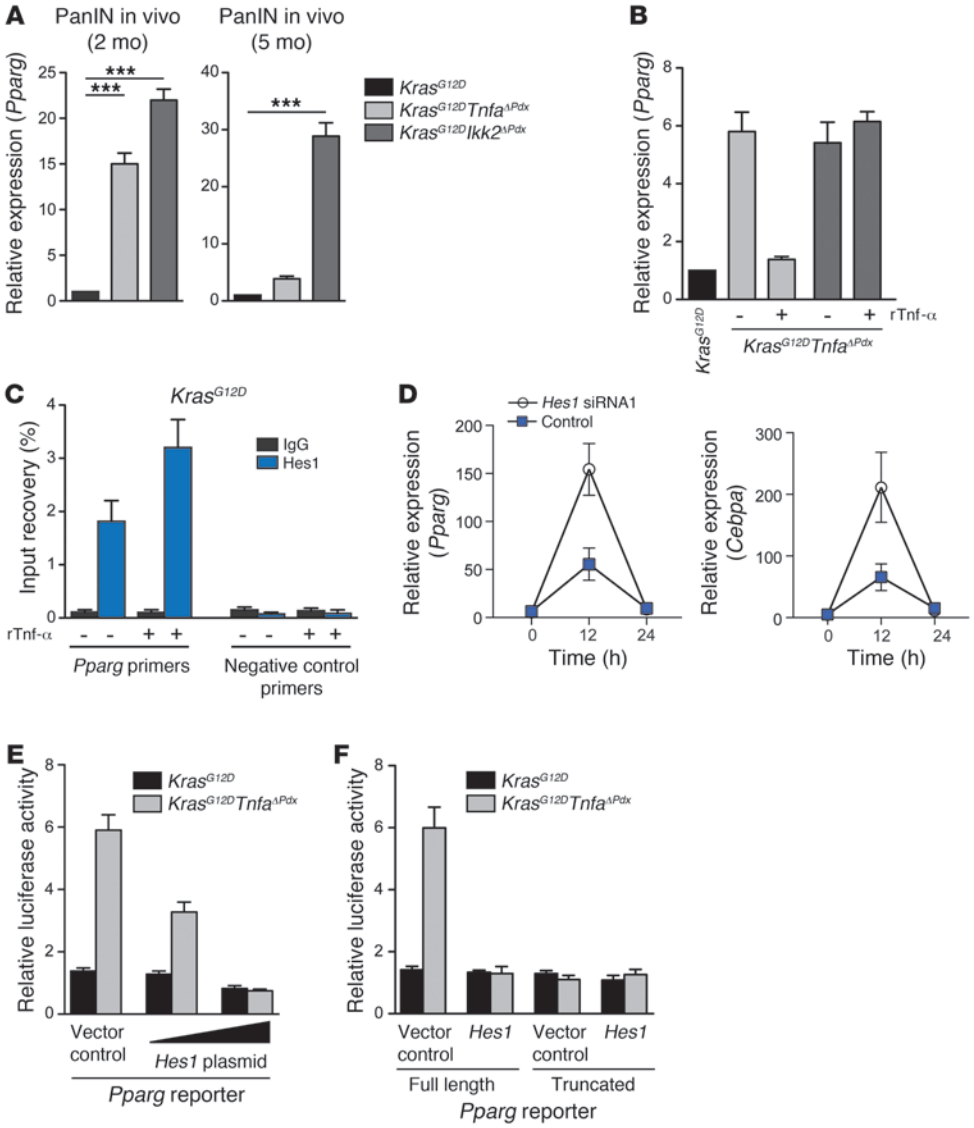

Figure 6

Tnf-α/NF-κB and Notch crosstalk leads to *Hes1*-mediated *Pparg* inhibition. (**A**) *Pparg* mRNA expression in 2- and 5-month-old $Kras^{G12D}Tnfa^{\Delta Pdx}$ and $Kras^{G12D}Ikk2^{\Delta Pdx}$ pancreases. Data were normalized to $Kras^{G12D}$ pancreases. Data are shown as mean + SD; $n = 6$. $^{***}P < 0.001$. The experiment was performed in duplicate. (**B**) Tnf-α stimulation (1 ng/ml) induced downregulation of *Pparg* in $Kras^{G12D}Tnfa^{\Delta Pdx}$ PanIN cell lines. (**C**) ChIP was performed on $Kras^{G12D}$ cells using anti-Hes1 or a control IgG. Precipitated DNA was amplified by real-time PCR using primers specific for *Pparg*. (**D**) siRNA knockdown of *Hes1* upregulated *Pparg* and *Cebpa* expression in $Kras^{G12D}$ PanIN cells. (**E**) $Kras^{G12D}$ and $Kras^{G12D}Tnfa^{\Delta Pdx}$ PanIN cells were cotransfected in duplicate with a *Pparg* reporter construct containing 1,500 bases of the proximal *Pparg* promoter (full length) and a *Hes1* expression plasmid or empty vector control. Twenty-four hours after transfection, cells were analyzed for luciferase activity. (**F**) Transfection of $Kras^{G12D}Tnfa^{\Delta Pdx}$ PanIN cells as described in **E** with a full-length *Pparg* reporter construct or a construct with a truncated Hes1-binding sequence. All data are shown as mean + SD from duplicate transfections and are representative of 3 independent experiments.

and downregulation of Notch target genes was observed. Notch signaling has oncogenic properties in pancreatic carcinogenesis; however, a link between this pathway and canonical NF-κB had not been previously appreciated (17–19).

Tnf-α is a major inflammatory cytokine that activates the NF-κB pathway and is regulated in its expression by NF-κB. We demonstrated that Tnf-α stimulation of initiated pre-malignant epithelial cells resulted in upregulated expression of classical Notch targets. This occurred at the level of transcription by Ikk2-mediated phosphorylation of histone H3, a modification that is linked with transcriptional activation (28–30). Accordingly, Tnf-α–mediated upregulation of *Hes1* and *Hey1* was independent of de novo protein synthesis but required canonical Notch signaling. Our data suggest that activation of NF-κB signaling can synergize with basal Notch signals to induce maximal expression of Notch target genes.

Conversely, Vilimas et al. have demonstrated that in T cell acute lymphoblastic leukemia, constitutively active Notch results in activation of the NF-κB pathway (13). Work from the same group demonstrated that the Notch/Hes1 signaling sustained NF-κB pathway activation by repressing the deubiquitinase CYLD, a negative Ikk complex regulator (41). In conjunction with our data, these studies indicate a bidirectional interaction between the NF-κB and Notch pathways that can result in bidirectional expression of target genes and enhanced malignant cell growth.

Within the tumor microenvironment, Tnf-α stems from two sources: the tumor-infiltrating immune cells and the malignant cells. In accordance with previous studies, we found an influx of inflammatory cells, predominantly macrophages and neutrophils, in $Kras^{G12D}$ mice as disease progressed (42). These cells were a major source of the cytokine in aged mice. We also showed that Kras-induced PanIN and PDAC cells constitutively secreted low levels of Tnf-α. Crosstalk between NF-κB and Notch signaling can therefore be fueled both by a constitutive autonomous activation of NF-κB signaling due to mutant *Kras* and by inflammatory cytokines provided by the immune cells. Our data suggested that early in the carcinogenic process, Tnf-α secreted by the malignant cells is critical for their growth, while at later stages, influx of immune cells constitutes the major source of the cytokine.

Table 2
Disease spectrum in *Kras*^{G12D} mice treated with rosiglitazone

ID	Age (d)	PDAC	Histology	Liver	Lung	PD	Ascites	Skin	BO
CHS601-8	421	N		N	N	N	N	N	N
CHS601-15	438	N		N	N	N	N	N	N
CHS601-19	567	N		N	N	N	N	N	N
CHS601-21	558	Y	Glandular	N	N	Y	Y	N	Y
CHS601-25	621	N		N	N	N	N	N	N
CHS601-27	521	Y	Glandular	Y	N	N	Y	N	Y
CHS601-30	504	Y	Glandular	N	N	Y	N	N	Y
CHS601-31	486	N		N	N	N	N	N	N
CHS601-33	531	N		N	N	N	N	N	N
CHS601-46	367	N		N	N	N	N	N	N
CHS601-55	422	N		N	N	N	N	N	N
CHS601-57	394	Y	Undifferentiated	Y	Y	N	N	N	Y
CHS601-67	357	Y	Glandular	Y	N	N	N	N	N
CHS601-68	547	Y	Glandular	Y	N	N	Y	N	Y
CHS601-69	555	N		N	N	N	N	N	N
CHS601-79	501	N		N	N	N	N	N	N
CHS601-80	408	N		N	N	N	N	N	N
CHS601-83	486	N		N	N	N	N	N	N
CHS601-84	433	N		N	N	N	N	N	N
CHS601-92	567	N		N	N	N	N	N	N
CHS601-96	555	N		N	N	N	N	N	N
CHS601-99	537	N		N	N	N	N	N	N
CHS601-108	521	N		N	N	N	N	N	N
CHS301-116	482	Y	Glandular	N	N	Y	Y	N	Y
CHS601-127	444	N		N	N	N	N	N	N
CHS601-128	518	N		N	N	N	N	N	N
CHS601-142	525	Y	Glandular	Y	N	N	N	N	Y
CHS601-144	367	N		N	N	N	N	N	N
CHS601-161	418	N		N	N	N	N	N	N
CHS601-167	632	N		N	N	N	N	N	N
CHS601-170	555	Y	Undifferentiated	Y	Y	N	N	N	N
CHS601-177	407	N		N	N	N	N	N	N
CHS601-178	634	N		N	N	N	N	N	N
CHS601-185	524	Y	Glandular	N	N	N	Y	N	Y
CHS601-192	301	N		N	N	N	N	N	N
CHS601-197	287	N		N	N	N	N	N	N
CHS601-201	425	N		N	N	N	N	N	N
CHS601-222	486	N		N	N	N	N	N	N
CHS601-224	411	Y	Glandular	Y	N	N	N	Y	N
CHS601-229	518	N		N	N	N	N	N	N
Median	493.5	27.5%	18% undifferentiated, 82% glandular	17.5%	5%	7.5%	12.5%	2.5%	20%

Inflammation induced extrinsically by tissue damage (i.e., pancreatitis) or inflammation related to metabolic stress has been shown to accelerate PanIN development (43–45). The underlying mechanism is a deregulated regeneration process whereby constitutively active Notch permits PanIN formation. By identifying a direct link between NF-κB signaling and enhanced Notch activity, we provide evidence that a major proinflammatory and a developmental signaling pathway can cooperate in the context of mutant *ras* to promote carcinogenesis.

Repression of inflammatory genes by the nuclear receptor Pparγ has been highlighted as an important mechanism by which cells can regulate inflammatory responses and homeostasis (46). Our findings demonstrated that a Tnf-α/Hes1–driven mechanism of Pparγ inhibition operates in initiated pre-malignant pancreatic epithelial cells. Hes1 suppressed *Pparg* expression by targeting E box elements in the promoter of the gene. We propose that the coordinated activity of NF-κB and Notch along with a suppression of antiinflammatory transcription factors such as Pparγ leads to a sustained expression of inflammatory genes and transcription factors and a constitutive production of inflammatory mediators and chemokines by the transformed cells. Pharmacological inhibition of the Notch pathway in *Kras*^{G12D} mice with a γ-secretase inhibitor resulted in attenuation of inflammatory gene expression by the transformed cells and downregulation of cytokine production in the pancreas. It has also been shown to significantly attenuate the development of PanINs (21).

Synthetic Pparγ ligands induce allosteric changes to the receptor and allow it to enter into a repression pathway (47). These agents are shown to have antiinflammatory activity in a variety of models of acute and chronic inflammation, as reviewed in ref. 35. By using rosiglitazone, a Pparγ ligand of the thiazolidinedione class, to treat

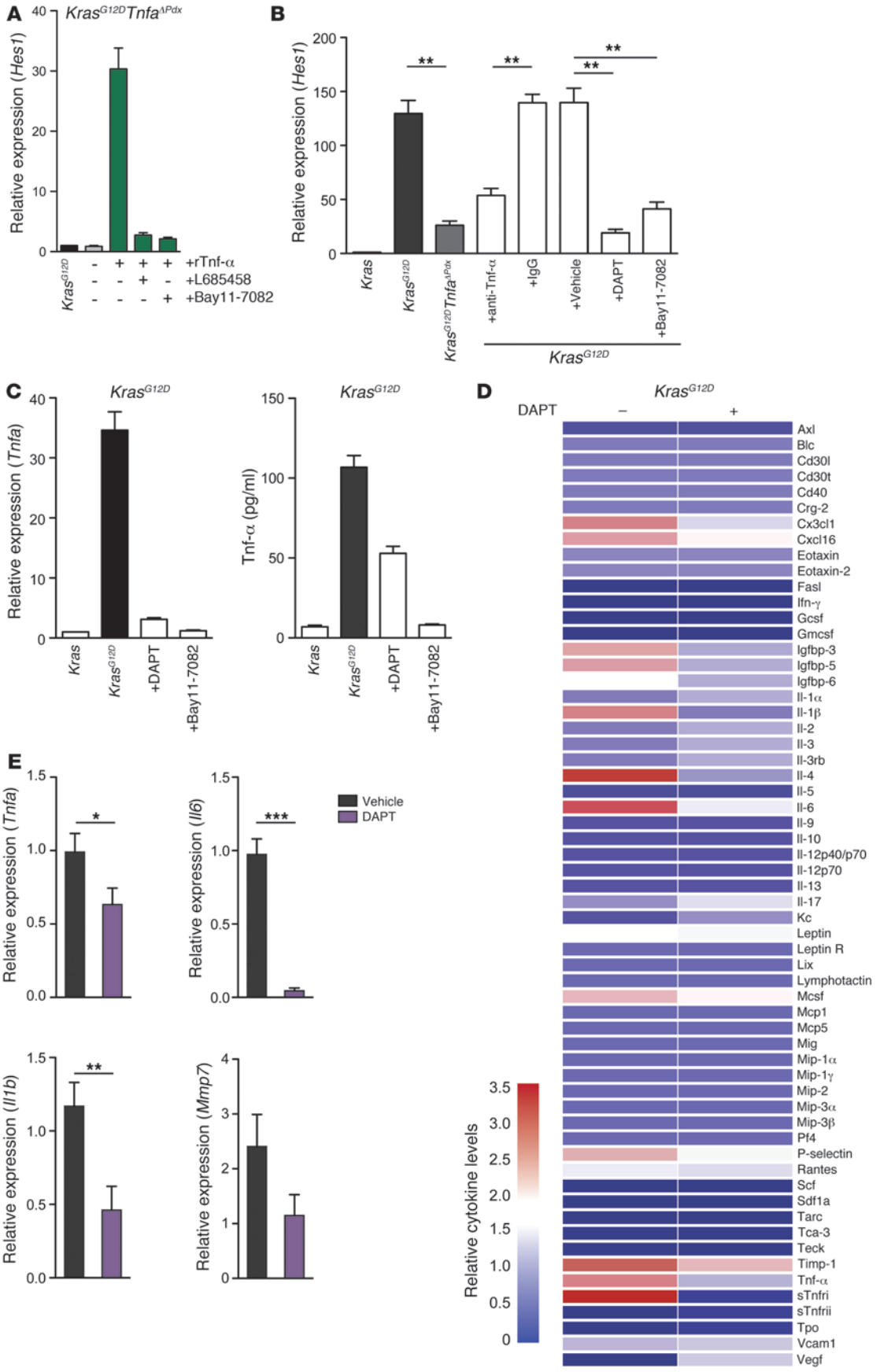
A
KrasG12DTnfaΔPdx
Relative expression (Hes1)
+rTnf-α
+L685458
+Bay11-7082
B
Relative expression (Hes1)
Kras
KrasG12D
KrasG12DTnfaΔPdx
+anti-Tnf-α
+IgG
+Vehicle
+DAPT
+Bay11-7082
KrasG12D
C
KrasG12D
Relative expression (Tnfa)
Tnf-α (pg/ml)
Kras
+DAPT
+Bay11-7082
D
KrasG12D
DAPT
Axl
Blc
Cd30l
Cd30t
Cd40
Crg-2
Cx3cl1
Cxcl16
Eotaxin
Eotaxin-2
Fasl
Ifn-γ
Gcsf
Gmcsf
Igfbp-3
Igfbp-5
Igfbp-6
Il-1α
Il-1β
Il-2
Il-3
Il-3rb
Il-4
Il-5
Il-6
Il-9
Il-10
Il-12p40/p70
Il-12p70
Il-13
Il-17
Kc
Leptin
Leptin R
Lix
Lymphotactin
Mcsf
Mcp1
Mcp5
Mig
Mip-1α
Mip-1γ
Mip-2
Mip-3α
Mip-3β
Pf4
P-selectin
Rantes
Scf
Sdf1a
Tarc
Tca-3
Teck
Timp-1
Tnf-α
sTnfri
sTnfrii
Tpo
Vcam1
Vegf
Relative cytokine levels
E
Vehicle
DAPT
Relative expression (Tnfa)
Relative expression (Il6)
Relative expression (Il1b)
Relative expression (Mmp7)

Figure 7
Inhibition of Notch/NF-κB signaling attenuates the inflammatory profile of malignant cells. (**A**) *Kras*^{G12D}*Tnfa*$^{\Delta Pdx}$ cells were stimulated with 1 ng/ml rTnf-α for 6 hours in the presence or absence of L685458 or Bay11-7082. *Hes1* mRNA expression was quantified by real-time PCR. Results were normalized to unstimulated *Kras*^{G12D} cells. Data are shown as mean + SD of triplicate determinants and are representative of 3 independent experiments. (**B**) *Hes1* mRNA expression in pancreases of 5-month-old untreated *Kras*^{G12D} and *Kras*^{G12D}*Ikk2*$^{\Delta Pdx}$ mice and of *Kras*^{G12D} mice treated with anti–Tnf-α, control IgG, DAPT, Bay11-7082, or the vehicle control. Results were normalized to *Kras* pancreases. Data are shown as mean + SD; $n = 6$. $^{**}P < 0.01$. The experiment was done in duplicate. (**C**) *Kras*^{G12D} PanIN cells were treated with DAPT or Bay11-7082. *Tnfa* mRNA expression and cytokine secretion are indicated. Data are shown as mean + SD of triplicate experiments and are representative of 3 independent experiments. (**D**) Cytokine and chemokine array on whole pancreases of DAPT or vehicle-treated 5-month-old *Kras*^{G12D} mice. The data are represented graphically as normalized signal intensity. (**E**) *Tnfa*, *Il6*, *Il1b*, and *Mmp7* expression in FACS-sorted EYFP-positive *Kras*^{G12D} cells treated for 1 week with DAPT or vehicle. Data are shown as mean + SD; $n = 12$. $^{*}P < 0.05$, $^{**}P < 0.01$, $^{***}P < 0.001$. Analysis of *Mmp7* expression did not reveal statistical significance.

Kras^{G12D} mice, we demonstrated a marked decrease in the frequency of PanINs and their progression into invasive carcinoma. Nevertheless, Pparγ has a wide range of effects on metabolism (48). Thiazolidinedione drugs are best characterized by their insulin-sensitizing action and have been used in the treatment of diabetes. Notably, individuals with type 2 diabetes receiving metformin, a glucose-lowering drug, have a decreased risk of developing pancreatic cancer (49, 50).

Our findings and an increasing body of studies highlight the requirement for inflammatory signaling pathways in the development of pancreatic cancer and reveal key molecular targets to assist current treatments.

Methods

Mouse strains. *Kras*$^{+/LSL\text{-}G12D}$, *Pdx1-cre* (5), *Tnfa*$^{fl/fl}$ (51), and *Ikk2*$^{fl/fl}$ strains (52) were interbred to obtain *Kras*^{G12D}, *Kras*^{G12D}*Tnfa*$^{\Delta Pdx}$, and *Kras*^{G12D}*Ikk2*$^{\Delta Pdx}$ triple mutant mice on a mixed 129/SvJaa/C57BL/6 background (see Supplement Figure 1 for the breeding plan). *Ikk2*$^{fl/fl}$ mice were a gift from Toby Lawrence (Inflammation Biology Group, Centre d'Immunologie de Marseille-Luminy, CNRS-INSERM-Université de la Méditerranée, Marseille, France). *Mx1-cre* mice were obtained from The Jackson Laboratory (53) and crossed to *Tnfa*$^{fl/fl}$ mice. The mice were genotyped at weaning by a commercial vendor (Transnetyx). Six-week-old *Kras*^{G12D} and *Kras*^{G12D}*Tnfa*$^{\Delta Pdx}$ female mice were lethally irradiated and underwent transplantation with bone marrow of female *Tnfa*$^{fl/fl}$ or *Tnfa*$^{fl/fl}$*Mx1-cre* mice ($n = 10$ each group). Two-month old mice were injected 3 times with 5 μg/g body weight poly(I:C) to delete *Tnfa*. Deletion was examined by Tnf-α ELISA of peripheral leukocytes upon ex vivo LPS stimulation. For in vivo experiments, we used rosiglitazone (Cayman Chemical) incorporated into standard rodent chow (3 mg/kg/d; 8 weeks); the Notch antagonist *N*-[*N*-(3,5-difluorophenacetyl)-L-alanyl]-*S*-phenylglycine *t*-butyl ester (DAPT/γ-secretase inhibitor IX, Calbiochem) at 100 mg/kg/d i.p.; L685458 (Sigma-Aldrich) and Bay11-7082 (Alexis) at 10 mg/kg/d i.p. or vehicle; anti–murine Tnf-α (R&D Systems) at 10 mg/kg/d or respective IgG control antibody (R&D Systems). Five-month-old mice were treated for 1 week.

Cell lines and reagents. Primary pancreatic ductal cell lines were derived from *Kras*^{G12D}, *Kras*^{G12D}*Tnfa*$^{\Delta Pdx}$, and *Kras*^{G12D}*Ikk2*$^{\Delta Pdx}$ mice as previously described (54). PanIN cell lines were derived from PanIN lesions with no invasive cancer present within the pancreas of the mouse. OP9-DL1 cells, a bone marrow–derived stromal cell line that ectopically expresses the Notch ligand Dll1 (55), were cocultured with *Kras*^{G12D}*Tnfa*$^{\Delta Pdx}$ pancreatic ductal cells. Cycloheximide and L685458 were purchased from Sigma-Aldrich. Recombinant mouse Tnf-α and Jagged-2/Fc chimeric protein were purchased from R&D Systems.

Histology and immunofluorescence. Histological analysis of pancreases was carried out by standard procedures. Specimens were harvested from time-matched animals, fixed in buffered formalin, and embedded in paraffin. Tissue sections (5 μm) were stained with hematoxylin and eosin or used for immunostaining. PanIN lesions and PDACs were graded as previously described (56). Proliferating cells were assessed by immunohistochemistry using an anti-PCNA antibody (BD Biosciences). Trichrome (Masson's) staining was carried out according to the manufacturer's instructions (Sigma-Aldrich). For immunofluorescence staining, cells were stained using anti-Hes1 (Santa Cruz Biotechnology Inc.) or anti–E-cadherin (Invitrogen) primary antibodies. Cell nuclei were counterstained with DAPI, and cells were visualized under a LSM 510 confocal microscope.

Flow cytometry. Pancreases were minced and digested with 2 mg/ml collagenase type IV (Sigma-Aldrich). Single-cell suspensions were prepared and cells were immunolabeled with fluorochrome-conjugated antibodies in PBS supplemented with 1% FBS. All antibodies were purchased from eBioscience: anti-F4/80–APC (clone BM8), anti-CD11b–PE (M1/70), anti-Ly6G–FITC (RB6-8C5). Flow cytometric data were subsequently acquired on a FACSCalibur flow cytometer (BD Biosciences) and analyzed using FlowJo software. For sorting of Eyfp-positive pancreatic epithelial cells, single-cell suspensions were further digested with 0.05% trypsin (Sigma-Aldrich), and EYFP-positive cells were collected using a FACSAria II sorter (BD Biosciences).

Real-time PCR analysis, protein expression, and kinase activity assay. Total tissue RNA was prepared using an RNeasy kit (QIAGEN). Quantitative PCR was performed as described previously (57). We performed antibody-based multiplex cytokine arrays analyzing the abundance of 62 cytokines and chemokines (Millipore). Tnf-α levels in cell culture supernatants were determined using a commercially available ELISA kit (R&D Systems) according to the manufacturer's instructions. Cells and tumors were lysed and analyzed by SDS-PAGE and immunoblotting (58) with antibodies to Hes1 and Rbp-j (both from Santa Cruz Biotechnology Inc.), Ikk2 (Cell Signaling Technology), and β-actin (Sigma-Aldrich). In vitro Ikk2 kinase activity was assessed using the Kinase Assay Kit (Cell Signaling Technology) according to the manufacturer's instructions.

ChIP. ChIP was performed with the EZ-ChIP Assay Kit (Millipore) in accordance with the manufacturer's instructions. A total of 10^6 PanIN cells were used per condition. Antibodies against phospho–histone H3 at serine 10 (Cell Signaling Technology), anti–total histone H3 (Cell Signaling Technology), and control rabbit IgG (R&D Systems) were used.

siRNA transfection. *Rbpj*-, *Ikk2*-, and *Hes1*-specific siRNAs and nontargeting control siRNAs were purchased from Dharmacon. siRNAs were transfected with Lipofectamine RNAiMAX reagent (Invitrogen).

Luciferase reporter assay. For *Hes1* reporter gene assays, primary *Kras*^{G12D}*Tnfa*$^{\Delta Pdx}$ and *Kras*^{G12D}*Ikk2*$^{\Delta Pdx}$ cells were transfected in duplicate in 24-well plates with a *Hes1* luciferase reporter construct containing the –194 to +160 promoter fragment of the *Hes1* gene inserted upstream of the luciferase gene in pGL2 (gift from Sangram S. Sisodia, Department of Neurobiology, University of Chicago, Chicago, Illinois, USA) and an internal control plasmid encoding *Renilla* luciferase (Promega) with Lipofectamine Plus reagent from Invitrogen (59, 60). On the next day, cells were stimulated with rTnf-α for 6 hours, and cell lysates were prepared and analyzed for firefly and *Renilla* luciferase activity with the Dual-Luciferase Reporter Assay System

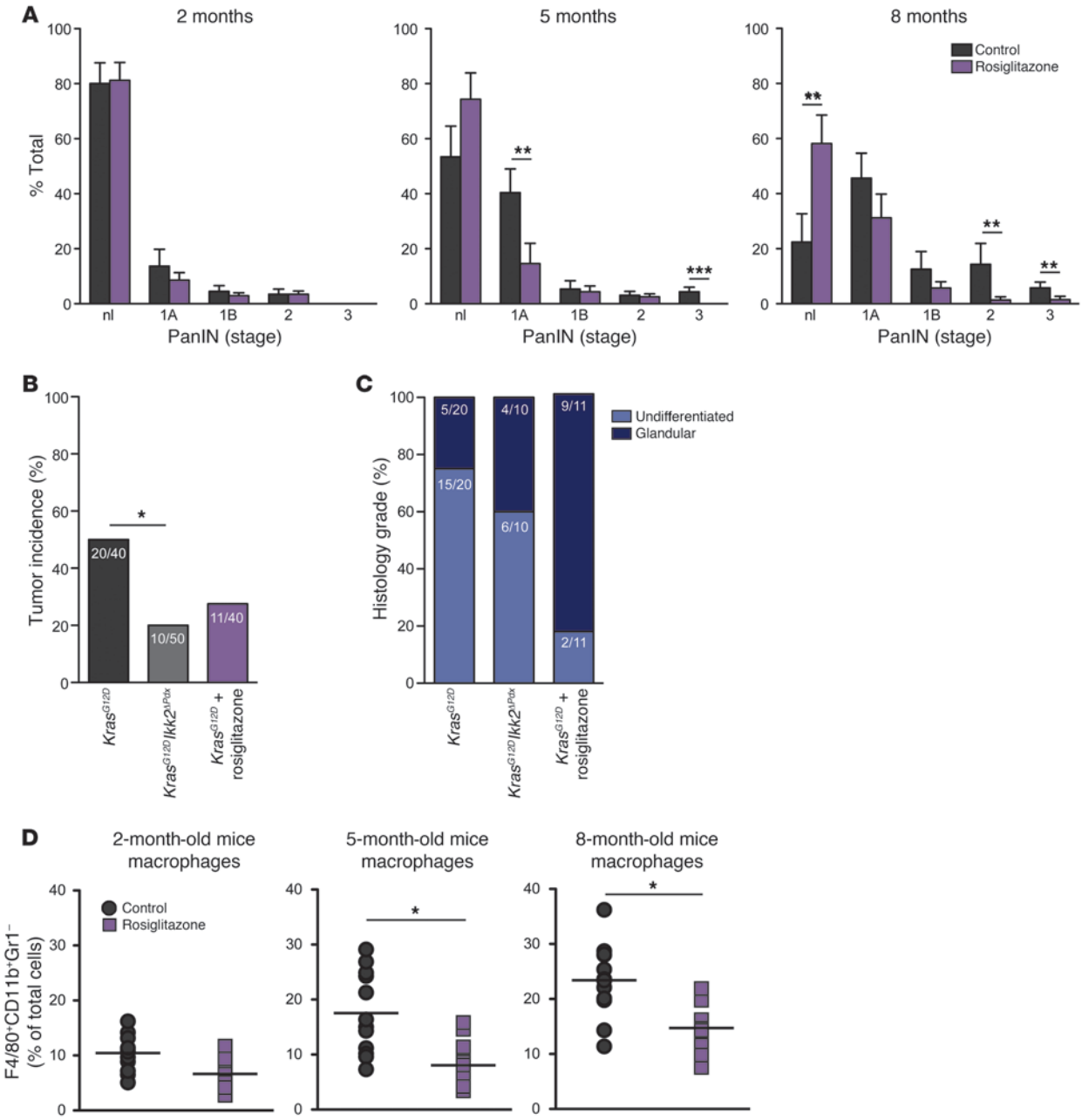

Figure 8

Rosiglitazone treatment blocks PanIN progression in *Kras*^{G12D} mice. (**A**) Quantification of the percentage or pancreatic parenchyma occupied by PanINs in *Kras*^{G12D} mice treated with rosiglitazone compared with untreated controls. Values are shown as mean + SD; $n = 12$. (**B**) Tumor incidence and (**C**) histology grade in rosiglitazone-treated *Kras*^{G12D} mice compared with untreated *Kras*^{G12D} and *Kras*^{G12D}*Ikk2*$^{\Delta Pdx}$ mice. (**D**) Percentage of F4/80$^+$CD11b$^+$Gr1$^-$ cells in the pancreas of 2-, 5-, and 8-month-old *Kras*^{G12D} mice treated with rosiglitazone or untreated as measured by flow cytometry. Each data point represents an individual mouse. Mean values are depicted by the horizontal lines; $n = 10$. $^*P < 0.05$, $^{**}P < 0.01$, $^{***}P < 0.001$.

(Promega). The *Pparg* reporter gene and *Hes1* plasmids (gifts from Marc Montminy, Salk Institute for Biological Studies, La Jolla, California, USA) have been previously described (31). Cells were transfected with the *Pparg* reporter plasmids and an expression plasmid encoding *Hes1* or a control vector as described for *Hes1* reporter gene assays. Results are shown as firefly normalized to *Renilla* luciferase activity.

Statistics. Results were tested for statistical significance using 1- or 2-way ANOVA and Bonferonni's multiple comparisons test on GraphPad Prism version 4.0c software. Tumor incidence was analyzed by Fisher's exact test. *P* values of 0.05 or less were considered statistically significant.

Study approval. Mice were maintained under specific pathogen–free conditions in the Biological Services Unit, Barts Cancer Institute, Queen Mary University of London, and used according to the established institutional guidelines under the authority of a UK Home Office project license (Guidance on Operation of Animals [Scientific Procedures] Act 1986; all animal studies were approved by the UK Home Office).

Acknowledgments

This work is supported by the Medical Research Council (grant G0601867) and Cancer Research UK (grant C18270/A11251). F.R. Balkwill acknowledges the support of the Higher Education Funding Council for England. D.A. Tuveson acknowledges the support of the University of Cambridge, Cancer Research UK, and Hutchison Whampoa Limited. We thank Simon Hallam (Barts Cancer Institute, United Kingdom) for critical review of the manuscript.

Received for publication July 19, 2011, and accepted in revised form September 28, 2011.

Address correspondence to: Thorsten Hagemann, Centre for Cancer and Inflammation, Barts Cancer Institute, Queen Mary University of London, John Vane Science Centre, Charterhouse Square, London EC1M 6BQ, United Kingdom. Phone: 44.20.7882.3590; Fax: 44.20.7882.3885; E-mail: t.hagemann@qmul.ac.uk.

1. Mantovani A, Allavena P, Sica A, Balkwill F. Cancer-related inflammation. *Nature*. 2008; 454(7203):436–444.
2. Downward J. Targeting RAS signalling pathways in cancer therapy. *Nat Rev Cancer*. 2003;3(1):11–22.
3. Jaffee EM, Hruban RH, Canto M, Kern SE. Focus on pancreas cancer. *Cancer Cell*. 2002;2(1):25–28.
4. Hruban RH, et al. Pancreatic intraepithelial neoplasia: a new nomenclature and classification system for pancreatic duct lesions. *Am J Surg Pathol*. 2001;25(5):579–586.
5. Hingorani SR, et al. Preinvasive and invasive ductal pancreatic cancer and its early detection in the mouse. *Cancer Cell*. 2003;4(6):437–450.
6. Guerra C, et al. Tumor induction by an endogenous K-ras oncogene is highly dependent on cellular context. *Cancer Cell*. 2003;4(2):111–120.
7. Meylan E, et al. Requirement for NF-kappaB signalling in a mouse model of lung adenocarcinoma. *Nature*. 2009;462(7269):104–107.
8. Bassères DS, Ebbs A, Levantini E, Baldwin AS. Requirement of the NF-kappaB subunit p65/RelA for K-Ras-induced lung tumorigenesis. *Cancer Res*. 2010;70(9):3537–3546.
9. Hagemann T, Biswas SK, Lawrence T, Sica A, Lewis CE. Regulation of macrophage function in tumors: the multifaceted role of NF-kappaB. *Blood*. 2009; 113(14):3139–3146.
10. Greten FR, et al. IKKbeta links inflammation and tumorigenesis in a mouse model of colitis-associated cancer. *Cell*. 2004;118(3):285–296.
11. Yang J, et al. Conditional ablation of Ikkb inhibits melanoma tumor development in mice. *J Clin Invest*. 2010;120(7):2563–2574.
12. Lu Z, et al. miR-301a as an NF-kappaB activator in pancreatic cancer cells. *EMBO J*. 2010;30(1):57–67.
13. Vilimas T, et al. Targeting the NF-kappaB signaling pathway in Notch1-induced T-cell leukemia. *Nat Med*. 2007;13(1):70–77.
14. Wu WK, et al. Dysregulation of cellular signaling in gastric cancer. *Cancer Lett*. 2010;295(2):144–153.
15. Miyamoto Y, et al. Notch mediates TGF alpha-induced changes in epithelial differentiation during pancreatic tumorigenesis. *Cancer Cell*. 2003;3(6):565–576.
16. Bray SJ. Notch signalling: a simple pathway becomes complex. *Nat Rev Mol Cell Biol*. 2006;7(9):678–689.
17. Mazur PK, et al. Notch2 is required for progression of pancreatic intraepithelial neoplasia and development of pancreatic ductal adenocarcinoma. *Proc Natl Acad Sci U S A*. 2010;107(30):13438–13443.
18. De La O JP, et al. Notch and Kras reprogram pancreatic acinar cells to ductal intraepithelial neoplasia. *Proc Natl Acad Sci U S A*. 2008;105(48):18907–18912.
19. Morris JP 4th, Cano DA, Sekine S, Wang SC, Hebrok M. β-catenin blocks Kras-dependent reprogramming of acini into pancreatic cancer precursor lesions in mice. *J Clin Invest*. 2010;120(2):508–520.
20. Kulbe H, et al. The inflammatory cytokine tumor necrosis factor-alpha generates an autocrine tumor-promoting network in epithelial ovarian cancer cells. *Cancer Res*. 2007;67(2):585–592.
21. Plentz R, et al. Inhibition of gamma-secretase activity inhibits tumor progression in a mouse model of pancreatic ductal adenocarcinoma. *Gastroenterology*. 2009;136(5):1741–1749.
22. Bash J, et al. Rel/NF-kappaB can trigger the Notch signaling pathway by inducing the expression of Jagged1, a ligand for Notch receptors. *EMBO J*. 1999;18(10):2803–2811.
23. Amsen D, Blander JM, Lee GR, Tanigaki K, Honjo T, Flavell RA. Instruction of distinct CD4 T helper cell fates by different notch ligands on antigen-presenting cells. *Cell*. 2004;117(4):515–526.
24. Fung E, et al. Delta-like 4 induces notch signaling in macrophages: implications for inflammation. *Circulation*. 2007;115(23):2948–2956.
25. Monsalve E, et al. Notch-1 up-regulation and signaling following macrophage activation modulates gene expression patterns known to affect antigen-presenting capacity and cytotoxic activity. *J Immunol*. 2006;176(9):5362–5373.
26. Palaga T, et al. Notch signaling is activated by TLR stimulation and regulates macrophage functions. *Eur J Immunol*. 2008;38(1):174–183.
27. Gordon WR, Arnett KL, Blacklow SC. The molecular logic of Notch signaling — a structural and biochemical perspective. *J Cell Sci*. 2008; 121(pt 19):3109–3119.
28. Anest V, Hanson JL, Cogswell PC, Steinbrecher KA, Strahl BD, Baldwin AS. A nucleosomal function for IkappaB kinase-alpha in NF-kappaB-dependent gene expression. *Nature*. 2003;423(6940):659–663.
29. Saccani S, Natoli G. Dynamic changes in histone H3 Lys 9 methylation occurring at tightly regulated inducible inflammatory genes. *Genes Dev*. 2002;16(17):2219–2224.
30. Yamamoto Y, Verma UN, Prajapati S, Kwak YT, Gaynor RB. Histone H3 phosphorylation by IKK-alpha is critical for cytokine-induced gene expression. *Nature*. 2003;423(6940):655–659.
31. Herzig S, Hedrick S, Morantte I, Koo SH, Galimi F, Montminy M. CREB controls hepatic lipid metabolism through nuclear hormone receptor PPAR-gamma. *Nature*. 2003;426(6963):190–193.
32. Fischer A, Gessler M. Delta-Notch — and then? Protein interactions and proposed modes of repression by Hes and Hey bHLH factors. *Nucleic Acids Res*. 2007;35(14):4583–4596.
33. Iso T, Kedes L, Hamamori Y. HES and HERP families: multiple effectors of the Notch signaling pathway. *J Cell Physiol*. 2003;194(3):237–255.
34. Tanigaki K, Honjo T. Regulation of lymphocyte development by Notch signaling. *Nat Immunol*. 2007;8(5):451–456.
35. Straus DS, Glass CK. Anti-inflammatory actions of PPAR ligands: new insights on cellular and molecular mechanisms. *Trends Immunol*. 2007;28(12):551–558.
36. Straus DS, et al. 15-deoxy-delta 12,14-prostaglandin J2 inhibits multiple steps in the NF-kappa B signaling pathway. *Proc Natl Acad Sci U S A*. 2000; 97(9):4844–4849.
37. Maeda S, Kamata H, Luo JL, Leffert H, Karin M. IKKbeta couples hepatocyte death to cytokine-driven compensatory proliferation that promotes chemical hepatocarcinogenesis. *Cell*. 2005;121(7):977–990.
38. Grivennikov SI, Greten FR, Karin M. Immunity, inflammation, and cancer. *Cell*. 2010;140(6):883–899.
39. Grivennikov SI, Karin M. Dangerous liaisons: STAT3 and NF-kappaB collaboration and crosstalk in cancer. *Cytokine Growth Factor Rev*. 2010;21(1):11–19.
40. Moore RJ, et al. Mice deficient in tumor necrosis factor-alpha are resistant to skin carcinogenesis. *Nat Med*. 1999;5(7):828–831.
41. Espinosa L, et al. The Notch/Hes1 pathway sustains NF-kappaB activation through CYLD repression in T cell leukemia. *Cancer Cell*. 2010;18(3):268–281.
42. Clark CE, Hingorani SR, Mick R, Combs C, Tuveson DA, Vonderheide RH. Dynamics of the immune reaction to pancreatic cancer from inception to invasion. *Cancer Res*. 2007;67(19):9518–9527.
43. Guerra C, et al. Chronic pancreatitis is essential for induction of pancreatic ductal adenocarcinoma by K-Ras oncogenes in adult mice. *Cancer Cell*. 2007; 11(3):291–302.
44. Khasawneh J, et al. Inflammation and mitochondrial fatty acid beta-oxidation link obesity to early tumor promotion. *Proc Natl Acad Sci U S A*. 2009; 106(9):3354–3359.
45. Siveke JT, Einwächter H, Sipos B, Lubeseder-Martellato C, Klöppel G, Schmid RM. Concomitant pancreatic activation of Kras(G12D) and Tgfa results in cystic papillary neoplasms reminiscent of human IPMN. *Cancer Cell*. 2007;12(3):266–279.
46. Glass CK, Saijo K. Nuclear receptor transrepression pathways that regulate inflammation in macrophages and T cells. *Nat Rev Immunol*. 2010;10(5):365–376.
47. Zoete V, Grosdidier A, Michielin O. Peroxisome proliferator-activated receptor structures: ligand specificity, molecular switch and interactions with regulators. *Biochim Biophys Acta*. 2007;1771(8):915–925.
48. Kota BP, Huang TH, Roufogalis BD. An overview on biological mechanisms of PPARs. *Pharmacol Res*. 2005;51(2):85–94.
49. Currie CJ, Poole CD, Gale EA. The influence of glucose-lowering therapies on cancer risk in type 2 diabetes. *Diabetologia*. 2009;52(9):1766–1777.
50. Evans JM, Donnelly LA, Emslie-Smith AM, Alessi DR, Morris AD. Metformin and reduced risk of cancer in diabetic patients. *BMJ*. 2005;330(7503):1304–1305.
51. Grivennikov SI, et al. Distinct and nonredundant in vivo functions of TNF produced by T cells and macrophages/neutrophils: protective and deleterious effects. *Immunity*. 2005;22(1):93–104.
52. Fong CH, et al. An antiinflammatory role for IKKbeta through the inhibition of "classical" macrophage activation. *J Exp Med*. 2008;205(6):1269–1276.
53. Kühn R, Schwenk F, Aguet M, Rajewsky K. Inducible gene targeting in mice. *Science*. 1995; 269(5229):1427–1429.
54. Schreiber FS, et al. Successful growth and characterization of mouse pancreatic ductal cells: functional properties of the Ki-RAS(G12V) oncogene. *Gastroenterology*. 2004;127(1):250–260.
55. Taghon TN, David ES, Zúñiga-Pflücker JC, Rothenberg EV. Delayed, asynchronous, and reversible T-lineage specification induced by Notch/Delta signaling. *Genes Dev*. 2005;19(8):965–978.
56. Hruban RH, et al. Pathology of genetically engineered mouse models of pancreatic exocrine cancer: consensus report and recommendations. *Cancer Res*. 2006;66(1):95–106.
57. Charles KA, et al. The tumor-promoting actions of TNF-α involve TNFR1 and IL-17 in ovarian cancer in mice and humans. *J Clin Invest*. 2009; 119(10):3011–3023.
58. Hagemann T, et al. "Re-educating" tumor-associated macrophages by targeting NF-kappaB. *J Exp Med*. 2008;205(6):1261–1268.
59. Jarriault S, Brou C, Logeat F, Schroeter EH, Kopan R, Israel A. Signalling downstream of activated mammalian Notch. *Nature*. 1995;377(6547):355–358.
60. Berechid BE, Thinakaran G, Wong PC, Sisodia SS, Nye JS. Lack of requirement for presenilin1 in Notch1 signaling. *Curr Biol*. 1999;9(24):1493–1496.